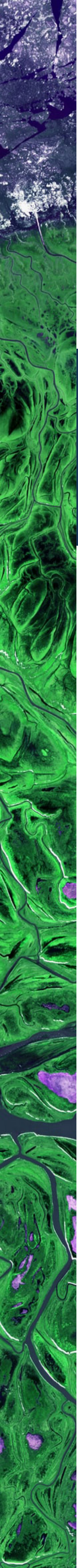

The Transition Institute 1.5

The ambition for an actual transition

WORKING PAPER

#6 - July 2026

Climate Exposed, Debt Decomposed, Reforms Proposed: Climate Disasters and Financing Solutions for Infrastructure in Sub-Saharan Africa

Estimating the Impact of Climate Risk and Sentiment on the Cost of Debt in Infrastructure in Sub-Saharan Africa for better informed financing solutions

BERGERO Jean[1], CARSON Louis[1], JESOVER Théo[1] & KIRKE Nile[1]

Under the Academic Supervision of: Dr ASSOUMOU Edi[2]
Under the Sponsorship of: Pr. MAÏZI Nadia[2]

[1] Students of the MSc Climate Change and Sustainable Finance, a double diploma programme offered jointly by the EDHEC Business School & Mines Paris - PSL.
[2] Mines Paris, PSL University, The Transition Institute 1.5, Center for Applied Mathematics (CMA), 06560 Valbonne, France.

DOI: 10.23646/qjp5-3h48

MINES PARIS | PSL | TTI.5° The Transition Institute

Climate Exposed, Debt Decomposed, Reforms Proposed: Climate Disasters and Financing Solutions for Infrastructure in Sub-Saharan Africa

Estimating the Impact of Climate Risk and Sentiment on the Cost of Debt in Infrastructure in Sub-Saharan Africa for better informed financing solutions

MSc Climate Change and Sustainable Finance

EDHEC Business School & MINES PARIS - PSL

Master Project Report

By:

BERGERO Jean, CARSON Louis, JESOVER Théo, KIRKE Nile

Under the Academic Supervision of:

Professor ASSOUMOU E.

Under the Sponsorship of:

The Transition Institute 1.5, Professor MAÏZI N.

May 2026

Abstract

Sub-Saharan Africa faces a large and persistent infrastructure financing gap, while climate change is increasing both the need for adaptation investment and the cost of capital. This thesis asks how infrastructure and adaptation finance can be scaled in Sub-Saharan Africa while keeping the cost of debt low enough to avoid debt distress.

To answer this question, the thesis decomposes the cost of debt itself. It brings three climate-related risk pricing channels and a behavioral climate sentiment channel from the sovereign level to the project level, where the association of these factors with Sub-Saharan African infrastructure debt pricing has not previously been analyzed at scale. The empirical analysis uses a cross-sectional dataset of 230 infrastructure projects across 1996-2025, assembled from the African Development Bank and World Bank Project Appraisal Documents, as well as data from the private infrastructure finance information platform IJGlobal. Relevant variables are extracted from more than 1,100 unstructured PDF documents using an LLM-assisted extraction pipeline. The all-in nominal interest rate clustered at financial close is regressed on hazard-decomposed climate exposure measures for flood, storm, and extreme heat events, an NLP-derived behavioral sentiment proxy, lender composition, and standard macroeconomic and project-level controls. The climate hazard risk indicators are constructed using climate data informed by satellite observations, combined with local weather station records.

The results show a structured pattern of selective pricing. Storm exposure is associated with a significant cost of debt premium of approximately 104 bps per unit increase in the storm risk index, and this result is robust across lender segments and alternative exposure constructions. Heat exposure is not robustly priced. Flood exposure is not priced as a simple residual risk premium. Rather, it appears to operate through lender-side selection, with our hypothesis being that commercial syndicates finance flood-exposed projects only where adaptation has already been credibly arranged. The behavioral sentiment proxy is priced by private commercial lenders at 114bps per unit increase in the sentiment score and is attenuated when mandate-driven institutions participate in the syndicate.

These findings imply that the climate premium in Sub-Saharan African infrastructure debt is not a single number, but a structured pattern of hazard-specific and lender-specific pricing. We analyze the effect of reducing the storm climate premium through investment in infrastructure resilience on a sample of 19 projects, using a cost-benefit DCF analysis of debt repayment that integrates a Hill-type exposure function. The case study does not provide evidence of any significant benefit in the total cost of debt financing over a project's lifetime from simply reducing debt by investing in adaptation. While not minimizing the importance of resilient infrastructure, this conclusion hints at the need of a deeper, structured, financial solution to scale capital. The thesis argues that the most effective policy response is a blended-finance architecture combining concessional and commercial capital, complemented by adaptation-linked instruments and targeted institutional reforms. A central recommendation is the reform of Basel III capital treatment for eligible blended finance instruments, particularly through lower effective CET1 capital requirements for credit-enhanced climate infrastructure exposures in Sub-Saharan Africa, in order to crowd in commercial capital at scale.

Keywords: Sub-Saharan Africa (SSA); Climate Finance; Infrastructure Debt; Cost of Debt; Blended Finance; Climate Risk Pricing; Climate Hazard Risk Index; Satellite Climate Data; Weather Station Data; Behavioral Climate Sentiment; Development Finance Institutions (DFIs); Basel III; CET1 Capital Requirements; Adaptation Pricing.

Acknowledgements

We would like to thank our supervisor, Professor Edi ASSOUMOU, researcher in applied mathematics at Mines Paris, PSL University, for his guidance throughout the course of this study,

Our sponsor, The Transition Institute 1.5 (TTI.5) and specifically Professor Nadia MAÏZI, Founder and Director of TTI.5, for entrusting us with this research topic and guiding us throughout the process.

We would also like to thank Professor Jeanne AMAR, Professor of finance and associate researcher at EDHEC Business School,

Professor David ZERBIB, Assistant Professor of Sustainable Finance at EDHEC Business School,

Valentine HUET, Head of Climate Adaptation Strategy at VINCI Concessions and Leonard,

Solène METAYER and Sébastien POSTIC, researcher in transition finance and research fellow in public finance and development at I4CE.

Finally, we thank all our Professors from the MSc Climate Change and Sustainable Finance course from EDHEC Business School and MINES Paris universities, our course directors Professor Sophie CLOT and Professor Gilles GUERASSIMOFF, and course coordinators Marie-Ange MANTUANO and Sabrina BEKLI.

Table of Contents

Table of Figures

Table of Tables

List of abbreviations

AfDB - African Development Bank

AI - Artifical Intelligence

API - Application Programming Interface

CAPM - Capital Asset Pricing Model

CDS - Copernicus Climate Data Store

CET1 - Common Equity Tier 1

CO2e - Carbon dioxide equivalent (units)

CoD - Cost of Debt

DCF - Discounted Cash Flows

DFI - Development Finance Institution

DFO - Dartmouth Flood Observatory

EMDE - Emerging Markets and Developing Economies

GDP - Gross Domestic Product

IATI - International Aid Transparency Initiative

IPCC - Intergovernmental Panel on Climate Change

LLM - Large Language Model

MDB - Multilateral Development Bank

ND-GAIN - Notre Dame Global Adaptation Initiative

NLP - Natural Language Processing

NPV - Net Present Value

OECD - Organisation for Economic Co-operation and Development

OLS - Ordinary Least Squares

PV - Photovoltaic

SSA - Subsaharan Africa

UNDRR - United Nations office for Disaster Risk Reduction

USD - United States Dollar

VIF - Volatility Inflation Factors

WACC - Weighted Average Cost of Capital

WBG - World Bank Group

WHO - World Health Organization

WMO - World Meteorological Organization

1 Introduction

Sub-Saharan Africa (SSA) is currently caught in a macroeconomic "pincer" between accelerating climate vulnerability and a prohibitively high cost of debt. These two pressures reinforce each other in a downward-spiraling feedback loop. On one side of this squeeze, the African continent has been warming faster than the global average: ~0.3°C per decade between 1991 and 2023. This is resulting in severe climate catastrophes, such as widespread flooding in East Africa that displaced approximately 2.4 million people during the April-June rainy season in 2023. More generally, Sub-Saharan Africa is the most vulnerable continent to climate change because it is *"multi-dimensional with socioeconomic, political, and environmental factors intersecting"* (Intergovernmental Panel On Climate Change (IPCC), 2023). As such, the continent is losing between 2% and 5% of its annual GDP to climate-driven shocks, which forces governments to divert up to 9% of national budgets toward unplanned disaster recovery, leaving less fiscal room for productive investment (World Meteorological Organization, 2024).

Developing countries' climate risks and vulnerabilities lead to a higher cost of capital, which means these countries receive less investment and or spend more on debt repayment. Climate vulnerability has already raised the cost of debt in developing countries by over 1%. By the end of the 2020s, it is estimated that total additional interest payments due to climate vulnerability will have amounted to USD$146-168 billion (Buhr et al., 2018). This effect can put climate-vulnerable developing countries in a downward spiral: climate adaptation becomes more expensive, so fewer projects are funded, leading to increased climate vulnerability and even greater adaptation costs.

On the other side of the squeeze, the global financial architecture imposes a punishing risk premium that leaves Sub-Saharan African sovereign borrowing costs nearly four times higher than those of the United States (United Nations Conference on Trade and Development, 2025). Median interest-to-revenue ratios exceed 12%, triple the average of developed economies as of 2025, and the fiscal space for growth is rapidly evaporating (Laws et al., 2025). The gap is significant even relative to other developing countries; Sub-Saharan African annual coupon rates were, on average, 1.3 percentage points higher than the average of EMDE countries from other regions between 2014 and 2021, implying a heavier interest burden relative to revenue (Gbohoui, 2023).

In essence, the financial architecture producing these costs, the system of credit ratings, risk premia, asset-pricing models, and multilateral lending consolidated after Bretton Woods and then throughout the end of the 20th century, was designed, in important respects, for different economies. It evolved to allocate capital among industrial and service economies whose risks were stationary, whose data were abundant, and whose currencies were broadly trusted. It assumed continuous price discovery in deep secondary markets, a representative investor with constant relative risk aversion, and a tail of disaster scenarios that could be calibrated from history. None of these assumptions hold fully in Sub-Saharan Africa. Project finance debt is illiquid and held to maturity. Climate hazards are non-stationary, increasingly compound, and concentrated in regions with the least historical data. Currencies are volatile, sometimes structurally so. Sovereign credit ratings are anchored to default histories that, in turn, reflect the punitive premiums. In fact, 22 out of the 54 African countries do not have any sovereign credit ratings from major credit agencies. The result is a financial framework whose key mathematical concepts (e.g., CAPM betas, WACC weights, sovereign spread regressions) remain largely intact, but whose empirical inputs are systematically biased against frontier markets. SSA infrastructure pays a premium that is part fundamental and part artifact of the system itself.

Against this backdrop, the African Development Bank estimates an annual SSA infrastructure financing gap of USD 181- 221 billion, of which adaptation alone represents approximately USD 580 billion over the 2020-2030 decade (African Development Bank Group, 2024b). Almost every credible scenario for closing this gap depends on lowering the borrowing cost faced by SSA sovereigns and infrastructure sponsors. This positions the cost of debt as the central object of analysis, both empirically and structurally. Empirically, infrastructure projects in our sample are debt-financed at an average leverage of 79%, with equity thin, frequently bundled with in-kind contributions from sponsors, and rarely valued through observable secondary markets. Structurally, the cost of debt is the binding constraint on infrastructure delivery: there is no liquid market in SSA infrastructure equity from which a cost-of-equity term structure could be inferred, and the weighted average cost of capital, while theoretically appealing, requires inputs that are not produced in market-clearing form in this setting.

This thesis asks a single central question: how can capital be scaled for Sub-Saharan Africa whilst maintaining a cost of debt low enough to bridge the adaptation and infrastructure financing gap?

The question has two parts that must be answered together. Scaling capital alone, at the prevailing cost of debt, does not close the gap because median commercial rates in our sample of 8.45% leave most adaptation and mitigation projects unbankable on standard terms. Lowering the cost of debt alone, without scaling, does not close it either, because concessional capital is constrained by the fiscal space of the institutions that supply it. The solutions our evidence supports operate on both margins simultaneously.

We approach the question in four movements. First, we develop a theoretical framework that begins with the CAPM, explains why the standard asset-pricing toolkit is institutionally mismatched to SSA project finance, and motivates the cost-of-debt regression as the empirically meaningful pricing primitive in a market where senior debt is the dominant marginal price of capital.

Second, to examine this structure empirically, we assemble a cross-sectional dataset of 230 infrastructure projects across Sub-Saharan Africa spanning 1996-2025. The dataset combines African Development Bank and World Bank Project Appraisal Documents with IJGlobal commercial transaction records. Project-level variables are extracted from more than 1,100 unstructured PDF documents through an LLM-coded document extraction pipeline. Climate exposure is measured using hazard-decomposed Climate Risk Indicators that distinguish flood, storm, and heat exposure, constructed from satellite-derived climate data and Sub-Saharan African weather station observations. We additionally construct an NLP-derived behavioral climate sentiment proxy capturing the informational environment surrounding each project's host country and sector prior to financial close.

Third, we develop a project-level adaptation debt trade-off optimization framework based on DCF analysis of payments to debtors to minimize total financing cost as a function of adaptation investment. We find that it generally fails to clear the trade-off, which in turn motivates the architectural response.

Fourth, we translate this empirical pattern into a financing architecture. The structured nature of the pricing pattern points to a structured rather than uniform policy response. The storm premium calls for first-loss subordination scaled to exposure. The sentiment channel calls for structured DFI participation in commercially priced transactions, a channel that widens rather than narrows as physical-risk salience advances. We anchor the discussion in a worked transaction from our sample, an off-grid distributed solar & storage Tanzania in 2016, to show that proper Basel III recognition of DFI subordination as credit risk mitigation could, in principle, compress this project's all-in cost of debt from its actual 8.59% to approximately 3.04% and, at the same time, increase capital flow towards blended finance.

Our central claim is that the climate premium in SSA is not a single number to be discovered, but a structured pattern of selective pricing in which different hazards, lender pools, and contractual structures interact with project-level exposure to produce the cost-of-debt distribution observed at financial close. Each pattern implies a specific reform, and together they outline what an SSA-aligned development finance architecture would look like: one that simultaneously scales capital and compresses the cost of debt by deploying the same volume of concessional resources to mobilize more commercial capital at lower senior rates.

2 Literature Review

This thesis estimates the cost of debt of Sub-Saharan African infrastructure projects as a function of project-level climate hazard exposure, decomposed into flood, storm, and heat, debt components, and a climate behavioral sentiment proxy. It draws on and aims to contribute to three partially developed strands of literature: the climate finance literature on whether and how climate physical risk is priced in debt markets, the climate vulnerability literature focused on Sub-Saharan Africa, and the project finance literature on infrastructure capital structure in Africa. Each of these strands has produced influential, methodical work on one or more of the dimensions that define our research question. We are not aware of work that brings all of them together in a single empirical setting, though the boundaries between these literatures are porous. Our objective in this literature review is to characterize this body of work carefully, identify the most relevant antecedents, and explain how our research design relates to and extends them.

2.1 The closest antecedents

2.1.1 Climate vulnerability and the cost of debt

The most important antecedent for the climate cost of debt nexus is (Kling et al., 2025). Using a panel of 46 advanced and developing economies from 1996 to 2016, they show that the 25 most climate-vulnerable countries pay approximately 117 basis points more on sovereign debt due to their climate exposure, equivalent to USD 62 billion in additional interest costs over 2007-2016. (Cevik & Jalles, 2022) also use this framework with 98 countries and document an attenuating role for climate resilience. (Zenios, 2024) synthesizes the evolving literature as evidence of a "climate-sovereign debt doom loop", discussing the effect of climate change on sovereign debt levels. (Kling et al., 2021) previously also performed a similar analysis at the firm level, examining the cost of debt for 15,265 firms across 71 countries and finding a 63-basis-point differential attributable to climate vulnerability. Another paper with a similar methodology to ours is that of (Li et al., 2024) who studied the impact of flood and drought risk on the cost of bond financing for water utilities in the US. To reach these conclusions, Li et al. assigned a drought or flood risk score to each water utility bond (using geographical and hydrological data), then fitted a regression model to estimate the effect of increased risk on the bond yield spread.

These contributions establish a robust empirical fact: aggregate climate vulnerability is priced into sovereign and, by extension, corporate borrowing costs across a wide range of countries. Our work takes this finding as a foundational premise. Two design choices in this literature distinguish it from ours and motivate our extension. Climate vulnerability is operationalized through composite indices, most often the Notre Dame Global Adaptation Initiative (ND-GAIN) score (University of Notre Dame, 2026), which aggregates exposure, sensitivity, and adaptive capacity across multiple sectors and hazards. As the authors acknowledge, this design is well-suited to document an aggregate vulnerability premium but is less informative about which specific hazards drive it. The unit of analysis is also the sovereign, or, in the firm-level extension, the corporate borrower, in each country, so that within-country variation in physical exposure across infrastructure projects is not the object of estimation. These features are appropriate to the questions Kling et al. set out to answer, and we make no claim that they represent oversights. They do, however, leave room for a country-level, hazard decomposed analysis to refine or qualify the aggregate finding, particularly in a region as physically heterogeneous as SSA.

2.1.2 Climate vulnerability and SSA public debt

More specifically, a particularly recent and SSA-focused contribution comes from (Egbétoké & Ureche-Rangau, 2026). Using annual data for 38 SSA countries over 2000-2022, they document a negative relationship between climate vulnerability and the debt-to-GDP ratio, which is robust to controls for financial crises, sovereign defaults, and debt relief. They interpret this as a "funding squeeze" through which climate vulnerability constrains SSA sovereigns on the quantity margin, with credit rationing supplementing whatever pricing channel may be operating.

The paper is valuable to our work because it provides direct, SSA-specific evidence that the climate-debt relationship documented globally by Kling et al. is also operative in Sub-Saharan Africa. This guards against an alternative reading in which the global climate-debt finding might dissolve in the SSA subsample. Our research design is best understood as complementary to theirs: they study the response of debt quantity to aggregate climate vulnerability at the sovereign level, while we study the response of debt price to project-level hazard exposure at the infrastructure-project level. The two channels: quantity rationing and price adjustment, are closely linked theoretically (Stiglitz & Weiss, 1981) but distinct empirically, and our sentiment variable is partly motivated by the credit-rationing logic they invoke.

2.1.3 Infrastructure financing in Africa

The closest antecedent on the project-level dimension is (Lu & Wilson, 2024), who examine infrastructure financing in Africa using project-level OLS regressions with country and year fixed effects. Their dependent variables are measures of capital structure, private ownership share, equity ratio, and the use of commercial debt, and their explanatory variables include aggregate infrastructure development, governance, and macroeconomic controls. Their findings confirm that financial institutions strongly prefer to supply debt rather than equity in African infrastructure, and that capital structure choices respond systematically to the level of infrastructure development and to country-level institutional quality.

Their methodology is, to our knowledge, the closest published precedent for a project-level OLS analysis of African infrastructure finance, and we draw on it directly to motivate our research design and our use of project-level fixed effects. Where our work departs from theirs is in the dependent variable (cost of debt) rather than capital structure, and in the central regressors of interest, which include a hazard-decomposed climate exposure factor rather than aggregate infrastructure-development indicators. Climate is not part of their specifications, which is appropriate given their research question. Still, it leaves open the empirical question of how climate exposure enters the pricing of African infrastructure debt, which we will investigate.

2.1.4 Physical climate risk and commercial loan pricing

A recent contribution in the *Journal of Environmental Economics and Management* (Kempa, 2026). This paper analyzes the pricing of physical climate risk in a global dataset of approximately 86,000 syndicated bank loans. The paper finds that the higher the climate vulnerability of the borrowing firm's host country, the higher the loan spreads, with the effects concentrated in long-maturity loans and among financially distressed borrowers. Adjacent work, including (Javadi & Masum, 2021) on physical climate risk and US corporate loan spreads, and (Nguyen et al., 2022) on the role of sea-level rise in collateral pricing, establish a similar pattern in advanced-economy banking markets.

The above literature provides important context for our work because it shows that commercial lenders actively price physical climate risk into loan terms, not only into bond yields or sovereign spreads, and it supports a loan-pricing rather than bond-spread approach as a methodological framework. The samples nonetheless consist primarily of corporate loans to large listed firms in advanced and middle-income economies. SSA infrastructure project finance, structurally distinct in its tenor, leverage, lender composition, and reliance on concessional and politically risk-insured capital, accounts for a small share of these datasets. The unit of analysis is the corporate borrower rather than the project, and climate exposure is again proxied by country-level composite scores. These design choices are reasonable for the questions their papers pose. However, our setting allows us to ask whether the qualitative pattern they document: that physical climate risk is partially and asymmetrically priced, extends to non-recourse project vehicles in SSA when exposure is measured at the project location for each hazard separately.

2.2 Position relative to the antecedents

These papers, taken together, mark out a literature in which the constituent dimensions of our research question have been studied with care, but in different combinations and in different empirical settings. The climate-cost-of-debt link has been established globally and at the firm level, though primarily through composite vulnerability scores. The SSA residual premium has been documented at the sovereign level, though largely without explicit climate variables. SSA-specific climate debt dynamics have been examined on the quantity margin at the sovereign level. Project-level African infrastructure finance has been analyzed in terms of capital-structure outcomes. Each of these strands lends our work both methodological tools and substantive priors.

Our reading of the literature is that the intersection of project-level cost of debt in SSA infrastructure finance and hazard-decomposed climate exposure remains relatively underexplored. What we observe is that each of the pieces of antecedent literature stops just short of the empirical question we pose, in different ways and for different reasons. We aim to occupy this intersection in a single, internally consistent empirical setting, drawing on the methodological conventions of each strand: the spread regressions of the climate-cost-of-debt framework, the residual-premium decomposition of the SSA risk premium literature, and the project-level OLS design of the African infrastructure finance literature.

2.3 Secondary literature

Three further bodies of work inform our specification.

There is considerable existing literature that describes how climate hazards translate into infrastructure cash-flow effects and, therefore, why a forward-looking lender should price them. Chronic stressors include thermodynamic derating of solar PV (Ondraczek et al., 2015). Acute shocks, floods, cyclones, and fires are modeled by (Gourio, 2012) as jump-diffusion processes that destroy capital instantaneously. (Hallegatte et al., 2019) distinguish asset damage from service-disruption losses, noting that NPV impacts of downtime can exceed direct repair costs. Together, these literatures inform our priors about the direction and asymmetric structure of climate effects on infrastructure debt pricing, but they do not themselves estimate the relationship in our setting.

A related strand of the climate finance literature asks whether adaptation, both at the country level through adaptive capacity and at the project level through resilience investments, attenuates the borrowing-cost premium associated with climate vulnerability. (Cevik & Jalles, 2022) find that climate resilience indicators significantly reduce sovereign spreads, partially offsetting the vulnerability premium they document.

A second, more policy-oriented group of literature examines the instruments through which adaptation finance, blended finance, and credit-enhancement mechanisms are designed to reduce financing frictions and borrowing costs in climate-vulnerable regions. Contributions from (OECD, 2025) concerning blended finance for climate action, characterize the architecture of concessional capital, partial credit guarantees, and DFI co-lending arrangements that shape the variation in lender composition we exploit empirically. (OECD & United Nations Capital Development Fund, 2019) provide quantitative assessments of the mobilization and cost-reduction effects of these instruments.

This literature is directly relevant to the interpretation of our findings, particularly the apparent shielding role of concessional finance against the storm premium. In the present section, we note their existence and defer the discussion to Sections 6 and 7, where the policy architecture and the adaptation-pricing channel can be evaluated against empirical evidence rather than in parallel with it.

2.4 Our paper's contribution

Five contributions follow from the empirical and architectural exercise we undertake.

The first is methodological and concerns the construction of the empirical setting itself. Project-level cost of debt data for SSA infrastructure is not available through any standardized disclosure channel, which is one reason the prior literature has focused on the sovereign or firm level rather than the project level. We address this in two ways. We assemble a cross-sectional dataset of 230 SSA infrastructure projects spanning 1996-2025 by combining African Development Bank and World Bank Project Appraisal Documents, extracted from 1,103 PDF documents through an AI-driven pipeline with a fixed extraction schema, validated against independent human readers via a binomial hypothesis test, with commercial transaction records from IJGlobal. We also construct bespoke project-level Climate Risk Indicators for flood, storm, and heat hazards, motivated by the observation that the climate damage functions most used in the literature are calibrated predominantly on data from regions other than SSA and carry a region-of-calibration bias when applied to this setting. Our CRIs draw directly on SSA-specific hazard data: ERA5-Land satellite temperature grids for heat exposure, and EM-DAT records of flood- and storm-affected populations for the acute hazards, evaluated at each project's geographic coordinates over its debt tenor. Both methodological contributions are described in full in Section 4 and the appendix so that subsequent work in this region can extend or replicate them.

The second is the central empirical contribution: we bring three pricing channels: climate-related risks exposure, behavioral sentiment, and the African premium, down from the sovereign level, where the literature reviewed in Section 2.1 has established their operation, to the project level, where their joint operation in SSA infrastructure debt has not previously been characterized at scale. The sovereign-level literature has documented one or more of these channels affecting aggregate sovereign or corporate borrowing costs, but, to our knowledge, no prior work has examined whether the same three channels operate jointly in pricing individual SSA infrastructure project debt. Establishing that they do, and characterizing how they do, is the substantive empirical claim the thesis advances.

The third is the structured pattern that emerges from this exercise, together with its refinement of the residual SSA premium. Storm exposure is associated with a positive and statistically significant cost of debt premium across both lender segments and both CRI constructions. Heat exposure is an insignificant null. We hypothesize that flood exposure is priced through a lender-side selection mechanism rather than a residual risk premium, with commercial syndicates financing flood-exposed projects only where adaptation has been credibly arranged ex ante. The behavioral sentiment proxy loads disproportionately on private commercial lenders and is attenuated, sometimes reversed, where mandate-driven institutions participate in the syndicate. This last pattern refines the interpretation of the SSA residual premium documented at the sovereign level, from a uniform "Africa discount" toward a more structured account that varies with project-level lender composition and physical exposure. The asymmetric structure is, by construction, invisible to specifications that rely on composite vulnerability scores or magnitude-only hazard measures, and it has direct implications for adaptation and policy design that an aggregate measure cannot capture. The refinement of the residual premium is offered in the spirit of complementing rather than displacing the existing sovereign-level evidence: the channels are the same, but their operation at the project level is segment-specific in a way the sovereign-level data cannot reveal.

The fourth contribution concerns adaptation pricing. The empirical observation that infrastructure cash flows are exposed to climate hazards through channels lenders only partially price, motivates a project-level optimization framework in which adaptation operates upstream of pricing rather than alongside it. We develop in Section 6 a total funding cost function that depends on adaptation investment, the level of protection a given adaptation measure provides, and the effectiveness with which that protection is delivered, drawing on a Hill equation-type exposure factor function inspired by the works of (Assab, 2024) and the EDHEC Climate Institute's ClimaTech database for sector- and hazard-specific calibration parameters. The framework asks how a sponsor, given a fixed climate exposure and the relationship between adaptation spend and risk reduction, can benefit from allocating capital to resilience from lower debt climate-related risk premium. This complements the existing adaptation finance literature, which has documented a resilience effect on borrowing costs but, to our knowledge, has not embedded it in a project-level optimization that the sponsor and lender can solve at the design stage.

The fifth contribution is architectural. The empirical pattern documented in Section 5 is, in our reading, not just a descriptive finding but a diagnostic that shapes the design of a financing and policy response. We anchor these proposals in a worked transaction from the regression sample of an off-grid distributed solar & storage project in Tanzania (2016), to quantify the regulatory capital channel and the concessional substitution channel through which a blended finance restructuring compresses the cost of debt. The contribution sits alongside the existing policy literature on blended finance done notably by the OECD, which has characterized the architecture of these instruments in general terms but has not, to our knowledge, calibrated their deployment against project-level empirical evidence on which pricing channels they should target.

These contributions are bounded. The sample is cross-sectional, the geography is restricted to SSA, the dataset is moderate in size, and the climate exposure measures, although constructed from SSA-specific data, remain ex-ante hazard-and-exposure proxies rather than realized loss histories. The adaptation-pricing framework is conceptual rather than empirically estimated. We do not claim to provide a definitive account of climate risk pricing or financing architecture in SSA infrastructure debt, but rather a first set of project-level, hazard-decomposed estimates, along with the architectural and analytical scaffolding that supports those estimates, which we hope will inform subsequent work.

3 Theoretical Framework: From CAPM to Cost of Debt

The introduction noted that the financial architecture inherited from the late-twentieth-century asset-pricing literature was developed primarily in settings whose institutional features differ from those of Sub-Saharan African project finance. This section develops that observation into a practical conceptual framework for our empirical work. We discuss why two standard asset pricing tools, the CAPM and the project-level WACC, are not well-suited to the SSA project finance setting, and why the cost of debt is a more appropriate empirical tool given the institutional structure of this market. The discussion is intended to provide the structure and rationale for the regression specification developed in Section 3.5, rather than to critique the underlying models in their original domains of application. The framework presented here reflects the empirical progression of our own work, an initial application of the CAPM, a subsequent attempt at the project-level WACC, and an eventual settlement on the cost of debt as the most consistent with the institutional structure of SSA project finance.

3.1 The CAPM

The canonical starting point for asset pricing is the CAPM, which expresses expected excess returns as the product of an asset's exposure to systematic risk and the market price of that risk:

$$\mathbb{E}\left[r_{i,t+1}^{e}\right] = \beta_i^{mkt}\lambda_{mkt,t} \tag{3.1}$$

Where:

$\beta_i^{mkt} = \frac{Cov_t\left[r_{i,t+1}, m_{t+1}^{mkt}\right]}{Var_t[m_{t+1}^{mkt}]}$ is the sensitivity of asset *i's* return to the market price kernel, and

$\lambda_{mkt,t}$ is the expected market excess return.

The CAPM in Equation (3.1), specified in expected returns, $r_{i,t+1}^{e}$requires, for empirical implementation, a time series of realized returns for each project. This requirement is not directly applicable to SSA infrastructure project debt. Project debt in this setting originates bilaterally, is priced once at financial close, and held to maturity. Therefore, a sequence of realized returns, from which β_i^{mkt}could be estimated, is not generated by the asset class. The CAPM is thus institutionally mismatched to our empirical setting: the model is sound in markets with continuous price discovery, but its empirical usefulness is limited where such repricing does not occur.

3.2 The Project-Level WACC

A natural alternative is the project-level Weighted Average Cost of Capital, computed at financial close:

$$WACC_i = \frac{E_i}{V_i} \times R_{e,i} + \frac{D_i}{V_i} \times R_{d,i} \times (1 - T) \tag{3.2}$$

Where:

- E_i is the market value of equity for asset i
- D_i is the market value of debt for asset i
- V_i is the total value of asset i
- $R_{e,i}$ is the cost of equity for asset i
- $R_{d,i}$ is the cost of debt for asset i
- T is the corporate tax rate

The WACC has the appeal of preserving CAPM logic at the project level while delivering a single price of capital that does not require a time series of returns. We explored this specification at length and encountered two limitations.

The first is that the cost of equity $R_{e,i}$ is rarely disclosed in SSA project finance documentation, whereas country-level estimates are documented. Our extraction efforts achieved a low success rate on equity IRR fields across project appraisal documents. The second, which we view as the more substantive concern, is that where $R_{e,i}$ is reported it is typically a target IRR set by the project sponsor rather than a market-clearing price. Equity stakes in SSA infrastructure are negotiated bilaterally and rarely valued through observable secondary transactions, which limits the interpretability of disclosed IRRs as analogs to the equity cost of capital implied by an asset-pricing model. The cross-sectional dispersion of any WACC constructed from these inputs would therefore reflect variation in sponsor targets at least as much as variation in systematic risk.

We do not read this as a failure of the WACC formula, which is correct in its standard domain. We read it as an indication that the WACC is of limited empirical usefulness in a setting where one of its required inputs is not produced in market-clearing form.

3.3 The cost of debt

The cost of debt $R_{d,i}$ is comparatively well supported by the institutional architecture of SSA project finance for three reasons:

First, it is observable. The senior debt interest rate is set at financial close, documented in loan agreements, and reported in project appraisal documents and (somewhat) in commercial databases such as IJGlobal. We extract $R_{d,i}$ at a 38% success rate from project appraisal documents and supplement this with IJGlobal data, yielding 230 usable observations.

Second, it is comparable across projects. Senior debt instruments share a common structure defined by coupon, maturity, and seniority, which permits cross-sectional comparison in a way that equity returns or sponsor IRRs do not.

Third, it is structurally central. SSA infrastructure projects in our sample carry an average leverage ratio of 79%, with debt providing the majority of project capital. The cost of debt is therefore the dominant marginal price at which infrastructure financing is allocated in this market, and lenders rather than equity sponsors are the agents whose risk-pricing behavior we seek to characterize.

Building the empirical framework around $R_{d,i}$ is therefore a matter of methodological fit: in a highly leveraged, illiquid, non-recourse infrastructure market, the cost of debt is an empirically meaningful pricing primitive.

3.4 A Heuristic Pricing Decomposition

To motivate the regression specification, it is useful to consider a simple reduced-form decomposition of the cost of debt. We present this as an intuitive heuristic rather than as a structural credit pricing model. For project i:

$$R_{d,i} = r_{f,i} + \mathrm{PD}_i \cdot \mathrm{LGD}_i + \pi_i \quad (3.3)$$

Where:

$r_{f,i}$ is a relevant risk-free benchmark,

$\mathrm{PD}_i$and $\mathrm{LGD}_i$are the project's probability of default over the loan tenor and loss given default, respectively,

$\pi_i$is a residual term capturing compensation that the lender requires above expected loss.

This decomposition organizes the variables that enter the empirical specification. Climate hazards plausibly enter through $\mathrm{PD}_i$and LGD_i. Acute shocks, such as floods and cyclones, can raise loss given default by damaging assets and disrupting cash flows. In contrast, chronic stressors, such as sustained heat, can raise the default probability by eroding operating margins over the loan tenor.

Behavioral and informational factors plausibly enter through π_i, in line with the literature on credit rationing (Stiglitz & Weiss, 1981) and the residual SSA premium (Gbohoui, 2023). Lender composition may vary across both channels, consistent with the differing mandates and information structures of development finance institutions and commercial banks.

Equation (3.3) is not estimated directly. It clarifies which variables we expect to appear in a cross-sectional pricing regression and why.

3.5 Empirical Specification

The empirical analog of the decomposition above is the cross-sectional regression:

$$R_{d,i} = \alpha + \beta_1 \mathrm{CI}_i^{\mathrm{flood}} + \beta_2 \mathrm{CI}_i^{\mathrm{storm}} + \beta_3 \mathrm{CI}_i^{\mathrm{heat}} + \gamma S_i + X_i^{\mathrm{macro}}\delta_1 + X_i^{\mathrm{proj}}\delta_2 + X_i^{\mathrm{sect}}\delta_3 + \varepsilon_i \quad (3.4)$$

Where:

$\mathrm{R}_{\mathrm{d,i}}$ is the senior debt interest rate at financial close for the project i

$\mathrm{CI}_{\mathrm{i}}^{\mathrm{flood}}$, $\mathrm{CI}_{\mathrm{i}}^{\mathrm{storm}}$, and $\mathrm{CI}_{\mathrm{i}}^{\mathrm{heat}}$are project-level Climate Damage Factors for each hazard, constructed from publicly available hazard layers evaluated at the project's geographic coordinates and combined with hazard-specific damage functions

S_{i} is a climate behavioral sentiment proxy capturing the prevailing perception of SSA risk over the period preceding financial close

$\mathrm{X}_{\mathrm{i}}^{\mathrm{macro}}$, $\mathrm{X}_{\mathrm{i}}^{\mathrm{proj}}$, $\mathrm{X}_{\mathrm{i}}^{\mathrm{sect}}$are vectors of macroeconomic, project-level, and sectoral controls, respectively.

Interaction terms between sentiment and lender type, and between flood exposure and concessional lender share, are introduced in extended specifications reported in the solutions section.

The specification is estimated using Ordinary Least Squares, with standard errors clustered at the year of the financial close. Year-level clustering reflects the prior that the dominant source of residual dependence in this cross-section is contemporaneous variation in global financial conditions and SSA wide sentiment affecting projects closing in the same year.

We interpret the coefficients in (3.4) as conditional correlations rather than causal effects. The cross-sectional design does not provide a source of exogenous variation in hazard exposure or sentiment, and we make no causal claim. The contribution of the regression is descriptive and exploratory: it characterizes, for a cross-section of 230 SSA infrastructure projects spanning three decades, how the cost of debt covaries with hazard-decomposed climate exposure, lender and debt composition, and behavioral sentiment, conditional on a set of standard controls.

4 Data and Methodology

This section sets out the empirical implementation of the cost of debt regression introduced in Section 3.5. Section 4.1 describes the construction of the project-level financial dataset from multilateral development bank Project Appraisal Documents and the IJGlobal infrastructure finance database, and addresses the sample selection structure that follows from the disclosure environment of SSA project finance. Section 4.2 describes the construction of project-level climate-related risk indicators for floods, storms, and extreme heat events, distinguishing between hazard layers, geographic exposure, and severity measurement. Section 4.3 describes the behavioral sentiment proxy and clarifies its interpretation. Section 4.4 summarizes the analytic dataset and the variable definitions. Section 4.4.1 sets out the empirical strategy: the estimating equation, the construction of standard errors, the multicollinearity diagnostics, the sample-split design, the interaction battery, and the robustness specifications. Throughout the section we frame the empirical exercise as descriptive of conditional associations.

4.1 Infrastructure Project Data

The unit of observation is an individual infrastructure project located in Sub-Saharan Africa, with the all-in nominal interest rate on senior debt at financial close as the dependent variable. The SSA infrastructure finance market does not produce the standardized, machine-readable disclosure that characterizes sovereign bond or syndicated-loan markets in advanced economies: senior loan terms are typically embedded in unstructured Project Appraisal Documents, transaction records, or sponsor disclosures, with substantial heterogeneity in how they are reported. We therefore combined two complementary sources of project-level data, each subject to its own selection structure.

4.1.1 Multilateral Development Bank Project Appraisal Documents

The first source is the corpus of Project Appraisal Documents (PADs) and equivalent appraisal reports published by the African Development Bank (AfDB) and the World Bank Group (WBG). These documents are released at financial close and typically describe the project rationale, sponsor structure, financing plan, debt terms, country context, and environmental and social considerations. PADs are the most consistent public source of project-level financial information for SSA infrastructure, but they are released as PDFs and are not available through any structured data interface.

We retrieved PADs via a Python web-scraping pipeline targeting the document portals of the two institutions and applied a series of filters to isolate the regression-ready sample. The pipeline operates on five stages:

1. Document retrieval, in which 1,746 PADs were obtained from the AfDB portal via the IATI Datastore (a 52% success rate against the indexed target list of 3,353 reports) and 164 from the WBG repository, the latter pre-filtered for infrastructure operations (African Development Bank, 2026; World Bank Group, 2026; IATI, 2026).
2. Infrastructure filtering, applied to the AfDB sample to retain projects in transport, energy, water and sanitation, digital infrastructure, agriculture, and mining, yielding 939 AfDB projects and 1,103 documents in total once combined with the WBG set.

3. Readability filtering, which dropped corrupted or non-text-recoverable PDFs and documents lacking financial-terms keywords, leaving 735 documents eligible for content extraction.
4. Information extraction, in which a large language model with a fixed extraction schema, deterministic settings, and strict JSON output was applied to each document.
5. Regression conditioning, which retained only those projects for which the dependent variable and a minimum set of project covariates were recovered. The full methodology can be found in Section 11.1.

For each document, the model returned a structured record covering the senior debt interest rate at financial close, the debt tenor, the project size, the financing structure (leverage, lender composition, fixed versus floating rate, concessional versus non-concessional terms), the project type (greenfield, expansion, refinancing), the sector classification, and project geocoordinates where available. Documents in which a required field was not present were marked as missing rather than imputed.

Extraction success varied substantially across fields: sector classification, project type, and country of operation were recovered for nearly all documents, while the cost of debt, our dependent variable, was reported in only 38% of the 735 documents analyzed. This is the binding empirical constraint on sample size and reflects the fact that multilateral lenders frequently report concessional terms in narrative form (for example, "on standard IDA terms" or "on AfDB concessional window terms") without quoting an explicit nominal rate.

After regression conditioning, the public-document pipeline yielded 165 AfDB and WBG infrastructure projects.

Because the extraction was performed by a language model rather than by human readers, we conducted a validation exercise on a stratified random sample of extracted records. For each sampled document, two members of the research team independently extracted the cost of debt and the leverage ratio from the underlying PAD, and the results were compared with the LLM output. Treating each document as a Bernoulli draw with success defined as agreement within a pre-specified tolerance band (10 basis points for the cost of debt, two percentage points for leverage), the observed agreement rate was sufficient to satisfy a one-sided binomial test of the null that the underlying agreement rate exceeds 90% at conventional significance levels. We interpret this as evidence that the LLM-extracted variables are of comparable quality to a careful human read for the purposes of cross-sectional regression analysis, while acknowledging that residual measurement error remains and is absorbed into the regression error term.

4.1.2 Private Project Finance Data

The PAD pipeline tilts the sample towards concessional MDB-financed projects, by construction: the AfDB and the WBG disclose appraisal documents only for operations they themselves finance, and these institutions operate predominantly through concessional or semi-concessional windows.

To recover variation across the lender-composition margin, we supplemented the PAD sample with project records drawn from IJGlobal, a commercial database that aggregates infrastructure project-finance transactions from sponsor disclosures, lender announcements, and the financial press (Green Street Infrastructure, 2026).

We obtained access through a trial subscription, extracted all SSA project-finance transactions for which the senior debt interest rate at financial close was disclosed, restricted the extract to completed onshore SSA transactions, excluded out-of-scope offshore hydrocarbon projects, and harmonized variable definitions to those of the public document sample. After these restrictions, 65 IJGlobal projects entered the analysis. With one exception, all are financed through private, non-concessional debt, reflecting the concentration of IJGlobal coverage in commercial transactions where lender disclosure is more common.

4.1.3 Structure of the Merged Sample

The combined dataset prior to merging climate and sentiment, therefore, comprises 230 projects: 165 from the AfDB-WBG pipeline and 65 from IJGlobal. After conditioning on the availability of the dependent variable, the climate exposure variables, and the sentiment proxy, and after dropping observations with implausible values (zero or negative interest rates and projects with financial close before 1996), the regression sample comprises 230 projects, of which 165 are concessional and 65 are non-concessional.

It is important to be explicit about the selection structure of this merged dataset. The two source pipelines are systematically biased in opposite directions. The PAD pipeline overrepresents concessional MDB-financed projects because MDBs are the institutions disclosing the appraisal documents on which it relies. IJGlobal over-represents commercially financed projects with disclosed pricing because its coverage is concentrated where commercial sponsors and syndicate banks publish loan terms. Neither source approximates a random draw from the population of SSA infrastructure projects, and their union does not either. The merged dataset is best understood as a sample of SSA infrastructure projects for which debt pricing information is observable, conditional on the disclosure practices of the financing institutions involved.

We treat this as an inherent feature of the infrastructure finance disclosure environment rather than a flaw in the research design. Cross-sectional empirical work on SSA project finance is constrained by market reporting, and a fully random sample of SSA infrastructure debt pricing is not feasible at present.

The selection structure has two implications for the empirical strategy that follows. First, the external generalizability of the estimates is limited: the coefficients describe pricing patterns within the set of disclosed projects rather than within the universe of SSA infrastructure debt. Second, because the two source pipelines load on different segments of the lender market, we exploit this variation analytically through the concessional versus market sample split design described in Section 4.1.3, which makes the divergent pricing behavior of the two segments visible rather than averaging over it.

The geographic coverage of the merged sample warrants a brief description before turning to the climate exposure variables, since the spatial footprint of the data conditions the variation that any subsequent regression can exploit. The 230 projects in the regression sample are distributed across 43 Sub-Saharan African countries, spanning every major sub-region of the continent. Coverage is most concentrated in West Africa and Southern Africa, reflecting the geographic distribution of MDB infrastructure lending and of commercial project finance in the IJGlobal database. East Africa and the Sahel are represented but with fewer projects per country. North African countries are excluded by construction, consistent with the regional scope of the thesis.

Figure 4-1: Geographic coverage of the regression sample

Note: Shaded countries are those represented in the regression sample (N = 230 projects across 43 countries).

Two implications of this geographic distribution are relevant for the empirical work that follows. First, the sample retains substantial cross-country variation in macroeconomic conditions, governance quality, and climate exposure, which supports the inclusion of macro controls and the use of project-level CIs rather than country-level aggregates. Second, several countries are represented by only a small number of projects, which reinforces the choice of year-level rather than country-level clustering for standard errors and motivates caution in interpreting any country-specific patterns that may emerge from the regression residuals.

4.2 Climate Risk Indicator

4.2.1 Motivations

The central impetus of this framework lies in the pricing of climate risk in infrastructure financing, we look to define a set of risk indicators that make a reasonable job in capturing the rational component of climate risk evaluation. The climate risk indicators are set to take into account the occurrences and severity of the three types of events we found to be the most relevant in literature on damages to infrastructure: flood, storm and extreme heat events (Assab, 2024, 2025; Eberenz et al., 2021; European Commission. Joint Research Centre., 2016; Verschuur et al., 2024; World Bank Group & Miyamoto International, 2019). While literature provides a set of well calibrated climate damage functions (Eberenz et al., 2021; European Commission. Joint Research Centre., 2016) these seem upon review to be better calibrated to other regions where data has been historically more available than in SSA to calibrate their functions, while making a reasonable attempt. Additionally, proxies have been used in literature to create indicators (Assab, 2024, 2025; DFO - Flood Observatory (DFO), 2026), which we take inspiration from to develop specific indicators using data from SSA countries. In the following framework, we design two indicators in order to test the relevance of socioeconomic indicators (inspired from (Assab, 2024) use of affected population for flood risks) and magnitude (used in the DFO flood impact function, (DFO - Flood Observatory (DFO), 2026)). We note that these indicators aim to capture the evolution of the occurrences and relative severity of each type of disaster independently from each other.

4.2.2 Setup: climate socioeconomic risk indicator

In the present iteration of the climate risk indicator, we distinguish extreme heat events as different from storms and floods and compose the heat risk indicator differently for the following reasons:

- Extreme weather damage databases (CRED EM-DAT, UNDRR Desinventar Sendai) report no significant extreme heat events impacts in SSA since 1900, yet the region presents strong evidence it has since then experienced a number of extreme heat events (Harrington & Otto, 2020),
- While floods and storms present acute destruction over a relatively short period (that is, relatively short in comparison to the observed durations of extreme heat events, see descriptive statistics in Appendix), and that extreme heat events affect efficiency (in terms of productivity or system efficiency) over longer periods.

For floods and storms, we use the EM-DAT database, specifically the number of occurrences of events, Nocc, the duration of events, de, and number of affected people, Apop, to compute an indicator mixing the (Assab, 2024) approach (use of affected people as severity) and DFO approach (accounting for duration of events). We use population data over cost data as we observe that it is reported more systematically. Equation 4.1 below presents the equation for this first indicator, CIpop:

$$CI_{pop,e,t} = d_p * \frac{\sum_{t=0}^{t}\left(N_{occ,e,t}\right)}{t} * \frac{\sum_{t=0}^{t}\left(d_e\right)}{t} * \frac{\sum_{t=0}^{t}\left(\frac{A_{pop}}{Pop_t}\right)}{t} \qquad (4.1)$$

With dp the duration of the project, e indicates the type of climate event (flood or storm), t the date of the financial close for the project, Pops the total population at the year t.

Equation 4.1 in this form accounts therefore for the historically observed average of the affected population (as a ratio of total population to account for population growth) and duration of events and the number of yearly occurrences which creates an indicator of the yearly expected percentage of affected population which is then multiplied by the duration of the population to determine the expected effect of a given climate disaster over the lifetime of the project. The methodology uses simple averages rather than more complex computations that would more appropriately account for the estimated increases in occurrence and severity, as these estimates have evolved significantly over the sample period (1986-2025).

For extreme heat events, we use data from ERA5-land database, with no sufficient reported data (Harrington & Otto, 2020), we use climate data, specifically ERA5-land (Muñoz-Sabater et al., 2021) to estimate occurrences and duration. For this task, we therefore had to define how we would quantify occurrences of extreme heat events. The definition varies amongst different organizations with the more commonly accepted ones being from the WMO, IPCC or WHO. However, to capture in what we believe to be the most appropriate manner the operational thresholds of infrastructure, we turn to research done by (Verschuur et al., 2024) who estimates this for electricity generation, T&D, airports, seaports, rail and telecoms, a group of sectors that we assume to be sufficient to generalize across all the sectors covered by our sample of projects. The thresholds (as specific points or ranges) are presented in Figure 4-2. These vary significantly, the lowest being at 25°C and highest 50°C. From this data we assume the most relevant threshold temperature is situated between 29 and 33°C which is where the three ranges overlap, and while transport and telecom have estimated thresholds above this range, it is a decent compromise so that we do not omit any impacting events. We round up to 35°C (red line, Figure 4-2) to suit the ERA5-land downloadable dataset, which we acknowledge introduces a conservative bias in the counting of extreme heat events with regards to the proxy sector thresholds.

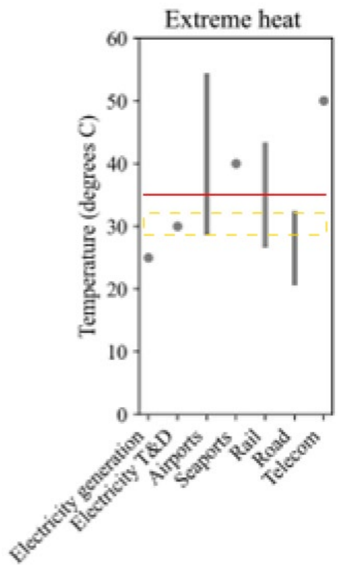

Figure 4-2 Temperature thresholds for different asset classes, (Verschuur et al., 2024)

We use the multi-origin C3S atlas from ERA5-land to obtain the monthly extreme-hot-day (>35°C) variable, which returns the number of days over 35°C each month over the period 1950-2024. As ERA5-land is a high-resolution grid dataset, the CDS API used to collect this data functions as a coordinates download; we defined boundaries for all the countries represented in the sample of infrastructure financing deals to obtain a specific dataset for each country. The boundaries are presented in Figure 4-3 below, while some boundaries extend across the borders over water, ERA5-land only accounts for land data, which means all grid cells above water are ignored in the downloads. The number of monthly extreme-hot days is computed as the average across the grid cells within the country's boundaries. (Muñoz-Sabater et al., 2021)

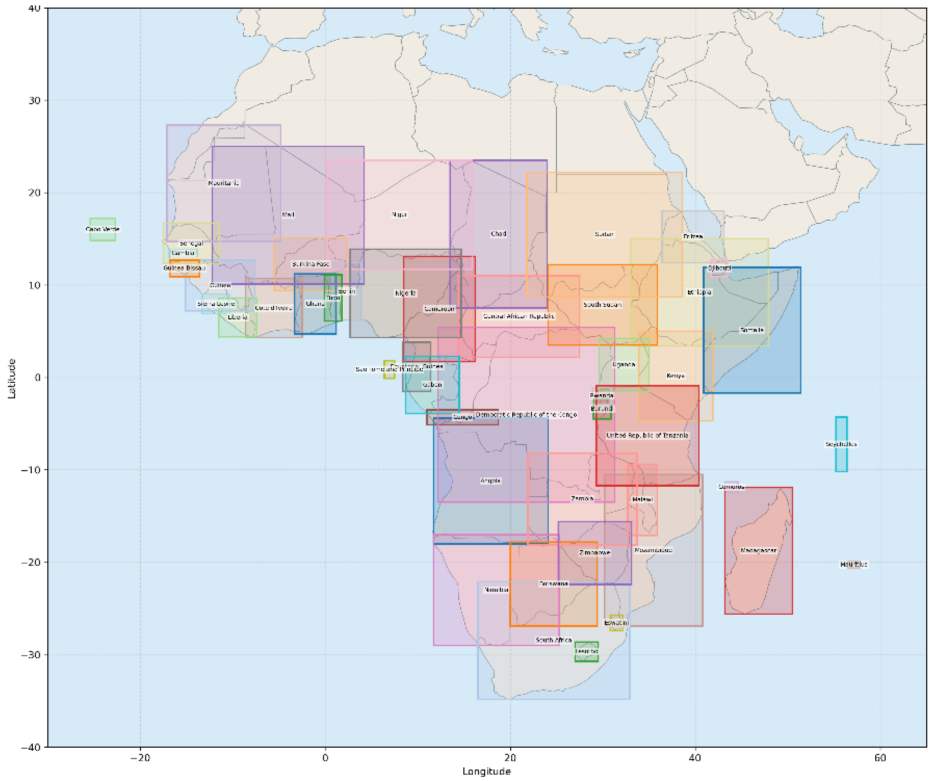

Figure 4-3: Estimated country boundaries

We use the 2-day (that is, consecutive days over 35°C) threshold from the IPCC definition as the minimum duration to count for one event, limiting the count for one event at one month, a simplification necessary due to how the data is aggregated, and that was chosen arbitrarily.

The indicator is then computed as follows:

$$CI_{pop,e,t} = d_p * \frac{\sum_{t=0}^{t}\left(N_{occ,e,t}\right)}{t} * \frac{\sum_{t=0}^{t}(d_e)}{t} \qquad (4.2)$$

The absence of a population index is relevant to the difficulty of assessing boundaries to an extreme heat event, noticed in literature (Harrington & Otto, 2020). Taking the average number of extremely hot days across all cells for each country permits us to consider that the entire population is affected at each occurrence. We notice this is a limitation to this framework, which was in part what motivated the multiplication of indicators in order to test the robustness of the assumptions we make to see if different configurations present the same answer, or what type of information investors are more sensible to when approaching climate risk in infrastructure projects.

4.2.3 Setup: climate magnitude risk indicator

The climate magnitude risk indicator presents the same characteristics as the previous, however we replace the cumulated yearly average affected percentage of population variable and replace it with a specific magnitude indicator for each type of event, similarly to the DFO methodology (DFO - Flood Observatory (DFO), 2026). For floods, we use the affected area given by EM-DAT, for storm the speed given by EM-DAT, and for extreme heat events we use the monthly daily maximum temperature variable of the ERA5-land database as our magnitude, mage. The formula for the indicator is presented below.

$$CI_{pop,e,t} = d_p * \frac{\sum_{t=0}^{t}(N_{occ,e,t})}{t} * \frac{\sum_{t=0}^{t}(d_e)}{t} * \frac{\sum_{t=0}^{t}(mag_e)}{t} \quad (4.3)$$

4.2.4 Resulting indicator description

As we will se in following sections, the indicators will be log-normalised: log(1+CI). In this section we compare normalized values of the indicators. While they were created to account for amplitudes and variations, rendering the core numeric value by itself useless, the normalized values allow for easier comparison between the indicators. Below we compare only the time variable component of each indicator, excluding therefore the project duration from the computation.

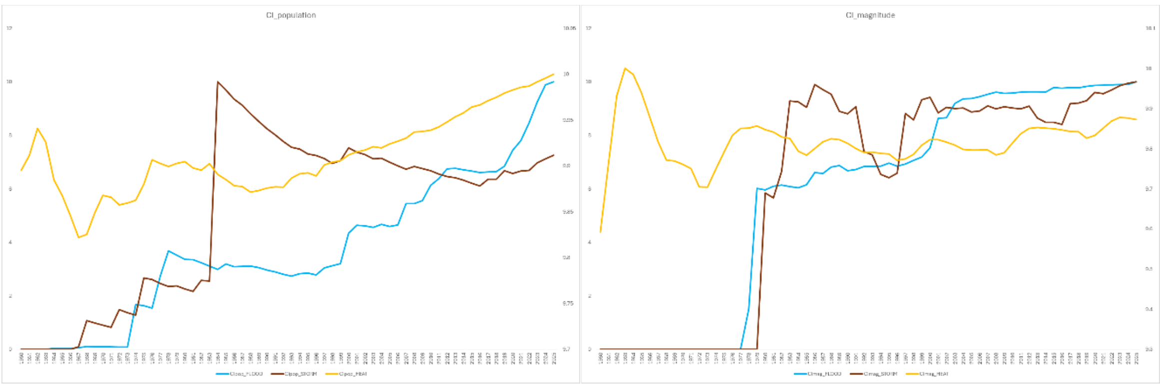

Figure 4-4 Timeplot of the variations in the normalized values of the population Climate Indicator, CIpop (left) and magnitude Climate Indicator CImag (right)

Due to the variations in the heat indicator being more subtle, the right vertical axis of each chart is specific to the heat indicator while the storm and flood indicators refer to the left vertical axis

Before any commentary, we remind the reader that these indicators represent the knowledge of events through either reported information (floods, storms) or climate observations and modelling (heat).

For storms, Figure 4-4 shows in both cases a peak around 1985, following which in the case of CI_pop, it presents a decreasing trend with only slight increases around the year 2000 and 2017 onwards. The magnitude indicator reacts differently to these shocks, reverting back to its near-max amplitude at each of these dates (around 1985, the year 2000 and a progressive increase since 2017). We assume this decoupling of magnitude and socioeconomic impact to be related to the evolution of preparedness and means of ensuring security of populations when storms occur, in other words, increase in adaptive capacity.

For floods, both indicators present a two-step progressive increase with a before and after 2000 mean level, however the magnitude indicator presents one main, severe, increase around 2000 whereas the population indicator is more progressive from the year 2000 onwards. This may reflect improvements in reporting (the Sendai Framework for Disaster Risk Reduction, established in 1994) and the urbanization of floodplains.

For extreme heat events, both indicators are created using the same data, and the magnitude indicator only introduces heat in addition to the other; we see that the trend, while continuing to rise, presents a “cyclical” aspect to it, dropping every 12 years approximately. The cyclical aspect may reflect oscillations due to El Niño (Southern Oscillation, SOI) or the Indian Ocean Dipole (IOD), which significantly impact temperature extremes in SSA, while the upwards trend is evidence of anthropogenic global warming.

4.3 Behavioral Sentiment Proxy

4.3.1 Motivations

The motivation for integrating this indicator into our regression model lies in the literature on the existence of an African risk premium (Gbohoui, 2023), hinting that a component of the cost of debt may stem from a purely behavioral aspect of investment. Behavioral economics literature has established that decisions made under conditions of genuine uncertainty are affected by a set of cognitive shortcuts and psychological pitfalls (Tversky & Kahneman, 1974) directly relating these to investment decisions (Daida et al., 2025; Idris, 2025; Katenova et al., 2025). The link between psychological pitfalls and biases and climate change is exposed by (Shefrin, 2023) as the big behavioral question, hinting that the psychology of climate change centers on fear of future climate-related damages, biases or misjudgments that hamper the efficiency of responses and hope with regards to emerging technologies that promise significant greenhouse gas reductions. As we are exploring the effects of climate change on the cost of debt for infrastructure projects in SSA, this has encouraged us to incorporate the behavioral question into our regression model as a variable that we estimate makes a reasonable attempt to capture the biases - notably the availability bias – that may have influenced investment decisions at the time of their closings. Two qualifications govern the interpretation of all results produced by this framework. First, the truthfulness of the information to which lenders were exposed is not the subject of this inquiry; only its directional valence and its plausible cognitive effect are at issue. Second, the heuristic mechanisms operate as distortions of rational cost-benefit analysis rather than as substitutes for it.

4.3.2 Sentiment model setup

To engage our framework on how to capture investor climate sentiment - a variable we will call the climate sentiment score, S - we must first define the availability bias which provides the foundation of the psychological mechanism we aim to capture. The concept is defined as the tendency to estimate the frequency or probability of an event by the ease with which instances or scenarios that present resemblance to a given choice or estimation task can be brought to mind, such that events rendered salient by recent, vivid, or extensively circulated discourse are judged disproportionately probable, regardless of their actual statistical frequency of even truthfulness. This signifies a “fresh memory” effect, suggesting a decay period for information embedded in memory (Tversky & Kahneman, 1974). We call the decay period d. For a transaction in our sample that occurs in year t, the lookback period would be t-d.

After the elimination of duplicate articles, we extend on the recommendations of (Daida et al., 2025) who advocate the use of natural language processing (NLP) tools as a potential solution to creating robust sentiment indices, introducing ClimateBERT [1]to conduct a sentiment analysis. The choice of a domain-specific, climate-trained model over a general-purpose sentiment classifier is deliberate as the nuance of climate-related discourse renders general classifiers systematically unreliable in this domain. The three output labels for each article are: (Webersinke et al., 2021)

- Risk (−1): the passage frames climate conditions as a threat — business downside risk, potential losses, adverse impacts on society or the environment, associated with specific negative adjectives applied to anticipated, past, or present developments;
- Opportunity (+1): the passage frames climate conditions as beneficial — business opportunities arising from adaptation or mitigation, positive environmental impacts, associated with specific positive adjectives applied to the topics covered;
- Neutral (0): the passage states facts or developments without directional framing, assigning neither specifically positive nor specifically negative adjectives to the entities or outcomes described.

The model does not cross-reference textual claims with external data, rendering it vulnerable to greenwashing: it rewards domain-specific syntax regardless of evidential quality. In the context of this study, however, this is a feature rather than a flaw (our purpose being to measure the tone of the information to which lenders were exposed, not to evaluate its truthfulness).

The sentiment score is then calculated as the arithmetic mean of all of the citation label sentiment scores (associating +1 to opportunity, -1 to risk and 0 to neutral), Cn, then dividing by the total number of citations, CN:

$$S_n = \frac{1}{C_N} * \left(C_{n,opportunity} - C_{n,risk}\right) \qquad (4.4)$$

By construction, it lies on the interval [−1, +1]: a score near −1 indicates that the preponderance of textual evidence in the project's information environment frames climate conditions as a risk. A score near +1 signals a predominantly opportunity-oriented framing. And a score near zero indicates either a balanced distribution of risk and opportunity signals or a corpus dominated by neutral passages.

We acknowledge that the core concepts of traditional and behavioral economics would lead us to integrate a coefficient of risk aversion, weighing C_n risk higher than the C_n opportunity. While this would allow for a more realistic approach, we do not incorporate this weight in our study to conduct a purely observational study that can serve as the basis for further research on calibrating this function.

4.3.3 Data collection

The first step of our process is to collect articles relevant to the sample of projects studied, for a decay period before each financial closing date. This means, for a given project that obtained financial closing in year t, all articles relevant to the project from year t-d to year t must be

[1] Specifically, the climatebert/distilroberta-base-climate-sentiment model, a DistilRoBERTa-based transformer architecture fine-tuned on a corpus of climate-related research abstracts, corporate disclosures, and general news reports to perform three-class directional sentiment analysis (Webersinke et al., 2022).

recovered to provide the best possible picture. In our study we set d to 3 years. We consider an article to be relevant to this study if it mentions climate-related disasters, the country of the project and the sector. This data collection is carried out using a project-specific scrape-search loop in Python. Keywords are defined for climate-related disasters (using vocabulary from the IPCC corpus), and we also use the names of countries as inputs and define lists of synonyms or linked terms for every project's sector. The list of collected citations reflects primarily the scholarly and institutional publication record rather than the broader media environment, a distinction that bears on the interpretation of the sentiment scores and is discussed further in the results section. Media source scraping did not return any citations. See appendix for detailed information on sources and methodology. We assume this to be a downfall of the methodology, while claiming that academic research does affect lender decisions in relatively new fields such as climate risk assessment, for which economic models used by banks rely on assumptions that are grounded in research (Abinzano et al., 2026; Kruse et al., 2024).

4.3.4 Resulting score description

The distribution across sources reveals a pronounced concentration in the peer-reviewed scholarly literature: Crossref contributed the largest share (11,729 articles, 37.0% of the total), followed by OpenAlex (10,535 articles, 33.2%), CORE (8,962 articles, 28.3%), Semantic Scholar (375 articles, 1.2%), and arXiv (104 articles, 0.3%). The mean number of articles per project is 133.2, with a standard deviation of 26.7.

Across all 33,172 classified chunks, the label distribution is as follows: neutral - 14,630 chunks (44.1% of the total); risk - 9,692 chunks (29.2%); and opportunity - 8,850 chunks (26.7%). The near symmetry of risk and opportunity counts at the corpus level conceals substantial heterogeneity at the project and sector levels. The mean ClimateBERT confidence score across directional (risk and opportunity) classifications, the precision statistic is 0.758, suggesting that, on average, the model assigns its directional predictions with moderate-to-high certainty. The standard deviation of the project-level precision is 0.038, indicating a relatively stable classification confidence across projects and suggesting that the cross-project variation in sentiment scores is driven primarily by differences in the substance of the retrieved corpus rather than by differences in model confidence.

The distribution of project-level sentiment scores spans the range [−0.566, +0.431], with a mean of -0.032 and a median of -0.051, both slightly negative, indicating a modest but consistent net risk orientation in the textual environment in which these 230 deals were closed. Of the 230 projects, (57.6%) carry a negative sentiment score, (41.2%) carry a positive score, and (1.3%) are exactly zero. This distributional asymmetry is consistent with the negativity bias documented in the psychological literature(Soroka et al., 2019) and with the prediction of the availability heuristic that adverse climate events, being more salient and vivid, will disproportionately populate the accessible information environment.

Sector-level disaggregation reveals heterogeneity. Water and Sanitation projects carry the most negative mean sentiment score (-0.301), followed by Transport (-0.130) and Mining (-0.108), all sectors whose infrastructure is most directly and visibly exposed to climate physical hazards such as flooding, drought, and extreme precipitation. Clean Energy and Networks, by contrast, exhibits the most positive mean sentiment score (+0.127), reflecting the extensive literature framing renewable energy infrastructure as a climate opportunity. Digital Infrastructure also posts a positive mean (+0.092). Fossil Energy occupies an intermediate positive position (+0.035), which at first glance may appear counterintuitive but is consistent with the composition of the corpus, dominated by peer-reviewed publications whose coverage of fossil fuel infrastructure in Sub-Saharan Africa emphasizes energy access as an opportunity rather than climate risk as a threat. Agriculture and Rural Development registers a modestly negative mean (-0.037), we interpret this as a translation of the exposure of this sector.

A temporal decomposition by decade of financial close reveals a tentative downward trend in mean sentiment, but increasing divergence in framing (in relation to the development of media sources, and increase in quantity of research): the three projects closed in the 1990s carry a mean score of -0.234, the 45 projects of the 2000s a mean of -0.054, the 152 projects of the 2010s a mean of -0.012, and the 37 projects of the 2020s a mean of -0.073. The single project from the 1980s posts a slightly positive score of +0.028. The limited number of observations in the earliest decades renders the pre-2000 figures highly sensitive to individual project characteristics. The 2010s and 2020s sub-samples are sufficiently large to suggest that the information environment became marginally more risk-oriented in the most recent period, plausibly reflecting the accumulation of climate science documenting escalating physical hazards. This does not mean that prior to this the sentiment was significantly more positive, as this reflects the data that we collected which we recognize is limited in sample size and source diversification (academic research only).

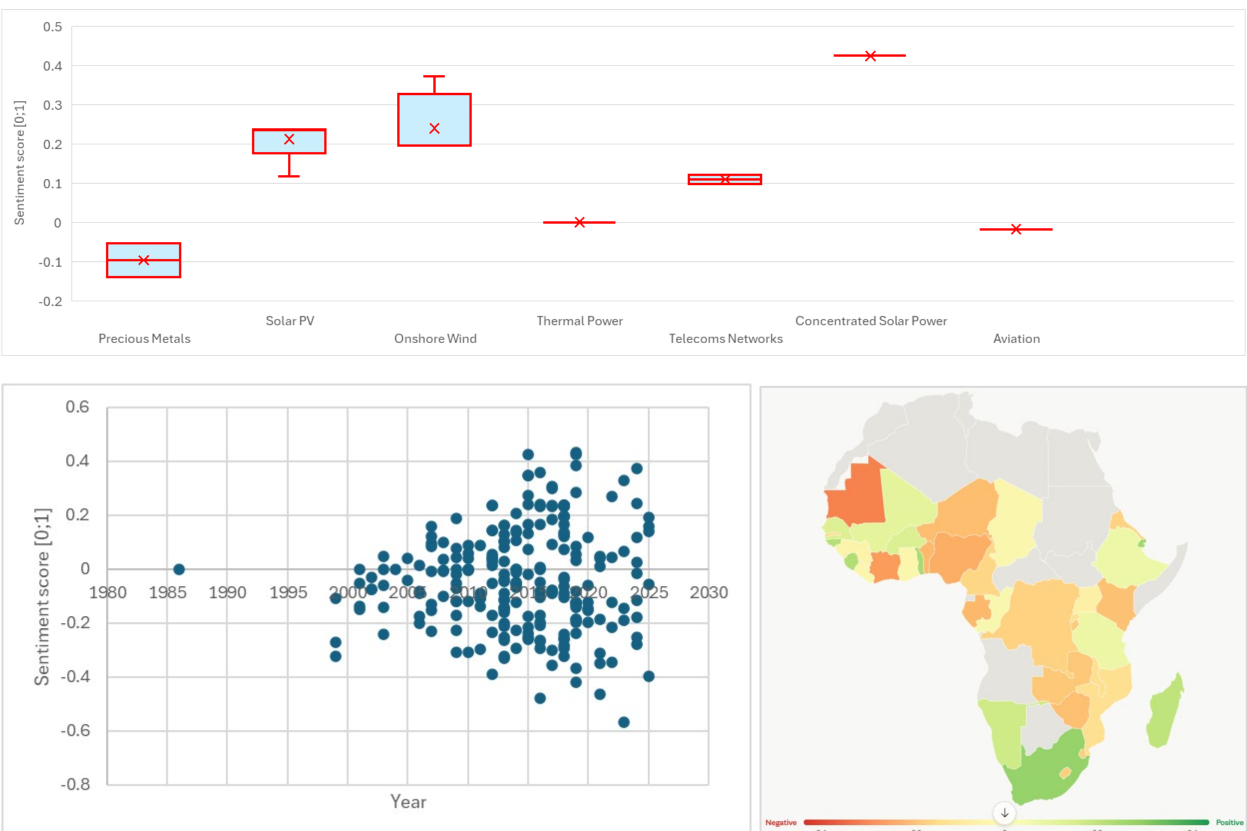

Figure 4-5 Sentiment score across sectors, time and country (average), result from NLP analysis

4.4 The Analytic Dataset

The final analytic dataset combines the project-level financial information described in Section 4.14.1.3, the climate-related risk variables of Section 4.2, the sentiment proxy of Section 4.3, and a vector of standard macroeconomic and project-level controls. Macroeconomic controls are merged at the country-year level and comprise GDP per capita (in natural logs, log_gdp), a country-risk composite, the Worldwide Governance Indicators rule-of-law score, and a currency-risk proxy capturing exchange-rate volatility around the time of the financial close. Table 11-3 distinguishes the 22 raw project-level variables collected from the data sources of Section 4.1 from the derived and transformed variables that enter the regression. Descriptive statistics for the regression sample of 230 projects are reported in Table 11-4 with the same panel structure.

A note on the role of the controls is in order before proceeding. Several variables on the right-hand side of the specification, in particular leverage, concessionality, lender composition, debt tenor, and the fixed-rate indicator, are themselves part of the loan contract and therefore part of the pricing mechanism rather than exogenous determinants of it. We retain them as conditioning variables because the section's empirical objective is to characterize the conditional descriptive association between climate exposure, sentiment, and the cost of debt, holding the loan's principal contractual features fixed. We do not interpret their coefficients as causal effects, nor do we interpret the climate or sentiment coefficients as estimates of the effect of those variables on the cost of debt that would obtain if the contractual structure were altered. The framework throughout is descriptive and conditional, not structural.Three features of the descriptive statistics condition the empirical work that follows. The cost of debt has a mean of 3.4% and a median of 1.1%, with a standard deviation of 3.7 percentage points and a maximum above 15%. The gap between the mean and median, combined with the right-skewness of the distribution, reflects the bimodal lender composition of the sample, with concessional projects clustering at low rates while commercial projects exhibit much wider price dispersion. Average leverage is 79%, consistent with the structural premise of Section 3 that SSA infrastructure is overwhelmingly debt-financed and that the cost of debt is the dominant marginal price of capital. Concessional projects represent 72% of the sample, an artifact of the disclosure asymmetry discussed in Section 4.1.1 and the principal motivation for the concessional/market sample-split strategy used alongside the full-sample baseline.

4.4.1 Empirical Strategy

The empirical analog of equation (3.4) is implemented in Python using *statsmodels*. The estimating equation is reproduced for clarity:

$$R_{d,i} = \alpha + \beta_1 \mathrm{CI}_i^{\mathrm{flood}} + \beta_2 \mathrm{CI}_i^{\mathrm{storm}} + \beta_3 \mathrm{CI}_i^{\mathrm{heat}} + \gamma S_i + \delta X_i + \varepsilon_i \tag{4.5}$$

Where

- $R_{d,i}$ is the all-in nominal interest rate at financial close (in percentage points),
- the three log-transformed CIs capture hazard-decomposed climate exposure,
- S_i is the behavioral sentiment proxy,

X_i is the vector of conditioning variables comprising the financial structure (leverage, log size, number of lenders, fixed-rate indicator, concessional indicator, tenor), the macroeconomic environment (country risk, log GDP per capita, rule of law, currency risk), the project type, the sector, the multi-country indicator, and the year of financial close.

Coefficients are estimated by Ordinary Least Squares. As discussed in Section 4.4, we interpret all coefficients throughout as conditional descriptive associations rather than as causal effects, consistent with the cross-sectional design and the absence of a credible source of exogenous variation in hazard exposure or sentiment.

4.5 Standard errors and clustering

Standard errors are clustered at the year of financial close. This choice reflects our prior that the dominant source of residual dependence in the cross-section is contemporaneous variation in global financial conditions and SSA-wide sentiment affecting projects closing in the same calendar year. Year-level clustering allows the residuals of two projects closing in the same year to be arbitrarily correlated while imposing independence across years. We considered two alternatives. Country-level clustering would absorb persistent country-specific factors but, given that several countries appear in only a small number of projects, would produce unreliable cluster-robust variance estimates. Two-way clustering by country and year was considered but rejected for similar reasons. For the smaller market sub-sample analyzed in isolation, where year clustering is less informative because of the relatively small number of years, we use heteroskedasticity-robust HC3 standard errors.

4.6 Multicollinearity diagnostics

Before estimation, we examined the variance inflation factors (VIF) of the right-hand-side variables to assess whether multicollinearity threatens the precision of individual coefficient estimates. The VIFs of the principal regressors are reported in Table 11-5.

All VIFs are below the conventional threshold of 5. The highest values, on is_concessional and fin_fixed_rate, reflect the substantive correlation between concessional financing and fixed-rate structures rather than a mechanical multicollinearity problem. The three climate-exposure variables have VIFs between 1.34 and 1.50, indicating that they capture genuinely distinct hazard channels and can be included jointly without inflating standard errors beyond a tolerable range.

4.7 Sample splits

The sample-selection structure documented in Section 4.1.3 motivates a sample-split strategy alongside the full-sample baseline. We partition the regression sample into a market sub-sample of 65 projects financed on non-concessional terms (predominantly the IJGlobal projects) and a concessional sub-sample of 165 projects financed by multilateral or development finance institutions (predominantly the AfDB-WBG projects) and re-estimate the baseline specification separately for each sub-sample. The market sample, by virtue of its smaller size, supports a parsimonious specification with a reduced macro-control vector; the concessional sample retains the full specification. The contrast between the two sets of estimates allows us to characterize within-segment patterns transparently rather than averaging across segments whose composition is itself the product of selective disclosure. The sample-split estimates are complementary to, rather than a substitute for, the interaction-based extensions described in Section 4.5.

4.8 Theoretically motivated interactions and exploratory extensions

The baseline specification of Equation (4.1) is the primary empirical object of the analysis, and the discussion in Section 5 is organized around it. We supplement the baseline with two distinct sets of interaction terms, which we keep conceptually separate to avoid the appearance of specification searching.

The first set is small and theoretically motivated. The framework of Section 3 generates three priors for which interactions are the natural empirical analog. The flood-exposure premium is expected to differ between concessional and non-concessional projects, reflecting the role of public lenders in absorbing physical risk; this motivates a flood × concessional interaction. The storm-exposure premium is expected to differ between private and public lenders, reflecting differences in risk-pricing behavior and in the willingness to underwrite tail-risk hazards; this motivates a storm × private-lender interaction. The sentiment premium is expected to load disproportionately on private commercial lenders, in line with the credit-rationing logic of Section 2.3; this motivates a sentiment × lender-type interaction. These three interactions, together with the baseline, constitute the set of confirmatory empirical tests directly tied to the section's theoretical priors.

The second set is broader and explicitly exploratory. Beyond the theoretically motivated interactions, we report a wider battery of approximately fifty interactions covering hazard-by-sector, hazard-by-lender-origin, hazard-by-project-characteristic, sentiment-by-sector, and concessional-by-sector combinations. We treat these as exploratory rather than as part of a pre-specified hypothesis structure. Given the sample size of N = 230 and the multiplicity of tests, we interpret isolated significant coefficients in this exploratory set with caution, particularly when they are not corroborated by the baseline specification, the sample splits, or the theoretically motivated interactions. The exploratory results are reported in full in the interest of methodological transparency, but the substantive interpretation in Section 5 leans on the baseline and the confirmatory interactions; exploratory findings are flagged as such where they are discussed.

4.9 Robustness specifications

We report three classes of robustness checks alongside the baseline. First, we estimate a no-macro specification in which the four macroeconomic controls are removed; this provides a sense of how much of the climate-exposure association is mediated by country-level conditions correlated with hazard exposure. Second, we estimate an aggregated-CI specification in which the three hazard variables are replaced by a single standardized composite. The contrast between this specification and the hazard-decomposed baseline is itself an empirical statement: an aggregated measure obscures the asymmetric pattern across hazards, which is one of the central findings of the analysis. Third, within the concessional sub-sample, we estimate a green-finance specification in which a clean-energy dummy and a climate-infrastructure indicator are added, to assess whether concessional finance prices these categories differentially.

All specifications are estimated on the same 230-project regression sample, except where the sample is explicitly partitioned into the market and concessional sub-samples. Coefficient estimates are reported as point estimates with cluster-robust standard errors and conventional significance stars (* for $p<0.10$, ** for $p<0.05$, *** for $p<0.01$). The full set of regression results, theoretically motivated and exploratory interactions, and robustness specifications is presented in Section 5.

5 Results and Interpretation

This section presents empirical estimates from the cost of debt regression developed in Section 3 and implemented in Section 4. The discussion is organized in seven subsections. Section 5.1 describes the construction of the Climate Risk Indicators and the rationale for the two alternative specifications used throughout the section. Section 5.2 reports the baseline specification on the full sample of 230 projects, alongside a parallel set of robustness specifications, and discusses the diagnostic properties of the OLS residuals. Section 5.3 turns to the segmentation analysis, presenting the within-concessional pricing pattern and the theoretically motivated interactions identified in Section 4.9 Section 5.4 covers additional exploratory analysis. Section 5.5 examines the robustness of the empirical pattern to an alternative construction of climate risk indicators. Section 5.6 synthesizes the empirical pattern that emerges across these specifications, and Section 5.7 sets out the boundaries of what the cross-section can and cannot establish. We retain throughout the descriptive framing of Section 4: estimated coefficients are reported as conditional associations rather than as causal effects, and we are explicit about the limits of generalization imposed by the sample selection structure.

5.1 A note on the climate risk indicator construction

The change in construction between CImag and CIpop is theoretically motivated rather than statistically motivated. Magnitude-weighted CIs measure hazard intensity in physical units. They are well suited to engineering applications in which the object of interest is the expected physical damage to a single asset of known specification. Lenders, however, do not price physical damage in isolation: they price the consequences of physical damage for project cash flows and, by extension, for the probability and loss-given default of the loan. Those consequences flow through channels that are population mediated rather than purely physical, including disruption to the customer base of revenue-generating infrastructure, displacement of the workforce on which operations and maintenance depend, breakdown of the supply chains that feed inputs to the project, and the political-economy response of the host country to a hazard that affects a large share of its citizens. The framework of (Hallegatte et al., 2019), makes this distinction explicit: asset damage and service-disruption losses are conceptually distinct, and the latter is the channel through which NPV impacts of downtime can exceed direct repair costs. A population-weighted exposure measure better proxies the service disruption channel than a magnitude only measure does.

We therefore present the CIpop estimates as the primary empirical results in Sections 5.1 through 5.3, and return in Section 5.4 to the comparison with the CImag construction as a robustness exercise. The headline finding of Section 5.4 is that three of the four central results the storm premium, the heat null, and the lender-segment-specific sentiment premium are stable across the two constructions, while the flood pattern reframes substantially between them in a way that we read as informative about the underlying channels through which flood exposure is priced.

5.2 Baseline specification and robustness on the full sample

Before turning to the regression estimates, the bimodal structure of the sample warrants a brief visual statement. Figure 5-1 plots the distribution of the all-in nominal interest rate at financial close separately for the 165 concessional and 65 non-concessional projects. The two segments are visibly distinct: concessional rates cluster between 0.5% and 2% with a median of 0.75% and a mean of 1.67%, while non-concessional rates span 2% to above 15% with a median of 8.45% and a mean of 7.93%. This bimodal structure is the empirical premise on which the segmentation analysis of Section 5.2 rests, and it is the main reason that pooled-sample coefficients on segment-specific variables are best read in conjunction with the within-segment estimates.

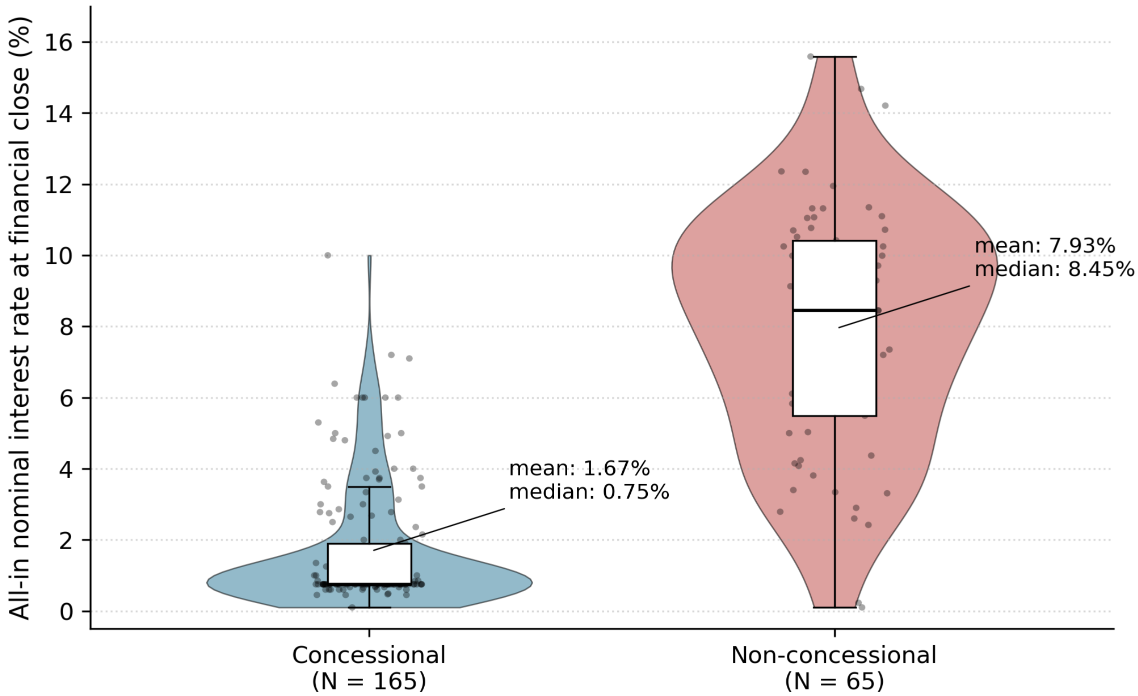

Figure 5-1: Cost of debt by lender segment (regression sample, N = 230)

Notes: Violin plot with overlaid box-and-whisker showing the within-segment distribution of the all-in nominal interest rate at financial close. Individual project observations are shown as jittered points. Concessional segment dominated by AfDB-WBG-financed projects; non-concessional segment dominated by IJGlobal commercial projects.

The baseline estimates of Equation (4.1) under the CIpop construction are reported in column (A) of Table 5-1. The specification fits the cross-section reasonably well, with an R^2 of 0.712 and 230 effective observations. Three results in the baseline are central to the discussion that follows. Storm exposure is associated with a positive and statistically significant cost-of-debt premium ($\beta = +1.042$, $p < 0.05$), so that, holding the other regressors fixed, a one-unit increase in log_cri_storm is associated with a 104-basis-point increase in the all-in nominal interest rate at financial close. Flood exposure has a negative point estimate that is not statistically significant in the pooled baseline ($\beta = -0.312$), and heat exposure has a small, insignificant coefficient ($\beta = +0.062$). The pooled sentiment proxy enters with a small positive point estimate that is not distinguishable from zero in the baseline ($\beta = +0.304$). The concessional indicator enters with a large negative coefficient ($\beta = -4.726$, $p < 0.01$), consistent with the price differential visible in Figure 5-1.

The pattern across columns (B) through (F) of Table 5-1 sharpens, rather than overturns, the baseline. Adding the flood × concessional interaction in column (B) is the single most informative new specification: the flood main effect, which now identifies the within-non-concessional flood pricing, falls to −2.401 with a p-value below 0.001, while the interaction term is +2.250 ($p < 0.01$). The implied within-concessional flood sensitivity is therefore approximately −2.401 + 2.250 ≈ −0.151, which is statistically and economically indistinguishable from zero. The pooled flood coefficient of -0.312 in column (A) is therefore best interpreted as a weighted average of a substantial negative value in a non-concessional pricing pattern and a near-zero value in a concessional pricing pattern. The association here is visualized in Figure 5-4. The storm coefficient is stable in sign and magnitude across columns (A) through (E), with point estimates between +1.022 and +1.266 and statistical significance preserved at the 5% level or better in every full-sample specification. The heat coefficient remains small and insignificant throughout. Figure 5-2 illustrates this stability across specifications.

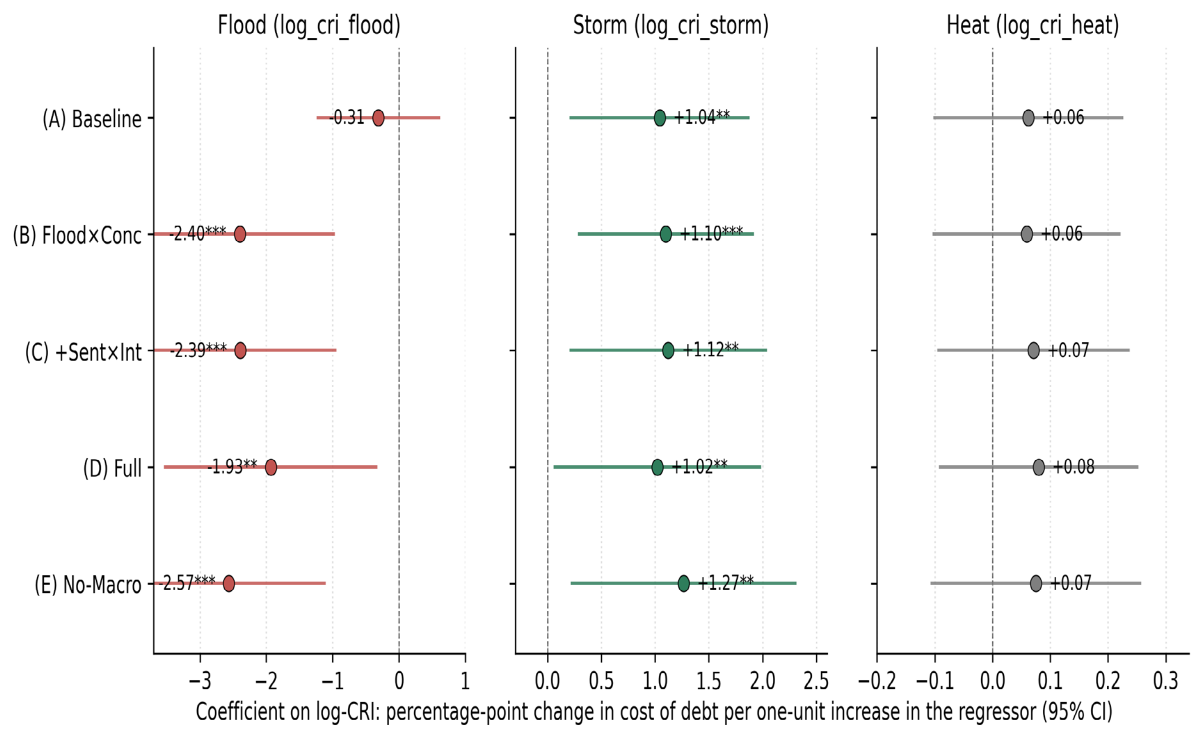

Figure 5-2: Coefficient stability across baseline and robustness specifications.

*Notes: Forest plot of the three CRI coefficients across the five full sample specifications of Table 5-1. Points are OLS estimates and horizontal bars are 95% confidence intervals using year-clustered standard errors. The flood panel reports the main-effect coefficient (within-non-concessional) for columns (B)-(E). Significance: * p<0.10, ** p<0.05, *** p<0.01.*

Two robustness specifications warrant comment. The no-macro specification in column (E) removes the four macroeconomic controls and produces estimates that are very close to those of column (B): the storm coefficient is +1.266 ($p < 0.05$), the flood main effect is -2.566 ($p < 0.001$), and the flood × concessional interaction is +2.411 ($p < 0.001$). We read this as evidence that neither the storm premium nor the flood-segmentation pattern is mediated through, or absorbed by, the country-level macro conditions correlated with hazard exposure. The aggregated specification in column (F) replaces the three hazard variables with a single standardized composite, *cri_total_z*. This composite enters with a coefficient of +0.013 that is not statistically significant at any conventional level ($p \approx 0.82$). The contrast between columns (A) through (E) and (F) is itself one of the central methodological findings of the section: an aggregated CRI measure does not reproduce the asymmetric hazard pattern that emerges when flood, storm, and heat are entered separately and the lender-segment dimension is allowed to interact with flood exposure.

Among the controls, currency-risk volatility (*macro_currency_risk*) enters with a positive and significant coefficient across columns (A) through (D) and (F), and *fin_leverage* enters with a positive coefficient that is significant at the 10% level or better across all specifications. The multi-country indicator enters with a positive and significant coefficient (+1.24, $p < 0.05$ in the baseline), consistent with cross-border infrastructure projects carrying an additional pricing premium beyond what is captured by the host-country macro variables.

Variable	(A) Baseline	(B) Flood×Conc	(C) +Sent×Int	(D) Full	(E) No-Macro	(F) Aggregated
log_cri_flood	−0.312	−2.401***	−2.391***	−1.934**	−2.566***	—
log_cri_storm	+1.042**	+1.100***	+1.123**	+1.022**	+1.266**	—
log_cri_heat	+0.062	+0.059	+0.071	+0.080	+0.075	—
cri_total_z	—	—	—	—	—	+0.013
beh_sw	+0.304	+0.131	+0.831	+0.118	+0.387	+0.570
is_concessional	−4.726***	−5.416***	−5.445***	−3.631***	−5.975***	−4.834***
log_cri_flood × is_conc.	—	+2.250***	+2.240***	+1.801**	+2.411***	—
beh_sw × lender_intl	—	—	−4.627*	−3.596	—	—
is_conc. × is_clean_energy	—	—	—	−2.860***	—	—
is_climate_infra	—	—	—	−0.469	—	—
macro_country_risk	−4.115	−3.662	−3.476	−2.960	—	−5.682
macro_currency_risk	+3.532**	+3.953**	+3.827**	+3.769**	—	+3.146**

Variable	(A) Baseline	(B) Flood×Conc	(C) +Sent×Int	(D) Full	(E) No-Macro	(F) Aggregated
log_gdp	+0.480*	+0.350	+0.266	+0.189	—	+0.592**
fin_leverage	+1.785*	+1.616*	+1.793*	+1.809**	+1.705*	+1.551
is_multicountry	+1.238**	+1.352**	+1.406**	+1.471***	+1.124**	+1.112*
R^2	0.712	0.727	0.732	0.742	0.717	0.707
N	230	230	230	230	230	230

Table 5-1: Baseline specification and robustness, full sample (N = 230)

*Notes: OLS estimates of equation (4.1) using the CIpop (population-weighted) CRI construction. The dependent variable is the all-in nominal interest rate at financial close in percentage points. Standard errors clustered at the year of financial close. Project-type, sector, and year coefficients estimated but suppressed for readability; full output in the Appendix. Stars: * p<0.10, ** p<0.05, *** p<0.01.*

5.2.1 Diagnostic assessment of the baseline

The diagnostic plots of the baseline residuals (Figure 5-3) display the features one would expect from a cross-sectional model fit to a bimodal lender market. The residuals-vs-fitted panel shows two visible clusters of fitted values, one centered near 1 and one near 10, reflecting the concessional and commercial segments of the sample. Within each cluster, the residuals are approximately mean-zero, with a moderate fan suggesting heteroskedasticity increases with the fitted value. The Q-Q plot shows light upper-tail and lower-tail departures from normality, attributable to a small number of high-coupon commercial projects and to the floor effect at very low concessional rates. The residual histogram is unimodal and approximately symmetric around zero, and the scale-location plot shows no systematic trend in residual variance once the bimodal structure is accounted for. We interpret these patterns as broadly consistent with the descriptive use of the OLS estimator. The clustering of standard errors at the year of the financial close addresses residual heteroskedasticity for inference.

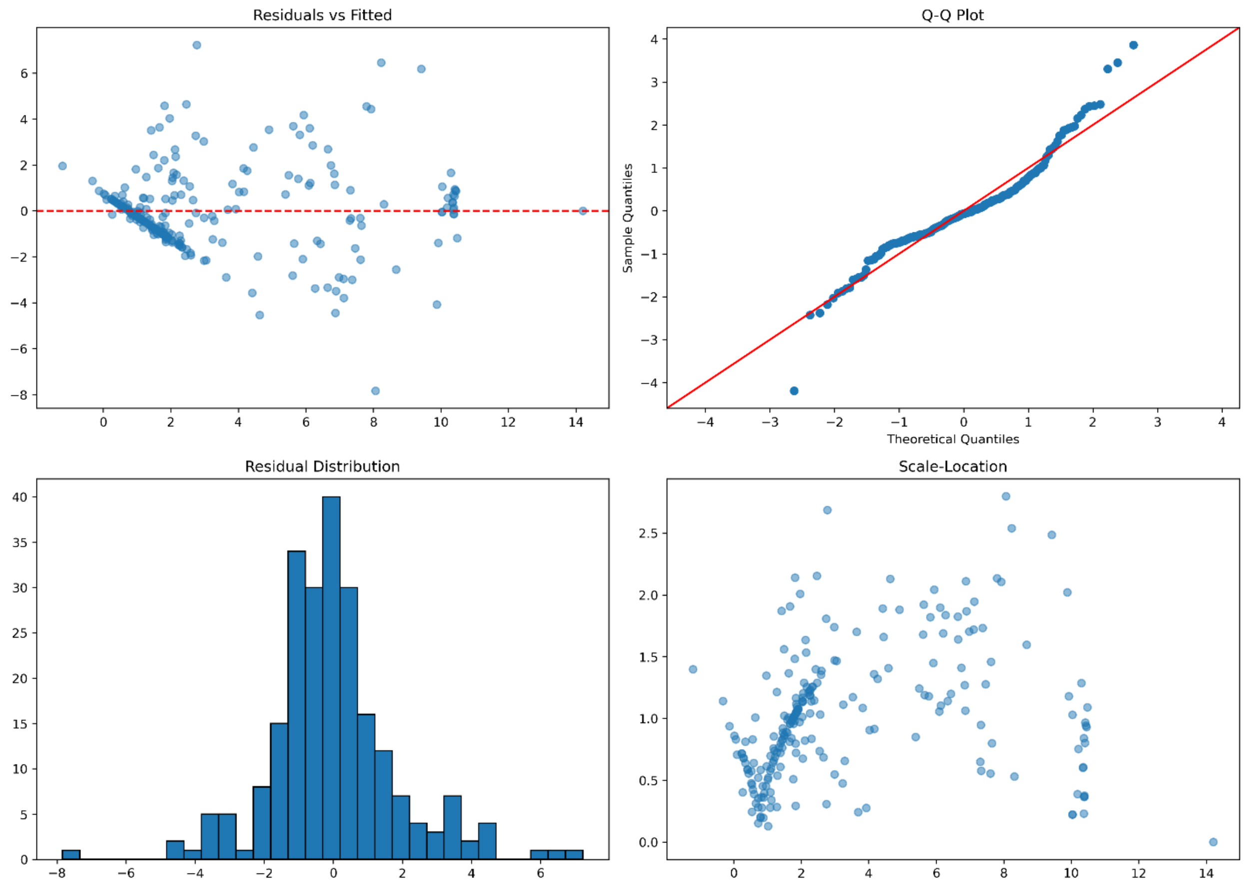

Figure 5-3: Diagnostic plots: residuals vs fitted, Q-Q, residual distribution, and scale-location for baseline column (A) under the CIpop construction

5.3 Segmentation: concessional sub-sample and theoretically motivated interactions

The full-sample baseline averages over two segments of the SSA infrastructure finance market that, as Section 4.1 documented, are structurally different in their pricing behavior and unequally represented in the data. We make the segment-level pattern visible through two complementary devices: a sample-split estimation on the 165-project concessional sub-sample, and a battery of interaction terms applied to the full-sample baseline. We do not report a corresponding sample-split estimate for the 65-project non-concessional sub-sample because the OLS specification on that sample under the CIpop is rank-deficient with respect to the full conditioning vector and yields non-interpretable inference. We identify the within-non-concessional pricing pattern through the interaction terms instead. This is a feature of the small commercial-segment sample size combined with the standardization of the CIpop, and is discussed further in Section 5.6.

5.3.1 Concessional sub-sample (C1)

Estimating the baseline specification on the 165-project concessional sub-sample (Table 5.2, top panel) yields a stark statement about the pricing of concessional infrastructure debt. Of the three climate-exposure variables, only storm enters significantly: the log_cri_storm coefficient is +1.069 ($p < 0.05$), close to the full-sample baseline of +1.042 and to the column (B) estimate of +1.100. The flood and heat coefficients are small and insignificant. The sentiment proxy is small and insignificant. The strongest non-climate associations are with project size (*log_size*, +0.355, $p < 0.001$) and leverage (*fin_leverage*, +1.146, $p < 0.10$), both consistent with multilateral pricing that scales modestly with project complexity. We read this as evidence that, within the concessional segment of our data, lenders price storm exposure into the modest dispersion of concessional rates while flood and heat exposure do not enter the pricing of the concessional component of the capital stack in any detectable way.

5.3.2 Theoretically motivated interactions

The framework of Section 3 generates three priors for which interactions are the natural empirical analog. The first concerns flood exposure and concessional financing. The framework predicts that flood exposure, if it is priced through fundamentals such as expected loss given default, should enter loan terms in the commercially priced segment of the market. Concessional finance is expected to absorb rather than price this risk. The estimates in column (B) of Table 5-1, which we reproduce in compact form in Table 5-2, support a more striking pattern than this prior anticipation. The within-non-concessional flood coefficient is *negative* and large ($\beta = -2.401$, $p < 0.001$), with the interaction reversing the sign within the concessional segment to approximately zero ($-2.401 + 2.250 = -0.151$). The non-concessional pattern is therefore not a flood pricing premium; it is a flood-pricing *discount*, and one of substantial magnitude: each unit of log_cri_flood is associated with approximately 240 basis points *lower* debt cost in the commercially priced segment. Figure 5-3 this segment-specific marginal-effect pattern.

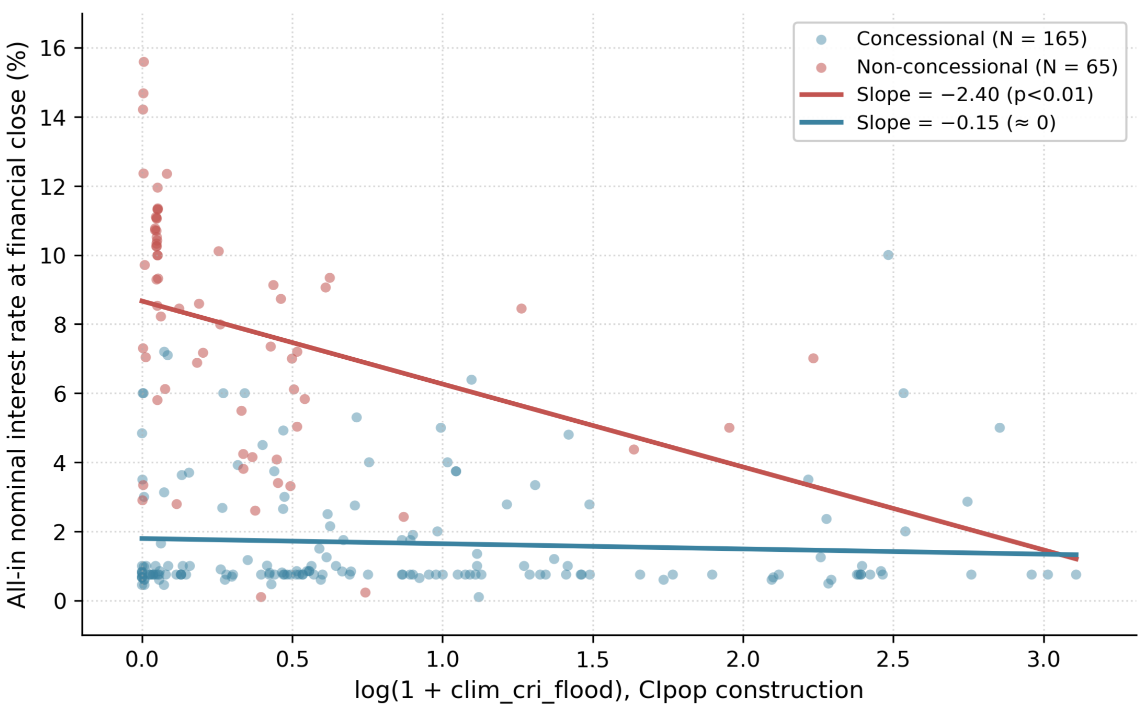

Figure 5-4: Marginal effect of flood exposure on the cost of debt by lender segment

WORKING PAPER #6

Notes: Predicted cost of debt as a function of log_cri_flood under the CIpop construction, plotted separately for the concessional and non-concessional segments. Slopes correspond to the column (B) estimates of Table 5-1 (within-non-concessional: -2.40, p < 0.01; within-concessional: -2.40 + 2.25 = -0.15, ≈ 0). Intercepts are calibrated to each segment's mean cost of debt at the segment-mean log_cri_flood. Underlying scatter shows the 230 individual project observations, colored by segment.

The most plausible reading of this finding is a selection effect, in line with the framing already articulated in the introduction of this thesis. Commercial syndicated lenders, faced with a pipeline of SSA infrastructure projects that are heterogeneous in their flood exposure, do not finance the most flood-exposed projects on standard terms. The projects they do finance in flood exposed locations are those for which sponsors have credibly mitigated the risk through engineering adaptation, insurance, contractual risk-sharing, or some combination of the three. Conditional on reaching financial close in the commercial segment, a higher value of log_cri_flood therefore signals not more residual lender-borne flood risk but less, because only the better-adapted projects in flood-exposed locations clear the commercial-financing threshold. The negative within-non-concessional coefficient is the cross-sectional shadow of this lender-side selection. Concessional lenders, whose mandates require them to finance infrastructure in high-vulnerability environments regardless of sponsor adaptation, do not exhibit this selection, and the within-concessional flood coefficient is correspondingly close to zero.

This reading is supported by the further interactions reported in Table 5-2. The flood × public-lender interaction is positive (+1.806, $p < 0.05$): public lenders, whose financing decisions are less constrained by commercial selection, exhibit a less negative, indeed, slightly positive, flood-pricing pattern than private lenders. The flood × multicountry interaction is positive (+1.521, $p < 0.05$) and the flood × large-project interaction is positive (+0.643, $p < 0.05$): in cross-border and large-scale projects, where adaptation is less of a binding selection criterion because the capital stack is larger and more heavily syndicated, the within-non-concessional flood discount narrows. The flood × refinancing interaction is negative (−2.293, $p < 0.10$), pointing in the opposite direction: refinancing transactions, which by construction involve assets with revealed operating performance, exhibit even steeper flood discounts. We interpret each of these as small but mutually consistent pieces of evidence that the central flood-pricing pattern is driven by a selection mechanism rather than by direct risk pricing.

The second prior concerns the storm premium and lender type. The framework predicts that the storm premium, if it is being priced by lenders responding to physical risk, should be larger among private commercial lenders than among public ones. The storm × private-lender interaction estimated on the full sample yields a coefficient of +29.70 ($p \approx 0.05$). This magnitude should not be interpreted literally as a 2,970-basis-point pricing increment, because log_cri_storm is concentrated near zero under the CIpop construction: the raw clim_cri_storm has a sample mean of 0.07, a median of essentially zero, and a maximum of 3.16, so that the log-transformed regressor has a mean of 0.05, a median near zero, a 95th percentile of 0.22, and a maximum of 1.42 (full distributional summary in Table 5.4). Applied at the sample mean of log_cri_storm, the +29.70 coefficient implies a within-private-lender storm pricing increment of approximately 140 basis points; applied at the 95th percentile the implied increment is on the order of 660 basis points, at the maximum observed value it is implausibly large. The headline coefficient is therefore best read as a slope estimate on a regressor whose support is narrow rather than as a structural pricing parameter, and the standard error is large in proportion to the point estimate. The *lender_private* indicator is sparsely represented in the sample and the coefficient is identified from a small private-lender sub-cell. We characterize this as qualitative confirmation that private commercial lenders price storm exposure more aggressively than the omitted lender categories, in a direction consistent with the storm × long-tenor and storm × large-project interactions reported in Table 5.2 (+2.145 and +1.451, both significant). We do not attribute precise structural meaning to the +29.70 magnitude.

The third prior concerns the climate behavioral sentiment premium and lender type. The full-sample sentiment coefficient is small and insignificant (β = +0.304 in the baseline), raising the possibility that any sentiment effect is heterogeneous across lender pools and is averaged out in the pooled specification. Interacting beh_sw with lender_private produces a coefficient of +11.42 ($p < 0.01$): private commercial lenders price our sentiment proxy into loans markedly more aggressively than the omitted lender categories, in a direction consistent with the credit-rationing logic of (Stiglitz & Weiss, 1981) and the residual SSA premium documented by (Gbohoui, 2023). The corresponding interactions with international and public lenders are negative (−4.69, $p < 0.10$ and −5.999, $p < 0.10$ respectively): in segments of the lender market dominated by mandate-driven institutions, the sentiment proxy enters with the opposite sign. As with the storm × private estimate, the +11.42 magnitude should not be read as a literal 1,142-basis-point increment: beh_sw has a sample mean of −0.03, a standard deviation of 0.20, and a range of [−0.57, +0.43] (Table 5.4), so the implied within-private-lender sentiment-pricing increment is on the order of tens to low hundreds of basis points across the observed range of the proxy rather than the four-digit number the headline coefficient suggests. The evidence is therefore best read as qualitative confirmation of differential sentiment pricing across lender types rather than as a precise structural estimate.

Test / specification	Term	Coefficient	Std. error	p-value
Concessional sub-sample (C1)	log_cri_flood	−0.048	0.167	0.772
Concessional sub-sample (C1)	log_cri_storm	+1.069**	0.496	0.031
Concessional sub-sample (C1)	log_cri_heat	+0.046	0.053	0.387
Concessional sub-sample (C1)	beh_sw	−0.881	1.110	0.428
Concessional sub-sample (C1)	log_size	+0.355***	0.086	0.000
Flood × Concessional	log_cri_flood (main effect)	−2.401***	0.723	0.001
Flood × Concessional	log_cri_flood : is_concessional	+2.250***	0.745	0.003
Storm × Private lender	log_cri_storm : lender_private	+29.70**	15.08	0.049

Test / specification	Term	Coefficient	Std. error	p-value
Sentiment × Private lender	beh_sw : lender_private	+11.42***	4.090	0.005
Sentiment × International	beh_sw : lender_intl	−4.690*	2.460	0.057
Sentiment × Public lender	beh_sw : lender_public	−5.999*	3.454	0.082
Concessional × Clean Energy	is_conc. : is_clean_energy	−3.639***	1.124	0.001
Concessional × Fossil	is_conc. : is_fossil	+3.759***	1.430	0.009
Climate Infra × Concessional	is_climate_infra : is_conc.	−0.796**	0.384	0.038
Flood × Public lender	log_cri_flood : lender_public	+1.806**	0.843	0.032
Storm × Long tenor	log_cri_storm : is_long_tenor	+2.145***	0.816	0.009
Flood × Long tenor	log_cri_flood : is_long_tenor	+0.741**	0.289	0.010
Flood × Large project	log_cri_flood : is_large	+0.643**	0.266	0.016
Flood × Multicountry	log_cri_flood : is_multicountry	+1.521**	0.635	0.017
Flood × Refinancing	log_cri_flood : is_refinancing	−2.293*	1.215	0.059

Table 5-2: Concessional sub-sample baseline and significant interaction terms

*Notes: The top panel reports baseline estimates for the 165-project concessional sub-sample. Subsequent rows report coefficients from separate regressions in which the indicated interaction term is added to the full-sample baseline. For the Flood × Concessional row, both the main effect and the interaction are reported jointly. Standard errors clustered at the year of financial close. Stars: * p<0.10, ** p<0.05, *** p<0.01.*

5.4 Additional exploratory tests

Beyond the three confirmatory interactions tied to the framework in Section 3, we estimate approximately 50 additional interaction tests covering hazard-by-sector, hazard-by-lender-origin, hazard-by-project-characteristic, sentiment-by-sector, and concessional-by-sector combinations. We treat these as exploratory and acknowledge that, with this many tests on N = 230, isolated significant coefficients should be interpreted with caution, particularly when they are not corroborated by the baseline, the concessional sub-sample, or the confirmatory interactions of Section 5.2. Within these limits, three exploratory results are sufficiently consistent with the broader pattern to be worth reporting.

First, the concessional × clean-energy interaction is large and negative (−3.639, $p < 0.01$) and reappears in column (D) of Table 5-1 with a similar magnitude and significance (−2.860, $p < 0.01$). Clean-energy projects financed on a concessional basis are priced approximately 290 to 360 basis points below other concessional projects, holding all other specifications constant. This is the empirical signature of the green-finance subsidy embedded in MDB lending and is one of the inputs to the policy discussion in Section 7. Second, the concessional × fossil-energy interaction is positive and significant (+3.759, $p < 0.01$): conditional on receiving concessional finance at all, fossil-energy projects appear to price approximately 380 basis points *above* other concessional projects, consistent with the gradual tightening of MDB fossil-fuel lending criteria over the sample period. Third, the climate-infrastructure × concessional interaction is negative and significant (−0.796, $p < 0.05$), pointing in the same direction as the clean-energy result: concessional finance prices climate-related infrastructure at a small but detectable discount.

The remaining significant exploratory results: flood × public, flood × long-tenor, flood × large-project, flood × multicountry, flood × refinancing, storm × long-tenor, storm × large-project were already discussed in Section 5.2 because they bear directly on the interpretation of the flood and storm pricing patterns and we draw the same conclusions there. We do not draw separate policy inferences from them in this section. The remaining interactions are not statistically significant at the 10% level and are not discussed individually.

5.5 Robustness across CI construction

The CIs entered in the regressions reported above are constructed using the CIpop measure described in Section 4.2. To assess the robustness of the empirical pattern to this choice of construction, we re-estimate the baseline specification in column (A) of Table 5-1 using the CImag CIs that were the subject of an earlier implementation of the empirical pipeline. Table 5-3 reports the headline coefficients from the two constructions side by side, on the same 230-project sample, with the same conditioning vector and the same year-clustered standard errors.

Coefficient	CImag (magnitude-weighted)	CIpop (population-weighted)	Stable / changed
log_cri_flood (baseline)	+0.036 (ns)	−0.312 (ns)	Sign flipped
log_cri_flood (main, with int.)	+0.126 (ns)	−2.401 ***	Magnitude and sign changed

Coefficient	CImag (magnitude-weighted)	CIpop (population-weighted)	Stable / changed
log_cri_flood × is_concessional	−0.114 (ns)	+2.250 ***	Sign flipped, now significant
log_cri_storm (baseline)	+0.289 ***	+1.042 **	Stable: positive, significant
log_cri_heat (baseline)	+0.021 (ns)	+0.062 (ns)	Stable: small, insignificant
beh_sw × lender_private	+9.975 **	+11.419 ***	Stable: positive, significant
is_concessional × is_clean_energy	−2.502 **	−3.639 ***	Stable: negative, significant
is_concessional (baseline)	-4.027 ***	-4.726 ***	Stable: large negative

Table 5-3: Baseline coefficients under the two CI constructions

*Notes: All coefficients are from full-sample OLS regressions on N = 230 with the identical conditioning vector and year-clustered standard errors. The CImag (magnitude-weighted) CIs are constructed as the cumulative product of hazard frequency, average event magnitude, and project tenor; the CIpop (population-weighted) CIs replace the magnitude term with the cumulative share of host-country population affected per year. Stars: * p<0.10, ** p<0.05, *** p<0.01.*

Three of the four central results survive the change in CI construction. The storm premium is positive and statistically significant in both versions, with a coefficient is +0.289 in the CImag baseline and +1.042 in the CIpop baseline. The point estimates are not directly comparable in magnitude because the two CIs are denominated in different units and live on different scales, but the qualitative finding, that storm exposure is associated with a positive cost-of-debt premium, is preserved across constructions and at conventional significance levels. The heat coefficient is small, insignificant, and stable across both constructions, supporting the heat-null reading developed in Section 5.5. The sentiment × private-lender interaction is positive and significant in both versions (+9.975 in CImag versus +11.42 in CIpop), supporting the lender-segment-specific reading of the residual SSA premium. The concessional × clean-energy interaction is large, negative, and significant in both versions.

The flood pattern, by contrast, reframes substantially between the two constructions. Under the CImag CIs, the flood coefficient is small and insignificant in the baseline (+0.036) and becomes positive but insignificant when interacted with the concessional indicator. Under the CIpop CRIs, the baseline coefficient is negative and insignificant (−0.312) but becomes large, negative, and highly significant once the flood × concessional interaction is included (−2.401, $p < 0.001$), with a positive concessional offset of comparable magnitude. Figure 5-5 visualizes the underlying difference between the two constructions at the project level and clarifies why the flood coefficient is sensitive to construction in a way that the storm and heat coefficients are not.

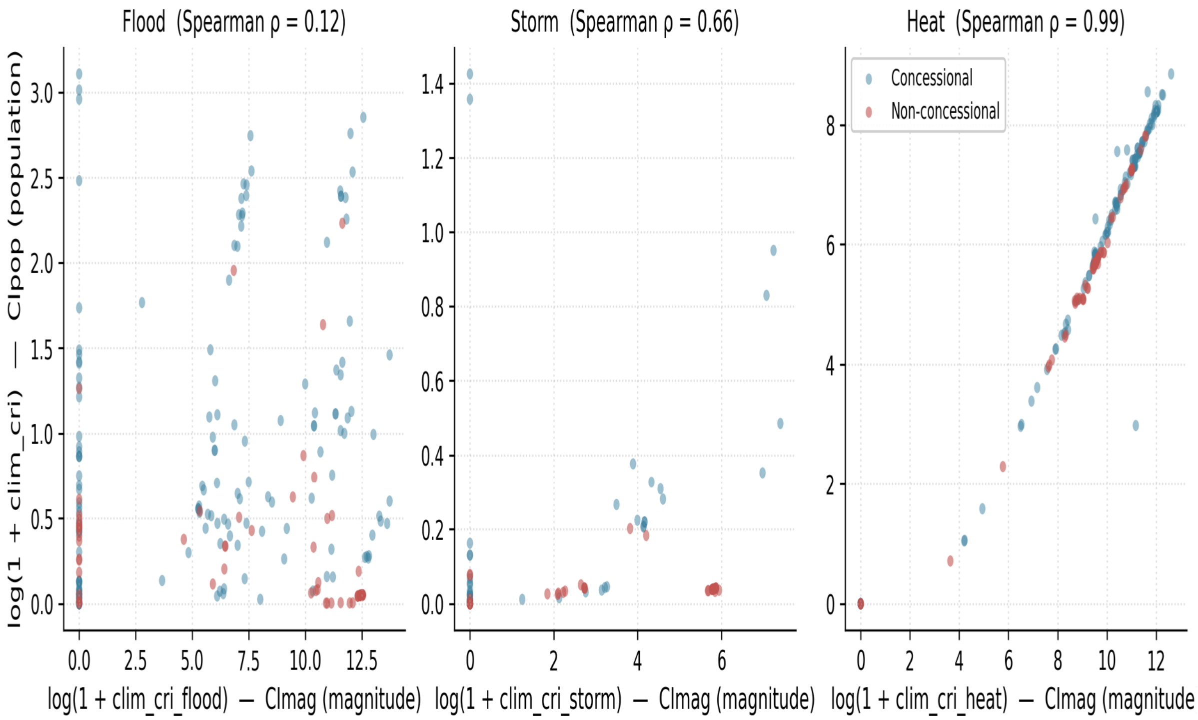

Figure 5-5: Project-level CIs under the two constructions

Notes: For each of the three hazards, the panel plots the log-transformed CIpop CI against the corresponding CImag CI, for the 230 projects in the regression sample. Spearman rank correlations indicate the extent to which the two constructions preserve the project-level ordering of exposure. Heat shows near-perfect rank agreement (ρ = 0.99, the heat CI is constructed identically across the two specifications, see Section 5.0); storm shows substantial but imperfect agreement (ρ = 0.66); flood shows essentially no rank agreement (ρ = 0.12). The flood pattern in the leftmost panel is therefore not a monotone re-scaling of CImag. The two constructions identify different projects as the flood-exposed ones, which is what generates the change in the flood coefficient between Table 5-3's two columns.

Two readings of this finding are mutually compatible. First, the CImag measure aggregates over events whose physical intensity may be high but whose population coverage is low, including remote upland flash floods and spatially concentrated cyclonic storm surges. Lenders pricing infrastructure debt do not respond uniformly to such events, because the cash-flow exposure of a project to a flood depends on whether the flood reaches the project's customer base, workforce, and supply chain, not only on the flood's hydrological magnitude. The CIpop measure aligns the CI with the cash-flow channel through which lenders actually price climate risk. Second, the selection mechanism developed in Section 5.3.2, by which commercial lenders finance only adapted projects in flood-exposed locations, operates at the level of perceived societal exposure rather than physical magnitude. A project in a high population share flood zone is more visible to commercial lenders as a flood-exposed project, which sharpens the selection mechanism and produces the negative within-non-concessional flood coefficient documented in Section 5.3.2 CImag measures, which do not distinguish high-population from low-population exposure, blur this signal. The Spearman ρ of 0.12 in the flood panel of Figure 5-5 quantifies how much project-level reranking the change in construction produces.

We therefore retain the CIpop CIs as the primary specification for the empirical analysis and for the policy discussion of Section 7, while documenting the CImag estimates in Appendix for transparency. The robustness pattern documented in Table 5-3, three central results stable across constructions, one result reframing in a way that is internally interpretable through the cash-flow channel and visualized in Figure 5-4, strengthens, rather than weakens, the empirical position taken in this section.

Variable	Mean	SD	Min	p25	Median	p75	p95	Max	% zero
log_cri_flood	0.701	0.781	0.000	0.057	0.464	1.038	2.411	3.108	3.0
log_cri_storm	0.046	0.165	0.000	0.000	0.000	0.025	0.222	1.425	34.8
log_cri_heat	5.043	2.836	0.000	4.011	5.792	7.255	8.222	8.854	19.6
beh_sw	−0.033	0.196	−0.566	−0.173	−0.051	0.113	0.279	0.431	1.3
clim_cri_flood (raw)	2.015	3.706	0.000	0.059	0.591	1.823	10.145	21.382	3.0
clim_cri_storm (raw)	0.068	0.318	0.000	0.000	0.000	0.025	0.249	3.158	34.8
clim_cri_heat (raw)	918.0	1226.4	0.0	54.3	326.5	1413.9	3722.9	6999.1	19.6

Table 5-4: Distributional summary of CIs and behavioral sentiment proxy

Notes: Distribution statistics for the regression sample (N = 230) under the CIpop construction. The four log-transformed regressors are the variables that actually enter equation (4.1); the three raw CIs are reported alongside for context. The % zero column reports the share of observations for which the raw CI (or, for beh_sw, the proxy) is exactly zero, reflecting projects in locations with no cumulative recorded exposure to the relevant hazard over the project's debt tenor.

5.6 Synthesis: a structured pattern of selective pricing

Taken together, the baseline, the concessional sub-sample, the confirmatory interactions, and the robustness exercise across CI constructions describe a structured, asymmetric, and segment-specific pattern of climate pricing in SSA infrastructure debt that is, by construction, invisible to specifications that rely on composite vulnerability scores or magnitude-only hazard measures. The pattern can be summarized in four points.

Storm exposure is associated with a measurable premium. The full-sample baseline coefficient of +1.042 ($p < 0.05$), the within-concessional estimate of +1.069 ($p < 0.05$), the storm × private-lender interaction (+29.70, $p \approx 0.05$), the storm × long-tenor interaction (+2.145, $p < 0.01$), and the stability of the storm premium across the two CI constructions all point to the same conclusion: in our sample, lenders charge a measurable premium on senior infrastructure debt for projects exposed to tropical-cyclone storm hazard, and the premium is identifiable across both lender segments and across alternative exposure constructions. This is the most robust empirical finding of the section.

We cannot say whether or not heat exposure is priced. Although the heat coefficient is consistently small across all six full-sample specifications, the concessional sub-sample, and both CI constructions, it is not statistically significant in any specification. As a result, we cannot draw any meaningful conclusion about the relationship between heat exposure and senior loan pricing from these estimates.

Flood exposure is priced through a selection mechanism rather than through a direct risk premium. The within-non-concessional flood coefficient under the CIpop CIs is large and negative (−2.401, $p < 0.001$), and the within-concessional flood coefficient is approximately zero. The most coherent reading of this pattern, visualized in Figure 5-3, is that commercial lenders do not finance the most flood-exposed projects on standard terms, and the flood-exposed projects that do reach financial close in the commercial segment are those for which sponsors have credibly mitigated the risk. The cross-sectional shadow of this selection is a flood-pricing *discount* rather than a flood-pricing premium. Concessional lenders, whose mandates do not impose this selection, exhibit no flood-pricing pattern in either direction. The pattern is sensitive to the construction of the flood CI, magnitude-only measures do not pick it up, but is robust across the macro-control vector and across the interaction battery once the CIpop CIs are used.

The climate behavioral premium loads on private lenders rather than on the sample as a whole. The pooled sentiment coefficient is small and insignificant in both CI constructions; the sentiment × private-lender interaction is large and significant in both (+9.975 under CImag, +11.42 under CIpop). The corresponding interactions with international and public lenders are negative. The empirical content of the residual SSA premium, as it shows up in our project-level data, is therefore not a uniform *Africa discount* but a lender-segment-specific perception premium concentrated where lender mandates make it most natural for it to live. Concessional finance, alongside its clean-energy subsidy and its apparent flood-neutrality, also appears to attenuate the sentiment channel by virtue of who its lenders are.

These four points together motivate the framing developed in Section 6: the climate premium in SSA infrastructure debt is not a single number to be discovered, but a structured pattern of selective pricing, in which different hazards, lender pools, and contractual structures interact with project-level exposure to produce the cost-of-debt distribution observed at financial close. The storm premium, the heat null, the flood selection mechanism, and the lender-segment-specific sentiment premium each imply a specific reform, and together they outline what an SSA-aligned development finance architecture would look like.

5.7 Limits of the empirical evidence

Six limits of the empirical evidence presented in this section should be made explicit before the policy discussion of Section 7 builds on it.

First, the cross-section comprises 230 projects observed once each at financial close. The design has no time-series dimension, no within-project variation, and no source of exogenous variation in hazard exposure or sentiment. Coefficients should be read as conditional descriptive associations and not as causal estimates of how the cost of debt would respond to a counterfactual change in hazard exposure, sentiment, or contractual structure.

Second, the sample is biased due to the sources from which we collected the data, as described in Section 4. The PAD pipeline over-represents concessional MDB-financed projects. IJGlobal over-represents commercially financed projects with disclosed pricing. The merged sample is best understood as a sample of SSA infrastructure projects for which debt-pricing information is observable, and the segmentation analysis is used to make the divergent pricing behavior of the two segments visible rather than to generalize from one segment to the other. The external validity of the estimates is bounded by what the SSA project-finance disclosure environment makes observable.

Third, a sample-split estimation on the 65 project non-concessional sub-sample under the CIpop CIs is rank-deficient with respect to the full conditioning vector and produces non-interpretable inference. We identify the within-non-concessional pricing pattern through interaction terms estimated on the pooled sample instead, which is the standard approach when a sub-sample does not support full-vector OLS. We acknowledge that interaction-based identification requires the assumption that the slopes on the conditioning variables that are not interacted are common across the two segments, an assumption we cannot test directly with the present sample. The robustness of the storm premium across the pooled, the concessional, and the interaction-based specifications offers some reassurance.

Fourth, the climate-exposure variables rely on publicly available hazard layers evaluated at the project's geographic coordinates and combined with hazard-specific exposure functions. The CIs are designed to be project-specific in ways that composite vulnerability scores are not, but they remain ex-ante proxies for hazard and exposure rather than realized loss histories. The choice between CImag and CIpop constructions is a substantive measurement choice, and Section 5.4 has transparently documented its empirical implications. The robustness of the storm premium, the heat null, and the sentiment × private-lender pattern across the two constructions offers reassurance that those findings are not artefacts of a single construction. The flood pattern is sensitive to the construction, and the framework in Section 5.3.2 has set out our reading of why.

Fifth, the sentiment proxy is constructed from a 36-month rolling NLP-scored corpus and is, by construction, a noisy measure of an unobservable. The pooled sentiment coefficient is small and insignificant in both CI constructions, and only when the proxy is interacted with private-lender presence does a clear signal emerge. We are therefore careful in Section 5.5 to characterize the sentiment finding as evidence of differential pricing across lender pools rather than as a uniform behavioral premium documented at the sample level.

Finally, in the regression, the independent variables include several contractual loan characteristics, including leverage, concessionality, lender composition, tenor, and the fixed-rate indicator. These variables are part of the loan agreement itself rather than strictly exogenous determinants. We retain them in the specification because the empirical objective is to characterize the descriptive association between climate exposure, climate sentiment, and the cost of debt, while holding the loan's principal contractual features fixed. We do not interpret the climate or sentiment coefficients as estimates of the effects that would obtain if the contractual structure were altered, and the policy discussion of Section 7 is careful to make that distinction.

These limits notwithstanding, the empirical pattern documented in this section is internally consistent across the baseline, the concessional sub-sample, the confirmatory interactions, and the robustness exercise, regardless of CI construction. The storm premium, the heat null, the selection-driven flood pattern, and the lender-segment-specific sentiment premium together provide a more structured account of climate pricing in SSA infrastructure debt than aggregate vulnerability indices have so far produced. Sections 6 and 7 build on these findings to develop the adaptation-pricing framework and the blended-finance proposals that constitute this thesis's policy contribution.

6 The Resilience–debt trade-off: could resilience lower the cost of debt?

After computing the regression and finding evidence that supports debt pricing fluctuates in tandem with the wind and flood indicators, we follow up with a natural question that comes to mind: can investing to reduce a project's exposure to climate-related disasters pay for itself through the reduction of debt interest payments? Or to phrase it in a more digestible manner: can adaptation pay for itself through debt? The simple idea explored in this section's case study is that, because a component of interest repayments is proportional to a climate indicator, CI_i, resilience measures that reduce the vulnerability of a physical asset can be considered to reduce the cost of debt. However, this comes at a cost, meaning the SPV would have to take on more debt to integrate this new investment. We propose a framework for conducting this cost-benefit analysis, testing it across 31 SSA energy projects to animate a discussion about the potential of resilience engineering to reduce total debt-funding costs.

In this section, we use a novel, conceptual optimization function inspired by the works of (Assab, 2024), specifically the exposure factor introduced in his study of the impact of floods on the cost of debt for a light railway transportation project in Costa Rica. While Assab (2024) examined the subject through the lens of the probability that a given infrastructure project will default, we use a cost-benefit DCF analysis aimed at minimizing the total funding cost from the SPV's perspective. After introducing our exposure factor, we expand the complete optimization function and propose a range of case studies.

In the previous sections, we presented evidence of a climate-related disaster risk premium, with this premium varying by a quantity β in relation to the climate indexes we defined, CIpop and CImag, in Section 4.2. We can therefore posit the following relation between the cost of debt and the climate index:

$$R = R_g + \sum_i I_{clim,i} * \beta_i \tag{6.1}$$

Where Rg represents the cost of debt excluding the climate-related disaster risk premium. Additionally, the beta can vary by sector, as the regression tested for sector premiums:

$$R = [\dots] + \beta_i * CI_i + \beta_{i\,x\,sector} * is_{sector} * CI_i \tag{6.2}$$

According to the IPCC (2022), risk is defined as the intersection of hazard exposure and vulnerability. Just as the climate indices in the regression expressed the severity of climate-related disasters (in two different manners) and consider exposure constant (assets 100% exposed). We introduce a variable to Equation (6.2), exposure, E(Ia), a function of investment into adaptation/resilience measures, that would vary between a minimum level of exposure that is to be defined in relation to the asset and adaptation measure and Equation (6.2) becomes:

$$R_a = R_g + \sum_i I_{clim,i} * \beta_i * E_i \tag{6.3}$$

6.1 The Exposure Factor

To accomplish this analysis, we formulate the relation between adaptation measures and exposure to climate risks. We start by putting in place some physical barriers to the exposure. We know that with no adaptation, the physical asset is fully exposed to the risks, so E(0) = 1. Investing in adaptation would reduce the exposure to climate-related disasters (the exposure factor), however there would theoretically always be a lower limit, we call the "level of protection" that any adaptation solution can get to. Let δ be the level of protection, with δ ∊ [0;1]. This can be understood as for example a flood barrier being of a certain height that it would protect an asset from a 1/100-year flood but a 1/500-year flood would go over, it is the probability of an event being higher than the designed limit of the adaptation measure. As Ia goes to +∞ then $E(I_a)$ should go towards 1- δ. Now we have the bounds of our function, to define the shape we inspire ourselves from (Assab, 2024) who uses a logic function that follows an 'S' curve, which presents the characteristics we are looking for, much like a dose-response function used in toxicology but also by (Hughes et al., 2010) as a central component for the assessment of infrastructure adaptation costs. To finish our formulation, we need to define a shape factor and a scaling factor. The shape factor determines how quickly we reach the maximum protection level (minimum exposure) by investing in adaptation. We use the effectiveness of the adaptation measures for the shape factor; we call this value 'η'. To determine the scaling of the adaptation measure, we define a quantity of investment, 'INV_a,s', that represents the cost at which point the measure becomes significant, or in other terms the point at which the marginal benefit of investment in adaptation is the highest (highest slope, absolute value). We fit a logical function to these characteristics:

$$E_{i,asset}(INV_a) = 1 - \delta * \frac{{INV_{a,i}}^{\exp(\eta)}}{{INV_{a,s,i}}^{\exp(\eta)} + {INV_{a,i}}^{\exp(\eta)}} \qquad (6.4)$$

INV_a,s is defined in relation to the adaptation measure and the asset (scale of the asset). We also express this quantity as a percentage of initial investment, INV_g, in which case we will write:

$$E_i(inv_a) = 1 - \delta * \frac{{inv_{a,i}}^{\exp(\eta)}}{{inv_{a,s,i}}^{\exp(\eta)} + {inv_{a,i}}^{\exp(\eta)}} \qquad (6.5)$$

To illustrate how the variables affect the level of adaptation, here are some examples of the function: (the numbers are chosen for illustrative purposes only)

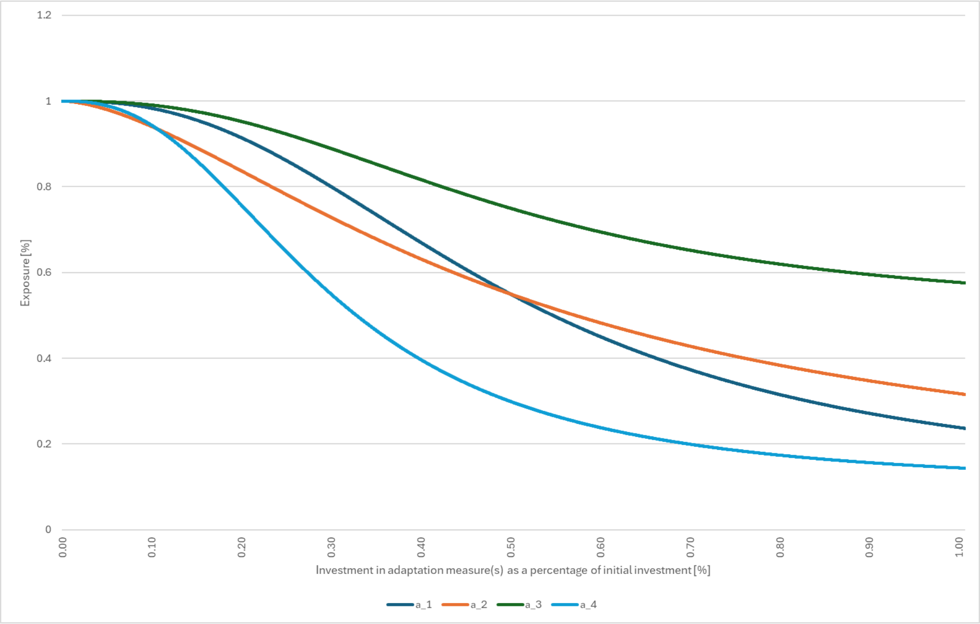

Considering:

	a_1	a_2	a_3	a_4
δ:	0.9	0.9	0.5	0.9
η:	0.9	0.5	0.9	0.9
Inv_a,s,i:	50%	50%	50%	30%

From these graphical examples we can illustrate the following variations:

Effectiveness η (from a_1 [0.9] to a_2 [0.5]) changes how fast the exposure factor decays, increase in η increases the speed. Scaling factor I_a,s determines the point at which the curvature goes from concave to convex (second derivative goes from negative to positive), a point at which the marginal utility is the highest. The level of protection changes the vertical asymptote as investment tends to infinity, since it represents the maximum level of protection (lowest exposure).

6.2 Optimization function

Using the formulas for the CoD and the function $E(I_a)$, we create an optimization function of the total debt funding cost, TFC. The formula we use for the TFC is as follows:

$$TFC = \sum_{t=1}^{T} \frac{P_t + int_t}{(1+r)^t} \tag{6.6}$$

With: P the principal repayments, Int interest repayments, r the discount rate (cost of capital or WACC from the SPV's point of view) and T the duration of the loan (years) while t corresponds to the period (year index). We start at year 1, not 0, since we are interested in comparing the NPV of the total cost of the debt for the project SPV (ultimately, how much they value the amount they have to repay). For now, this is a classic DCF analysis. Before incorporating the investment in adaptation, Ia, we first consider in this study that the additional investment in adaptation measures to be funded through debt, meaning the initial drawdown will include I_a, increasing the principal repayments while the CoD function reduces interest rate:

$$INV = INV_g + INV_a \tag{6.7}$$

With INV_g the initial (gross) investment (debt drawdown related to total project cost and the leverage). The exposure factor is integrated into the CoD equation (6.1). The interest is:

$$int_t = R * \left(INV - \sum_{t_1 \to t-1} P_t \right) \tag{6.8}$$

We expand equation (6.8) to express TFC as a function of inv_a to create our final optimization function TFC(inv_a), combining all the math presented in this section: (in blue the principal repayment and in green the interest repayment)

$$TFC(INV_{a,i}) =$$

$$\sum_{t=1}^{T} \left[\frac{\boldsymbol{P_t} + \left(\boldsymbol{INV_g} + \sum_i [\boldsymbol{I_{a,i}}] - \sum_{t_1 \to t-1} [\boldsymbol{P_t}]\right) * \left(\boldsymbol{R_g} + \sum_i \left[\boldsymbol{log}(1 + \boldsymbol{CI_{clim,i}}) * \boldsymbol{\beta_i} * \left(\mathbf{1} - \delta * \frac{\boldsymbol{INV_{a,i}}^{\exp(\eta)}}{\boldsymbol{INV_{a,s,i}}^{\exp(\eta)} + \boldsymbol{INV_{a,i}}^{\exp(\eta)}}\right)\right]\right)}{(1 + WACC)^t} \right] \tag{6.9}$$

The function is bounded at inv_a=0, when the TFC is equal to the no-adaptation base case scenario, and when inv_a grows, TFC tends to infinity. It is, as it is shown in Figure 6-1, what happens between those two points that most interests us. When resilience presents a payoff of which the NPV reimburses the initial investment in resilience, the curve will dip (Figure 6-1, red curve) whereas in other cases, when the benefit is marginal, the curve will rise in a relatively straight line (Figure 6-1, blue curve).

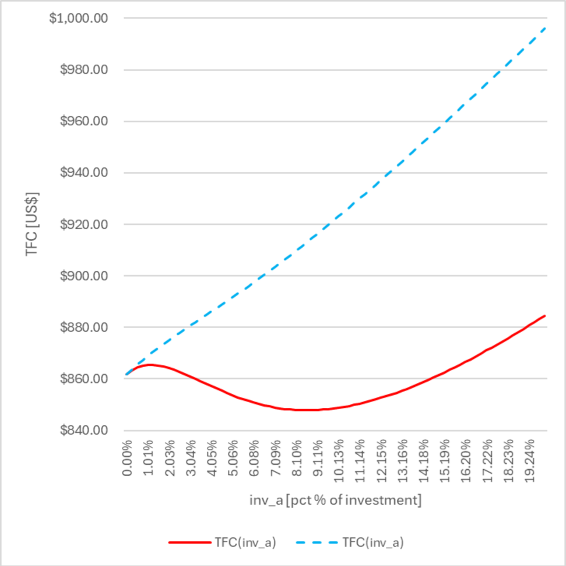

Figure 6-1 TFC function examples: illustration of adaptation-sensitive and non-sensitive projects

WORKING PAPER #6

6.3 Case study setup

We have seen in the results of the regressions that there is evidence of a storm premium with both climate risk indicators. We confront the opportunity of reducing the TFC with adaptation against wind for a set of projects from our sample (39 case studies on 29 projects in two samples), integrating for each project a credible adaptation measure against wind using the EDHEC Climate Institute (ECI) ClimaTech database on adaptation (and mitigation though not relevant to our study) solutions for infrastructure (Verschuur et al., 2024).

The inputs needed to complete the optimization function are:

- Adaptation measure variables for level of protection, δ, and effectiveness, η
- The scaling factor for investment in adaptation, INV_a,s or inv_a,s
- Discount rate, WACC

The adaptation measure variables δ and η are collected from the ECI ClimaTech database, we select the solution that presents the most promising characteristics. The figures presented are based on the best available research (academic publications, technical reports, industry guidance documents, engineering manuals and case studies) at the time of the creation of the database and reflect current understanding. In the ECI ClimaTech database the level of protection, δ, is presented in a manner that reflects the return period that the measure protects from as follows:

- Very High: > 1:1000 year event
- High: 1:100 < x ≤ 1:1000 year event
- Medium: 1:50 < x ≤ 1:100 year event
- Low: ≤ 1:50 year event

The level of protection represents in our function the maximum protection level gained through the adaptation measure, which we define as the percentage of events that the measure protects from. This means that, if the level of protection corresponds to a return period of 1:100, then it is also protected against a 1:50 year event or a 1:20 year event, and so on, but not against a 1:200 year event or a 1:1000 year event for which it would be completely ineffective. The best illustration of this would be a flood barrier; when designed for a certain return period (say 1:100 year) then it is designed for a certain depth above which (so, for a rarer flood return period say 1:200 year) then the water would run right over the flood barrier. So, we consider that δ is, for wind, equal to:

$$\delta = 1 - return\_period$$

The return period used will be the median for measures classed as having "High" and "Medium" levels of protection, for "Low" and "Very High," we use the given thresholds. Note that, while in designing for a 100-year flood, the engineer looks at the characteristics of the 100-year flood on the basis of evidence of storms up to the current date when using this methodology in a prospective analysis, the level of protection should be stochastic as a rarer flood today may be more frequent tomorrow due to climate change (Hughes et al., 2010).

Concerning effectiveness, the ECI ClimaTech database defines it as:

- Very High ≥95%

- High 65-94%
- Medium 35-64%
- Low 5-34%
- Very Low <5%

We use these values directly as η, applying the same rule of median for “High”, “Medium” and “Low” and threshold for “Very High” and “Very Low”.

The next component to be defined is the scaling level of investment in adaptation, which presents a more complex task as the reality is that it is specific to the selected adaptation measure and the type of asset. First, we define some clear guidelines of what we require from the scaling factor in order to choose the best source of information. It must:

- be adapted to lower-middle income, low income, and upper-middle income countries (Metreau et al., 2024)
- be adapted to the specificities of each type of infrastructure,
- be representative of the amount of investment in adaptation, as a percentage of the investment, that presents the highest marginal benefit of inv_a,I,
- be specific to adaptation to wind.

We collect the most appropriate database (to the best of our knowledge) from (World Bank Group & Miyamoto International, 2019), who provide an overview of engineering options for increasing infrastructure resilience, a report that provides detailed information on what infrastructure is exposed to damage from wind, while also providing the investment needed to reduce this exposure as a percentage of the cost of the project. We use this for our inv_a,s metric. In this paper, an estimated implementation cost, as a percentage of total cost, is presented for adapting to wind, floods, liquefaction, and earthquakes across 21 types of infrastructure, and, in relation to this measure, a damage index is presented before and after implementation. The estimated cost of improvement presented in this report is considered to be the cost of the complete (full) implementation of the resilience measure. We therefore consider the scaling factor to be half of the estimated cost of improvement reported in the report (aligning with the structure of the logic function).

To compute the WACC (discount rate) we refer to the following simplified formula:

$$WACC = Leverage * Cost_{of_{debt}} + (1 - Leverage) * Cost_{of_{equity}} \tag{6.10}$$

The leverage is the percentage of financing from debt. We collect the cost of equity from (Dato et al., 2025). We consider in this case study that the projects are financed through debt and equity, no grants. The cost of debt used in this calculation corresponds to R, meaning that this part of the WACC is endogenous to the model and therefore decreases with investment in adaptation. This feature means that investment in adaptation lowers the discount rate, making future repayments to debtors have more weight in the overall NPV relative to the initial discounting, which has a negative effect on the TFC. This feature is justified in the point of view that we take in this analysis (of the SPV), since easing the access to debt ultimately eases access to capital, reducing WACC.

We define two samples (one for each wind climate indicator type) that can be defined by the following guidelines:

- All projects are from the energy sector, which were shown to present an increased sensitivity to wind in the regression results (wind x energy premium),
- Infrastructure is deemed vulnerable to wind (World Bank Group & Miyamoto International, 2019),
- Financial close is post-2015 and up to 2024,
- The projects are situated in a country for which the wind climate indicator, CI_wind, is not null on the year of the financial close.

These constraints are mainly due to data scarcity. The total sample comprises 19 projects. The samples are described below in the Appendix, showing geographical and sector coverage. We note that both samples present many solar farm projects (photovoltaic), over 68% for sample 1 and over 50% for sample 2. Additionally, projects are concentrated in South Africa (18 out of 19) and in solar energy.

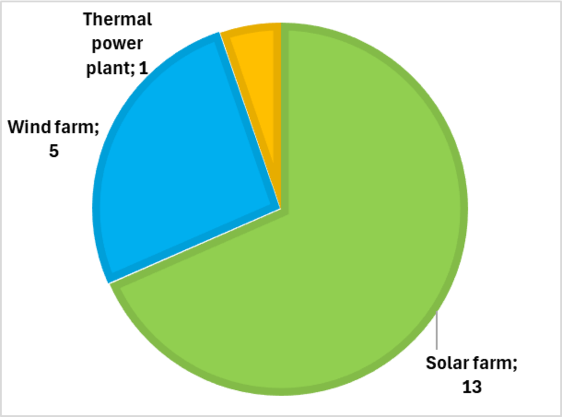

Figure 6-2: Adaptation case studies sector breakdown

Figure 6-3: Adaptation case studies country breakdown (South Africa & Mozambique)

The full data table used in this study, including the selected projects, is included in the Appendix of this report.

6.4 Case study results

Across the 19x2 case studies, only one presents an optimal TFC with investment in adaptation (inv_a > 0%). This project (project ID 23, Thermal Power plant in Mozambique, concessional loan, 2020) finds an optimal TFC only when using magnitude as the storm risk indicator, with 8.62% of investment in resilience (windbreaks), 1.12% above the scaling level of investment (7.5%). The characteristics of this project are listed below:

Table 6-1 Project 23: Thermal Power plant, Mozambique 2020, concessional loan; CI_mag optimization results and project characteristics

Gross cost of debt (excl. climate):	2.93%
Cost of equity:	19.78%
Leverage:	57%
Gross investment (excl. adaptation):	1,306 mUSD
Loan tenure:	25
Storm β:	0.667%
Storm climate indicator, log(1+CI):	4.61
Scaling resilience investment as percentage of investment:	7.5%
Selected resilience strategy (name):	Storm breaks – structural
Effectiveness of resilience strategy:	Medium
Level of protection of resilience strategy:	High
Optimized level of investment in resilience strategy:	8.62%
Exposure factor:	45%
Resulting cost of debt:	4.30%
Resulting discount rate:	10.96%
Total funding cost:	847.82 mUSD
Exposure factor and total funding cost shown as a function of the investment in resilience measure:	

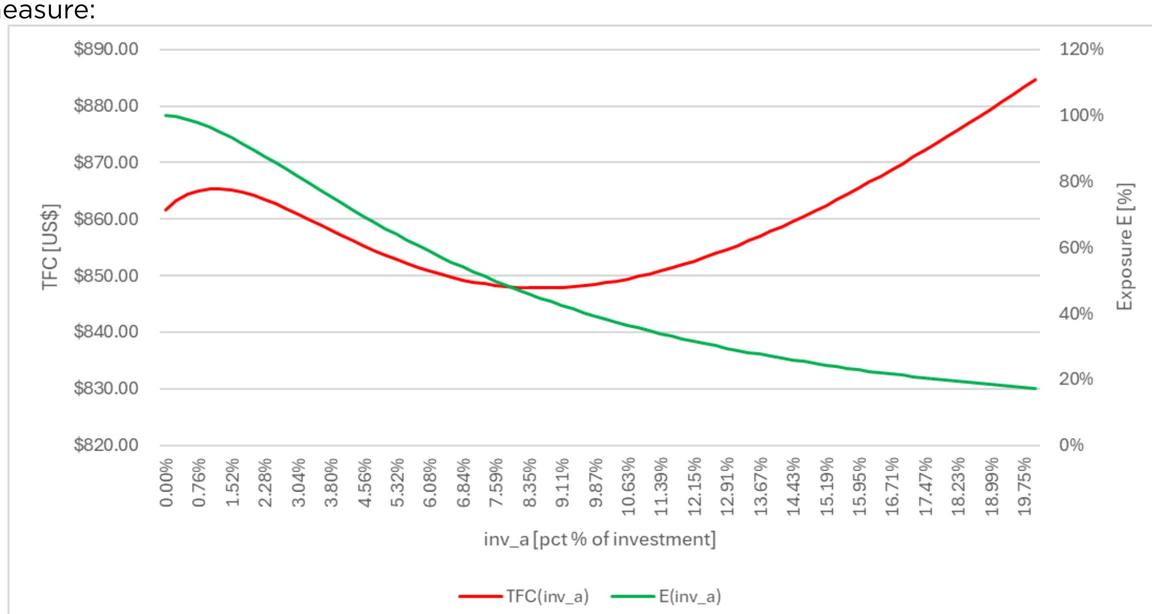

Across the 19x2 case studies, only one presents an optimal TFC with investment in adaptation (inv_a > 0%). This project (project ID 23, Thermal Power plant in Mozambique, concessional

loan, 2020) finds an optimal TFC only when using magnitude as the storm risk indicator, with 8.62% of investment in resilience (windbreaks), 1.12% above the scaling level of investment (7.5%). The characteristics of this project are listed below:

Table 6-1 shows several figures that, when compared to the other projects, can explain why the optimization leads to investment in adaptation only in this case. We compare below these characteristics amongst the two samples.

The difference between the two samples is the storm indicator and the beta. In terms of magnitude, the portion of the debt explained by variations in the climate indicator (CI_mag or CI_pop) is greater when using magnitude than when using population. We remind ourselves that the CI_mag results were less significant than those for CI_pop (two stars instead of three). The mean part of debt that covaries with the CI_pop indicator is slightly higher than for the CI_pop:

- CI_mag: mean part of debt related directly to 3.72%
- CI_pop: mean part of debt related directly to 0.15%

We conclude from our study that this methodological difference significantly affects the outcome of the cost-benefit analysis.

The most significant difference between project 23 and the others is leverage. Project 23 has relatively low leverage at 57% in comparison to the mean of the sample which stands at 77%. This has a consequence on the denominator of the optimisation function. Cost of equity has more weight in the WACC, meaning the discount rate is less affected by the reduction of the cost of debt in comparison to the interest rate. Additionally, the cost of equity is amongst the highest. The sample mean is 11.6% and for project 23, 19.78%. While this does not lead to an above average WACC, seen as this project is the only concessional project of the sample, the cost of debt is relatively small (6% originally, with 3.07% related to the climate indicator, falling to 4.3% with investment in resilience), the difference is noticeable when comparing the difference between the WACC and the cost of debt, we see the cost of debt, R, is 5.93% below the WACC without adaptation, and 6.66% with adaptation whereas the average difference is of 0.52%. Mathematically, this means that the interest payments are relatively heavily discounted and therefore less significant and reducing the cost of debt exacerbates this difference as it reduces interest more than it reduces the WACC. We conclude on the case of project 23 that while this is a specific case that works within our framework, it only helps to identify a specific scenario in which adaptation could help reduce the cost of debt, and, the total funding cost of debt. While we have initiated this exploration, significant scale would have to be obtained, and combination with a cost-benefit analysis of O&M, in order to bring any substantial evidence to the claims that adaptation can reduce the cost of debt.

Detailed results for each project TFC analysis are presented in the Appendix.

The case study does not establish that adaptation generally pays for itself through debt compression at the project level, and we do not claim it does. The 18 of 19 projects in which the optimization yields no payoff are not a failure of the framework but a feature of the underlying economics: at prevailing leverage ratios, cost-of-equity levels, and climate beta magnitudes, the present value of compressed interest payments does not, on its own, offset the additional debt drawn to finance resilience. Project 23 is informative about the conditions under which the trade-off can clear low leverage, a large cost of equity premium relative to the cost of debt, concessional baseline rates but those conditions are not the modal case in our sample.

The implication is not that adaptation is unaffordable. It is that the financing channel through which adaptation pays back cannot be sponsor-side debt compression alone. If commercial debt compression at the sponsor level does not generate sufficient NPV savings to fund resilience investment, the case for absorbing some of that cost through credit enhancement, concessional subordination, or regulatory capital relief none of which the sponsor can deliver unilaterally becomes correspondingly stronger. This is the architectural response developed in section 7.

7 Policy Recommendations: Blended Finance as a Result of Structural Mispricing

7.1 The structural financing problem

The empirical section has documented a high degree of variability in SSA infrastructure costs of debt that is bimodal in its lender market and structured in its climate pricing. Storm exposure is associated with a measurable cost of debt premium across both lender segments and across both Climate Risk Indicator constructions. For extreme heat, the coefficients are insignificant and approximately zero, hence, if the results were significant, we would conclude that heat exposure is not priced. Flood exposure is priced through what we read as a lender-side selection mechanism rather than through a direct risk premium, with commercial syndicates financing flood-exposed projects only where adaptation has been credibly arranged ex ante. The climate behavioral sentiment proxy enters the cost of debt asymmetrically across lender pools, loading on private commercial lenders and offset, sometimes reversed, where mandate-driven institutions are present in the syndicate. The next sections of this section ask how these findings should shape the policy response. Before turning to that question, we set out the structural financing problem within which any policy response has to operate.

The cost of debt distribution, documented in Figure 5-1, is bimodal because the lender market is bimodal. Within the regression sample of 230 projects, the 165 concessional projects price senior debt at a median of 0.75% and a mean of 1.67%, while the 65 non-concessional projects price at a median of 8.45% and a mean of 7.93%. The gap between these two rates is the empirical magnitude of the financing problem in our sample, and it cannot be closed by any one of the three pools of capital that finance SSA infrastructure: sovereign, multilateral, or commercial, acting alone. The structural case for a different financing model rests on three constraints, which we set out in turn.

7.1.1 Sovereign fiscal space is exhausted

The IMF's most recent Regional Economic Outlook for Sub-Saharan Africa documents that the ratio of interest payments to revenue has more than doubled over the past decade, and that "high imbalance" status defined to include public interest payments above 20% of revenues, now characterizes a substantial share of the region (International Monetary Fund, 2025). Median public debt has stabilized at around 60% of GDP in 2024, but at a level that leaves limited room for direct sovereign infrastructure investment, and 13 African countries were identified by the IMF and World Bank as being at high risk of debt distress as of late 2023, with seven already in distress (African Legal Support Facility, 2024). It is estimated that SSA needs to invest approximately 7.1% of GDP annually in infrastructure to meet its sustainable development objectives, against current investment of roughly half that amount, with governments bearing approximately 90% of the burden and the private sector contributing only 10% (Chinzara et al., 2023). Direct sovereign expansion of infrastructure investment at the required scale is, in present fiscal conditions, not feasible across most of the region.

7.1.2 Multilateral capital is finite

The African Development Bank's outstanding development-related portfolio reached USD 27.3 billion in 2025, and a USD 117 billion General Callable Capital Increase was approved by its Board of Governors in 2024 to preserve and leverage its lending headroom (African Development Bank Group, 2024a). Aggregate reform efforts under the G20 Capital Adequacy Framework review have, since mid-2024, increased projected MDB lending headroom by more than USD 250 billion over the next decade, bringing the total to over USD 650 billion across all regions of operation. S&P estimates that further methodological updates could unlock USD 600-800 billion in additional sovereign lending capacity across the system over time (Goko, 2025). These figures are substantial in aggregate but must be set against the African Development Bank's own estimate of an annual SSA infrastructure financing gap of USD 181-221 billion with adaptation alone accounting for roughly USD 580 billion over the 2020-2030 decade (Ijjasz-Vasquez & Saghir, 2023). The arithmetic is unambiguous: even on the most ambitious reform trajectories, multilateral headroom over a decade is of the same order of magnitude as a single year of regional financing need.

7.1.3 Commercial capital is structurally expensive

The empirical section has documented why: the 8.45% median rate within the 65-project non-concessional sub-sample reflects the joint operation of country-risk premia, currency-risk premia, hazard-specific physical-risk premia, and a behavioral premium that, based on our evidence, loads disproportionately onto private commercial lenders. The regression demonstrates that physical climate risk and sentiment are part of the structure that produces this rate, rather than idiosyncratic features of individual transactions. The directional implication, set out in the empirical section and revisited here, is that the rate is not stationary: as physical-risk salience increases over the coming decade, the sentiment channel that loads onto private lenders will plausibly amplify rather than attenuate.

The structural problem is therefore not that one of the three pools of capital is insufficient. It is that none of the three is sufficient on its own, that each is insufficient for different reasons, and that the model best suited to combining them in a single transaction is a financing architecture none of them implements unilaterally.

7.2 Why blended finance emerges as the response

7.2.1 What blended finance is, and what it does

Blended finance is the structured deployment of concessional public capital alongside commercial private capital within a single transaction, configured such that the public layer absorbs risk, subordinates its claim, or extends a guarantee that improves the risk-return profile of the commercial layer (OECD, 2025). The model is not new, its institutional origins lie in concessional co-financing arrangements that multilateral lenders have used since the 1980s but its formalization as a distinct financing category dates from the work of the OECD Development Assistance Committee in the late 2010s and from the consolidation of practitioner standards through institutions such as Convergence and the Blended Finance Taskforce. The OECD definition, which we adopt, frames blended finance as the use of concessional public funds to mobilize additional commercial capital toward sustainable-development objectives, with the public component priced or structured below market terms and the commercial component priced at risk-adjusted market terms (OECD and UNCDF, 2019; OECD, 2025).

What the model does, mechanically, is alter the risk-return profile faced by the commercial lender. Three structural devices are most commonly used. A first-loss subordinated tranche absorbs the initial portion of any realized credit losses, leaving the senior commercial tranche shielded until that subordinated layer is exhausted. This compresses the loss-given-default that the senior tranche faces and therefore the spread the senior lender charges. A partial credit guarantee from a multilateral institution covers a defined share of senior-tranche losses up to a contractual ceiling, thereby compressing the perceived probability of default rather than the loss given default. A foreign-exchange or interest-rate hedging facility, often provided by specialist DFIs or by dedicated currency-risk vehicles such as TCX, transfers a specific component of macroeconomic risk away from the project balance sheet. These devices are not mutually exclusive, and well-structured transactions combine them. The common feature is that concessional capital is deployed in a position that produces a multiplier effect every dollar of concessional capital placed in a subordinated or guarantee position mobilizes several dollars of commercial capital that would not otherwise have entered the transaction at the rate it does.

7.2.2 Why blended finance fits the SSA cost-of-debt problem

Three features of the SSA infrastructure financing problem make blended finance a particularly well-matched response. The first is the leverage feature: SSA infrastructure projects in our sample carry an average debt-to-capital ratio of 79%, which means that the cost of debt is the dominant marginal price at which infrastructure financing is allocated and that any instrument that compresses the cost of debt has a disproportionate effect on overall project bankability. The second is the lender-segmentation feature: the bimodal distribution of debt costs documented in Section 5.1 reflects two segments of the lender market that operate on different mandates, different cost of capital, and different risk-pricing behavior, and blended finance is the only model that systematically combines them. The third is the empirical evidence that combination already attenuates the pricing patterns documented in the empirical section: the flood × concessional interaction in Table 5-1 and the sentiment × lender-type interactions in Table 5-2 are both observed in the data without any deliberate policy intervention, and both are consistent with concessional presence already producing a measurable mitigation effect on the margin. Systematizing and amplifying that effect, rather than inventing it, is the operative reform.

A further consideration is what blended finance avoids. The two principal alternatives direct sovereign expansion of infrastructure investment, and direct concessional substitution for commercial lending both fail the scaling test set out in Section 6. Sovereign expansion is constrained by fiscal space. Direct concessional substitution is constrained by multilateral balance-sheet headroom. Blended finance is the only model in which the same volume of concessional capital can be made to do more work, by acting on the multiplier through which commercial capital is crowded in, rather than substituting for it.

7.2.3 The current state of play

Convergence reports that aggregate blended-finance deal flow has been broadly stable since the late 2010s, with cumulative transactions exceeding USD 213 billion to date but with annual flows that have not scaled at the pace required by the climate and infrastructure financing gaps (African Development Bank Group, 2019). The OECD reports that climate-related blended finance has grown faster than the aggregate but remains a small share of total commercial flows into emerging and developing economies (OECD, 2025). Within SSA specifically, blended-finance volumes are concentrated in clean energy and financial-sector intermediation, with infrastructure project finance representing a smaller share than the financing gap arithmetic would suggest. This is, in part, a function of the institutional frictions that the policy literature has begun to document, Basel III risk-weight treatment of credit-mitigated exposures, currency-risk hedging coverage gaps, and the transaction costs of structuring blended deals at scale (International Chamber of Commerce, 2025) and we return to these institutional frictions in Section 7.4. The state of play, in short, is that blended finance exists as an established model, has demonstrated mobilization effects in specific transaction types, but operates at a scale that is an order of magnitude below what the SSA infrastructure financing gap would require. The policy task, on our reading, is to characterize the shape the model should take if it were scaled, and the institutional reforms that would accompany that scaling.

7.3 How the empirical results shape the design of blended finance

The empirical evidence of Section 5 supports a particular shape for the blended-finance response, rather than a generic endorsement of the model. We develop two design propositions in this section, each tied to a specific empirical finding, and we set them against the descriptive lender-composition pattern visible in our database, which conditions the deployment of marginal blended-finance.

7.3.1 Where capital currently flows, and where it should

Table 7-1 summarizes the lender-composition pattern within the regression sample.

Lender configuration	N	Climate-infra share	Mean cost of debt	Sectoral concentration
International, Private	10	10%	6.72%	7 Mining, 2 Fossil, 1 Clean Energy
International, Public/Private mix	3	0%	7.25%	3 Mining
International, Public	25	72%	3.33%	17 Clean Energy, 4 Mining, 2 Fossil, 1 Agri, 1 Digital

Lender configuration	N	Climate-infra share	Mean cost of debt	Sectoral concentration
African-origin, Private	26	58%	9.72%	15 Clean Energy, 4 Mining, 3 Fossil, 3 Digital, 1 Transport
African-origin, Public	103	75%	1.22%	40 Transport, 20 Water, 19 Clean Energy, 14 Agri, 7 Digital
African-origin, Public/Private mix	5	80%	10.31%	4 Clean Energy, 1 Mining
Intl & African, Private	6	0%	5.11%	3 Mining, 1 Transport, 1 Digital, 1 Fossil
Intl & African, Public	46	76%	2.56%	17 Clean Energy, 11 Transport, 9 Water, 6 Fossil
Intl & African, Public/Private mix	6	17%	6.64%	3 Fossil, 1 Mining, 1 Clean Energy, 1 Transport
Total / regression sample	230	66%	3.44%	—

Table 7-1: Sectoral composition by lender origin and type, regression sample (N = 230)

Notes: Cost of debt is the all-in nominal interest rate at financial close. The "Climate-infra share" is the proportion of projects flagged as climate-related infrastructure under the dataset's classification. Sectoral concentration shows the dominant sectors within each lender cell. The Africa Public/Private mix and International/African mixed-private cells are small (5 and 6 projects respectively) and the cost levels in those cells should be read as descriptive of those few transactions rather than as segment-level averages.

Three features of this composition deserve emphasis because they bear directly on how blended finance should be designed. First, international private capital, in our sample, is almost entirely a vehicle for extractive-industry finance: of the ten observed international private lender projects, seven are in mining and two in fossil energy, with only one in clean energy and none in water, transport, agriculture, or digital infrastructure. The pattern sharpens further when international private participation in mixed-type transactions is included: ten of the thirteen projects involving any international private participation are in mining. International private capital, when it enters SSA on commercial terms, is therefore not currently flowing to the climate-infrastructure pipeline that the financing gap is principally about.

The most plausible explanation for this concentration is institutional and historical rather than rational risk pricing in the strict sense. SSA mining has been integrated into international commodity markets for over a century, with project sponsors that are themselves listed in OECD jurisdictions, with offtake contracts denominated in hard currency, and with revenue streams that are by construction insulated from local-currency depreciation. The asset class additionally benefits from a long-standing architecture of host-country mining codes, stabilization clauses, and political-risk insurance products designed around extractive sector cash flows. There is also a demand side dimension worth naming: extractive output flows back to consumers in lender countries, while the output of clean energy or water infrastructure stays in SSA. International private capital has no direct consumption interest in the latter, which removes a channel, supply-chain integration, that has historically conditioned the willingness of developed origin lenders to engage with SSA sectors. None of these features is climate-relevant, and several have been the object of policy critique in their own right. But together they make extractives a familiar and well-instrumented asset class in a way that climate-resilient infrastructure is not. The structural inefficiency the policy section must address is that the institutional architecture currently channeling international private capital into SSA was built around a different sectoral composition than the one the climate financing gap requires.

Second, African-origin private lenders are more engaged in climate-related infrastructure (58% of their portfolio in our sample) but finance these projects at the highest mean cost of any lender cell (9.72%). Within African private financing of clean energy specifically (15 projects), the mean rate rises to roughly 10.7%. The capital that is most aligned with the climate infrastructure pipeline is also the most expensive. Third, concessional finance, of both African and international origin, prices roughly seven to nine percentage points below the private segments, but its volume is bounded by the fiscal space of the institutions that supply it, as documented in Section 7.

The structural inefficiency that emerges from this composition is therefore a misalignment, not a shortage. International private capital flows to extractives but not to climate infrastructure. African-origin private capital flows to climate infrastructure but at rates that compromise project viability. Concessional capital is well-priced but capacity-constrained. A blended-finance architecture that is responsive to this composition would aim to do two things at once: redirect international private capital toward the climate infrastructure pipeline by altering the risk-return profile of those transactions through concessional layering, and compress the rate at which African-origin private capital can finance climate infrastructure through the same mechanism applied within a different lender configuration.

7.3.2 Design proposition one: concessional first-loss tranching calibrated to the storm premium

Storm exposure is the only hazard for which our regression identifies a positive, significant, and construction-robust cost-of-debt premium, with a baseline coefficient of approximately +1.04 percentage points per unit of log-CI and a within-private-lender interaction whose direction confirms that the premium is concentrated in the segment of the market most exposed to commercial pricing. This is the empirical anchor for a financial instrument response.

A blended-finance structure designed around this finding would deploy concessional public capital as a first-loss, subordinated tranche within transactions exposed to high storm-CI hazard, calibrated so that the senior commercial tranche carries a reduced loss-given-default profile upon the realization of a storm event. The economic logic follows directly from the heuristic decomposition of the cost of debt presented in Section 3.3: a first-loss tranche compresses the LGD term, which is the channel through which storm exposure plausibly enters loan pricing in our framework. Figure 7-1 illustrates the structure schematically.

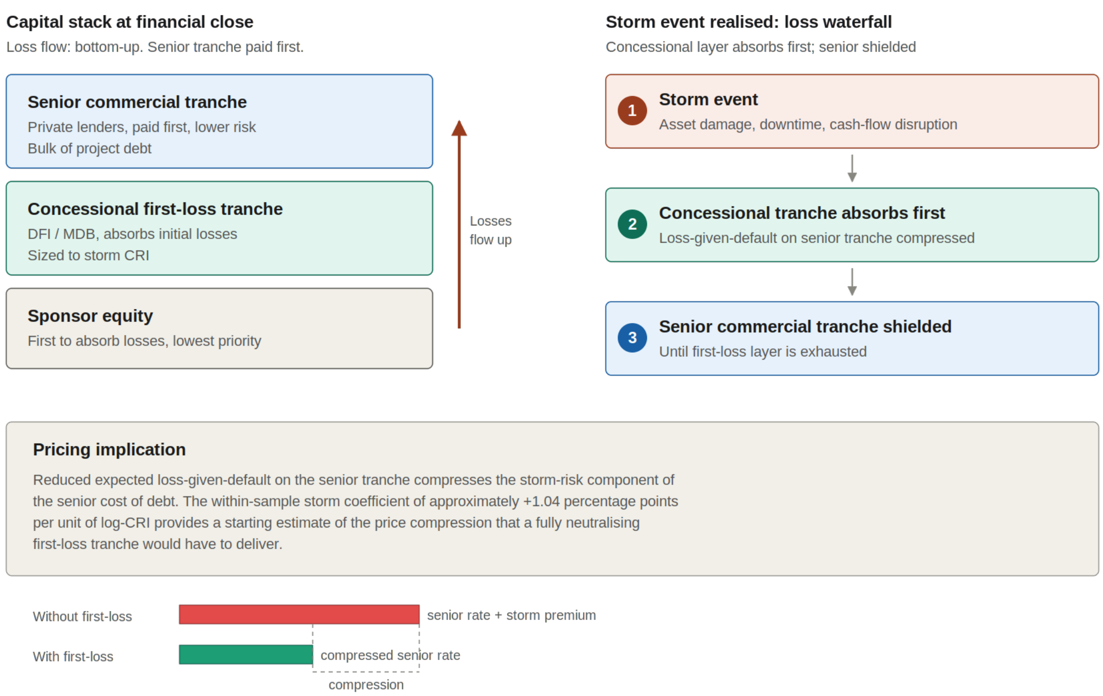

Figure 7-1: Blended Finance Structure for a Storm Exposed SSA Infrastructure Project

Note: This is a schematic representation of a blended-finance structure responding to the storm-exposure premium. The concessional first-loss tranche, sized to the project's storm CI, absorbs initial losses from a storm event and compresses the loss-given-default that the senior commercial tranche faces. The compression of the senior cost of debt is the channel through which the empirical storm premium is mitigated.

The size of the first-loss tranche should scale with the project-level storm CI rather than be set as a flat percentage of project cost, on the view that the empirical premium varies with exposure and the concessional response should track that variation. We do not propose a specific calibration: the magnitude of the storm coefficient in our regression provides a starting estimate of the price compression that a fully neutralizing first-loss tranche would have to deliver, but the cross-sectional nature of our evidence and the identification limits set out in Section 5.6 mean we do not interpret this magnitude as a precise structural target. The directional proposition, first-loss subordination scaled to storm exposure, is what the empirical pattern supports.

The same instrument is not the appropriate response to flood exposure or to heat exposure. Flood exposure operates through the selection mechanism documented in Section 5.2 rather than through a residual pricing premium that a first-loss tranche could compress. The corresponding policy response, financing the adaptation that allows flood-exposed projects to clear the commercial selection threshold, is taken up directly in the adaptation debt trade-off framework of Section 6 and is not a free-standing blended-finance instrument here. Heat exposure does not appear robustly priced in our regression, and a blended-finance instrument designed to compress a heat premium would be operating on a premium that the data does not support. The differentiated mapping from finding to instrument is itself a feature of the design proposition: the storm-pricing finding is what supports a first-loss tranche; the other findings support different responses.

7.3.3 Design proposition two: structured DFI participation against the sentiment channel

The sentiment × private-lender interaction estimated in Table 5.2 supports a reading whereby the residual SSA premium documented at the sovereign level by (Gbohoui, 2023) loads, in our project-level data, specifically on the private commercial-lender segment and is attenuated where mandate-driven institutions participate in the syndicate. The interactions with international and public lender presence are negative in both CI constructions, consistent with this reading.

The instrument-level implication is that the architecture of a blended finance transaction can be designed to deliver a measurable sentiment-mitigation effect by ensuring DFI co-investment in transactions otherwise dominated by private commercial lenders. The mechanism is informational rather than purely capital-based: DFI presence functions as a signal that the transaction has cleared a mandate-driven due diligence process whose criteria differ from those a commercial syndicate would apply on a stand-alone basis, and the empirical evidence in Section 5.2 is consistent with private lenders responding to that signal. We propose, on the strength of this evidence, that blended-finance structures targeting projects with high sentiment-proxy values, projects closing in periods of negatively framed climate discourse about the host country or sector, should carry a minimum DFI participation share, set at a level sufficient to produce the attenuating effect visible in the regression. We do not have a precise structural estimate of the threshold at which this effect becomes operative; the interaction coefficient is a slope rather than a threshold, and the sample size in the private lender cell is too small to identify a non-linearity reliably.

A particular feature of this design proposition deserves emphasis. The behavioral sentiment proxy used in the empirical section is constructed from textual material whose negative framing of SSA climate exposure increased modestly over the most recent decade of our sample (Section 4.6). The regression demonstrates that this proxy is priced into commercial debt costs through the private-lender channel. The combination has a directional implication: as climate change advances, the salience and adverse framing of SSA climate exposure in the textual environment to which lenders are exposed will plausibly intensify rather than attenuate. To the extent that the sentiment channel operates through the availability heuristic, an increase in the frequency and visibility of climate-disaster reporting on SSA, itself an expected consequence of accelerating physical-risk realization, will mechanically increase the input variable on which the private-lender sentiment premium loads. The unmitigated commercial cost of debt for SSA infrastructure may therefore drift upward over time even if fundamentals remain unchanged.

This makes the mandate-driven attenuation channel, DFI participation that empirically dampens the sentiment loading on private lenders, not a static correction but a structural buffer whose importance grows with the rate of physical risk realization. The case for designing blended finance structures around sentiment mitigation is stronger if the channel they address is widening over time than if it were stationary.

7.3.4 A note on sectoral steering

The clean-energy concessional differential, documented in Section 5.3, shows that concessional clean-energy projects priced 290 to 360 basis points below other concessional projects, already demonstrates that the deployment of concessional capital can be conditioned on sector. Mining, by contrast, is financed entirely on non-concessional terms in our sample, which suggests that an implicit sectoral differential is already operating in MDB lending criteria over the sample period. We do not propose this sectoral differential as a new policy instrument, but rather note that it is internally consistent with the broader architecture of concessional steering: the same logic that supports first-loss subordination against storm-exposed clean energy projects also supports the absence of concessional support for sectors whose climate value is ambiguous. Making the differential more transparent and more measurable against standardized criteria is the policy adjustment our evidence supports.

7.4 Institutional reforms required to scale the model

The design propositions mentioned before cannot scale to address the SSA infrastructure financing gap without a corresponding set of institutional reforms that relax the constraints currently binding on each pool of capital. We discuss four such reforms here, each tied to a specific empirical or institutional friction identified in the preceding sections.

7.4.1 Basel III risk-weight clarifications and capital relief for credit-mitigated exposures

Commercial bank participation in SSA infrastructure debt is constrained, in part, by the capital charges imposed by the Basel III framework on long-tenor lending in low-rated jurisdictions. To convey the magnitude of the differential, it is useful to anchor the discussion in an actual transaction from our regression sample. We take project ID 183, the Off-Grid Electric Tanzania solar and battery storage project, which reached financial close in 2016 with a USD 40 million senior loan provided by an international private syndicate of four lenders led by New Island Capital Management, at an all-in nominal rate of 8.59% over a 16.5-year tenor. The project is greenfield clean-energy infrastructure in a non-investment-grade jurisdiction. We then ask what an OECD-domiciled commercial bank holding the same USD 40 million exposure would have allocated in regulatory capital, and what return on regulatory equity it would have generated, under three configurations: (A) a hypothetical OECD operational comparator project benefiting from the standardized approach's preferential treatment of high-quality project finance, (B) the actual Tanzania transaction, and (C) the same Tanzania transaction restructured with a concessional first-loss tranche. The numerical exercise uses a CET1-plus-buffer ratio of 10.5%, representative of large G-SIBs after capital conservation and countercyclical buffers, and a 200-basis-point net interest margin held constant across the three configurations. The point of the exercise is not to claim a precise structural estimate of the SSA premium, but to make the regulatory mechanism explicit, separating the capital channel from the country-risk and sentiment channels documented elsewhere in our analysis.

Under the Basel III standardized approach, an unrated project finance exposure carries a 130% risk weight during the pre-operational phase and 100% during the operational phase, with a preferential 80% risk weight available to operational-phase exposures classified as "high-quality" (KPMG, 2025). The "high-quality" criteria, set out in paragraph 71 of the BIS framework, require, among other conditions, that the project finance entity's revenue depend on a main counterparty that is itself rated 80% RW or lower, that is, an investment-grade central government, public-sector entity, or corporate. The European CRR additionally provides an Infrastructure Supporting Factor that reduces capital requirements on qualifying infrastructure exposures by 25% (EBA, 2022). Sub-Saharan African sovereigns and state-owned utilities are typically rated below the threshold required to access the 80% RW bucket, and the Infrastructure Supporting Factor in its current form does not extend to projects in non-OECD jurisdictions on the same terms. The result, applied to the Tanzania project, is that the same loan economics translate into materially different capital allocations and returns on regulatory equity. Figure 6-2lays out the comparison.

7.4.2 Assumptions and method

To make the comparison reproducible, we explicitly set out the assumptions and the calculation method. The exercise uses a single bank perspective and holds five parameters constant across scenarios. The bank's minimum capital ratio is set at 10.5%, comprising the Basel III CET1 minimum of 4.5%, the capital conservation buffer of 2.5%, an indicative G-SIB surcharge of 1.5%, and an indicative countercyclical capital buffer of 2.0%, which is representative of large internationally active banks subject to additional supervisory loadings (Basel Committee on Banking Supervision, 2024). The bank's net interest margin is held at 200 basis points across Scenarios A and B, on the assumption that the bank prices its loans to deliver an identical spread over its own cost of funds in both jurisdictions; in Scenario C, the senior tranche's NIM is derived endogenously by holding the bank's target return on regulatory equity constant at the OECD comparator's level. The bank's cost of funds is set at 200 basis points, representative of long-tenor wholesale funding for an OECD-domiciled investment-grade bank in 2016. The DFI subordinated tranche in Scenario C is priced at 1.5%, representative of the midpoint of AfDB African Development Fund concessional lending rates that range from zero-interest loans for grant-eligible countries to roughly 4.2% for blend-eligible borrowers (Mathiasen & Martinez, 2025), adjusted upward to reflect the additional risk associated with subordination relative to senior concessional facilities. The senior commercial tranche in Scenario C is assigned an effective risk weight of 50%, conditional on full regulatory recognition of DFI subordination as credit risk mitigation; the derivation of this figure is set out in the box below. Risk weights for Scenarios A and B follow directly from the Basel III standardized approach, with Scenario A applying the 80% high-quality bucket and the EU CRR Infrastructure Supporting Factor (a 25% reduction in own-funds requirements), and Scenario B applying the 130% pre-operational project finance bucket without either preferential treatment.

The return on regulatory equity in each scenario is then computed as

$$RoE = (loan \times NIM) \div (loan \times RW \times capital\ ratio) \qquad (7.1)$$

where loan × RW gives the risk-weighted assets, the product of risk-weighted assets and the capital ratio gives the regulatory capital allocated to the loan, and loan × NIM gives the bank's annual net interest income from the position. In Scenario C, where the bank holds only the senior tranche, "loan" in both terms refers to the senior tranche notional of USD 28 million rather than the full project debt of USD 40 million. The arithmetic for each scenario is reported in Figure 7-2 and discussed in the following paragraphs.

Derivation of the 50% effective risk weight in Scenario C

The 50% effective risk weight applied to the senior commercial tranche in Scenario C is derived from the Basel III treatment of credit-mitigated exposures, applied to a tranched-cover structure. The bank's USD 28 million senior position sits above a USD 12 million DFI first-loss tranche, giving it an attachment point of 30% and a detachment point of 100% on the underlying USD 40 million exposure. Two channels of regulatory relief are then available, conditional on full recognition under the Basel framework.

First, the substitution approach allows the protected portion of the bank's exposure to inherit the protection provider's risk weight. Qualifying multilateral development banks carry a 0% risk weight under Basel III, and where DFI subordination meets the eligibility criteria for credit risk mitigation, 30% of the bank's senior exposure inherits a 0% risk weight on this basis. Second, the credit enhancement provided by the DFI subordination strengthens the case for treating the senior tranche as eligible for the high-quality operational project finance bucket at 80%, rather than the 130% pre-operational bucket that would apply to the underlying unmitigated exposure. Combining the two channels, the effective risk weight on the senior tranche is calculated as a weighted average:

effective RW = (0.30 × 0%) + (0.70 × 80%) = 56%, rounded to approximately 50%

The 50% figure used in Figure 6.2 is therefore a slight conservative simplification of the 56% point estimate. Two sensitivities are worth noting. If the substitution approach applies but the high-quality reclassification does not — that is, if the senior tranche retains its 130% pre-operational risk weight on the unprotected portion — the effective risk weight rises to (0.30 × 0%) + (0.70 × 130%) = 91%, the capital allocation rises to USD 2.68 million, and the return on regulatory equity falls to approximately 20.9%, still above Scenario B but well below the OECD comparator. If neither recognition channel applies, the senior tranche carries the underlying 130% risk weight in full, and Scenario C collapses back toward Scenario B in capital terms. The 50% figure, therefore, represents the upper end of what the structure can deliver under economically appropriate Basel treatment; the gap between 50% and the 91% or 130% alternatives is the empirical content of the Basel reform proposals discussed in the rest of this section, which call for the regulatory framework to recognize the credit-mitigation effect that the structure produces in economic terms.

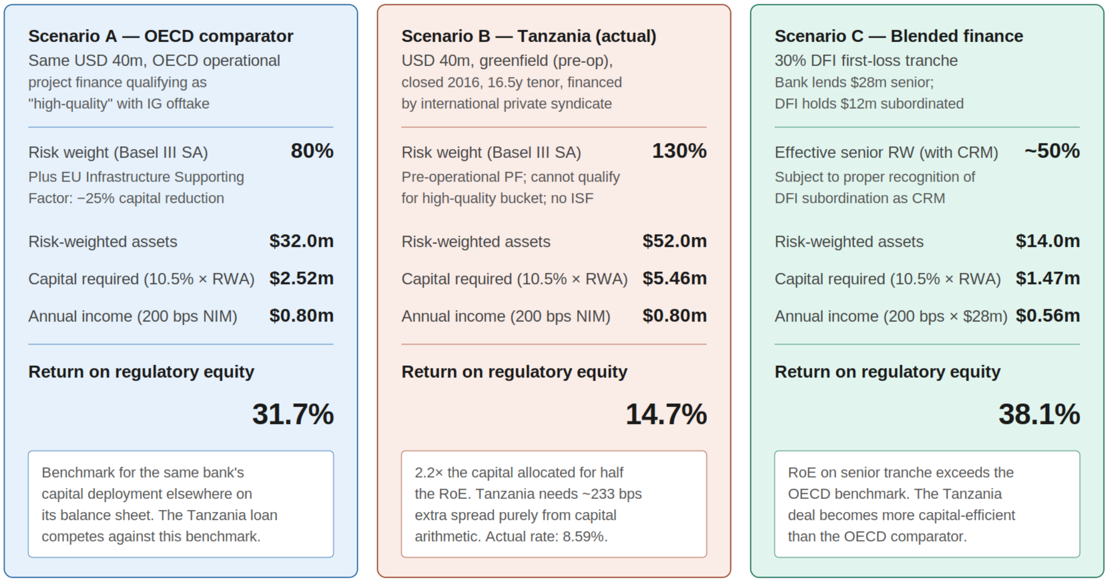

Figure 7-2: Capital and ROE Off-Grid Electric Plant Tanzania versus OECD Country

Note: The Tanzanian case study project is a USD 40m greenfield clean-energy project, financial close 2016. Standardized approach: CET1+buffer 10.5%, 200bps NIM. Capital and return-on-equity comparison anchored on the Off-Grid Electric Tanzania solar and battery storage project (regression sample ID 183, 2016 financial close). The comparison shows what an OECD domiciled commercial bank would have allocated in regulatory capital, and what return on regulatory equity it would have generated, under three configurations: (A) a hypothetical OECD operational comparator project qualifying for the standardized approach's 80% high-quality risk weight and the EU Infrastructure Supporting Factor, (B) the Tanzania transaction as actually structured (greenfield, falling under the 130% pre-operational project finance risk weight at financial close, with no access to the high-quality bucket or the Infrastructure Supporting Factor), and (C) the same Tanzania transaction restructured with a 30% concessional first-loss tranche held by a DFI. The comparison isolates the regulatory capital channel under common assumptions of a 10.5% CET1-plus-buffer ratio and a 200 basis-point net interest margin.

The mechanism producing the differential between the OECD comparator and the Tanzania transaction is institutional rather than purely risk-based. The hypothetical OECD comparator, with an investment-grade utility offtake counterparty, qualifies for the 80% RW under the standardized approach and benefits from the 25% capital reduction provided by the Infrastructure Supporting Factor; the resulting capital allocation against a USD 40 million loan is approximately USD 2.52 million, supporting a return on regulatory equity of 31.7% at the assumed 200 basis-point spread. The Tanzania transaction, identical in size, falls into the 130% pre-operational project finance bucket because the project was greenfield at financial close, and is not eligible for either the high-quality treatment or the Infrastructure Supporting Factor; the same loan accordingly absorbs USD 5.46 million in capital, more than twice the OECD comparator, and the implied return on regulatory equity at the same 200 basis-point spread drops to 14.7%. The arithmetic indicates that, holding everything else constant, the Tanzania project would have needed to charge approximately 233 additional basis points over the OECD comparator's spread to generate the same return on regulatory equity from the lender's perspective. This is purely the capital-channel differential, before any pricing for country risk, currency risk, or the sentiment premium identified in our regression. The 8.59% all-in rate that the Tanzania project actually paid in 2016 reflects this capital-channel differential layered on top of the bank's cost of funds and the additional premia for which our regression provides empirical evidence: the basis-point magnitudes implied by the capital channel alone are of the same order as the storm premium and the sentiment × private-lender effect documented in Section 5, suggesting that the Basel III architecture is itself one of the structural mechanisms producing the cost-of-debt differential we observe.

A blended-finance restructuring of the same transaction, with a 30% concessional first-loss tranche held by a DFI, substantially alters the picture, conditional on regulatory recognition of DFI subordination as a credit-risk mitigant. The senior commercial tranche is now USD 28 million rather than USD 40 million, and its effective risk weight, under proper recognition of the credit substitution effect, falls to approximately 50%: a figure we use as illustrative rather than as a precise calibration. The capital allocation against the senior tranche drops to roughly USD 1.47 million, and the return on regulatory equity rises to 38.1%, exceeding even the OECD comparator. The capital efficiency of the Tanzania transaction, structured this way, would surpass that of the OECD baseline. Whether this efficiency would be realized in practice depends on the regulatory treatment of the credit-mitigation structure, which is the subject of the policy reform proposals discussed below.

The arithmetic above is on the bank side and addresses how regulatory capital allocation shapes a lender's willingness to participate. From the project sponsor's perspective, the more directly relevant question is what blended rate the restructured transaction would deliver on the cost of debt. The blended rate decomposes into two tranche-specific rates, each priced according to the channel that produces it. The senior commercial tranche, having absorbed less regulatory capital under the credit-mitigation structure, can be priced at a lower spread for the same lender return. Working backward from the OECD comparator's 31.7% return on regulatory equity, the senior tranche would need to generate annual income of approximately USD 0.466 million on its USD 28 million notional, implying a net interest margin of around 166 basis points rather than the 200 basis points that the standalone Tanzania structure would have required. Adding an OECD-bank representative cost of funds of approximately 200 basis points for long-tenor lending in 2016 yields a senior tranche rate of approximately 3.7%. The concessional first-loss tranche, by contrast, is priced according to DFI mandate rather than commercial return targets. AfDB lending rates on its African Development Fund window range from zero-interest concessional loans for grant-eligible countries to roughly 4.2% for blend-eligible borrowers (Mathiasen & Martinez, 2025); for project-finance subordinated tranches, which take more risk than budget-support concessional facilities, a representative midpoint is approximately 1.5%. The blended rate the sponsor pays is then the weighted average across the two tranches: 70% × 3.7% + 30% × 1.5% = 3.04%. Compared to the 8.59% all-in rate that the Tanzania project actually paid in 2016, the blended structure delivers a cost-of-debt compression of approximately 555 basis points, of which 233 basis points is attributable to the bank-side capital channel and the remaining 320 basis points to the substitution channel through which a portion of the loan is funded at concessional rather than commercial terms. The empirical content of this decomposition is that blended finance compresses the cost of debt through two distinct mechanisms operating in parallel (regulatory capital relief on the senior tranche, and concessional substitution on the subordinated tranche) and that the relative weight of the two channels in any given transaction depends on the size of the concessional layer and on whether the credit-mitigation effect of that layer is fully recognized in the senior tranche's capital treatment.

The relevant policy literature has converged on a set of targeted clarifications and adjustments. The Basel framework already recognizes a 0% risk weight for direct exposures to qualifying multilateral development banks, including the African Development Bank and the World Bank Group entities (Basel Committee on Banking Supervision, 2024), but the recognition of credit-mitigated exposures, that is, commercial loans backed by MDB or DFI guarantees, partial credit guarantees, or first-loss subordination structures, is, in practice, restrictive enough that many real-world blended-finance instruments do not qualify for capital relief proportionate to their economic risk-mitigation effect (International Chamber of Commerce, 2025). The ICC presents a closely analogous worked example involving a B-rated SSA solar project with a long-term power purchase agreement and MIGA political-risk insurance, and shows that under current rules the bank cannot obtain capital relief proportionate to the credit-mitigation effect of the insurance, with the consequence that the loan does not generate a competitive return on capital. Three specific clarifications follow from this body of work, and each is consistent with the empirical evidence we have produced. First, recognition of MDB and DFI credit-risk-mitigation tools should be updated to reflect real-world contract structures, including standard market exclusions such as war and nuclear clauses that currently disqualify guarantees from capital relief even though they substantially reduce real-world credit risk (International Chamber of Commerce, 2025). Second, blended risk weights should apply to exposures covered by partial guarantees, reflecting the genuine residual exposure on the uncovered portion rather than treating the entire exposure as if uncovered (International Chamber of Commerce, 2025). Third, a scaling factor for high-quality climate-related exposures in EMDEs, analogous to the existing SME Supporting Factor under Basel III or the Infrastructure Supporting Factor under the EU Capital Requirements Regulation, would directly relax the constraint on commercial participation in eligible blended-finance transactions.

The empirical justification for these clarifications, in our setting, is that DFI participation already attenuates the sentiment premium and the broader pricing pattern in our data. Regulatory recognition of the credit-enhancement effect of DFI subordination would convert this empirically observable mitigation into a Tier 1 capital benefit on commercial bank balance sheets, which is the channel through which the regulatory adjustment translates into incremental commercial participation. The Basel framework's treatment of these instruments is technical and is currently the subject of active policy consultation; we do not develop the specifications here but refer to recent papers from the ICC and the IIF for detailed proposals. The directional case our evidence supports is that recognition of credit-mitigated exposures within blended-finance structures, calibrated to the empirically observable attenuation effects, would relax the most binding regulatory constraint on commercial scaling of the model.

7.4.3 Concessional capital at a meaningful scale

The proposed reform outlined above presupposes that concessional capital is available at sufficient scale to subordinate, to guarantee, or to hedge the volumes of commercial capital required to close the infrastructure gap. As documented in Section 7, the current scale of concessional resources is bounded by the AfDB's USD 27.3 billion outstanding portfolio, by IDA and bilateral DFI commitments to SSA, and by aggregate MDB lending headroom of approximately USD 650 billion across all regions of operation over the next decade. The combined CAF reform agenda and the AfDB callable capital increase have begun to expand this envelope, but the order of magnitude remains an order of magnitude smaller than the cumulative SSA infrastructure financing gap over the same horizon.

A scaling-up of concessional resources, whether through a dedicated SSA climate-infrastructure facility, through the redirection of existing concessional flows toward subordination rather than direct lending, through hybrid capital issuance of the kind initiated by the AfDB in 2024 (Mathiasen & Martinez, 2025), or through some combination of these, is a precondition for the design propositions of Section 7.3 to operate at the scale the financing gap requires. We do not advance a specific institutional design for such a facility here. The existing literature on blended finance for climate action (OECD, 2025; OECD & United Nations Capital Development Fund, 2019; United Nations Conference on Trade and Development, 2025) discusses several candidate architectures, and the choice among them is properly the subject of separate work. What our empirical evidence supports is the directional proposition that, given the same volume of concessional resources, a deployment biased toward subordinated and guarantee-based positions in commercial syndicates will mobilize more total capital than direct senior concessional lending because it acts on the multiplier through which concessional capital crowds in commercial capital, rather than substituting for it. The flood × concessional interaction in Table 5-1, the sentiment × lender-type pattern in Table 5-2, and the clean-energy concessional differential are each consistent with concessional capital already producing a measurable mobilization effect on the margin. The empirical case for using existing concessional resources differently, rather than only for using more of them, is the contribution our evidence makes to a debate that is otherwise often conducted at the level of aggregate volumes.

8 Further Research

Several directions would strengthen and extend the findings of this thesis. The most immediate limitation is the cross-sectional structure of the dataset, which allows us to infer robust associations but does not permit causal identification. A difference-in-differences approach exploiting plausibly exogenous variation in hazard realization, for instance, the timing of major cyclone landfalls relative to financial close, could test whether the storm premium documented here reflects ex-ante pricing or ex-post repricing.

The flood selection mechanism developed in Section 5.3 is, in our reading, the most plausible interpretation of the negative within-non-concessional flood coefficient, but it remains a hypothesis rather than a verified finding. Direct tests would require project-level data on adaptation measures present at financial close which would allow the flood coefficient to be conditioned on revealed adaptation. A complementary research agenda is to assemble a pipeline of failed or withdrawn SSA infrastructure transactions and compare their climate exposure to the financed sample. The selection mechanism predicts systematic differences. The absence of such differences would weaken the interpretation.

On the data side, scaling the LLM extraction pipeline to the full IJGlobal and Dealogic universes, and establishing direct data-sharing arrangements with development finance institutions for portfolio-level loan records, would substantially increase statistical power and enable panel specifications with country and time fixed effects that the current sample of 230 projects cannot support. Benchmarking the storm premium and flood selection mechanism against comparable emerging market infrastructure in Southeast Asia and Latin America would test whether these are SSA specific phenomena or features of frontier infrastructure markets more broadly.

Finally, the analysis is restricted to senior debt pricing for reasons of both theory and data availability. A complete picture of the financing constraint requires modeling the full capital stack, including junior and mezzanine debt, and equity. Potential improvements include incorporating local-currency lending rates alongside hard-currency rates to isolate the FX risk premium, extending the framework to guarantee and insurance instruments as DFI reporting expands, and constructing a cost-of-equity estimate from the growing pool of listed infrastructure funds with SSA exposure. This would allow derivation of project-level WACC for specific Sub-Saharan African projects, providing a more complete foundation for the institutional reforms recommended in Section 7. The Basel III counterfactual presented in Section 7.4 is itself a candidate for empirical testing: identifying transactions where DFI subordination was formally recognized as credit risk mitigation and comparing their pricing to matched non-recognized transactions would convert the calibration into an estimate.

9 Conclusion

This thesis set out to ask how capital can be scaled for Sub-Saharan African infrastructure while keeping the cost of debt low enough to bridge the adaptation and infrastructure financing gap. Working from a cross-section of 230 projects assembled from over 1,100 unstructured appraisal documents and commercial transaction records, we have argued that the climate premium in SSA infrastructure debt is not a single number to be discovered, but a structured pattern of selective pricing across hazards and lender pools.

The adaptation–debt trade-off explored in section 6 shows that, at prevailing leverage ratios and climate beta magnitudes, sponsor-side debt compression alone rarely justifies the resilience investment it would require. This is itself the empirical case for a financing architecture that the sponsor cannot deliver unilaterally.

Section 7 argues that what is needed is not a new financing instrument but a structural reform of how the existing system treats blended capital. Blended finance already exists, what limits it, is the regulatory and institutional architecture surrounding it. In particular the Basel III treatment of credit-mitigated exposures, the recognition of DFI subordination as a credit risk mitigant, FX risk coverage, and the scale at which concessional resources are deployed in subordinated rather than senior positions. The empirical pattern documented in section 5 maps onto some specific reforms: first-loss subordination scaled to storm exposure, structured DFI participation against the sentiment channel,

A Tanzania transaction from our sample illustrates the combined effect: proper regulatory recognition of credit-mitigated exposures, together with concessional substitution in a 30% first-loss tranche, would compress the all-in cost of debt from 8.59% to approximately 3.04% while lifting the lender's return on regulatory equity above the OECD comparator. The second effect is what makes the reform a scaling mechanism rather than a subsidy: the same volume of concessional capital mobilizes more commercial capital because the regulatory architecture finally recognizes the risk mitigation the concessional layer already provides in economic terms.

The contribution we hope to have made is not a definitive account of climate risk pricing in SSA infrastructure, but a first set of project-level, hazard-decomposed estimates together with the architectural scaffolding those estimates support. The central claim is simple: the same volume of concessional capital, deployed within a reformed regulatory framework, can mobilize substantially more commercial capital at meaningfully lower senior rates, and the structure of any such deployment should track the structure of the pricing pattern the empirical evidence has revealed.

10 Bibliography

Abinzano, I., Corredor, P., & Mansilla-Fernández, J. M. (2026). Physical climate risk and banks' credit risk: Worldwide evidence. *The North American Journal of Economics and Finance*, *81*, 102550. https://doi.org/10.1016/j.najef.2025.102550

African Development Bank. (2026). *AfDB Projects & Operations*. African Development Bank. https://www.afdb.org/en/documents/projects-operations

African Development Bank Group. (2019, May 15). *Africa Economic Brief - Closing Africa's Infrastructure Gap: Innovative Financing and Risks* [Text]. African Development Bank Group. African Development Bank Group. https://www.afdb.org/en/documents/document/africa-economic-brief-closing-africas-infrastructure-gap-innovative-financing-and-risks-23430

African Development Bank Group. (2024a). *African Development Bank Group Board of Governors approves $117 billion General Callable Capital Increase*. https://www.afdb.org/en/news-and-events/press-releases/african-development-bank-group-board-governors-approves-117-billion-general-callable-capital-increase-71459

African Development Bank Group. (2024b, August 2). *Scaling up financing is key to accelerating Africa's structural transformation* [Text]. African Development Bank Group. African Development Bank Group. https://www.afdb.org/en/news-and-events/scaling-financing-key-accelerating-africas-structural-transformation-73244

African Legal Support Facility. (2024). *African Legal Support Facility Annual Report*. https://africanlegalsupportfacility.com/docs/Report%20Layout%20English%20v27%20-%20Justified%20Text%20v5%20Web%20Version.pdf

Assab, A. (2024). Theoretical Foundation for Pricing Climate-Related Loss and Damage in Infrastructure Financing. *Journal of Risk and Financial Management*, *17*(4), 133. https://doi.org/10.3390/jrfm17040133

Assab, A. (2025). Did we open the flood gates? Climate risk and infrastructure loans probability of default. *Journal of Climate Finance*, *11*, 100066. https://doi.org/10.1016/j.jclimf.2025.100066

Basel Committee on Banking Supervision (Ed.). (2024). *Core principles for effective banking supervision*. Bank for International Settlements. https://www.bis.org/bcbs/publ/d573.pdf

Buhr, B., Volz, U., Donovan, C., & Kling, G. (2018). *Climate Change and the Cost of Capital in Developing Countries*. Imperial College London; SOAS University of London; UN Environment. https://soas-repository.worktribe.com/output/381483/climate-change-and-the-cost-of-capital-in-developing-countries?__cf_chl_tk=Yk4KhqfSdXK9WEp37W6gWfiz0PFIhbssxFZHqZ1Vhx8-1778503113-1.0.1.1-8nwL2nENocpBHe6cH2SIaBf__Bfy5ZbihdXwCrNjQTM

Cevik, S., & Jalles, J. T. (2022). This changes everything: Climate shocks and sovereign bonds∗. *Energy Economics*, *107*, 105856. https://doi.org/10.1016/j.eneco.2022.105856

Chinzara, Z., Dessus, S., & Dreyhaupt, S. (2023). *Infrastructure in Africa: How Institutional Reforms Can Attract More Private Investment*. International Finance Corporation (IFC). https://www.ifc.org/content/dam/ifc/doc/2023/working-paper-infrastructure-in-africa.pdf

Daida, D. S., Yadav, D. Y., Sontakke, D. K. K., Bagkar, D. A., Kaustubh, D., Sontakke, A., & Pathak, D. A. (2025). Behavioral Finance and Investor Psychology: Understanding Market Volatility in Crisis Scenarios. *Advances in Consumer Research.*

Dato, P., Dioha, M., Hessou, H., Houenou, B., Mukhaya, B., Okyere, M. A., & Odarno, L. (2025). Computation of weighted average cost of capital (WACC) in the power sector for African countries and the implications for country-specific electricity technology cost. *Applied Energy*, *397*, 126333. https://doi.org/10.1016/j.apenergy.2025.126333

DFO - Flood Observatory (DFO). (2026). *Global Flood Records* (Version 0.9.0) [Dataset]. Zenodo. https://doi.org/10.5281/ZENODO.19288170

EBA. (2022). *REPORT ON THE APPLICATION OF THE INFRASTRUCTURE SUPPORTING FACTOR* (p. 70). https://www.eba.europa.eu/sites/default/files/document_library/Publications/Reports/2022/1042869/Report%20on%20the%20application%20of%20the%20Infrastructure%20Supporting%20Factor.pdf

Eberenz, S., Lüthi, S., & Bresch, D. N. (2021). Regional tropical cyclone impact functions for globally consistent risk assessments. *Natural Hazards and Earth System Sciences*, *21*(1), 393–415. https://doi.org/10.5194/nhess-21-393-2021

Egbétoké, A., & Ureche-Rangau, L. (2026). Vulnerability to climate change and funding squeeze in Sub-Saharan Africa. *Journal of International Financial Markets, Institutions and Money*, *107*, 102281. https://doi.org/10.1016/j.intfin.2025.102281

European Commission. Joint Research Centre. (2016). *Global flood depth-damage functions: Methodology and the database with guidelines.* Publications Office. https://doi.org/10.2760/16510

Gbohoui, W. (2023). Sub-Saharan Africa's Risk Perception Premium: In the Search of Missing Factors. *IMF Working Papers*, *2023*(130), 1. https://doi.org/10.5089/9798400242144.001

Goko, C. (2025). *African development banks set to expand lending as capital buffers rise, S&P says*. CNBC Africa. https://www.cnbcafrica.com/2025/african-development-banks-set-to-expand-lending-as-capital-buffers-rise-sp-says

Gourio, F. (2012). Disaster Risk and Business Cycles. *American Economic Review*, *102*(6), 2734–2766. https://doi.org/10.1257/aer.102.6.2734

Green Street Infrastructure. (2026). *IJGlobal* [Dataset]. https://eu.greenstreet.com/products/infrastructure/

Hallegatte, S., Rentschler, J., & Rozenberg, J. (2019). *Lifelines: The Resilient Infrastructure Opportunity*. World Bank Group (Open Knowledge Repository). https://openknowledge.worldbank.org/entities/publication/c3a753a6-2310-501b-a37e-5dcab3e96a0b

Harrington, L. J., & Otto, F. E. L. (2020). Reconciling theory with the reality of African heatwaves. *Nature Climate Change*, *10*(9), 796–798. https://doi.org/10.1038/s41558-020-0851-8

Hughes, G., Chinowsky, P., & Strzepek, K. (2010). *The Costs of Adapting to Climate Change for Infrastructure* (Discussion Paper No. 56660). The World Bank.

IATI. (2026). *International Aid Transparency Initiative Datastore* [Dataset]. IATI. https://iatistandard.org/en/

Idris, H. (2025). A Systematic Literature Review of Investor Financial Behavior: Determinants, Biases, and Decision-Making Patterns. *Golden Ratio of Data in Summary*, *5*(4), 1053–1063. https://doi.org/10.52970/grdis.v5i4.1022

Ijjasz-Vasquez, & Saghir, J. (2023). *Climate adaptation finance in Africa*. https://www.brookings.edu/articles/climate-adaptation-finance-in-africa/

Intergovernmental Panel On Climate Change (IPCC). (2023). Climate Change 2022 – Impacts, Adaptation and Vulnerability: Working Group II Contribution to the Sixth Assessment

Report of the Intergovernmental Panel on Climate Change (1st ed.). Cambridge University Press. https://doi.org/10.1017/9781009325844

International Chamber of Commerce. (2025). *Enhancing climate finance in EMDEs through prudential regulatory clarification and reform*. https://iccwbo.org/news-publications/policies-reports/targeted-regulatory-reforms-offer-opportunity-to-boost-climate-finance-flows

International Monetary Fund. (2025). *Regional economic outlook. Sub-Saharan Africa: Recovery interrupted*. International Monetary Fund. https://www.imf.org/-/media/files/publications/reo/afr/2025/april/english/text.pdf

Ipcc. (2022). Global Warming of 1.5°C: IPCC Special Report on Impacts of Global Warming of 1.5°C above Pre-industrial Levels in Context of Strengthening Response to Climate Change, Sustainable Development, and Efforts to Eradicate Poverty (1st ed.). Cambridge University Press. https://doi.org/10.1017/9781009157940

Javadi, S., & Masum, A.-A. (2021). The impact of climate change on the cost of bank loans. *Journal of Corporate Finance*, *69*, 102019. https://doi.org/10.1016/j.jcorpfin.2021.102019

Katenova, M., Frolova, Y., & Schmunkamp, P. (2025). Behavioral Finance in the sphere of investment: Systematic Review of Literature between 2020 and 2025. *F1000Research*, *14*, 949. https://doi.org/10.12688/f1000research.166104.1

Kempa, K. (2026). Physical climate risk and the pricing of bank loans. *Journal of Environmental Economics and Management*, *137*, 103280. https://doi.org/10.1016/j.jeem.2025.103280

Kling, G., Lo, Y. C., Murinde, V., & Volz, U. (2025). Climate vulnerability and the cost of debt. *Oxford Open Economics*, *4*, odaf003. https://doi.org/10.1093/ooec/odaf003

Kling, G., Volz, U., Murinde, V., & Ayas, S. (2021). The impact of climate vulnerability on firms' cost of capital and access to finance. *World Development*, *137*, 105131. https://doi.org/10.1016/j.worlddev.2020.105131

KPMG. (2025). Changes in MNB ICAAP-ILAAP-BMA methodology manuals (p. 4).

Kruse, T., Mohnen, M., & Sato, M. (2024). Do Financial Markets Respond to Green Opportunities? *Journal of the Association of Environmental and Resource Economists*, *11*(3), 549–576. https://doi.org/10.1086/727370

Laws, A., Lemaire, T., Pafadnam, R., Spatafora, N., & Khandelwal, K. (2025). Breaking the Trend: Debt Stabilization in Sub-Saharan Africa. *IMF Notes*, *2025*(001), 1. https://doi.org/10.5089/9798229008679.068

Li, D., Saigal, R., & Adriaens, P. (2024). Impact of Flooding and Drought Risks on the Cost of Bond Financing for Water Utilities. *Environmental Science & Technology*, *58*(32), 14068–14077. https://doi.org/10.1021/acs.est.4c01863

Lu, Q., & Wilson, C. (2024). Infrastructure financing in Africa. *Journal of International Financial Markets, Institutions and Money*, *91*, 101954. https://doi.org/10.1016/j.intfin.2024.101954

Mathiasen, K., & Martinez, N. (2025). *The African Development Fund Replenishment and the Resource Curse of 2025*. Center for Global Development. https://www.cgdev.org/publication/african-development-fund-replenishment-and-resource-curse-2025

Metreau, E., Young, E., & Eapen, S. G. (2024). *World Bank country classifications by income level for 2024-2025* (Data Blog) [Blog]. World Bank Group.

Muñoz-Sabater, J., Dutra, E., Agustí-Panareda, A., Albergel, C., Arduini, G., Balsamo, G., Boussetta, S., Choulga, M., Harrigan, S., Hersbach, H., Martens, B., Miralles, D. G., Piles, M., Rodríguez-Fernández, N. J., Zsoter, E., Buontempo, C., & Thépaut, J.-N. (2021). ERA5-Land:

A state-of-the-art global reanalysis dataset for land applications. *Earth System Science Data*, *13*(9), 4349–4383. https://doi.org/10.5194/essd-13-4349-2021

Nguyen, D. D., Ongena, S., Qi, S., & Sila, V. (2022). Climate Change Risk and the Cost of Mortgage Credit. *Review of Finance*, *26*(6), 1509–1549. https://doi.org/10.1093/rof/rfac013

OECD. (2025). *OECD DAC Blended Finance Guidance 2025* [Best Practices in Development Co-operation]. https://doi.org/10.1787/e4a13d2c-en

OECD & United Nations Capital Development Fund. (2019). *Blended Finance in the Least Developed Countries 2019*. OECD Publishing. https://doi.org/10.1787/1c142aae-en

Ondraczek, J., Komendantova, N., & Patt, A. (2015). WACC the dog: The effect of financing costs on the levelized cost of solar PV power. *Renewable Energy*, *75*, 888–898. https://doi.org/10.1016/j.renene.2014.10.053

Shefrin, H. (2023). *The Behavioral Economics and Politics of Global Warming: Unsettling Behaviors* (1st ed.). Cambridge University Press. https://doi.org/10.1017/9781009454919

Soroka, S., Fournier, P., & Nir, L. (2019). Cross-national evidence of a negativity bias in psychophysiological reactions to news. *Proceedings of the National Academy of Sciences*, *116*(38), 18888–18892. https://doi.org/10.1073/pnas.1908369116

Stiglitz, J. E., & Weiss, A. (1981). Credit Rationing in Markets with Imperfect Information. *The American Economic Review*, *71*(3), 393–410.

Tversky, A., & Kahneman, D. (1974). Judgment under Uncertainty: Heuristics and Biases: Biases in judgments reveal some heuristics of thinking under uncertainty. *Science*, *185*(4157), 1124–1131. https://doi.org/10.1126/science.185.4157.1124

United Nations Conference on Trade and Development. (2025). *A world of debt 2025: It is time for reform*.

University of Notre Dame. (2026). *Notre Dame Global Adaptation Initiative Country Index (ND-GAIN)* [Dataset]. https://gain.nd.edu/

Verschuur, J., Fernández-Pérez, A., Mühlhofer, E., Nirandjan, S., Borgomeo, E., Becher, O., Voskaki, A., Oughton, E. J., Stankovski, A., Greco, S. F., Koks, E. E., Pant, R., & Hall, J. W. (2024). Quantifying climate risks to infrastructure systems: A comparative review of developments across infrastructure sectors. *PLOS Climate*, *3*(4), e0000331. https://doi.org/10.1371/journal.pclm.0000331

Webersinke, N., Kraus, M., Bingler, J. A., & Leippold, M. (2021). *ClimateBert: A Pretrained Language Model for Climate-Related Text* (Version 3). arXiv. https://doi.org/10.48550/ARXIV.2110.12010

World Bank Group. (2026). *World Bank Projects & Operations*. World Bank Group. https://projects.worldbank.org/en/projects-operations/project-search

World Bank Group, & Miyamoto International. (2019). *Overview of Engineering Options for Increasing Infrastructure Resilience* (Institutional No. 7183546). https://documents1.worldbank.org/curated/en/474111560527161937/pdf/Final-Report.pdf

World Meteorological Organization. (2024, September 2). *Africa faces disproportionate burden from climate change and adaptation costs*. https://wmo.int/news/media-centre/africa-faces-disproportionate-burden-from-climate-change-and-adaptation-costs

Zenios, S. A. (2024). The climate-sovereign debt doom loop: What does the literature suggest? *Current Opinion in Environmental Sustainability*, *67*, 101414. https://doi.org/10.1016/j.cosust.2024.101414

11 Appendix

11.1 Downloading Project summary & financial data

11.1.1 Full Methodology for downloading AfDB project appraisals using Python

We extracted project appraisal reports from the International Aid Transparency Initiative (IATI) Datastore (International Aid Transparency Initiative, n.d.), a centralised repository of development finance data published in a standardised XML format. We submitted an HTTP GET request to the Datastore's activity endpoint (/api/1/access/activity.xml), filtered by the reporting organisation reference code XM-DAC-46002, which uniquely identified the African Development Bank (AfDB). We set a streaming parameter to True to accommodate the anticipated size of the response, and supplied a browser-like User-Agent header to minimise the risk of request rejection.

We parsed the saved XML file using Python's xml.etree.ElementTree module, iterating over every <iati-activity> node in the document tree. For each activity, we extracted the following structured fields: the unique IATI project identifier, the project title, the recipient country (both ISO code and full name), and the primary sector. We further enumerated all associated <document-link> elements and retrieved the document URL, title, and category code. We deliberately retained projects lacking any document links as null-URL records, ensuring that no project metadata was silently discarded. We consolidated the resulting records into a pandas DataFrame and exported them to a CSV file.

We subsequently filtered the full document inventory to isolate records of specific relevance to our research. We applied two Boolean conditions conjunctively: the document URL field had to be non-null and non-empty, and the document title had to match the exact string "Appraisal Report". We removed duplicate URLs via deduplication and exported the resulting subset — representing Project Appraisal Reports (PARs) with valid download links — to a separate CSV file.

We observed that many of the document URLs retrieved from the IATI data did not point directly to PDF files, but instead to an intermediate web viewer whose actual file path was encoded as a query parameter. We therefore applied a URL-parsing function to each entry: where a viewer pattern was detected, we decoded the real PDF URL from the query string using urllib.parse, and stripped fragment identifiers (i.e., # anchors) in all cases. We wrote the cleaned, direct PDF URLs back into the DataFrame and re-exported it to disk.

With a clean list of direct PDF URLs in hand, we proceeded to download the documents using Selenium WebDriver controlling a Chrome browser. We adopted this browser-based approach — rather than a simple HTTP request — because some document URLs were subject to redirects or JavaScript-rendered download triggers that would defeat a plain requests.get() call.

Prior to initiating downloads, we specified a target country via a two-letter ISO 3166-1 alpha-2 code and enforced a geographic exclusion list that prevented the retrieval of documents associated with North African countries (Morocco, Libya, Algeria, Tunisia, Egypt). We created the download destination folder and initialized a tracker CSV from any PDF files already present on disk, enabling resumable execution across sessions.

We then filtered the appraisal report inventory to the target country and excluded entries whose filename was already present in the local folder. For each remaining URL, we navigated the browser to the PDF link, having configured Chrome's download preferences to save PDFs directly to disk. We implemented a polling loop that checked the download folder at one-second intervals for up to fifteen seconds, confirming file arrival by filename. We detected and deleted duplicate files saved by the browser with a suffix, and logged each successful or failed download to the tracker CSV. We introduced a randomized inter-request delay of between one and six seconds to reduce server load and mitigate the risk of rate-limiting.

Table 11-1 summarizes the Project Appraisal Reports retrieved from the AfDB project portal, showing the number of documents successfully downloaded relative to the total available, by country.

Code	Country	Downloaded	Total	% downloaded
MU	Mauritius	28	31	90.3%
SO	Somalia	44	52	84.6%
SZ	Eswatini	30	37	81.1%
SS	South Sudan	38	50	76.0%
SD	Sudan	38	51	74.5%
NG	Nigeria	105	141	74.5%
GQ	Equatorial Guinea	14	19	73.7%
GM	Gambia	52	71	73.2%
BJ	Benin	59	81	72.8%
KM	Comoros	32	44	72.7%
TG	Togo	40	57	70.2%
SC	Seychelles	23	33	69.7%
ZW	Zimbabwe	53	76	69.7%

Code	Country	Downloaded	Total	% downloaded
SL	Sierra Leone	37	54	68.5%
ZM	Zambia	43	63	68.3%
ST	Sao Tome and Principe	23	34	67.6%
CF	Central African Republic	45	67	67.2%
LR	Liberia	44	66	66.7%
GA	Gabon	28	43	65.1%
GH	Ghana	67	103	65.0%
MR	Mauritania	42	65	64.6%
RW	Rwanda	65	101	64.4%
CI	Cote d'Ivoire	69	110	62.7%
CM	Cameroon	55	90	61.1%
TD	Chad	47	79	59.5%
TZ	Tanzania	70	118	59.3%
CG	Congo	21	36	58.3%
MZ	Mozambique	60	107	56.1%
CV	Cape Verde	32	57	56.1%
LS	Lesotho	20	36	55.6%
SN	Senegal	81	147	55.1%
NE	Niger	37	69	53.6%
MW	Malawi	49	95	51.6%

Code	Country	Downloaded	Total	% downloaded
UG	Uganda	47	92	51.1%
GW	Guinea-Bissau	23	46	50.0%
MG	Madagascar	46	95	48.4%
ER	Eritrea	11	23	47.8%
BI	Burundi	18	63	28.6%
KE	Kenya	32	131	24.4%
ET	Ethiopia	21	89	23.6%
DJ	Djibouti	8	43	18.6%
AO	Angola	11	60	18.3%
GN	Guinea	10	69	14.5%
ML	Mali	11	83	13.3%
ZA	South Africa	6	49	12.2%
CD	Dem. Rep. of Congo	11	103	10.7%
BF	Burkina Faso	0	96	0.0%
BW	Botswana	0	28	0.0%
	Total	1746	3353	52.1%

Table 11-1: Project Appraisal Reports retrieved from the AfDB website

11.1.2 Full Methodology for downloading WBG project appraisals using Python

We retrieved World Bank Project Appraisal Documents (PADs) by submitting paginated HTTP GET requests to the World Bank's open document search API. We filtered results to documents classified under the African administrative regions (Western and Central Africa, and Eastern and Southern Africa), within the thematic area of Infrastructure Economics and Finance, and of document type "Project Appraisal Document." We requested 200 results per page, sorted by date in descending order, and iterated through pages by incrementing an offset parameter until the API returned fewer results than the page size, at which point we inferred that the final page had been reached. Throughout the pagination loop, we tracked previously seen document identifiers to prevent the inclusion of duplicates, appending each new record — comprising the document ID, title, date, and PDF URL — to a master list. A short delay was applied between requests to avoid overwhelming or being blocked by the server.

We loaded the collected records into a pandas DataFrame and retained only those entries for which a PDF URL was available, removing any remaining duplicates. We then iterated over each row and downloaded the corresponding PDF file via a direct HTTP GET request, saving it to a local folder. Files that had already been downloaded in a previous session were identified by their filename on disk and skipped, making the download process resumable. Failed or empty responses were logged to the console

11.2 Extracting key AfDB & WBG project information using an LLM

Having assembled a collection of 1103 project appraisal documents from both the AfDB and WBG, we developed an automated pipeline to extract structured financial and operational data from each PDF using an LLM.

At the outset of each run, we loaded the filenames of all PDFs previously processed successfully, as well as those that had previously failed or been skipped, from persistent logs on disk. This allowed the pipeline to resume seamlessly across multiple sessions without reprocessing files already handled.

Before submitting a document to the language model, we extracted its full text using PyMuPDF and applied a keyword filter. Only documents containing at least one of a predefined set of loan- and credit-related terms — in both English and French — were forwarded for analysis. Documents failing this check were logged as skipped, as their absence of financing-related language indicated they were unlikely to contain the financial variables of interest.

For each document that passed the pre-filter, we constructed a detailed prompt instructing Google Gemini 2.5 Flash to act as a senior infrastructure financial analyst and extract twenty specific variables from the document text. The prompt given was as followed:

" You are a meticulous Senior Infrastructure Financial Analyst. Read the provided project report. Extract the following 20 data points.

CRITICAL INSTRUCTIONS TO PREVENT OMISSIONS:

1. *You must search the entire text. Do not skip sections.*
2. *The report may be in English or French. You must analyze and extract the information accurately regardless of the language.*
3. *Authors may not use the exact variable names. Look for synonyms, implicit data, or financial context in both languages.*
4. *If a value is genuinely missing, or cannot be reasonably deduced, you MUST output exactly: "/!\ NOT FOUND"*

VARIABLES TO EXTRACT:

- *dep_wacc: Weighted Average Cost of Capital (look for WACC, hurdle rate, discount rate) / Coût moyen pondéré du capital (CMPC, taux de rentabilité minimum, taux d'actualisation).*
- *fin_project_size_musd: Total cost or Capex of the project. Convert to Millions of USD if possible, otherwise state the raw amount / Coût total ou Capex du projet. Convertir en millions de dollars américains (USD) si possible, sinon indiquer le montant brut.*
- *fin_cost_equity: Target return on equity, equity IRR, etc. / Objectif de rentabilité des capitaux propres, TRI des capitaux propres, etc.*
- *fin_cost_debt_senior: Interest rate or pricing on the senior debt/loans / Taux d'intérêt ou tarification de la dette senior/des prêts de premier rang.*
- *fin_cost_debt_junior: Interest rate or pricing on subordinated/junior/mezzanine debt / Taux d'intérêt ou tarification de la dette subordonnée/junior/mezzanine.*

- *fin_debt_share: Percentage of total funding coming from debt (leverage ratio) / Pourcentage du financement total provenant de la dette (ratio d'endettement/effet de levier).*
- *fin_equity_share: Percentage of total funding coming from equity / Pourcentage du financement total provenant des capitaux propres.*
- *fin_is_concessional_loan: "Yes" or "No". Look for mentions of soft loans, subsidized rates, grants, or development bank concessional windows / "Yes" ou "No". Rechercher les mentions de prêts à des conditions de faveur, prêts bonifiés, taux subventionnés, subventions ou guichets concessionnels.*
- *fin_junior_debt_funders: Names of institutions providing junior/mezzanine debt / Noms des institutions fournissant la dette junior/mezzanine.*
- *fin_senior_debt_funders: Names of banks/institutions providing the main senior loans / Noms des banques/institutions fournissant les principaux prêts senior.*
- *geo_country: Country where the project is located / Pays où se situe le projet.*
- *geo_subregion: Specific state, province, or geographic subregion / État, province ou sous-région géographique spécifique.*
- *time_financial_close_year: The year the project reached financial close or final investment decision (FID) / L'année où le projet a atteint le bouclage financier ou la décision finale d'investissement (DFI).*
- *proj_lifetime_years: Operating period, concession length, or PPA duration in years / Période d'exploitation, durée de la concession ou durée du PPA (contrat d'achat d'électricité) en années.*
- *sect_sector: Broad sector (e.g., Energy, Transport, Water, Health) / Secteur général (ex: Énergie, Transport, Eau, Santé).*
- *infra_type: Specific type (e.g., Onshore Storm, Toll Road, Desalination Plant) / Type spécifique (ex: Éolien terrestre, Autoroute à péage, Usine de dessalement).*
- *infra_is_climate: "Yes" or "No". Is this project related to climate change mitigation (e.g., renewables, green transit)? / "Yes" ou "No". Ce projet est-il lié à l'atténuation du changement climatique (ex: énergies renouvelables, transports écologiques) ?*
- *clim_has_adaptation: "Yes" or "No". Does the project include climate resilience or adaptation measures (e.g., flood defenses, weather-proofing)? / "Yes" ou "No". Le projet inclut-il des mesures de résilience ou d'adaptation au climat (ex: défenses contre les inondations, protection contre les intempéries) ?*
- *eco_irr: Economic Internal Rate of Return (look for EIRR, ERR, Economic IRR) / Taux de rentabilité économique (TRE, TRIE, rentabilité socio-économique).*
- *fin_irr: Financial Internal Rate of Return (look for FIRR, Project IRR, Financial IRR) / Taux de rentabilité financière (TRF, TRIF, TRI du projet).*

Return the data STRICTLY as a JSON object matching these exact variable names as keys. Do not include markdown formatting or extra text. Output all extracted values in English, even if the source text is in French. "

Upon receiving the model's response, we parsed the JSON output and wrote the extracted values as a row in a structured output file, flushing the buffer immediately after each successful write to guard against data loss in the event of an interruption. For each document, we also counted the number of variables successfully retrieved — defined as those not flagged as missing, null, or empty — providing a real-time measure of extraction quality. Documents that triggered API rate-limit errors were deferred for retry in a subsequent session, while those that failed due to document-level errors were permanently logged as failed and excluded from future runs. Table 11-2 shows the success rate for retreiving different figures.

Metric	Success Rate
WACC	74%
Project Capex (USDm)	96%
Equity IRR	5%
Senior Debt Interest Rate	38%
Junior Debt Interest Rate	1%
Debt Share (%)	91%
Equity Share (%)	80%
Concessional Financing (Yes/No)	100%
Junior Debt Funders	3%
Senior Debt Funders	76%
Country	100%
Subregion	93%
Financial Close Year	96%
Project Lifetime (Years)	82%
Sector	100%
Infrastructure Type	99%
Climate Mitigation? (Yes/No)	100%
Climate Adaptation? (Yes/No)	95%
Economic IRR	84%
Financial IRR	38%

Table 11-2: Success rate in extracting project summary information and financial data from WB/AfDB Project Appraisal Reports

11.3 Climate indicators formulation

11.3.1 Extreme heat event definition from ERA5-land data collection

The definition of the occurrences, duration and severity of extreme heat events relies on the acquisition of high-resolution historical climate data across 49 countries in Sub-Saharan Africa. We collect data from the Copernicus Climate Data Store (CDS) via the cdsapi library to access the ERA5-Land monthly aggregated dataset. We specifically use the ERA5-Land monthly averaged data on single levels, specifically the monthly extreme hot days (MEHD) and the monthly-daily maximum temperature (MDMT). This data provides a gridded reconstruction of the global climate at a native resolution of approximately 9km, covering a temporal span from January 1950 to the present, each variable captures:

- MEHD: number of days with temperature above 35°C each month, providing data used to determine number of occurrences (Nocc) and duration (dh) of extreme heat events,
- MDMT: maximum daily temperature for each month in degrees Celsius (°C), used to determine the severity of each occurrence.

The period of analysis is defined from 1950 to 2024.

The data collection is initialized by constructing a comprehensive spatial reference table for Sub-Saharan Africa. This table comprises 49 countries. To handle the granular nature of the data and comply with API request limits, each country is defined by a geographical bounding box. These boxes are specified in decimal degrees using the WGS-84 coordinate system following the CDS API convention: [North, West, South, East]. The coordinates are calibrated to be sufficiently generous to ensure total coverage of each national landmass while maintaining efficient data volume for the subsequent matrix calculations.

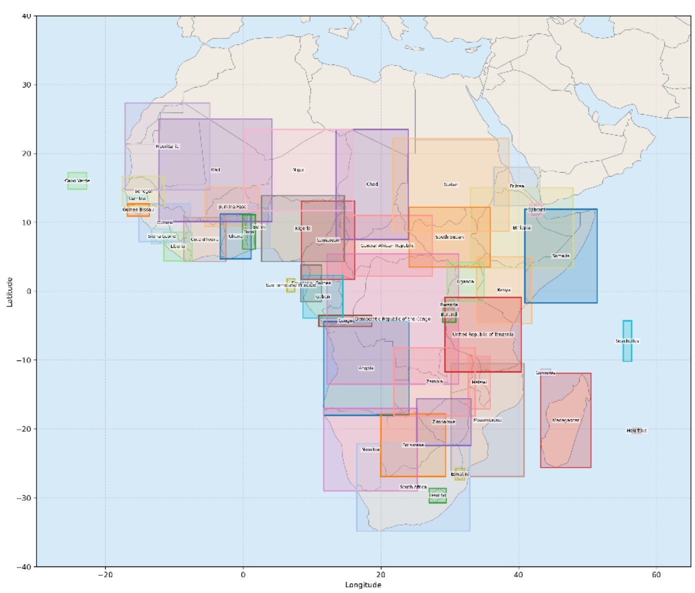

Figure 11-1 Map of the coordinate bounding for all SSA countries in the CDS API ERA5-land data collection

We used a python pipeline that loops through the 49 defined countries, submitting a dedicated request for each. The parameters for each request are listed below.

```
FIXED_PARAMS = {
    "origin":          "era5_land",
    "domain":          "global",
    "period":          "1950_2024",
    "variable":
"monthly_daily_maximum_temperature"                  or
"monthly_extreme_hot_days",
    "bias_adjustment": "no_bias_adjustment",
    "format":          "zip",
}
```

The raw output contained gridded climate matrices. In order to define the occurrence and duration of extreme heat events, and since the data collected for each country is aggregated into a collection of data from individual grid cells, we use the average number of MEHD over all the grid cells that compose each country and count one occurrence if in a given month this count is superior to 2 days. Therefore, a month can't present more than one occurrence. Additionally, we do not count a single heatwave for consecutive months that are above this threshold. This means that if we find in a given country there were 3 days average extreme hot days in October, and 5 in November, we still consider one extreme heat event in October and one in November. The duration is the average MEHD of a month when the average MEHD is superior to 2. The images below show the occurrences and duration of extreme heat events for every country.

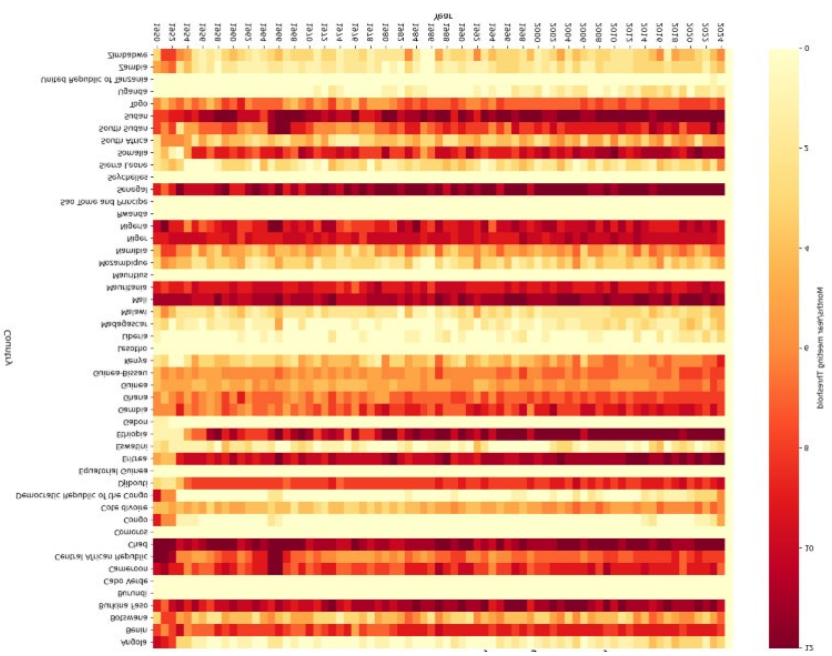

Figure 11-2 Heatmap of the yearly number of occurences of extreme heat events for all studied SSA countries

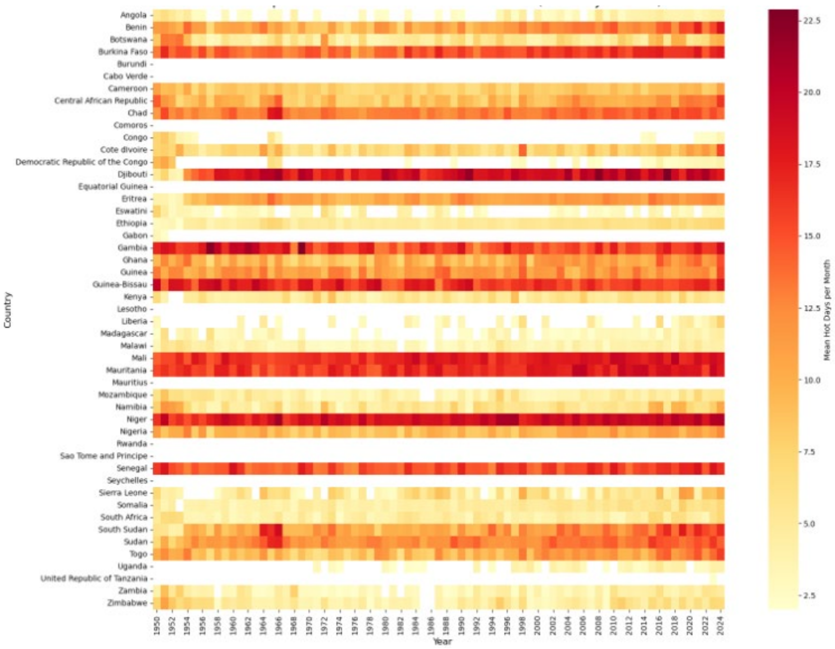

Figure 11-3 Heatmap of the yearly average duration of extreme heat events for all studied SSA countries

We use the MDMT variable to determine severity, using simply the value in degrees Celsius (°C) of every month during which we considered there was an occurrence of an extreme heat event.

11.3.2 Socioeconomic indicator: affected population, CIpop

The socioeconomic indicator is constructed using:

- EM-DAT data on number of occurrences for floods and storms, duration and number of affected people for each recorded event,
- World Bank data on population.

We compute the CI_pop indicator for floods and storms using country / year matrices for yearly occurrences (each line corresponding to a year from 1960 to 2025) and country / year matrices for duration and affected people for each event (lines are years, however there can be more than one line for a given year if there are multiple occurrences in that same year). The number of affected people values are divided by the population of the country in the year of each event, resulting in affected population as a percentage of total country population. We multiply each cell from the duration matrix to the corresponding cell from the affected populations matrix. For each country we compute the cumulative average at every year of the sample, resulting in a country / year matrix of cumulative average (same dimension matrix as for occurrences). A cumulative average number of yearly occurrences matrix is also created. These two matrixes are multiplied by each other (that is, the matrix of cumulative average number of yearly occurrences and the matrix of cumulative average affected population times duration). Finally, for each project the resulting indicator corresponding to the country and financial close year of the project is multiplied by the duration of the project to consider the long-term exposure to the climate-related risks.

The equation below summarizes these calculations.

$$CI_{pop,e,t} = d_p * \frac{\sum_{t=0}^{t}\left(N_{occ,e,t}\right)}{t} * \frac{\sum_{t=0}^{t}\left(d_e\right)}{t} * \frac{\sum_{t=0}^{t}\left(\frac{A_{pop}}{Pop_t}\right)}{t}$$

For the heat indicator, we do not use an affected population indicator and consider therefore that 100% of the population is affected when there is an occurrence.

The table below details the variation of climate indicators across the different projects of our sample.

Concessional projects (WBG, AfDB)	Private projects (IJGlobal)

ID	country(ies)	close year	dp	CI_pop FLOOD	CI_pop WNID	CI_pop HEAT
1	Senegal	1986	6	0.01	0.00	7.73
2	Rwanda	2009	20	5.84	0.00	0.00
3	Mozambique	2010	20	7.80	1.57	6.55
4	Tanzania	2010	30	1.10	0.00	0.00
5	Uganda	2001	35	0.27	0.00	0.00
6	Nigeria	2001	20	0.24	0.00	8.50
7	Cameroon	2012	50	0.43	0.00	9.29
8	Côte d'Ivoire, Liberia, Sierra Leone, Guinea	2012	30	2.01	0.01	8.39
9	Uganda	2001	30	0.24	0.00	0.00
10	Ethiopia, Kenya	2012	25	3.20	0.00	7.83
11	Zambia	2013	30	7.99	0.00	6.40
12	Burundi, Rwanda, Tanzania	2014	50	8.17	0.92	0.00
13	Guinea	2002	15	1.28	0.00	7.58
14	Burundi	2014	50	0.44	0.92	0.00
15	Ethiopia	2014	20	0.87	0.00	7.59
16	Uganda	2016	40	2.90	0.00	0.00
17	Seychelles	2017	6	0.02	0.08	0.00
18	Togo	2017	6	1.42	0.00	6.73
19	Ethiopia	2018	30	1.29	0.00	8.06
20	Mauritania	2018	26	1.53	0.00	9.32
21	Cameroon	2018	50	0.47	0.00	9.29

22	Guinea	2019	20	1.36	0.00	7.95
23	Mozambique	2020	25	8.15	1.97	6.84
24	Mali	2019	40	1.34	0.00	10.00
25	Eritrea	2004	25	0.00	0.03	8.54
26	Burkina Faso	2005	20	2.43	0.00	9.06
27	Rwanda	2005	6	3.16	0.00	0.00
28	Malawi, Mozambique	2007	30	9.18	2.30	7.02
29	Burkina Faso	2007	25	3.22	0.00	9.32
30	Ghana	2007	25	2.30	0.00	8.40
31	Angola	2015	25	1.91	0.00	5.72
32	Uganda	2014	25	2.14	0.00	0.00
33	Zambia	2019	30	7.71	0.00	6.40
34	Benin	1999	20	4.79	0.00	8.44
35	Benin	2018	20	6.76	0.01	8.47
36	Benin	2013	25	7.65	0.01	8.71
37	Benin	2023	8	4.21	0.00	7.44
38	Benin	2024	6	3.53	0.00	7.12
39	Benin	2010	20	7.12	0.01	8.46
40	Benin	2025	25	7.13	0.01	8.73
41	Benin	2018	30	7.93	0.01	8.93
42	Benin	2017	40	8.84	0.01	9.25
43	Benin	2019	25	7.35	0.01	8.72
44	Benin	2015	15	6.10	0.00	8.14
45	Cabo Verde	2021	3	0.03	0.01	0.00
46	Cabo Verde	2018	20	0.02	0.05	0.00
47	Cabo Verde	2022	25	0.20	0.06	0.00
48	Cameroon	2014	20	0.18	0.00	8.25
49	Cameroon	2013	50	0.42	0.00	9.29
50	Cameroon	2002	20	0.01	0.00	8.26
51	Cameroon	2021	25	0.24	0.00	8.52

52	Cameroon	2010	20	0.17	0.00	8.25
53	Cameroon	2009	50	0.42	0.00	9.29
54	Cameroon	2009	50	0.42	0.00	9.29
55	Cameroon	2021	30	0.28	0.00	8.72
56	Cameroon	2016	20	0.19	0.00	8.26
57	Cameroon	2024	20	1.51	0.00	8.27
58	Cameroon	2015	15	0.15	0.00	7.93
59	Congo, Cameroon	2009	20	1.59	0.00	8.25
60	Cameroon	2002	40	0.02	0.00	9.05
61	Cabo Verde	2013	20	0.02	0.06	0.00
62	Cabo Verde	2013	25	0.03	0.07	0.00
63	Chad	2025	25	7.27	0.00	9.23
64	Comoros	2017	40	1.53	1.46	0.00
65	Congo	2012	30	2.08	0.00	5.27
66	Congo	2016	15	1.13	0.00	4.42
67	Côte d'Ivoire	2018	25	0.00	0.00	7.50
68	Côte d'Ivoire	2018	20	0.00	0.00	7.25
69	Côte d'Ivoire	2017	10	0.00	0.00	6.46
70	Côte d'Ivoire	2022	30	0.00	0.00	7.72
71	Côte d'Ivoire	2025	25	0.00	0.00	7.53
72	Côte d'Ivoire	2021	30	0.00	0.00	7.72
73	Côte d'Ivoire	2016	3	0.00	0.00	5.10
74	Djibouti	2013	50	10.00	0.24	9.66
75	Djibouti	2013	6	4.09	0.03	7.27
76	Democratic Republic of the Congo	2019	20	0.10	0.00	5.35
77	Eritrea	2016	25	0.00	0.03	8.57
78	Eswatini	2018	25	4.79	10.00	5.17
79	Eswatini	2021	24	4.57	9.52	5.12
80	Ethiopia	2010	50	1.93	0.00	8.60
81	Ethiopia	2011	20	0.90	0.00	7.57

82	Ethiopia	2014	40	1.56	0.00	8.37
83	Ethiopia	2017	40	1.65	0.00	8.38
84	Gabon	2018	20	1.38	0.16	1.19
85	Gabon	2019	20	1.37	0.15	1.18
86	Ghana	2006	25	1.51	0.00	8.40
87	Ghana	2017	30	4.56	0.00	8.63
88	Ghana	2019	20	3.59	0.00	8.18
89	Ghana	2014	50	3.63	0.00	9.20
90	Ghana	2009	40	3.27	0.00	8.93
91	Ghana	2019	20	3.59	0.00	8.18
92	Guinea-Bissau	2015	40	1.90	0.03	9.40
93	Kenya	2009	50	4.54	0.00	7.56
94	Kenya	2010	50	4.71	0.00	7.57
95	Kenya	2017	35	3.91	0.00	7.24
96	Kenya	2019	20	2.97	0.00	6.63
97	Kenya	2013	20	2.79	0.00	6.57
98	Kenya	2018	20	2.87	0.00	6.62
99	Kenya	2013	40	4.26	0.00	7.35
100	Kenya	2016	20	2.78	0.00	6.59
101	Kenya	2016	20	2.78	0.00	6.59
102	Kenya and Ethiopia	2011	50	4.70	0.00	8.60
103	Lesotho	2013	20	1.72	0.22	0.00
104	Lesotho	2016	30	2.24	0.32	0.00
105	Lesotho	2009	30	2.42	0.36	0.00
106	Lesotho	2022	25	1.81	0.26	0.00
107	Lesotho	2013	10	0.97	0.11	0.00
108	Lesotho	2019	30	2.16	0.30	0.00
109	Liberia	2013	20	0.08	0.00	3.39
110	Liberia	2024	4	0.04	0.00	1.79
111	Liberia	2021	20	0.12	0.00	3.35

112	Liberia	2016	40	0.25	0.01	4.08
113	Liberia	2019	30	0.18	0.01	3.83
114	Madagascar	2013	20	0.12	5.82	4.81
115	Madagascar	2014	25	0.15	6.66	5.07
116	Malawi	2013	15	2.87	0.02	5.73
117	Mauritania	2012	5	0.37	0.00	7.46
118	Mauritius	2023	30	0.00	3.41	0.00
119	Mauritius	2014	20	0.00	2.47	0.00
120	Mozambique	2012	20	7.70	1.54	6.54
121	Mozambique	2012	20	7.70	1.54	6.54
122	Mozambique	1999	30	5.33	2.64	7.00
123	Mozambique	2013	30	8.88	2.17	7.01
124	Mozambique	1999	20	4.32	1.87	6.54
125	Mozambique	2016	20	7.67	1.44	6.58
126	Burundi and Rwanda	2012	20	5.68	0.39	0.00
127	Congo, Cameroon	2009	50	3.07	0.00	9.29
128	Malawi, Zambia	2013	20	6.82	0.03	6.06
129	Gabon, Congo	2013	20	1.50	0.17	4.80
130	The Gambia, Senegal	2011	30	1.98	1.14	9.60
131	Zambia	2010	50	9.70	0.00	6.96
132	Côte d'Ivoire, Guinea, Liberia	2014	20	0.08	0.00	3.37
133	Nigeria	2008	30	0.50	0.00	8.96
134	Niger	2008	30	1.99	0.00	9.61
135	Niger	2025	6	3.46	0.00	7.81
136	Niger	2019	20	4.15	0.00	9.16
137	Niger	2012	25	3.61	0.00	9.41
138	Nigeria	2019	20	3.36	0.00	8.52
139	Nigeria	2011	20	0.51	0.00	8.51
140	Nigeria	2019	6	1.42	0.00	7.17
141	Nigeria	2013	3	0.84	0.00	6.37

142	Nigeria	2014	30	4.41	0.00	8.97
143	Uganda	2011	25	2.22	0.00	0.00
144	Uganda	2013	20	1.84	0.00	0.00
145	Uganda	2022	20	1.66	0.00	0.00
146	Uganda	2023	20	1.64	0.00	0.00
147	Uganda	2016	20	1.77	0.00	0.00
148	Uganda	2015	20	1.79	0.00	0.00
149	Nigeria	2019	20	3.36	0.00	8.52
150	Rwanda	2014	20	5.58	0.00	0.00
151	Tanzania	2020	50	1.51	0.20	0.00
152	Tanzania	2018	25	0.86	0.00	0.00
153	Tanzania	2025	20	1.87	0.09	0.00
154	Tanzania	2015	25	0.89	0.00	0.00
155	Togo, Burkina Faso	2012	20	3.51	0.00	9.07
156	Togo	2022	20	3.38	0.00	8.10
157	Togo	2019	15	2.74	0.00	7.77
158	Togo	2023	30	4.25	0.00	8.56
159	Uganda	2020	20	1.68	0.00	0.00
160	Uganda	2020	30	2.28	0.01	0.00
161	Uganda	2019	10	0.96	0.00	0.00
162	Uganda	2008	40	3.15	0.00	0.00
163	Uganda	2009	50	3.57	0.00	0.00
164	Uganda	2015	20	1.79	0.00	0.00
165	Uganda	2016	40	2.90	0.00	0.00
166	Uganda	2018	20	1.72	0.00	0.00
167	Zambia	2013	50	9.52	0.00	6.97
168	Zambia	2015	25	7.38	0.00	6.20
169	Zambia	2016	25	7.33	0.00	6.19
170	Zambia	2015	20	6.74	0.00	5.94
171	Zambia	2015	30	7.91	0.00	6.40

172	Sierra Leone	2024	17	0.17	0.01	5.72
173	Mozambique	2024	9	5.27	1.42	5.74
174	South Africa	2018	18	0.17	0.30	6.54
175	South Africa	2018	17	0.16	0.27	6.44
176	South Africa	2018	15	0.14	0.24	6.31
177	South Africa	2018	15	0.14	0.25	6.33
178	South Africa	2018	17	0.16	0.28	6.48
179	South Africa	2018	17	0.16	0.27	6.45
180	South Africa	2018	17	0.15	0.27	6.42
181	South Africa	2018	17	0.16	0.28	6.46
182	South Africa	2018	17	0.16	0.28	6.46
183	Tanzania	2016	17	0.61	0.00	0.00
184	Mali	2024	11	1.38	0.00	8.57
185	Namibia	2023	9	4.06	0.00	6.62
186	Nigeria	2020	9	2.01	0.00	7.67
187	Democratic Republic of the Congo	2016	9	0.03	0.00	4.47
188	Nigeria	2010	15	0.40	0.00	8.18
189	Nigeria	2006	15	0.25	0.00	8.18
190	Zimbabwe	2007	9	0.82	0.00	6.01
191	Ghana	2014	9	1.07	0.00	7.31
192	Ghana	2016	16	1.61	0.00	7.92
193	Gabon	2019	11	0.84	0.09	0.80
194	Zambia	2015	17	6.29	0.00	5.76
195	Botswana	2021	9	1.27	0.00	6.63
196	Burkina Faso	2015	9	1.66	0.00	8.22
197	Kenya	2018	9	1.66	0.00	5.76
198	Nigeria	2007	15	0.27	0.00	8.18
199	Uganda	2017	20	1.74	0.00	0.00
200	Zambia	2006	9	1.97	0.00	5.07
201	Liberia	2013	9	0.04	0.00	2.59

202	Botswana	2011	9	1.44	0.00	6.63
203	Malawi, Mozambique	2018	18	7.19	1.28	6.43
204	South Africa	2019	17	0.16	0.27	6.45
205	Senegal	2017	15	1.08	0.53	8.83
206	Senegal	2015	15	1.09	0.55	8.83
207	Kenya	2006	9	1.49	0.00	5.67
208	Kenya	2012	9	1.59	0.00	5.70
209	Nigeria	2007	11	0.20	0.00	7.86
210	Zambia	2003	9	1.18	0.00	5.03
211	Tanzania	2013	9	0.37	0.00	0.00
212	South Africa	2001	9	0.01	0.19	5.74
213	Botswana	2003	9	1.46	0.00	6.62
214	Uganda	2009	11	1.21	0.00	0.00
215	Ghana	2008	15	1.63	0.00	7.82
216	South Africa	2003	11	0.01	0.24	5.95
217	Democratic Republic of the Congo	2009	9	0.01	0.00	4.51
218	Angola	2007	9	0.59	0.00	4.60
219	Ghana	2006	9	0.65	0.00	7.29
220	Nigeria	2020	15	2.80	0.00	8.20
221	Nigeria	2014	11	2.39	0.00	7.87
222	South Africa	2009	9	0.01	0.17	5.76
223	South Africa	2018	17	0.15	0.27	6.43
224	South Africa	2012	17	0.17	0.30	6.39
225	South Africa	2012	17	0.17	0.30	6.39
226	South Africa	2018	18	0.17	0.30	6.54
227	South Africa	2018	18	0.17	0.29	6.51
228	South Africa	2018	18	0.17	0.29	6.52
229	South Africa	2017	17	0.16	0.27	6.41
230	South Africa	2003	9	0.01	0.20	5.74
231	South Africa	2003	17	0.02	0.36	6.41

232	South Africa	2024	15	0.15	0.23	6.32
233	South Africa	2008	11	0.02	0.21	5.96
234	South Africa	2015	17	0.16	0.29	6.45
235	South Africa	2024	17	0.16	0.25	6.43
236	Namibia	2007	11	1.41	0.00	6.81
237	Senegal	2024	15	1.03	0.48	8.84

11.3.3 Physical indicator: magnitude, CImag

The magnitude indicator does not use affected population, instead uses physical indicators from EM-DAT (km² for floods, kph for storms) and from ERA5-land for heat (°C). The magnitude data is collected in a matrix similar to affected population, we then use the cumulative average since the first recorded year (t=0) to the year of the project (year t).

$$CI_{mag,e,t} = d_p * \frac{\sum_{t=0}^{t}\left(N_{occ,e,t}\right)}{t} * \frac{\sum_{t=0}^{t}(d_e)}{t} * \frac{\sum_{t=0}^{t}\left(mag_e\right)}{t}$$

The table below details the variation of climate indicators across the different projects of our sample.

Concessional projects (WBG, AfDB)	Private projects (IJGlobal)

ID	country(ies)	close year	dp	CI_mag FLOOD	CI_mag WIND	CI_mag HEAT
1	Senegal	1986	6	0.00	0.00	8.51
2	Rwanda	2009	20	0.00	0.00	0.00
3	Mozambique	2010	20	8.41	5.39	7.61
4	Tanzania	2010	30	5.10	0.00	0.00
5	Uganda	2001	35	0.00	0.00	0.00
6	Nigeria	2001	20	7.53	0.00	8.97
7	Cameroon	2012	50	0.00	0.00	9.55
8	Côte d'Ivoire, Liberia, Sierra Leone, Guinea	2012	30	6.09	0.00	8.82
9	Uganda	2001	30	0.00	0.00	0.00
10	Ethiopia, Kenya	2012	25	9.48	0.00	8.37
11	Zambia	2013	30	0.00	0.00	7.50

12	Burundi, Rwanda, Tanzania	2014	50	5.55	0.00	0.00
13	Guinea	2002	15	4.86	0.00	8.29
14	Burundi	2014	50	2.67	0.00	0.00
15	Ethiopia	2014	20	9.21	0.00	8.21
16	Uganda	2016	40	4.37	0.00	0.00
17	Seychelles	2017	6	0.00	1.68	0.00
18	Togo	2017	6	4.07	0.00	7.73
19	Ethiopia	2018	30	9.45	0.00	8.54
20	Mauritania	2018	26	0.00	0.00	9.58
21	Cameroon	2018	50	5.33	0.00	9.55
22	Guinea	2019	20	5.89	0.00	8.51
23	Mozambique	2020	25	8.81	6.22	7.79
24	Mali	2019	40	0.00	0.00	10.00
25	Eritrea	2004	25	0.00	0.00	8.26
26	Burkina Faso	2005	20	8.15	0.00	9.31
27	Rwanda	2005	6	0.00	0.00	0.00
28	Malawi, Mozambique	2007	30	9.15	5.85	7.97
29	Burkina Faso	2007	25	8.54	0.00	9.48
30	Ghana	2007	25	5.46	0.00	8.85
31	Angola	2015	25	6.21	0.00	6.94
32	Uganda	2014	25	4.01	0.00	0.00
33	Zambia	2019	30	5.38	0.00	7.50
34	Benin	1999	20	4.23	0.00	8.93
35	Benin	2018	20	5.00	0.00	8.90
36	Benin	2013	25	5.23	0.00	9.07
37	Benin	2023	8	4.38	0.00	8.19
38	Benin	2024	6	4.19	0.00	7.96
39	Benin	2010	20	4.98	0.00	8.90
40	Benin	2025	25	5.22	0.00	9.08
41	Benin	2018	30	5.30	0.00	9.22

42	Benin	2017	40	**5.52**	**0.00**	**9.45**
43	Benin	2019	25	**5.15**	**0.00**	**9.07**
44	Benin	2015	15	**4.83**	**0.00**	**8.67**
45	Cabo Verde	2021	3	**0.00**	**0.00**	**0.00**
46	Cabo Verde	2018	20	**0.00**	**0.00**	**0.00**
47	Cabo Verde	2022	25	**0.00**	**0.00**	**0.00**
48	Cameroon	2014	20	**0.00**	**0.00**	**8.82**
49	Cameroon	2013	50	**0.00**	**0.00**	**9.55**
50	Cameroon	2002	20	**0.00**	**0.00**	**8.85**
51	Cameroon	2021	25	**4.53**	**0.00**	**9.00**
52	Cameroon	2010	20	**0.00**	**0.00**	**8.81**
53	Cameroon	2009	50	**0.00**	**0.00**	**9.53**
54	Cameroon	2009	50	**0.00**	**0.00**	**9.53**
55	Cameroon	2021	30	**4.67**	**0.00**	**9.14**
56	Cameroon	2016	20	**4.64**	**0.00**	**8.82**
57	Cameroon	2024	20	**4.46**	**0.00**	**8.82**
58	Cameroon	2015	15	**4.45**	**0.00**	**8.59**
59	Congo, Cameroon	2009	20	**4.67**	**0.00**	**8.80**
60	Cameroon	2002	40	**0.00**	**0.00**	**9.40**
61	Cabo Verde	2013	20	**0.00**	**0.00**	**0.00**
62	Cabo Verde	2013	25	**0.00**	**0.00**	**0.00**
63	Chad	2025	25	**8.61**	**0.00**	**9.47**
64	Comoros	2017	40	**0.00**	**5.60**	**0.00**
65	Congo	2012	30	**5.11**	**0.00**	**6.61**
66	Congo	2016	15	**4.55**	**0.00**	**6.00**
67	Côte d'Ivoire	2018	25	**0.00**	**0.00**	**8.25**
68	Côte d'Ivoire	2018	20	**0.00**	**0.00**	**8.07**
69	Côte d'Ivoire	2017	10	**0.00**	**0.00**	**7.51**
70	Côte d'Ivoire	2022	30	**0.00**	**0.00**	**8.37**
71	Côte d'Ivoire	2025	25	**0.00**	**0.00**	**8.24**

72	Côte d'Ivoire	2021	30	0.00	0.00	8.38
73	Côte d'Ivoire	2016	3	0.00	0.00	6.55
74	Djibouti	2013	50	0.00	0.00	9.24
75	Djibouti	2013	6	0.00	0.00	7.56
76	Democratic Republic of the Congo	2019	20	0.00	0.00	6.67
77	Eritrea	2016	25	0.00	0.00	8.58
78	Eswatini	2018	25	0.00	0.00	6.68
79	Eswatini	2021	24	0.00	0.00	6.59
80	Ethiopia	2010	50	10.00	0.00	8.92
81	Ethiopia	2011	20	9.33	0.00	8.20
82	Ethiopia	2014	40	9.71	0.00	8.75
83	Ethiopia	2017	40	9.67	0.00	8.76
84	Gabon	2018	20	0.00	0.00	3.35
85	Gabon	2019	20	0.00	0.00	3.34
86	Ghana	2006	25	5.39	0.00	8.85
87	Ghana	2017	30	8.48	0.00	9.05
88	Ghana	2019	20	8.26	0.00	8.73
89	Ghana	2014	50	8.77	0.00	9.45
90	Ghana	2009	40	8.42	0.00	9.25
91	Ghana	2019	20	8.26	0.00	8.73
92	Guinea-Bissau	2015	40	0.00	0.00	9.50
93	Kenya	2009	50	0.00	0.00	8.23
94	Kenya	2010	50	0.00	0.00	8.24
95	Kenya	2017	35	0.00	0.00	8.00
96	Kenya	2019	20	0.00	0.00	7.53
97	Kenya	2013	20	0.00	0.00	7.54
98	Kenya	2018	20	0.00	0.00	7.57
99	Kenya	2013	40	0.00	0.00	8.09
100	Kenya	2016	20	0.00	0.00	7.55
101	Kenya	2016	20	0.00	0.00	7.55

102	Kenya and Ethiopia	2011	50	10.00	0.00	8.92
103	Lesotho	2013	20	0.00	3.73	0.00
104	Lesotho	2016	30	0.00	4.41	0.00
105	Lesotho	2009	30	0.00	0.00	0.00
106	Lesotho	2022	25	0.00	4.25	0.00
107	Lesotho	2013	10	0.00	2.87	0.00
108	Lesotho	2019	30	0.00	4.35	0.00
109	Liberia	2013	20	0.00	0.00	5.18
110	Liberia	2024	4	0.00	0.00	3.92
111	Liberia	2021	20	0.00	0.00	5.15
112	Liberia	2016	40	0.00	0.00	5.69
113	Liberia	2019	30	0.00	0.00	5.50
114	Madagascar	2013	20	0.00	9.55	6.29
115	Madagascar	2014	25	0.00	9.78	6.47
116	Malawi	2013	15	7.77	0.00	7.01
117	Mauritania	2012	5	0.00	0.00	8.26
118	Mauritius	2023	30	0.00	10.00	0.00
119	Mauritius	2014	20	0.00	9.43	0.00
120	Mozambique	2012	20	8.43	5.62	7.59
121	Mozambique	2012	20	8.43	5.62	7.59
122	Mozambique	1999	30	8.72	5.25	7.95
123	Mozambique	2013	30	8.74	6.14	7.92
124	Mozambique	1999	20	8.42	4.72	7.63
125	Mozambique	2016	20	8.58	5.59	7.62
126	Burundi and Rwanda	2012	20	2.02	0.00	0.00
127	Congo, Cameroon	2009	50	5.34	0.00	9.53
128	Malawi, Zambia	2013	20	7.98	0.00	7.24
129	Gabon, Congo	2013	20	4.80	0.00	6.27
130	The Gambia, Senegal	2011	30	5.18	0.00	9.74
131	Zambia	2010	50	0.00	0.00	7.88

132	Côte d'Ivoire, Guinea, Liberia	2014	20	5.83	0.00	8.86
133	Nigeria	2008	30	8.17	0.00	9.26
134	Niger	2008	30	7.49	0.00	9.70
135	Niger	2025	6	6.49	0.00	8.44
136	Niger	2019	20	7.28	0.00	9.37
137	Niger	2012	25	7.59	0.00	9.59
138	Nigeria	2019	20	7.56	0.00	8.97
139	Nigeria	2011	20	7.98	0.00	8.97
140	Nigeria	2019	6	6.69	0.00	8.02
141	Nigeria	2013	3	6.60	0.00	7.47
142	Nigeria	2014	30	8.29	0.00	9.30
143	Uganda	2011	25	3.97	0.00	0.00
144	Uganda	2013	20	3.86	0.00	0.00
145	Uganda	2022	20	4.25	0.00	0.00
146	Uganda	2023	20	4.26	0.00	0.00
147	Uganda	2016	20	3.86	0.00	0.00
148	Uganda	2015	20	3.84	0.00	0.00
149	Nigeria	2019	20	7.56	0.00	8.97
150	Rwanda	2014	20	0.00	0.00	0.00
151	Tanzania	2020	50	9.92	0.00	0.00
152	Tanzania	2018	25	9.32	0.00	0.00
153	Tanzania	2025	20	8.93	0.00	0.00
154	Tanzania	2015	25	9.26	0.00	0.00
155	Togo, Burkina Faso	2012	20	8.65	0.00	9.36
156	Togo	2022	20	5.00	0.00	8.71
157	Togo	2019	15	4.71	0.00	8.45
158	Togo	2023	30	5.28	0.00	9.01
159	Uganda	2020	20	4.15	0.00	0.00
160	Uganda	2020	30	4.44	0.00	0.00
161	Uganda	2019	10	3.52	0.00	0.00

162	Uganda	2008	40	4.30	0.00	0.00
163	Uganda	2009	50	4.45	0.00	0.00
164	Uganda	2015	20	3.84	0.00	0.00
165	Uganda	2016	40	4.37	0.00	0.00
166	Uganda	2018	20	3.88	0.00	0.00
167	Zambia	2013	50	0.00	0.00	7.91
168	Zambia	2015	25	5.26	0.00	7.36
169	Zambia	2016	25	5.25	0.00	7.36
170	Zambia	2015	20	5.10	0.00	7.18
171	Zambia	2015	30	5.39	0.00	7.51
172	Sierra Leone	2024	17	0.00	0.00	6.90
173	Mozambique	2024	9	7.85	5.16	7.02
174	South Africa	2018	18	9.11	7.93	7.65
175	South Africa	2018	17	9.05	7.82	7.59
176	South Africa	2018	15	8.97	7.67	7.49
177	South Africa	2018	15	8.98	7.68	7.50
178	South Africa	2018	17	9.08	7.87	7.61
179	South Africa	2018	17	9.06	7.83	7.59
180	South Africa	2018	17	9.04	7.79	7.57
181	South Africa	2018	17	9.06	7.84	7.60
182	South Africa	2018	17	9.06	7.83	7.59
183	Tanzania	2016	17	9.00	0.00	0.00
184	Mali	2024	11	5.56	0.00	9.02
185	Namibia	2023	9	0.00	0.00	7.73
186	Nigeria	2020	9	6.88	0.00	8.37
187	Democratic Republic of the Congo	2016	9	0.00	0.00	6.05
188	Nigeria	2010	15	7.70	0.00	8.73
189	Nigeria	2006	15	7.63	0.00	8.71
190	Zimbabwe	2007	9	0.00	0.00	7.23
191	Ghana	2014	9	7.55	0.00	8.12

192	Ghana	2016	16	7.99	0.00	8.55
193	Gabon	2019	11	0.00	0.00	2.89
194	Zambia	2015	17	4.98	0.00	7.06
195	Botswana	2021	9	0.00	0.00	7.74
196	Burkina Faso	2015	9	8.14	0.00	8.73
197	Kenya	2018	9	0.00	0.00	6.97
198	Nigeria	2007	15	7.68	0.00	8.71
199	Uganda	2017	20	3.89	0.00	0.00
200	Zambia	2006	9	0.00	0.00	6.60
201	Liberia	2013	9	0.00	0.00	4.58
202	Botswana	2011	9	0.00	0.00	7.83
203	Malawi, Mozambique	2018	18	8.48	5.68	7.51
204	South Africa	2019	17	9.13	7.86	7.58
205	Senegal	2017	15	4.71	0.00	9.16
206	Senegal	2015	15	4.70	0.00	9.18
207	Kenya	2006	9	0.00	0.00	6.91
208	Kenya	2012	9	0.00	0.00	6.92
209	Nigeria	2007	11	7.47	0.00	8.49
210	Zambia	2003	9	0.00	0.00	6.58
211	Tanzania	2013	9	4.31	0.00	0.00
212	South Africa	2001	9	7.95	2.50	7.17
213	Botswana	2003	9	0.00	0.00	7.83
214	Uganda	2009	11	3.37	0.00	0.00
215	Ghana	2008	15	5.15	0.00	8.46
216	South Africa	2003	11	8.12	3.07	7.32
217	Democratic Republic of the Congo	2009	9	0.00	0.00	6.07
218	Angola	2007	9	0.00	0.00	6.16
219	Ghana	2006	9	4.68	0.00	8.07
220	Nigeria	2020	15	7.23	0.00	8.75
221	Nigeria	2014	11	7.57	0.00	8.52

222	South Africa	2009	9	8.72	2.83	7.16
223	South Africa	2018	17	9.04	7.80	7.57
224	South Africa	2012	17	9.14	3.69	7.55
225	South Africa	2012	17	9.14	3.69	7.55
226	South Africa	2018	18	9.11	7.93	7.65
227	South Africa	2018	18	9.10	7.90	7.63
228	South Africa	2018	18	9.10	7.91	7.64
229	South Africa	2017	17	9.05	7.82	7.56
230	South Africa	2003	9	7.99	2.85	7.17
231	South Africa	2003	17	8.42	3.58	7.64
232	South Africa	2024	15	8.97	7.90	7.47
233	South Africa	2008	11	8.81	3.01	7.30
234	South Africa	2015	17	9.14	3.71	7.59
235	South Africa	2024	17	9.04	8.02	7.55
236	Namibia	2007	11	0.00	0.00	7.95
237	Senegal	2024	15	8.13	0.00	9.19

11.4 Extracting sentiment scores from article scraping

11.4.1 Inputs and article scraping

The pipeline is a media-sourced Natural Language Processing (NLP) workflow built with python. The inputs used in this pipeline are:

- Unique project identifiers (n° from 1 to 237),
- Country name(s) for the location of the project,
- Financial close year,
- Sector and subsector labels.

Additional inputs that were not directly related to the project database were added to ensure the identification of articles related to the different projects but that do not use the specific wording, or country name:

- Country synonyms and city names were defined and matched to each country in a table,
- Climate-related keywords sourced from the IPCC AR6 corpus (Ipcc, 2022), a list that covers 90 terms related to physical hazards, long-run climate changes, vulnerability concepts and Sub-Saharan African regional climate phenomena (Sahel drought, West African monsoon), and an additional set of climate query terms such as climate change, flood, heatwave…,
- Sector- and subsector-related keywords.

The sector list used was:

- Agriculture and rural development
- Clean energy
- Energy networks
- Digital infrastructure
- Fossil energy
- Mining
- Transportation
- Water and sanitation

While this list does not come from an official sector list, we remind that this pipeline is defined for scraping and therefore must consider that articles do not always follow exact sector wording from official lists (GICS, TICCS). The decomposition we defined to best reflect the different sectors present in our project database. Subsector list defines each type of infrastructure project related to these sectors.

Specific parameters were defined for the pipeline; they are related to either the functionalities or assumptions for the computation of the sentiment score:

- Decay period set at 3 years (e.g. for a close year in 2010, the search is conducted on articles from 2007 to 2010)
- Maximum articles per source set at 50,
- Word count per chunk set at 350, this is the word count per text chunk sent to ClimateBERT for inference,

- Minimum characters set at 20, this corresponds to the minimum character count from which a text is considered,
- Request delay and max retries were also parametered to ensure functionality of the pipeline, exponential back-off and a pause between every request.

To collect articles, we used a dedicated function covering the following strategies for the following sources:

Source	Type	Query method
GDELT Doc API v2	News media	Boolean and query on country x subsectpr keyword x climate term
RSS Feeds (27 feeds*)	News media	Parse all feeds, filter by country, sector and climate keyword matching
NewsAPI	News media	Keyword query per year
Semantic Scholar	Academic	Plain keyword query, filter by year range, sorted by citation count
Crossref	Academic	Keyword query with data filter, title and abstract returned
OpenAlex	Academic	Keyword search, abstract reconstructed from inverted index
CORE	Academic	Keyword query with year filter
arXiv	Academic preprints	Boolean all-field query on country x sector x climate

*The 27 feeds from international outlets includes: BBC Africa, The Guardian, Reuters, Nature Climate Change, Carbon Brief, IEA; alongside African regional media: Daily Maverick, The Eastern African, Mongabay Africa, The Africa Report, ReliefWeb, The New Humanitarian.

For sources that return broad results (notably RSS feeds), each article was passed through a relevance gate before being retained. An article was kept only if its combined title and summary text contained:

- At least one project country-related keyword,
- At least one sector keyword or at least one climate keyword.

This feature was implemented to avoid accumulating articles that were geographically or thematically irrelevant.

11.4.2 NLP sentiment classification using ClimateBERT

ClimateBERT (Hugging Face model ID: climatebert/distilroberta-base-climate-sentiment) is a DistilRoBERTa model fine-tuned on climate-related text. It assigns each text passage one of three labels:

Label	Numeric value	Interpretation
Risk	-1	The text frames climate in negative terms: hazards, damage, loss, uncertainty.
Neutral	0	The text makes no clear directional claim about climate impacts.
Opportunity	+1	The text frames climate in positive terms: adaptation gains, investment, resilience.

Inference was performed on CPU.

The aforementioned chunking of article texts ensures inference calls to ClimateBERT respect the 512 token limit per inference call. Each chunk was classified indeêndantly.

For each chunk, ClimateBERT returns the predicted label and its confidence score [0 to 1]. The model's input is capped at 2,048 characters per chunk (prevents excessively long tokens being passed to the tokeniser).

The project-level climate sentiment score is the arithmetic mean of the numeric values assigned to each chunk across all articles retrieved for that project:

$$S = mean\ (numeric_i); for\ i = 1\ to\ N\ chunks$$

The precision metric captures CLimateBERT's average certainty on its predicted sentiment labelling:

$$Precision = mean\ (confidence_i); for\ chunks\ where\ label \in [risk; opportunity]$$

Neutral chunks were excluded from the precision calculation as they represent the absence of directional signal. When all chunks are neutral, the pipeline returned 'NaN'.

For each article, the label that is retained is the dominant label: the chunk label prediction with the highest confidence score. This gives a single interpretable classification per article without averaging away the signals in the project-level scoring. This point relates only to the returned intermediate article result which is not presented in this appendix but can be made available upon request, these intermediary results are not part of the sentiment score construction, it was created only to provide us with a view of the pipeline process intermediate steps. Across the 230 projects 31,705 articles were retrieved: 37% Crossref, 33% OpenAlex, 28% CORE, 1% Semantic Scholar, <1% arXiv. 42% had neutral, 29% risk and 25% opportunity labels. The news source scraping (GDELT, NewsAPI, RSS) did not find any articles,

The main result, the sentiment scores per project, the resulting dataset presented a sentiment score ranging from -0.57 to +0.43 with a mean at -0.03 and precision scores ranging from 0.61 and 0.85 with a mean at 0.76. The variables in this results file are:

Column	Description
project_id	Project the article was retrieved for
source	Origin (e.g. 'Crossref', 'CORE', 'RSS:guardian_climate')
date	Publication date as returned by the source
title	Article or paper title
url	Link to the original article
cb_label	ClimateBERT dominant label: risk / neutral / opportunity / insufficient_text

Column	Description
cb_confidence	Confidence for the dominant label (0–1)
cb_numeric	Numeric value of the dominant label (−1, 0, +1)
n_chunks	Number of chunks the article was split into
text	Full text submitted for classification (title + abstract/summary)
query	Search query used to retrieve this article

The table below presents the project sentiment scores alongside the other variables detailed in the table above: (sentiment score and precision are expressed in percentage in order to propose a more readable table).

project_id	sentiment_score	precision	country	subsector	close_year	n_articles	n_chunks_total	n_risk	n_opportunity	n_neutral
1	2.82%	62.4%	Senegal	Power Networks	1986	84	71	7	9	55
2	-1.87%	76.5%	Rwanda	Power Networks	2009	100	107	24	22	61
3	0.00%	74.8%	Mozambique	Power Networks	2010	100	102	25	25	52
4	5.81%	76.3%	Tanzania	Power Networks	2010	148	155	37	46	72
5	-13.83%	67.4%	Uganda	Hydro power	2001	90	94	30	17	47
6	-5.19%	68.6%	Nigeria	Power Networks	2001	74	77	18	14	45
7	4.35%	76.6%	Cameroon	Hydro power	2012	147	161	49	56	56

8	3.80%	78.8 %	Côte d'Ivoire, Liberia, Sierra Leone, Guinea	Power Networks	2012	147	158	37	43	78
9	-13.83%	67.4 %	Uganda	Hydropower	2001	90	94	30	17	47
10	2.94%	74.1 %	Ethiopia, Kenya	Power Networks	2012	99	102	28	31	43
11	12.74%	75.2 %	Zambia	Power Networks	2013	147	157	34	54	69
12	-5.26%	77.5 %	Burundi, Rwanda, Tanzania	Hydropower	2014	142	152	48	40	64
13	-3.17%	72.3 %	Guinea	Power Networks	2002	117	126	25	21	80
14	-5.70%	77.2 %	Burundi	Hydropower	2014	149	158	50	41	67
15	21.79%	66.4 %	Ethiopia	Geothermal	2014	149	156	17	51	88
16	30.83%	77.5 %	Uganda	Power Networks	2016	149	133	20	61	52
17	-35.76%	80.6 %	Seychelles	Fisheries & Natural Resources	2017	147	151	74	20	57
18	23.18%	77.5 %	Togo	Power Networks	2017	152	151	29	64	58

19	12.26%	77.0 %	Ethiopia	Power Networks	2018	148	155	40	59	56
20	-3.95%	78.1 %	Mauritania	Oil & Gas	2018	149	152	37	31	84
21	13.42%	76.0 %	Cameroon	Power Networks	2018	147	149	33	53	63
22	8.28%	74.5 %	Guinea	Power Networks	2019	152	157	36	49	72
23	11.61%	76.1 %	Mozambique	Gas-to-Power	2020	147	155	38	56	61
24	28.48%	76.0 %	Mali	Power Networks	2019	150	151	30	73	48
25	0.00%	68.6 %	Eritrea	Power Networks	2004	95	107	24	24	59
26	4.12%	76.7 %	Burkina Faso	Thermal Power	2005	102	97	16	20	61
27	-4.11%	73.7 %	Rwanda	Power Networks	2005	71	73	18	15	40
28	8.57%	77.9 %	Malawi, Mozambique	Power Networks	2007	149	175	37	52	86
29	15.91%	76.8 %	Burkina Faso	Power Networks	2007	96	88	10	24	54
30	-1.01%	74.9 %	Ghana	Power Networks	2007	100	99	28	27	44

31	-26.09%	79.6 %	Angola	Water Supply & Distribution	2015	151	161	70	28	63
32	10.53%	76.3 %	Uganda	Agricultural Markets & Value Chains	2014	148	152	42	58	52
33	-18.59%	77.6 %	Zambia	Livestock Infrastructure	2019	152	156	67	38	51
34	-32.35%	78.4 %	Benin	Fisheries & Natural Resources	1999	66	68	28	6	34
35	-28.40%	76.7 %	Benin	Roads	2018	149	162	66	20	76
36	10.14%	76.1 %	Benin	Irrigation & Agricultural Infrastructure	2013	144	148	26	41	81
37	-56.63%	84.7 %	Benin	Drainage & Flood Management	2023	149	166	113	19	34
38	-25.45%	79.8 %	Benin	Water Supply & Distribution	2024	150	165	83	41	41
39	-11.93%	74.9 %	Benin	Roads	2010	100	109	34	21	54

40	15.72%	82.0%	Benin	Power Networks	2025	150	159	43	68	48
41	7.28%	79.1%	Benin	Power Networks	2018	147	151	39	50	62
42	30.60%	79.1%	Benin	Power Networks	2017	147	134	23	64	47
43	-41.83%	84.6%	Benin	Drainage & Flood Management	2019	148	153	87	23	43
44	-21.79%	79.4%	Benin	Water Supply & Distribution	2015	148	156	62	28	66
45	3.92%	76.6%	Cabo Verde	E-Government & Public Services	2021	147	153	35	41	77
46	-3.13%	75.7%	Cabo Verde	Ports, Rail & Other	2018	129	128	25	21	82
47	4.49%	73.3%	Cabo Verde	Technology Parks & Data Centres	2022	148	156	30	37	89
48	-6.76%	77.4%	Cameroon	Roads	2014	147	148	46	36	66
49	8.05%	77.7%	Cameroon	Irrigation & Agricultural	2013	141	149	31	43	75

				Infrastructure						
50	-7.55%	71.2%	Cameroon	Oil & Gas	2002	148	159	33	21	105
51	-31.25%	76.4%	Cameroon	Roads	2021	150	160	72	22	66
52	-0.64%	76.6%	Cameroon	Power Networks	2010	144	156	32	31	93
53	-22.64%	77.7%	Cameroon	Water Supply & Distribution	2009	151	159	62	26	71
54	-11.92%	74.7%	Cameroon	Roads	2009	149	151	42	24	85
55	-46.54%	82.8%	Cameroon	Drainage & Flood Management	2021	151	159	92	18	49
56	-8.39%	76.0%	Cameroon	Roads	2016	148	143	45	33	65
57	-27.85%	73.7%	Cameroon	Roads	2024	148	158	73	29	56
58	27.27%	63.2%	Cameroon	Fibre & Broadband Networks	2015	101	110	13	43	54
59	-17.17%	76.5%	Congo, Cameroon	Roads	2009	100	99	34	17	48
60	-7.55%	71.2%	Cameroon	Oil & Gas	2002	148	159	33	21	105
61	-4.55%	67.2%	Cabo Verde	Aviation	2013	102	110	19	14	77

62	2.81%	69.9%	Cabo Verde	Technology Parks & Data Centres	2013	150	178	16	21	141
63	19.25%	80.6%	Chad	Power Networks	2025	176	187	47	83	57
64	-9.02%	72.3%	Comoros	Roads	2017	120	133	33	21	79
65	14.43%	75.8%	Congo	Power Networks	2012	98	97	16	30	51
66	23.85%	62.5%	Congo	Fibre & Broadband and Networks	2016	105	109	18	44	47
67	-32.50%	78.0%	Côte d'Ivoire	Power Networks	2018	50	40	15	2	23
68	-24.24%	77.5%	Côte d'Ivoire	Roads	2018	52	33	10	2	21
69	-7.95%	78.7%	Côte d'Ivoire	Aviation	2017	96	88	22	15	51
70	-21.43%	77.6%	Côte d'Ivoire	Power Networks	2022	50	42	19	10	13
71	-5.73%	73.5%	Côte d'Ivoire	Roads	2025	141	157	50	41	66
72	-35.11%	82.8%	Côte d'Ivoire	Drainage & Flood Management	2021	98	94	50	17	27

73	-26.92%	60.6 %	Côte d'Ivoire	Power Networks	2016	50	26	10	3	13
74	16.26%	69.3 %	Djibouti	Geothermal	2013	119	123	18	38	67
75	16.26%	69.3 %	Djibouti	Geothermal	2013	119	123	18	38	67
76	-12.58%	77.2 %	Democratic Republic of the Congo	Roads	2019	148	159	58	38	63
77	-19.61%	76.8 %	Eritrea	Rural Livelihoods & Social Infrastructure	2016	99	102	45	25	32
78	-25.93%	76.2 %	Eswatini	Roads	2018	53	54	15	1	38
79	4.84%	74.5 %	Eswatini	Irrigation & Agricultural Infrastructure	2021	59	62	20	23	19
80	3.77%	75.9 %	Ethiopia	Power Networks	2010	149	159	41	47	71
81	-11.04%	74.9 %	Ethiopia	Roads	2011	147	154	50	33	71
82	-22.84%	82.3 %	Ethiopia	Water Supply & Distribution	2014	151	162	66	29	67

83	29.85%	77.0 %	Ethiopia	Power Networks	2017	148	134	25	65	44
84	-25.81%	83.0 %	Gabon	Water Supply & Distribution	2018	150	155	67	27	61
85	-13.33%	75.1 %	Gabon	Roads	2019	100	105	36	22	47
86	1.30%	73.3 %	Ghana	Sewerage & Wastewater	2006	143	154	42	44	68
87	-30.13%	81.3 %	Ghana	Sewerage & Wastewater	2017	148	156	74	27	55
88	-12.50%	76.7 %	Ghana	Roads	2019	146	152	58	39	55
89	14.29%	75.3 %	Ghana	Power Networks	2014	101	84	20	32	32
90	7.64%	75.7 %	Ghana	Roads	2009	147	157	33	45	79
91	-12.50%	76.7 %	Ghana	Roads	2019	146	152	58	39	55
92	13.33%	77.2 %	Guinea - Bissau	Power Networks	2015	148	135	24	42	69
93	-30.92%	79.8 %	Kenya	Water Supply & Distribution	2009	149	152	68	21	63
94	8.67%	77.2 %	Kenya	Power Networks	2010	150	150	33	46	71

95	-8.02%	79.2 %	Kenya	Aviation	2017	148	162	47	34	81
96	-14.11%	75.0 %	Kenya	Roads	2019	150	163	62	39	62
97	-11.61%	76.8 %	Kenya	Roads	2013	148	155	55	37	63
98	-10.56%	79.3 %	Kenya	Sewerage & Waste water	2018	150	161	61	44	56
99	-26.25%	80.5 %	Kenya	Water Supply & Distribution	2013	151	160	72	30	58
100	-26.54%	81.3 %	Kenya	Water Supply & Distribution	2016	155	162	77	34	51
101	-17.31%	73.8 %	Kenya	Roads	2016	101	104	40	22	42
102	-11.04%	74.9 %	Kenya and Ethiopia	Roads	2011	147	154	50	33	71
103	-32.99%	82.9 %	Lesotho	Water Supply & Distribution	2013	98	97	48	16	33
104	0.72%	75.2 %	Lesotho	Power Networks	2016	147	138	38	39	61
105	4.38%	73.7 %	Lesotho	Hydro power	2009	128	137	31	37	69
106	-34.50%	83.2 %	Lesotho	Water Supply &	2022	149	171	87	28	56

				Distrib ution						
107	-3.81%	74.9 %	Lesoth o	E-Govern ment & Public Service s	2013	100	105	26	22	57
108	3.03%	76.5 %	Lesoth o	E-Govern ment & Public Service s	2019	144	165	33	38	94
109	-11.32%	73.3 %	Liberia	Roads	2013	150	159	50	32	77
110	2.52%	74.4 %	Liberia	E-Govern ment & Public Service s	2024	148	159	39	43	77
111	0.99%	77.4 %	Liberia	Agricul tural Market s & Value Chains	2021	99	101	31	32	38
112	16.43%	76.0 %	Liberia	Power Networ ks	2016	148	140	28	51	61
113	5.31%	75.3 %	Liberia	Hydro power	2019	98	113	31	37	45
114	10.26%	75.0 %	Madag ascar	Irrigati on & Agricul tural Infrastr ucture	2013	83	78	15	23	40

115	13.70%	75.2 %	Madagascar	Irrigation & Agricultural Infrastructure	2014	140	146	32	52	62
116	-14.38%	74.3 %	Malawi	Roads	2013	148	153	53	31	69
117	-38.99%	82.5 %	Mauritania	Water Supply & Distribution	2012	149	159	78	16	65
118	33.01%	79.2 %	Mauritius	Power Networks	2023	100	103	11	45	47
119	20.50%	72.5 %	Mauritius	Thermal Power	2014	150	161	32	65	64
120	-17.20%	77.7 %	Mozambique	Roads	2012	150	157	52	25	80
121	5.33%	76.9 %	Mozambique	Irrigation & Agricultural Infrastructure	2012	148	150	36	44	70
122	-26.99%	77.2 %	Mozambique	Water Supply & Distribution	1999	148	163	62	18	83
123	-25.32%	79.3 %	Mozambique	Water Supply & Distribution	2013	148	158	70	30	58

124	-10.75%	69.1 %	Mozambique	Irrigation & Agricultural Infrastructure	1999	86	93	26	16	51
125	-4.86%	78.5 %	Mozambique	Roads	2016	147	144	46	39	59
126	-23.38%	74.1 %	Burundi and Rwanda	Roads	2012	147	154	56	20	78
127	-11.92%	74.7 %	Congo, Cameroon	Roads	2009	149	151	42	24	85
128	-15.03%	74.7 %	Malawi, Zambia	Roads	2013	148	153	53	30	70
129	-9.09%	67.9 %	Gabon, Congo	Roads	2013	100	99	29	20	50
130	-8.92%	75.4 %	The Gambia, Senegal	Roads	2011	144	157	47	33	77
131	-21.19%	76.2 %	Algeria, Chad, Niger	Roads	2013	148	151	54	22	75
132	5.63%	73.8 %	Zambia	Roads	2010	149	160	36	45	79
133	-12.33%	72.8 %	Côte d'Ivoire, Guinea	Roads	2014	146	146	47	29	70

			, Liberia							
134	-10.27%	73.5 %	Nigeria	Roads	2008	147	146	42	27	77
135	3.40%	75.0 %	Niger	Hydro power	2008	138	147	35	40	72
136	-39.61%	83.4 %	Niger	Water Supply & Distribution	2025	150	154	89	28	37
137	-23.75%	77.5 %	Niger	Roads	2019	146	160	65	27	68
138	14.29%	74.6 %	Niger	Irrigation & Agricultural Infrastructure	2012	149	147	35	56	56
139	-18.79%	79.5 %	Nigeria	Roads	2019	143	149	60	32	57
140	-29.68%	79.6 %	Nigeria	Water Supply & Distribution	2011	148	155	72	26	57
141	-36.63%	82.5 %	Nigeria	Water Supply & Distribution	2019	159	172	93	30	49
142	-32.32%	78.7 %	Nigeria	Roads	2013	99	99	51	19	29
143	-29.45%	81.6 %	Nigeria	Water Supply & Distribution	2014	155	163	74	26	63

144	8.72%	74.8 %	Uganda	Irrigation & Agricultural Infrastructure	2011	150	172	43	58	71
145	-15.89%	77.1%	Uganda	Roads	2013	146	151	50	26	75
146	-12.50%	78.2 %	Uganda	Roads	2022	149	160	64	44	52
147	-19.14%	76.7 %	Uganda	Roads	2023	150	162	68	37	57
148	-21.05%	78.0 %	Uganda	Roads	2016	146	152	58	26	68
149	34.81%	76.0 %	Uganda	Power Networks	2015	148	135	18	65	52
150	43.14%	72.8 %	Nigeria	Gas-to-Power	2019	153	153	14	80	59
151	-1.35%	74.5 %	Rwanda	Roads	2014	146	148	37	35	76
152	-6.06%	79.3 %	Tanzania	Hydro power	2020	150	165	59	49	57
153	16.56%	74.7 %	Tanzania	Power Networks	2018	150	151	36	61	54
154	14.02%	82.2 %	Tanzania	Power Networks	2025	151	164	44	67	53
155	-17.65%	75.8 %	Tanzania	Ports, Rail & Other	2015	149	153	56	29	68
156	1.31%	76.4 %	Togo, Burkina Faso	Roads	2012	148	153	39	41	73
157	26.88%	77.4 %	Togo	Solar PV	2022	148	160	31	74	55

158	38.51%	78.1 %	Togo	Solar PV	2019	147	161	21	83	57
159	-14.56%	82.2 %	Togo	Rural Livelihoods & Social Infrastructure	2023	150	158	65	42	51
160	-15.38%	77.9 %	Uganda	Roads	2020	145	156	58	34	64
161	-14.65%	77.2 %	Uganda	Roads	2020	145	157	58	35	64
162	-19.87%	77.7 %	Uganda	Roads	2019	145	151	59	29	63
163	-0.61%	75.8 %	Uganda	Power Networks	2008	148	164	38	37	89
164	-1.89%	73.6 %	Uganda	Roads	2009	100	106	24	22	60
165	34.81%	76.0 %	Uganda	Power Networks	2015	148	135	18	65	52
166	-48.08%	82.3 %	Uganda	Water Supply & Distribution	2016	103	104	63	13	28
167	-29.49%	83.9 %	Uganda	Water Supply & Distribution	2018	149	156	76	30	50
168	-20.26%	81.1%	Zambia	Livestock Infrastructure	2013	149	153	60	29	64
169	-25.25%	80.4 %	Zambia	Sewerage &	2015	99	99	41	16	42

				Waste water						
170	-29.25%	80.8 %	Zambia	Water Supply & Distribution	2016	103	106	50	19	37
171	-23.91%	75.4 %	Zambia	Roads	2015	100	92	37	15	40
172	-1.96%	75.6 %	Zambia	Agricultural Markets & Value Chains	2015	100	102	33	31	38
173	24.27%	75.0 %	Sierra Leone	Gas-to-Power	2024	100	103	16	41	46
174	-11.70%	79.0 %	Mozambique	Industrial Minerals	2024	100	94	32	21	41
177	19.61%	73.3 %	South Africa	Onshore Wind	2018	152	153	35	65	53
178	23.16%	75.2 %	South Africa	Solar PV	2018	157	177	35	76	66
179	23.16%	75.2 %	South Africa	Solar PV	2018	157	177	35	76	66
180	12.69%	74.6 %	South Africa	Solar PV	2018	115	134	31	48	55
181	23.73%	75.3 %	South Africa	Solar PV	2018	157	177	35	77	65
182	23.73%	75.3 %	South Africa	Solar PV	2018	157	177	35	77	65
183	23.73%	75.3 %	South Africa	Solar PV	2018	157	177	35	77	65
184	23.73%	75.3 %	South Africa	Solar PV	2018	157	177	35	77	65

185	23.73%	75.3%	South Africa	Solar PV	2018	157	177	35	77	65
186	23.18%	76.9%	Tanzania	Solar PV	2016	151	151	28	63	60
187	-17.72%	78.4%	Mali	Industrial Minerals	2024	150	158	62	34	62
188	6.67%	77.7%	Namibia	Base Metals	2023	144	165	45	56	64
190	-19.87%	79.1%	Nigeria	Precious Metals	2020	146	151	64	34	53
191	-10.38%	71.7%	Democratic Republic of the Congo	Base Metals	2016	100	106	27	16	63
192	-30.99%	74.8%	Nigeria	Oil & Gas	2010	148	142	60	16	66
193	-8.44%	75.3%	Nigeria	Oil & Gas	2006	152	154	37	24	93
195	-12.96%	72.8%	Zimbabwe	Precious Metals	2007	100	108	31	17	60
196	-4.91%	76.6%	Ghana	Precious Metals	2014	148	163	44	36	83
197	35.81%	70.1%	Ghana	Gas-to-Power	2016	151	148	14	67	67
198	-8.28%	78.8%	Gabon	Oil & Gas	2019	148	157	41	28	88
201	16.56%	73.3%	Zambia	Thermal Power	2015	151	157	24	50	83

202	-18.83%	79.6 %	Botswana	Precious Metals	2021	146	154	56	27	71
204	7.43%	71.2 %	Burkina Faso	Precious Metals	2015	149	148	33	44	71
205	-6.55%	72.7 %	Kenya	Industrial Minerals	2018	149	168	57	46	65
206	-23.23%	74.3 %	Nigeria	Oil & Gas	2007	100	99	35	12	52
207	9.21%	75.1 %	Uganda	Hydro power	2017	148	152	38	52	62
209	-17.65%	77.7 %	Zambia	Base Metals	2006	81	85	26	11	48
210	-14.68%	74.7 %	Liberia	Precious Metals	2013	100	109	34	18	57
214	-14.01%	74.6 %	Botswana	Base Metals	2011	150	157	48	26	83
215	-8.98%	72.5 %	Malawi, Mozambique	Ports, Rail & Other	2018	149	167	54	39	74
216	42.48%	72.3 %	South Africa	Concentrated Solar Power	2019	150	153	18	83	52
217	18.59%	75.2 %	Senegal	Thermal Power	2017	150	156	28	57	71
218	23.78%	72.6 %	Senegal	Thermal Power	2015	148	164	28	67	69
219	-20.18%	74.6 %	Kenya	Industrial	2006	100	109	35	13	61

				Minerals						
221	-5.42%	75.5 %	Kenya	Industrial Minerals	2012	148	166	51	42	73
222	9.48%	71.8 %	Nigeria	Telecoms Networks	2007	108	116	21	32	63
223	-24.32%	74.6 %	Zambia	Base Metals	2003	73	74	23	5	46
224	-1.88%	72.6 %	Tanzania	Precious Metals	2013	147	160	45	42	73
225	-14.84%	71.9 %	South Africa	Precious Metals	2001	149	155	40	17	98
226	-5.88%	71.9 %	Botswana	Precious Metals	2003	68	68	15	11	42
227	18.85%	69.1 %	Uganda	Telecoms Networks	2009	103	122	18	41	63
229	-0.77%	71.5 %	Ghana	Ports, Rail & Other	2008	135	130	26	25	79
230	4.58%	73.1 %	South Africa	Telecoms Networks	2003	127	131	26	32	73
231	-7.01%	73.8 %	Democratic Republic of the Congo	Base Metals	2009	146	157	37	26	94

232	-15.48%	75.6%	Angola	Base Metals	2007	129	155	45	21	89
233	-8.97%	74.3%	Ghana	Precious Metals	2006	144	156	41	27	88
234	-12.50%	80.5%	Nigeria	Oil & Gas	2020	160	176	60	38	78
236	-30.00%	79.9%	Nigeria	Oil & Gas	2014	114	120	57	21	42
237	-5.30%	74.1%	South Africa	Precious Metals	2009	148	151	42	34	75
238	23.73%	75.3%	South Africa	Solar PV	2018	157	177	35	77	65
239	23.60%	75.4%	South Africa	Solar PV	2012	150	161	28	66	67
240	23.60%	75.4%	South Africa	Solar PV	2012	150	161	28	66	67
241	19.61%	73.3%	South Africa	Onshore Wind	2018	152	153	35	65	53
242	19.61%	73.3%	South Africa	Onshore Wind	2018	152	153	35	65	53
243	19.61%	73.3%	South Africa	Onshore Wind	2018	152	153	35	65	53
244	23.46%	75.1%	South Africa	Solar PV	2017	161	179	41	83	55
245	-14.02%	72.9%	South Africa	Precious Metals	2003	100	107	33	18	56
246	0.00%	73.1%	South Africa	Thermal Power	2003	148	148	34	34	80
247	37.27%	79.1%	South Africa	Onshore Wind	2024	152	161	24	84	53
248	9.87%	71.4%	South Africa	Telecoms	2008	144	152	33	48	71

				Networks						
249	42.50%	73.9%	South Africa	Concentrated Solar Power	2015	150	160	23	91	46
250	11.73%	80.9%	South Africa	Solar PV	2024	157	162	54	73	35
251	12.09%	75.8%	Namibia	Telecoms Networks	2007	78	91	15	26	50
252	-1.74%	77.4%	Senegal	Aviation	2024	148	172	45	42	85

11.5 Regression variables and results

Variable	Type	Description
Panel A. Raw variables		
dep_cost_debt	Continuous (%)	All-in nominal interest rate on senior debt at financial close. Dependent variable.
fin_fixed_rate	Binary (Yes/No)	Indicates whether the senior debt carries a fixed coupon.
fin_concessional	Binary (Yes/No)	Indicates presence of concessional financing (below-market terms, subsidies, or blended finance).
fin_leverage	Continuous	Debt-to-total-capital ratio at financial close.
fin_project_size_musd	Continuous (USD m)	Total project capital expenditure.

Variable	Type	Description
fin_numb_lenders	Count	Number of distinct lenders in the financing syndicate.
fin_orig_lenders	Categorical	Geographic origin of lenders: International, Africa, or International & Africa.
fin_type_lenders	Categorical	Institutional type of lenders: Public, Private, or Mixed.
macro_currency_risk	Continuous	Proxy for exchange-rate volatility against USD around the time of financial close.
macro_gdp_per_capita	Continuous (USD)	Host-country GDP per capita in the year of financial close.
macro_country_risk	Continuous (index)	Composite country-risk score for the host country in the year of financial close.
macro_rule_of_law	Continuous (index)	Worldwide Governance Indicators rule-of-law score for the host country.
time_financial_close_year	Year	Year in which the project reached financial close. Used as the clustering variable for standard errors.
time_duration_years	Continuous (years)	Tenor of the senior debt at financial close.
sect_sector	Categorical	Sector: Agriculture & Rural Development, Clean Energy & Networks, Digital Infrastructure, Fossil Energy, Mining, Transport, or Water & Sanitation.
geo_multinational_project	Binary (Yes/No)	Indicates a cross-border / regional project.
project_type	Categorical	Type of project development: Greenfield, Expansion, or Refinancing.

Variable	Type	Description
clim_infra_is_climate	Binary (Yes/No)	Indicates whether the project qualifies as climate-related infrastructure.
clim_CI_flood	Continuous	Climate risk indicators, two different versions are used: (for each type of climate-related disaster) - a socioeconomic indicator, CIpop, that translates the probable percentage of the population affected by climate events during the project loan life - a physical magnitude indicator, CImag, that translates the probable cumulative severity of climate-related disasters during the project loan life
clim_CI_storm	Continuous	
clim_CI_heat	Continuous	
beh_S	Continuous	Behavioural sentiment proxy constructed from a NLP-scored corpus (ClimaBERT) over the 36 months preceding financial close.
Panel B. Derived and transformed variables		
dep_cost_debt_pct	Continuous (%)	dep_cost_debt expressed in percentage points (× 100). Used as the dependent variable in the regression.
log_size	Continuous	ln(fin_project_size_musd).
log_gdp	Continuous	ln(macro_gdp_per_capita).
log_CI_flood	Continuous	log(1 + clim_CI_flood). Enters the regression in place of the raw CI.
log_CI_storm	Continuous	log(1 + clim_CI_storm). Enters the regression in place of the raw CI.
log_CI_heat	Continuous	log(1 + clim_CI_heat). Enters the regression in place of the raw CI.
is_concessional	Binary (0/1)	1 if fin_concessional = Yes.

Variable	Type	Description
is_multicountry	Binary (0/1)	1 if geo_multinational_project = Yes.
is_climate_infra	Binary (0/1)	1 if clim_infra_is_climate = Yes.
is_greenfield, is_expansion, is_refinancing	Binary (0/1)	Project-type dummies derived from project_type.
is_clean_energy, is_fossil, is_mining, is_transport, is_water, is_digital	Binary (0/1)	Sector dummies derived from sect_sector. Agriculture & Rural Development is the omitted base.
lender_intl, lender_africa, lender_mixed	Binary (0/1)	Lender-origin dummies derived from fin_orig_lenders.
lender_public, lender_private	Binary (0/1)	Lender-type dummies derived from fin_type_lenders. "Mixed" lender type is the omitted base.

Table 11-3: Variable definitions

Variable	Mean	SD	Min	Median	Max
Panel A. Dependent variable					
dep_cost_debt_pct (%)	3.435	3.655	0.100	1.090	15.592
Panel B. Climate exposure (raw and log-transformed)					
clim_CI_flood	67,860.7	143,550.3	0.0	621.9	914,869.5
clim_CI_storm	51.8	193.2	0.0	0.0	1,645.1
clim_CI_heat	38,936.3	51,353.2	0.0	14,554.5	299,647.0
log_CI_flood	5.996	5.042	0.000	6.434	13.727
log_CI_storm	0.931	1.963	0.000	0.000	7.406
log_CI_heat	8.069	4.220	0.000	9.586	12.610

Variable	Mean	SD	Min	Median	Max
Panel C. Behavioural sentiment					
beh_sw	-0.033	0.196	-0.566	-0.051	0.431
Panel D. Financial structure					
fin_leverage	0.794	0.193	0.047	0.842	1.000
fin_project_size_musd	275.4	732.4	4.0	121.4	10,000.0
log_size	4.777	1.244	1.386	4.799	9.210
fin_numb_lenders	2.157	1.936	1	1	20
time_duration_years	22.395	11.605	3	20	50
fin_fixed_rate (0/1)	0.530	0.500	0	1	1
is_concessional (0/1)	0.717	0.451	0	1	1
Panel E. Macroeconomic environment					
macro_country_risk	0.090	0.042	0.012	0.083	0.278
macro_gdp_per_capita (USD)	5,685.7	5,029.4	218.0	3,886.4	31,595.7
log_gdp	8.313	0.821	5.384	8.265	10.361
macro_rule_of_law	-0.574	0.514	-1.883	-0.640	0.960
macro_currency_risk	0.089	0.064	0.000	0.080	0.288
Panel F. Project characteristics					
is_multicountry (0/1)	0.065	0.247	0	0	1
is_climate_infra (0/1)	0.657	0.476	0	1	1

Variable	Mean	SD	Min	Median	Max
is_greenfield (0/1)	0.596	0.492	0	1	1
is_expansion (0/1)	0.204	0.404	0	0	1
is_refinancing (0/1)	0.048	0.214	0	0	1
Panel G. Sector dummies (agriculture omitted)					
is_clean_energy (0/1)	0.322	0.468	0	0	1
is_fossil (0/1)	0.083	0.276	0	0	1
is_mining (0/1)	0.104	0.306	0	0	1
is_transport (0/1)	0.235	0.425	0	0	1
is_water (0/1)	0.126	0.333	0	0	1
is_digital (0/1)	0.057	0.231	0	0	1
Panel H. Lender characteristics					
lender_intl (0/1)	0.165	0.372	0	0	1
lender_africa (0/1)	0.583	0.494	0	1	1
lender_mixed (0/1)	0.252	0.435	0	0	1
lender_public (0/1)	0.757	0.430	0	1	1
lender_private (0/1)	0.183	0.387	0	0	1

Table 11-4: Descriptive statistics, regression sample (N = 230)

Variable	VIF
is_concessional	2.73
fin_fixed_rate	2.55

Variable	VIF
macro_country_risk	2.49
macro_rule_of_law	2.06
log_gdp	2.06
is_climate_infra	1.53
time_duration_years	1.52
log_size	1.51
log_CI_storm	1.50
log_CI_flood	1.44
beh_sw	1.36
is_multicountry	1.35
log_CI_heat	1.34
fin_numb_lenders	1.25
macro_currency_risk	1.13
fin_leverage	1.13

Table 11-5: Variance Inflation Factors

11.6 Storm resilience case study detailed results, TFC and Exposure curve

This appendix presents the complete and detailed results of the storm resilience case study, which aims to assess the potential of financing resilience in reducing the funding cost through debt only.

The method uses a hill curve equation to calculate the reduction in exposure from financing resilience measures using inputs from the EDHEC CLIMATECH database (ECI_ClimaTech_Reducing_Infrastructure_Climate_an_overview, n.d.) .

The cost of equity comes from a country level database (Dato et al., 2025).

The scaling level of investment comes from the WBG, Miyamoto study from 2019 (Overview of Engineering Options for Increasing Infrastructure Resilience, Final Report, 2019).

Other data comes from the sample collected from WBG and AfDB PADs and the IJGlobal database (see sections 8.1, 8.2 and 4.3).

The complete optimization function is detailed below:

$$TFC(INV_{a,i}) =$$

$$\sum_{t=1}^{T}\left[\frac{P_t + \left(INV_g + \sum_i[I_{a,i}] - \sum_{t_1 \to t-1}[P_t]\right) * \left(R_g + \sum_i\left[log(1 + CI_{clim,i}) * \beta_i * \left(1 - \delta * \frac{INV_{a,i}^{\exp(\eta)}}{INV_{a,s,i}^{\exp(\eta)} + INV_{a,i}^{\exp(\eta)}}\right)\right]\right)}{\left(1 + Leverage * \left(R_g + \sum_i\left[\log(1 + CI_{clim,i}) * \beta_i * \left(1 - \delta * \frac{INV_{a,i}^{\exp(\eta)}}{INV_{a,s,i}^{\exp(\eta)} + INV_{a,i}^{\exp(\eta)}}\right)\right]\right) + (1 - L) * R_e\right)^t}\right] \quad (8.1)$$

The table of all the variables is detailed below:

Symbol	Unit	Definition
TFC(INV_a)	Currency (US$)	Total Funding Cost, quantifies the net present value of all debt repayment (P+I) cash flows.
TFC(inv_a)	% of total 'gross' investment	
INV_a,i	Currency (US$)	Quantifies the amount of investment in adaptation measure(s) related to climate-disaster 'i'.
inv_a,i	% of total 'gross' investment	
CI_clim,i	/	Climate risk indicator for climate-related disaster 'I' (can be mag for magnitude related or pop for affected population related).
B_i	%	Coefficient related to climate-related disaster 'I'.
CoD_g	%	Gross Cost of Debt, cost of debt without the part that is explained by climate-related risks (see regression).
CoD	%	Cost of Debt (all components, total).
CoD_a	%	Adapted Cost of Debt encompassing the reduction of exposure to climate-related disasters (exposure factor).
E_i(INV_a,i or inv_a,i)	%	Exposure factor: level of exposure of the physical, financed asset to a given climate-related disaster.
η	%	Effectiveness of an adaptation measure defined as the _

δ	%	Level of protection of an adaptation measure defined as the maximum level of disaster that the measure would protect against.
L	%	Leverage (debt / total project cost)
INV_g	Currency (US$) or 100%	Total 'gross' investment.
INV	Currency (US$) or % of total 'gross' investment	Total investment with adaptation (INV_g + INV_a or 1 + inv_a).
INT_t	Currency (US$) or % of total 'gross' investment	Interest repayment at year 't'.
P_t	Currency (US$) or % of total 'gross' investment	Principal repayment at year 't'.
R_e	%	Cost of equity

*betas take into account sector beta.

All financial quantities are in million US dollars.

11.6.1 Sample 1: magnitude climate indicator

11.6.1.1 Project ID 23: Thermal Power plant, Mozambique, concessional, 2020

Gross cost of debt (excl. climate):	2.93%
Cost of equity:	19.78%
Leverage:	57.00%
Gross investment (excl. adaptation):	$ 1,306.00
Loan tenure:	25
Wind β	0.667%
Wind climate indicator, log(1+CI):	4.61
Scaling resilience investment as percentage of investment:	7.50%
Selected resilience strategy (name):	Wind breaks - structural
Effectiveness of resilience strategy:	49.50%
Level of protection of resilience strategy:	99.45%
Optimized level of investment in resilience strategy:	8.62%
Exposure factor:	44.61%
Resulting cost of debt:	4.30%
Resulting discount rate:	10.96%
Total funding cost:	$ 847.82
Exposure factor and total funding cost shown as a function of the investment in resilience measure:	

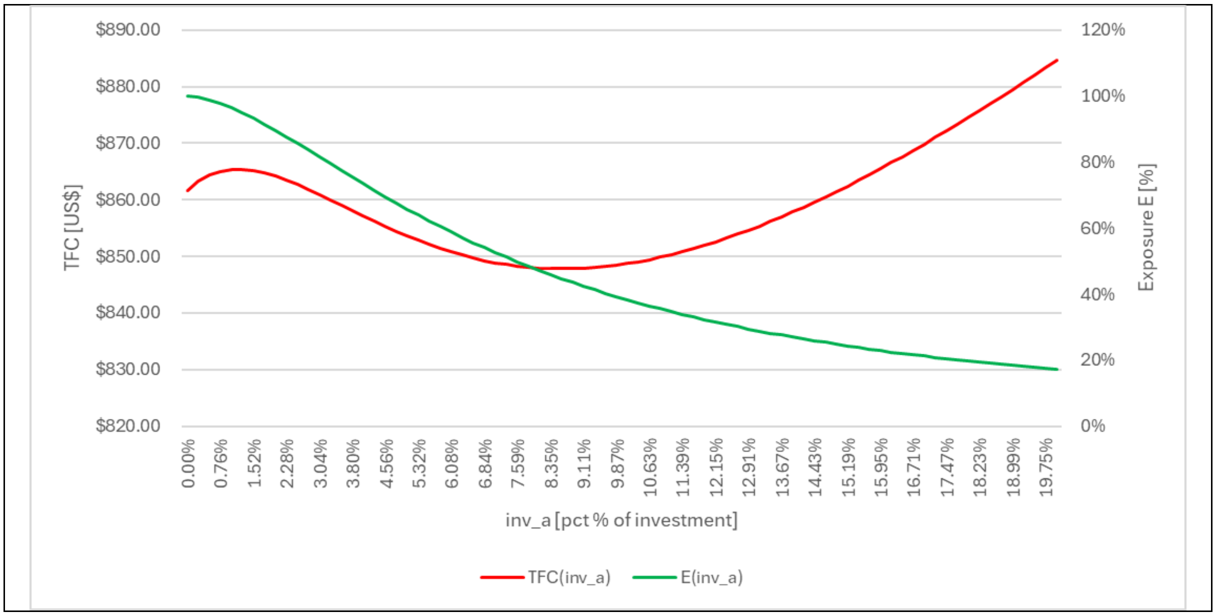

11.6.1.2 Project ID 174: Wind farm, South Africa, private, 2018

Gross cost of debt (excl. climate):	7.43%
Cost of equity:	10.42%
Leverage:	78.66%
Gross investment (excl. adaptation):	$ 253.00
Loan tenure:	40
Wind β :	0.667%
Wind climate indicator, log(1+CI):	5.87
Scaling resilience investment as percentage of investment:	7.50%
Selected resilience strategy (name):	Structural improvement
Effectiveness of resilience strategy:	79.50%
Level of protection of resilience strategy:	98.50%
Optimized level of investment in resilience strategy:	0.00%
Exposure factor:	100.00%
Resulting cost of debt:	11.35%
Resulting discount rate:	11.15%
Total funding cost:	$ 255.67
Exposure factor and total funding cost shown as a function of the investment in resilience measure:	

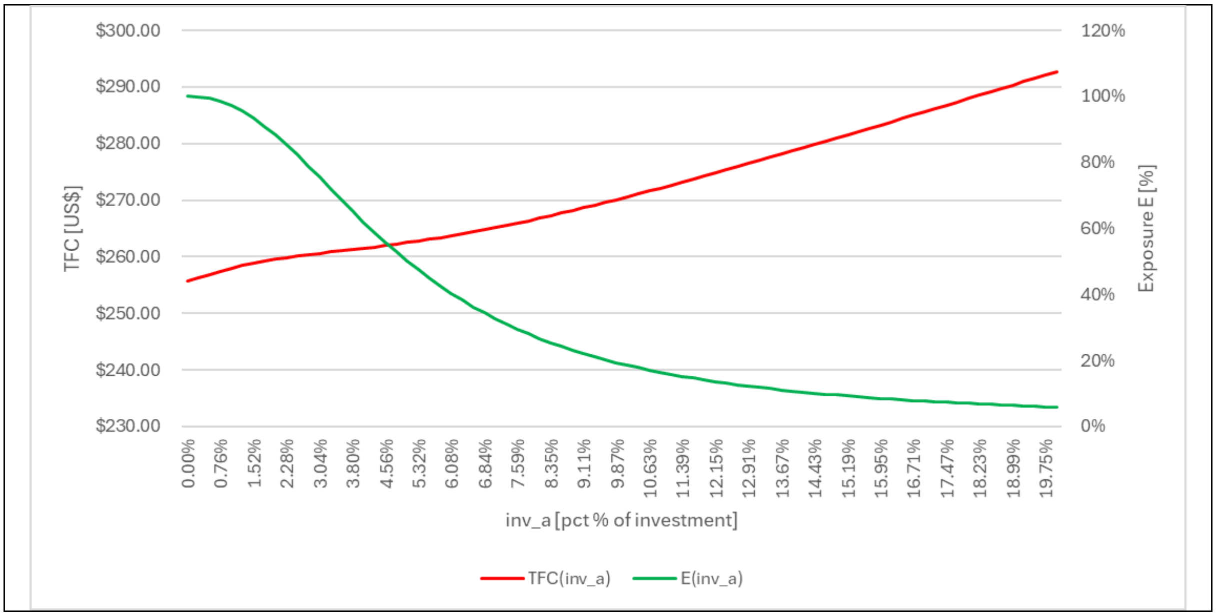

11.6.1.3 Project ID 175: Zeerust Solar farm, 86.19MW, South Africa, private, 2018

Gross cost of debt (excl. climate):	7.21%
Cost of equity:	10.42%
Leverage:	78.99%
Gross investment (excl. adaptation):	$ 119.00
Loan tenure:	20
Wind β:	0.667%
Wind climate indicator, log(1+CI):	5.79
Scaling resilience investment as percentage of investment:	7.50%
Selected resilience strategy (name):	Wind breaks - structural
Effectiveness of resilience strategy:	49.50%
Level of protection of resilience strategy:	99.45%
Optimized level of investment in resilience strategy:	0.00%
Exposure factor:	100.00%
Resulting cost of debt:	11.07%
Resulting discount rate:	10.94%
Total funding cost:	$ 119.83
Exposure factor and total funding cost shown as a function of the investment in resilience measure:	

WORKING PAPER #6

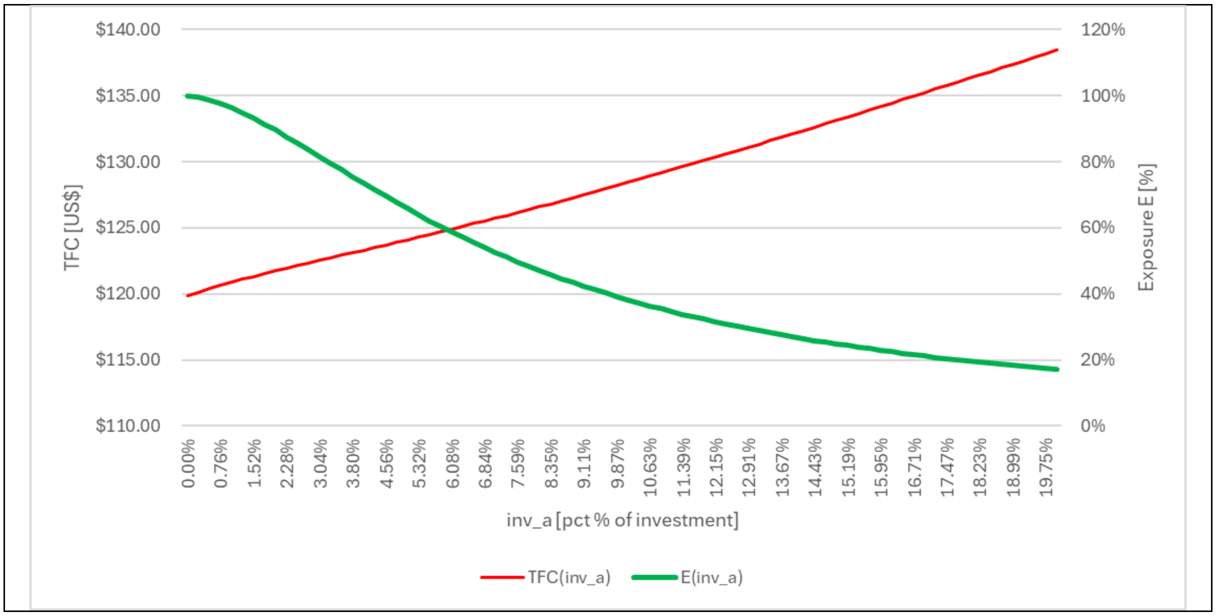

11.6.1.4 Project ID 176: Waterloo Solar farm, 86.2MW, South Africa, private, 2018

Gross cost of debt (excl. climate):	6.93%
Cost of equity:	10.42%
Leverage:	78.83%
Gross investment (excl. adaptation):	$ 137.00
Loan tenure:	25
Wind β:	0.667%
Wind climate indicator, log(1+CI):	5.68
Scaling resilience investment as percentage of investment:	7.50%
Selected resilience strategy (name):	Wind breaks - structural
Effectiveness of resilience strategy:	49.50%
Level of protection of resilience strategy:	99.45%
Optimized level of investment in resilience strategy:	0.00%
Exposure factor:	100.00%
Resulting cost of debt:	10.72%
Resulting discount rate:	10.65%
Total funding cost:	$ 137.43
Exposure factor and total funding cost shown as a function of the investment in resilience measure:	

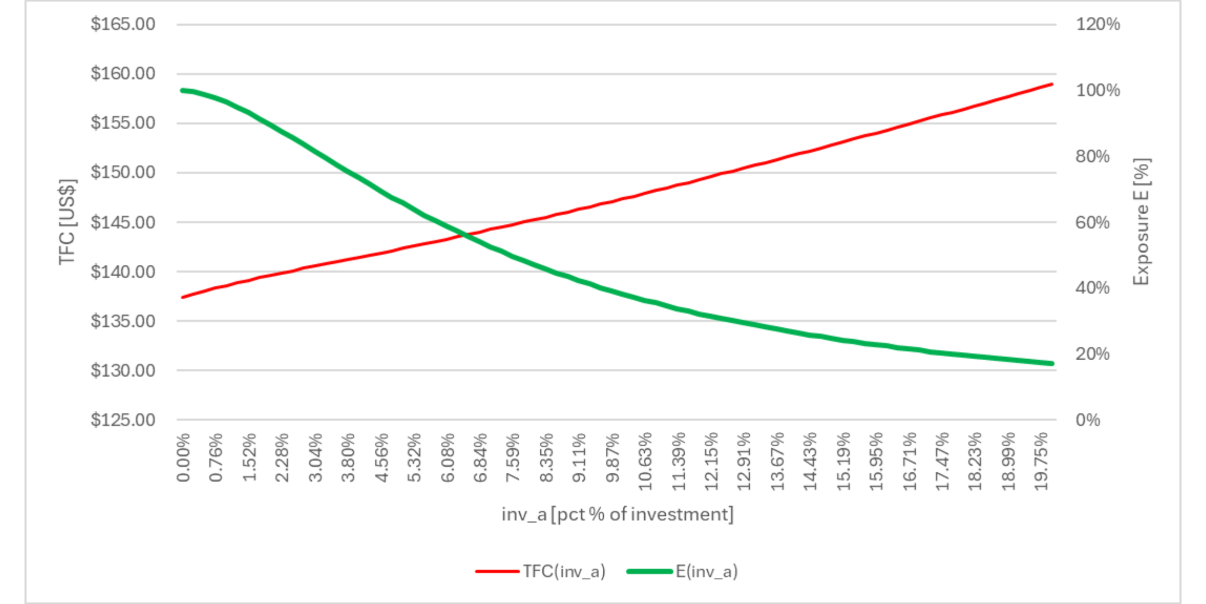

11.6.1.5 Project ID 177: De Wildt Solar farm, 57.68MW, South Africa, private, 2018

Gross cost of debt (excl. climate):	6.98%
Cost of equity:	10.42%
Leverage:	72.83%
Gross investment (excl. adaptation):	$ 92.00
Loan tenure:	20
Wind β:	0.667%
Wind climate indicator, log(1+CI):	5.69
Scaling resilience investment as percentage of investment:	7.50%
Selected resilience strategy (name):	Wind breaks - structural
Effectiveness of resilience strategy:	49.50%
Level of protection of resilience strategy:	99.45%
Optimized level of investment in resilience strategy:	0.00%
Exposure factor:	100.00%
Resulting cost of debt:	10.77%
Resulting discount rate:	10.68%
Total funding cost:	6.98%
Exposure factor and total funding cost shown as a function of the investment in resilience measure:	

WORKING PAPER #6

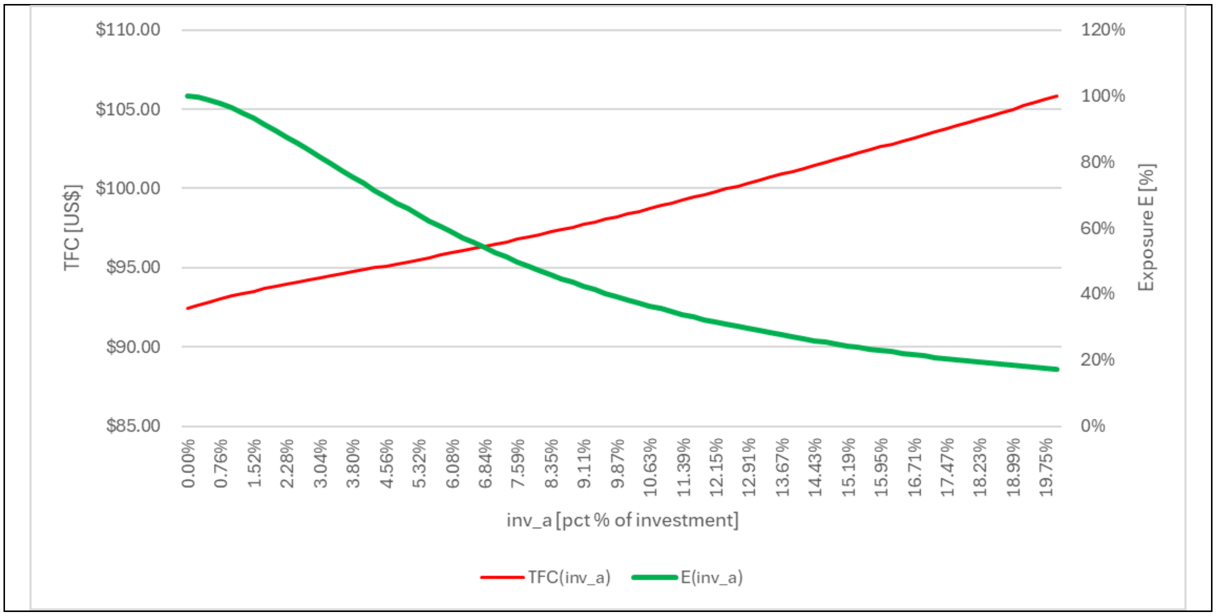

11.6.1.6 Project ID 178: Greefspan II Solar farm, 63.2MW, South Africa, private, 2018

Gross cost of debt (excl. climate):	6.54%
Cost of equity:	10.42%
Leverage:	79.09%
Gross investment (excl. adaptation):	$ 110.00
Loan tenure:	18
Wind β:	0.667%
Wind climate indicator, log(1+CI):	5.83
Scaling resilience investment as percentage of investment:	7.50%
Selected resilience strategy (name):	Wind breaks - structural
Effectiveness of resilience strategy:	49.50%
Level of protection of resilience strategy:	99.45%
Optimized level of investment in resilience strategy:	0.00%
Exposure factor:	100.00%
Resulting cost of debt:	10.42%
Resulting discount rate:	10.42%
Total funding cost:	6.54%
Exposure factor and total funding cost shown as a function of the investment in resilience measure:	

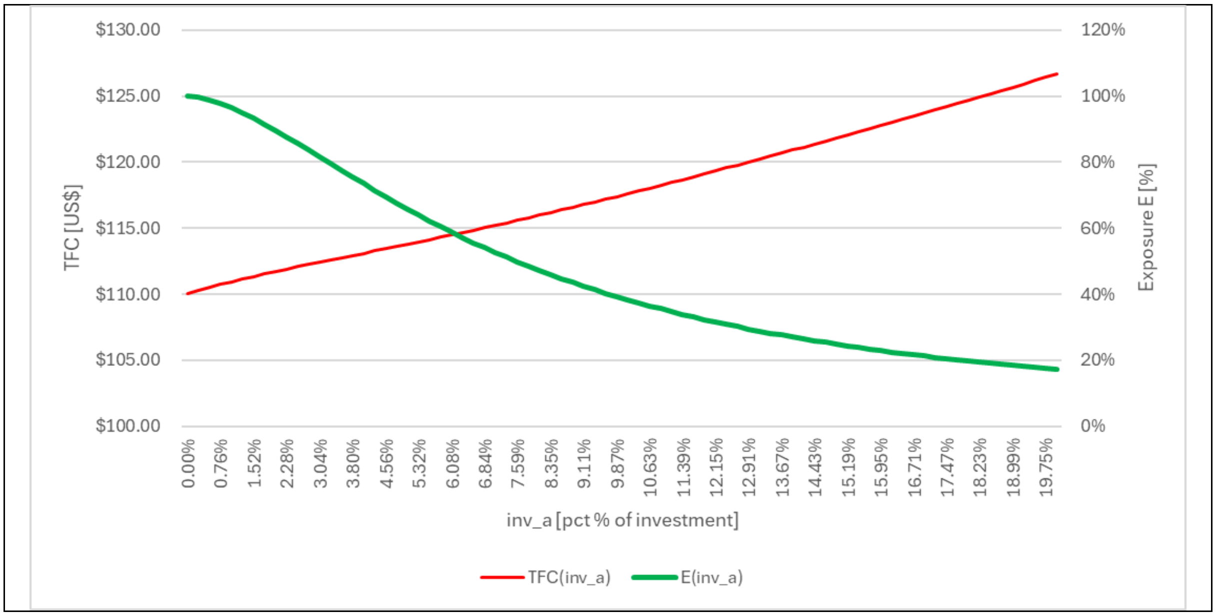

11.6.1.7 Project ID 179: Bokamoso Solar farm, 67.9MW, South Africa, private, 2018

Gross cost of debt (excl. climate):	7.18%
Cost of equity:	10.42%
Leverage:	80.80%
Gross investment (excl. adaptation):	$ 125.00
Loan tenure:	19
Wind β:	0.667%
Wind climate indicator, log(1+CI):	5.80
Scaling resilience investment as percentage of investment:	5.00%
Selected resilience strategy (name):	Wind breaks - structural
Effectiveness of resilience strategy:	49.50%
Level of protection of resilience strategy:	99.45%
Optimized level of investment in resilience strategy:	0.00%
Exposure factor:	100.00%
Resulting cost of debt:	11.05%
Resulting discount rate:	10.93%
Total funding cost:	7.18%
Exposure factor and total funding cost shown as a function of the investment in resilience measure:	

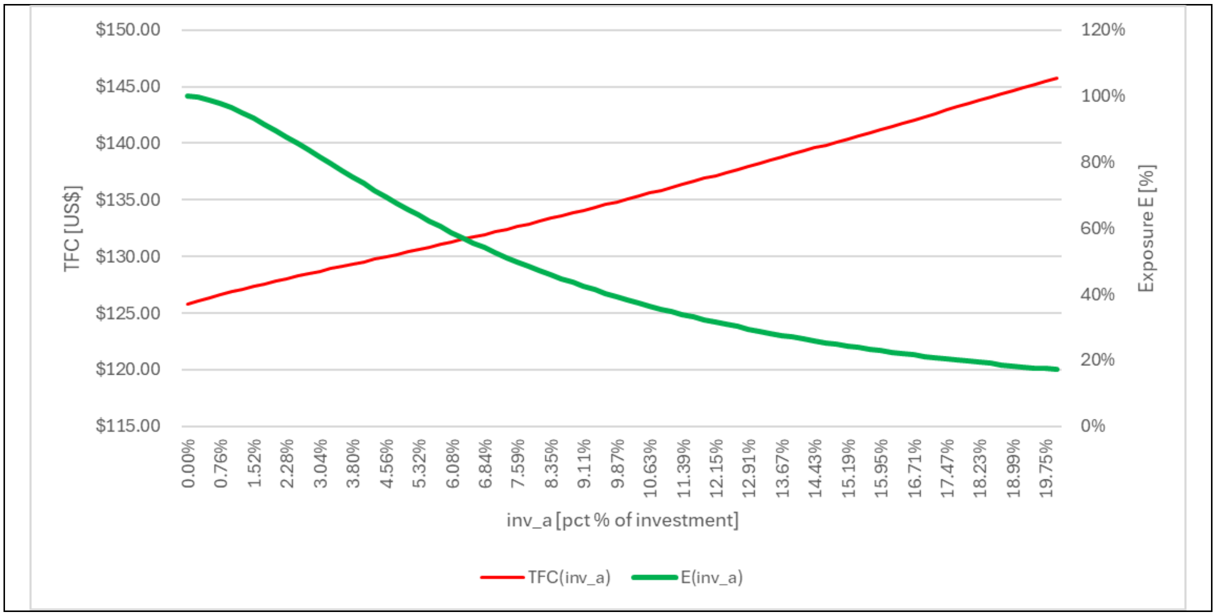

11.6.1.8 Project ID 180: Sirius Solar farm, 75MW, South Africa, private, 2018

Gross cost of debt (excl. climate):	6.40%
Cost of equity:	10.42%
Leverage:	79.29%
Gross investment (excl. adaptation):	$ 140.00
Loan tenure:	17
Wind β:	0.667%
Wind climate indicator, log(1+CI):	5.77
Scaling resilience investment as percentage of investment:	7.50%
Selected resilience strategy (name):	Wind breaks - structural
Effectiveness of resilience strategy:	49.50%
Level of protection of resilience strategy:	99.45%
Optimized level of investment in resilience strategy:	0.00%
Exposure factor:	100.00%
Resulting cost of debt:	10.25%
Resulting discount rate:	10.28%
Total funding cost:	6.40%
Exposure factor and total funding cost shown as a function of the investment in resilience measure:	

WORKING PAPER #6

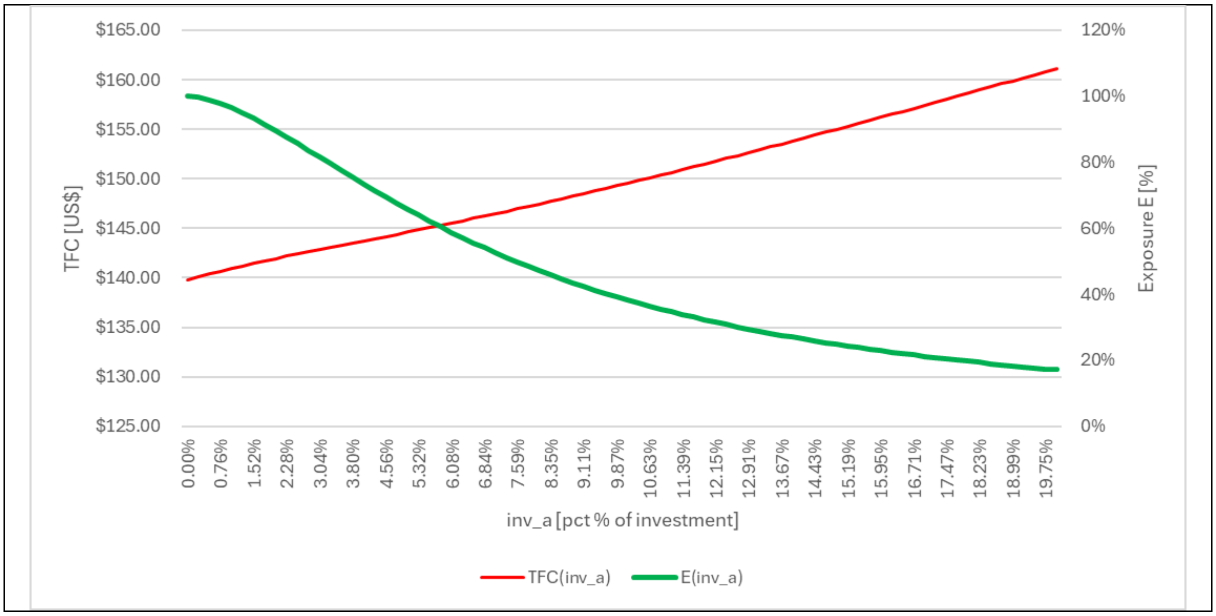

11.6.1.9 Project ID 181: Dayson's Klip 2 Solar farm, 75MW, South Africa, private, 2018

Gross cost of debt (excl. climate):	6.64%
Cost of equity:	10.42%
Leverage:	79.29%
Gross investment (excl. adaptation):	$ 140.00
Loan tenure:	16
Wind β:	0.667%
Wind climate indicator, log(1+CI):	5.81
Scaling resilience investment as percentage of investment:	7.50%
Selected resilience strategy (name):	Wind breaks - structural
Effectiveness of resilience strategy:	49.50%
Level of protection of resilience strategy:	99.45%
Optimized level of investment in resilience strategy:	0.00%
Exposure factor:	100.00%
Resulting cost of debt:	10.52%
Resulting discount rate:	10.50%
Total funding cost:	6.64%
Exposure factor and total funding cost shown as a function of the investment in resilience measure:	

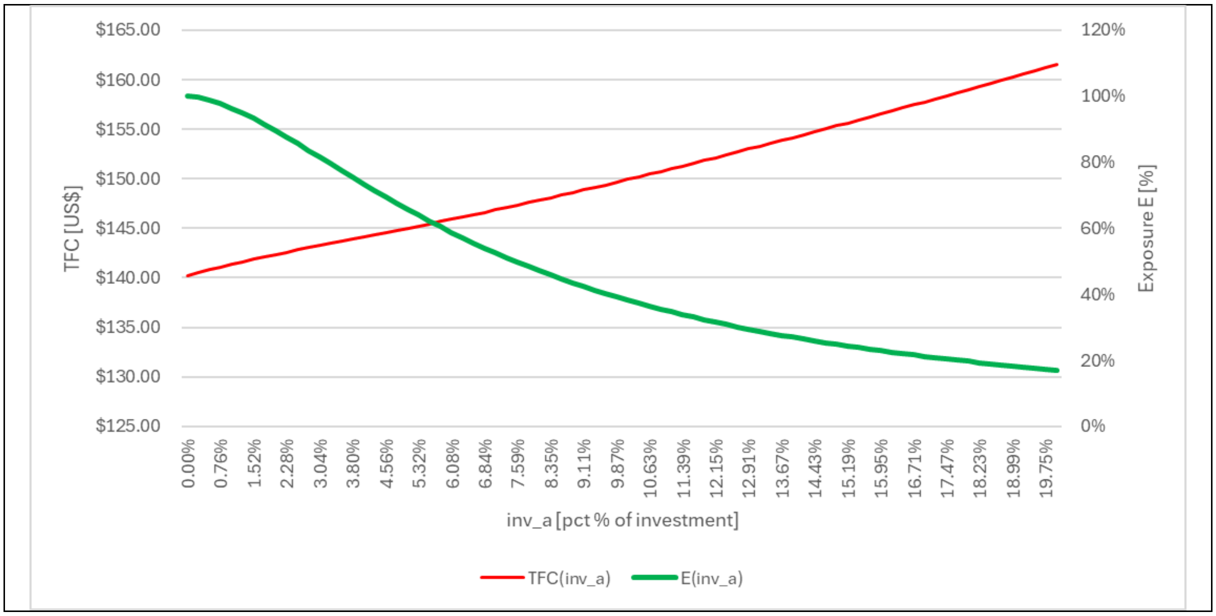

11.6.1.10 Project ID 182: Dayson's Klip 1 Solar farm, 75MW, South Africa, private, 2018

Gross cost of debt (excl. climate):	6.37%
Cost of equity:	10.42%
Leverage:	79.43%
Gross investment (excl. adaptation):	$ 141.00
Loan tenure:	16
Wind β:	0.667%
Wind climate indicator, log(1+CI):	5.80
Scaling resilience investment as percentage of investment:	7.50%
Selected resilience strategy (name):	Wind breaks - structural
Effectiveness of resilience strategy:	49.50%
Level of protection of resilience strategy:	99.45%
Optimized level of investment in resilience strategy:	0.00%
Exposure factor:	100.00%
Resulting cost of debt:	10.25%
Resulting discount rate:	10.28%
Total funding cost:	6.37%
Exposure factor and total funding cost shown as a function of the investment in resilience measure:	

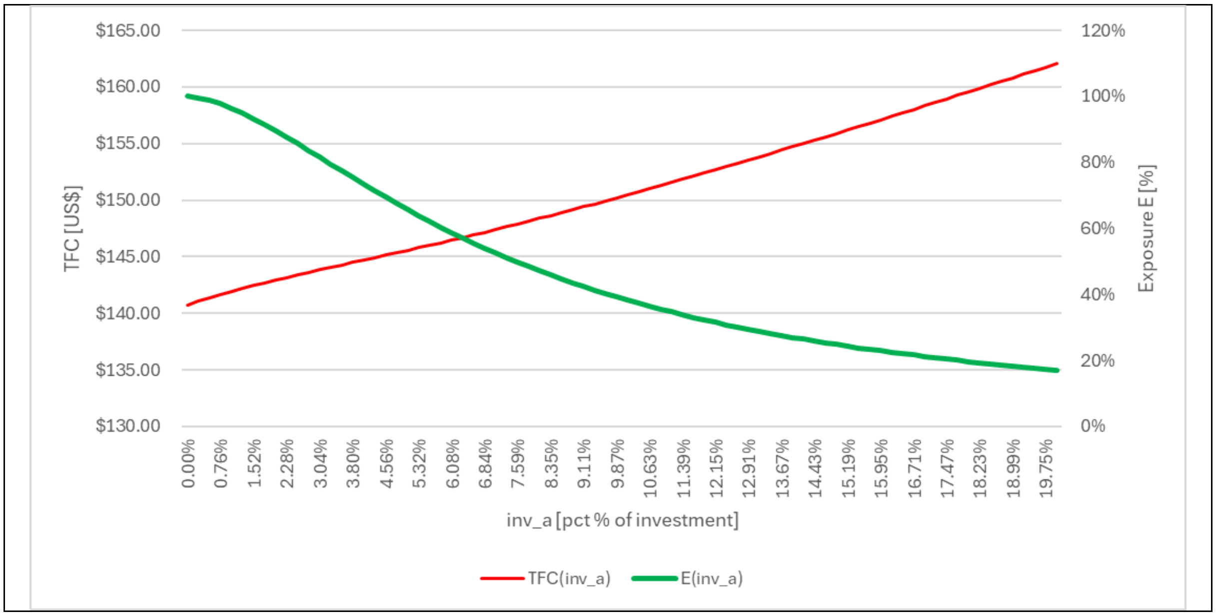

11.6.1.11 Project ID 204: Redstone CSP plant, 100MW, South Africa, private, 2019

Gross cost of debt (excl. climate):	5.41%
Cost of equity:	8.33%
Leverage:	83.75%
Gross investment (excl. adaptation):	$ 800.00
Loan tenure:	18
Wind β:	0.667%
Wind climate indicator, log(1+CI):	5.82
Scaling resilience investment as percentage of investment:	7.50%
Selected resilience strategy (name):	Wind breaks - structural
Effectiveness of resilience strategy:	49.50%
Level of protection of resilience strategy:	99.45%
Optimized level of investment in resilience strategy:	0.00%
Exposure factor:	100.00%
Resulting cost of debt:	9.29%
Resulting discount rate:	9.13%
Total funding cost:	5.41%
Exposure factor and total funding cost shown as a function of the investment in resilience measure:	

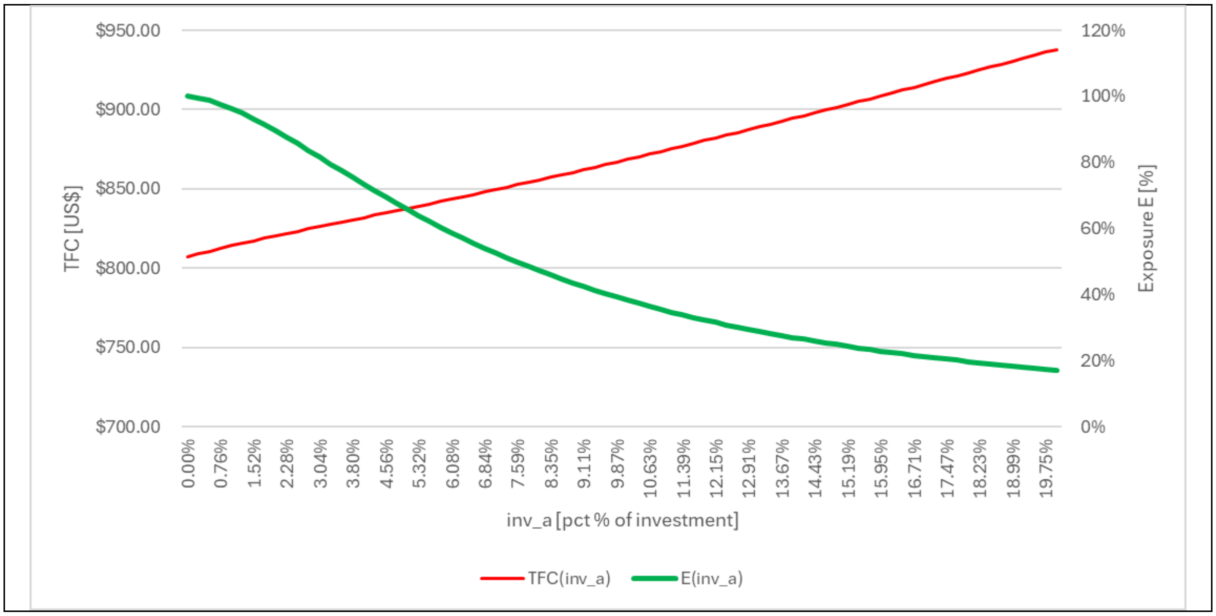

11.6.1.12 Project ID 223: Droogfontein 2 Solar farm, 86.23MW, South Africa, private, 2018

Gross cost of debt (excl. climate):	6.85%
Cost of equity:	10.42%
Leverage:	77.69%
Gross investment (excl. adaptation):	$ 121.00
Loan tenure:	17
Wind β:	0.667%
Wind climate indicator, log(1+CI):	5.78
Scaling resilience investment as percentage of investment:	7.50%
Selected resilience strategy (name):	Wind breaks - structural
Effectiveness of resilience strategy:	49.50%
Level of protection of resilience strategy:	99.45%
Optimized level of investment in resilience strategy:	0.00%
Exposure factor:	100.00%
Resulting cost of debt:	10.70%
Resulting discount rate:	10.64%
Total funding cost:	121.4 mUSD
Exposure factor and total funding cost shown as a function of the investment in resilience measure:	

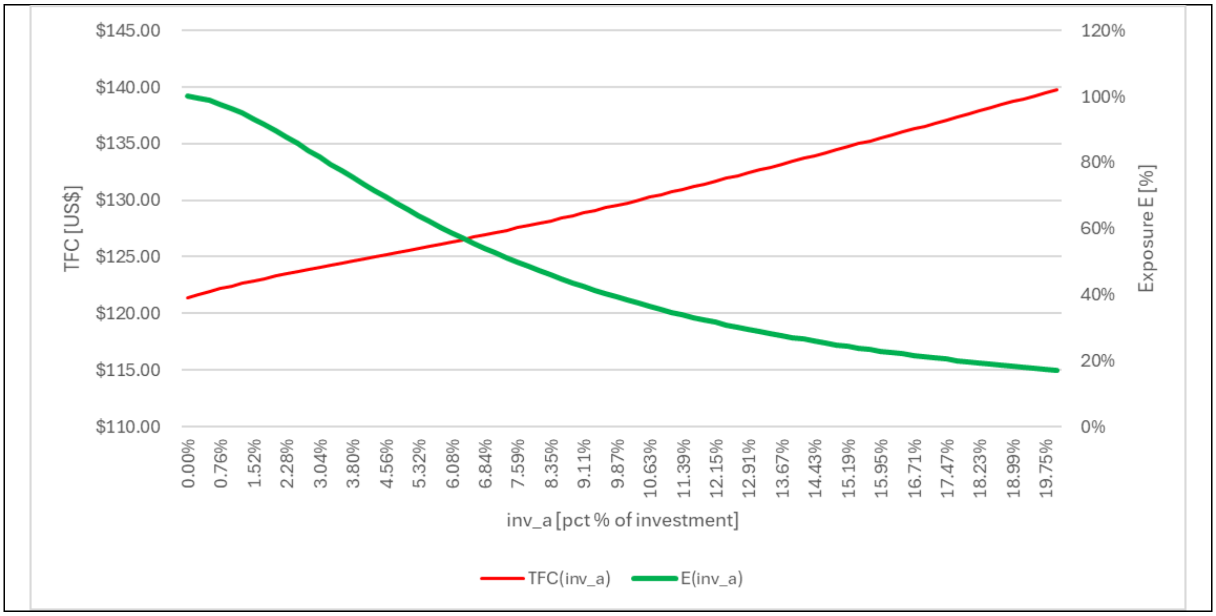

11.6.1.13 Project ID 226: Karusa Wind farm, 142MW, South Africa, private, 2018

Gross cost of debt (excl. climate):	7.40%
Cost of equity:	10.42%
Leverage:	79.48%
Gross investment (excl. adaptation):	$ 268.00
Loan tenure:	17
Wind β:	0.667%
Wind climate indicator, log(1+CI):	5.87
Scaling resilience investment as percentage of investment:	7.50%
Selected resilience strategy (name):	Wind breaks - structural
Effectiveness of resilience strategy:	79.50%
Level of protection of resilience strategy:	98.50%
Optimized level of investment in resilience strategy:	0.00%
Exposure factor:	100.00%
Resulting cost of debt:	11.32%
Resulting discount rate:	11.13%
Total funding cost:	270.64 mUSD
Exposure factor and total funding cost shown as a function of the investment in resilience measure:	

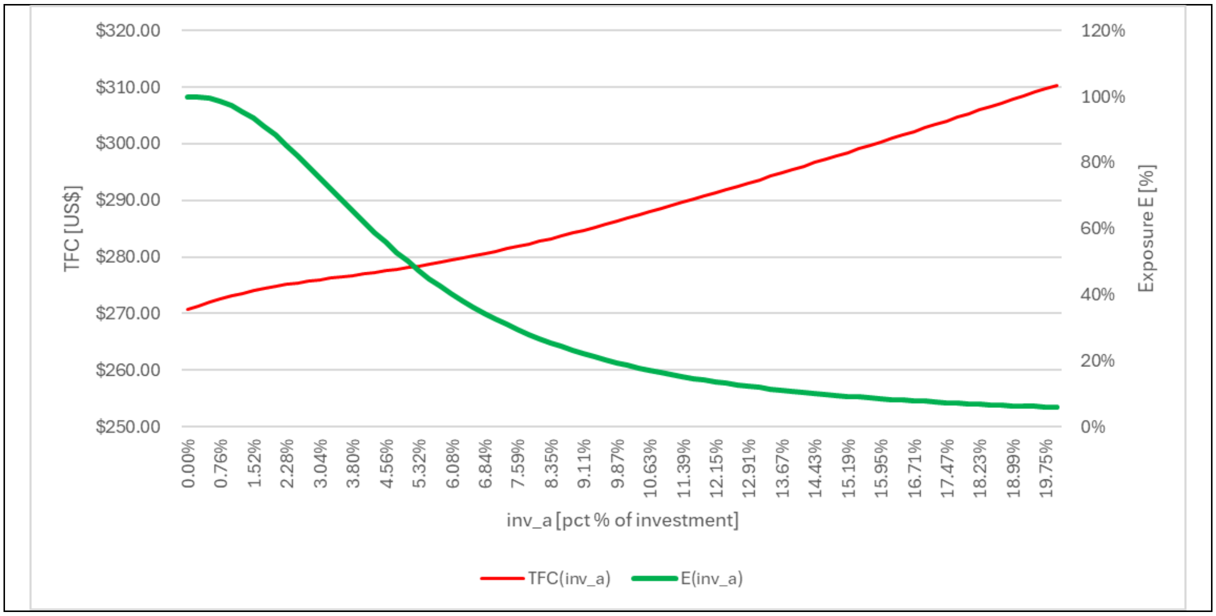

11.6.1.14 Project ID 227: Garob Wind farm, 144.9MW, South Africa, private, 2018

Gross cost of debt (excl. climate):	7.41%
Cost of equity:	10.42%
Leverage:	80.26%
Gross investment (excl. adaptation):	$ 304.00
Loan tenure:	18
Wind β:	0.667%
Wind climate indicator, log(1+CI):	5.85
Scaling resilience investment as percentage of investment:	7.50%
Selected resilience strategy (name):	Wind breaks - structural
Effectiveness of resilience strategy:	79.50%
Level of protection of resilience strategy:	98.50%
Optimized level of investment in resilience strategy:	0.00%
Exposure factor:	100.00%
Resulting cost of debt:	11.32%
Resulting discount rate:	11.14%
Total funding cost:	306.79 mUSD
Exposure factor and total funding cost shown as a function of the investment in resilience measure:	

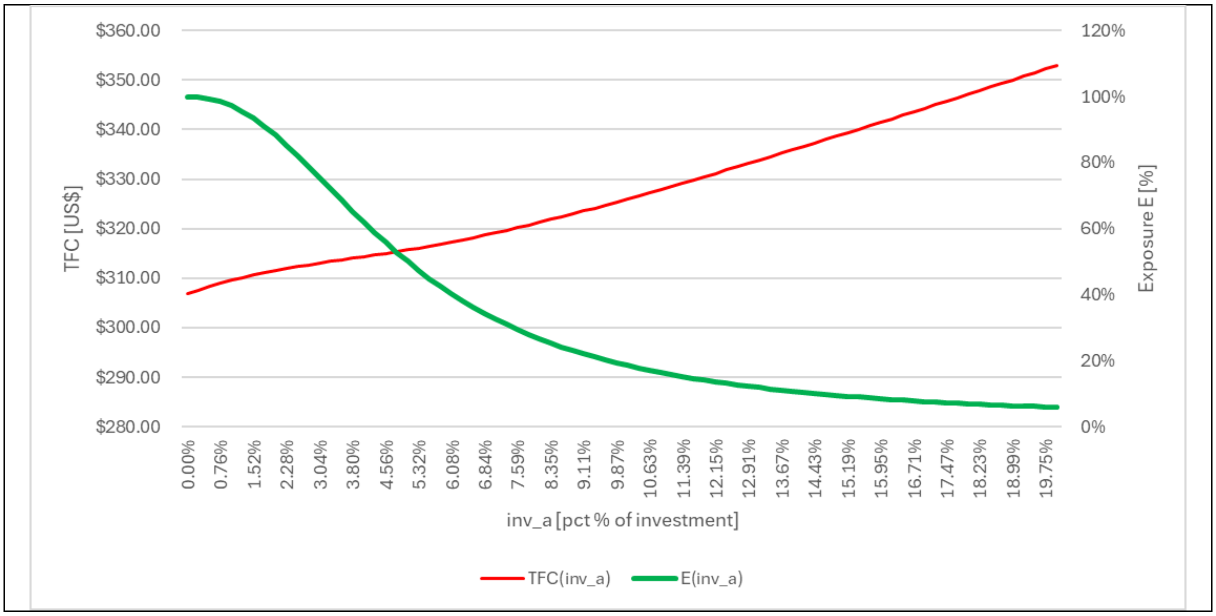

11.6.1.15 Project ID 228: Roggeveld Wind farm, 147MW, South Africa, private, 2018

Gross cost of debt (excl. climate):	8.04%
Cost of equity:	10.42%
Leverage:	71.06%
Gross investment (excl. adaptation):	$ 387.00
Loan tenure:	18
Wind β:	0.667%
Wind climate indicator, log(1+CI):	5.86
Scaling resilience investment as percentage of investment:	7.50%
Selected resilience strategy (name):	Structural improvement
Effectiveness of resilience strategy:	79.50%
Level of protection of resilience strategy:	98.50%
Optimized level of investment in resilience strategy:	0.00%
Exposure factor:	100.00%
Resulting cost of debt:	11.95%
Resulting discount rate:	11.51%
Total funding cost:	11.51%
Exposure factor and total funding cost shown as a function of the investment in resilience measure:	

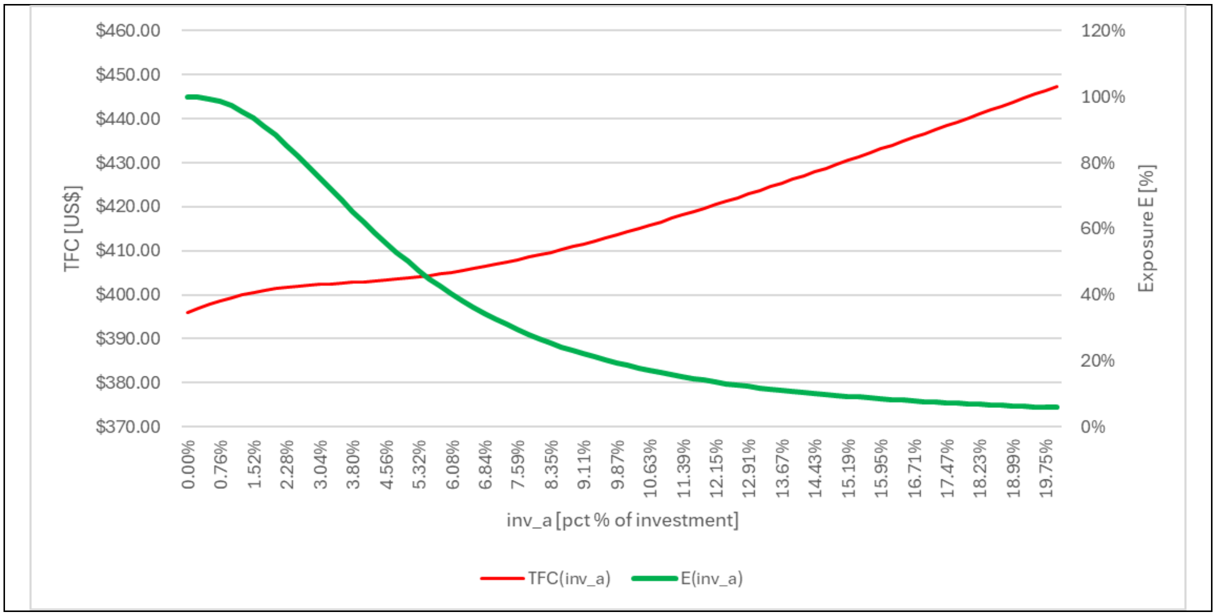

11.6.1.16 Project ID 229: Mettle Solar portfolio, 5MW, South Africa, private, 2017

Gross cost of debt (excl. climate):	6.47%
Cost of equity:	8.96%
Leverage:	75.00%
Gross investment (excl. adaptation):	$ 4.00
Loan tenure:	17
Wind β:	0.667%
Wind climate indicator, log(1+CI):	5.79
Scaling resilience investment as percentage of investment:	7.50%
Selected resilience strategy (name):	Wind breaks - structural
Effectiveness of resilience strategy:	49.50%
Level of protection of resilience strategy:	99.45%
Optimized level of investment in resilience strategy:	0.00%
Exposure factor:	100.00%
Resulting cost of debt:	10.33%
Resulting discount rate:	9.99%
Total funding cost:	$4.07
Exposure factor and total funding cost shown as a function of the investment in resilience measure:	

11.6.1.17 Project ID 232: Impofu Wind farm, 330MW, South Africa, private, 2024

Gross cost of debt (excl. climate):	7.19%
Cost of equity:	18.79%
Leverage:	79.63%
Gross investment (excl. adaptation):	$ 594.00
Loan tenure:	17
Wind β:	0.667%
Wind climate indicator, log(1+CI):	5.85
Scaling resilience investment as percentage of investment:	7.50%
Selected resilience strategy (name):	Structural improvement
Effectiveness of resilience strategy:	79.50%
Level of protection of resilience strategy:	98.50%
Optimized level of investment in resilience strategy:	0.00%
Exposure factor:	100.00%
Resulting cost of debt:	11.10%
Resulting discount rate:	12.66%
Total funding cost:	$551.37
Exposure factor and total funding cost shown as a function of the investment in resilience measure:	

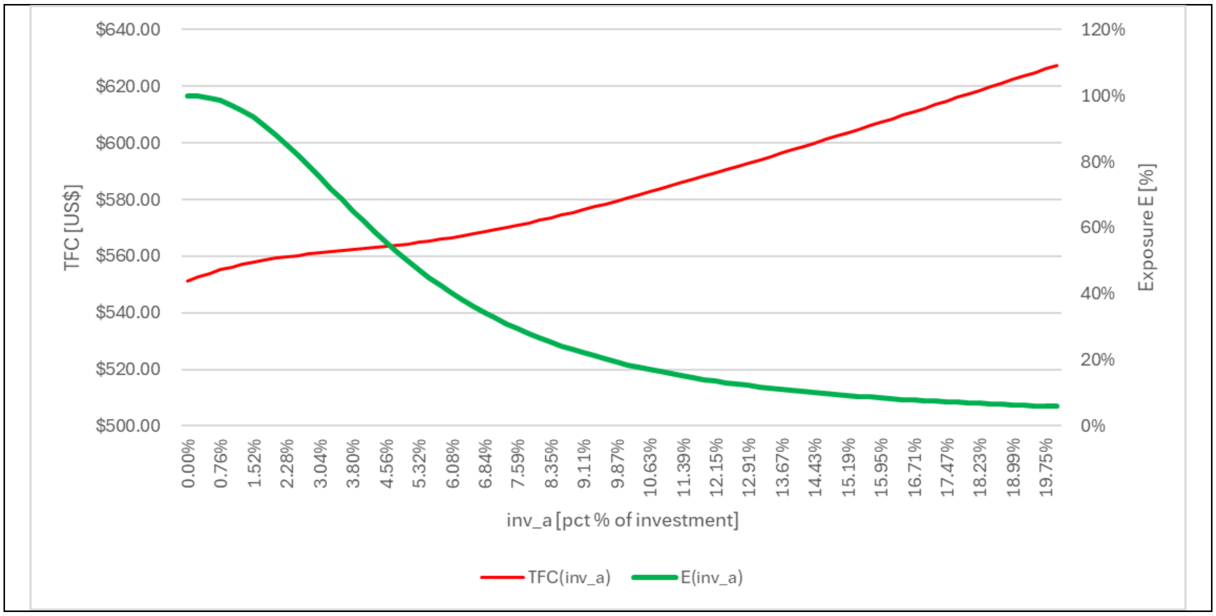

11.6.1.18 Project ID 234: Xina CSP plant, 100MW, South Africa, private, 2015

Gross cost of debt (excl. climate):	3.96%
Cost of equity:	10.25%
Leverage:	72.37%
Gross investment (excl. adaptation):	$ 854.00
Loan tenure:	15
Wind β:	0.667%
Wind climate indicator, log(1+CI):	2.75
Scaling resilience investment as percentage of investment:	7.50%
Selected resilience strategy (name):	Structural improvement
Effectiveness of resilience strategy:	49.50%
Level of protection of resilience strategy:	99.45%
Optimized level of investment in resilience strategy:	0.00%
Exposure factor:	100.00%
Resulting cost of debt:	5.80%
Resulting discount rate:	7.03%
Total funding cost:	$ 790.11
Exposure factor and total funding cost shown as a function of the investment in resilience measure:	

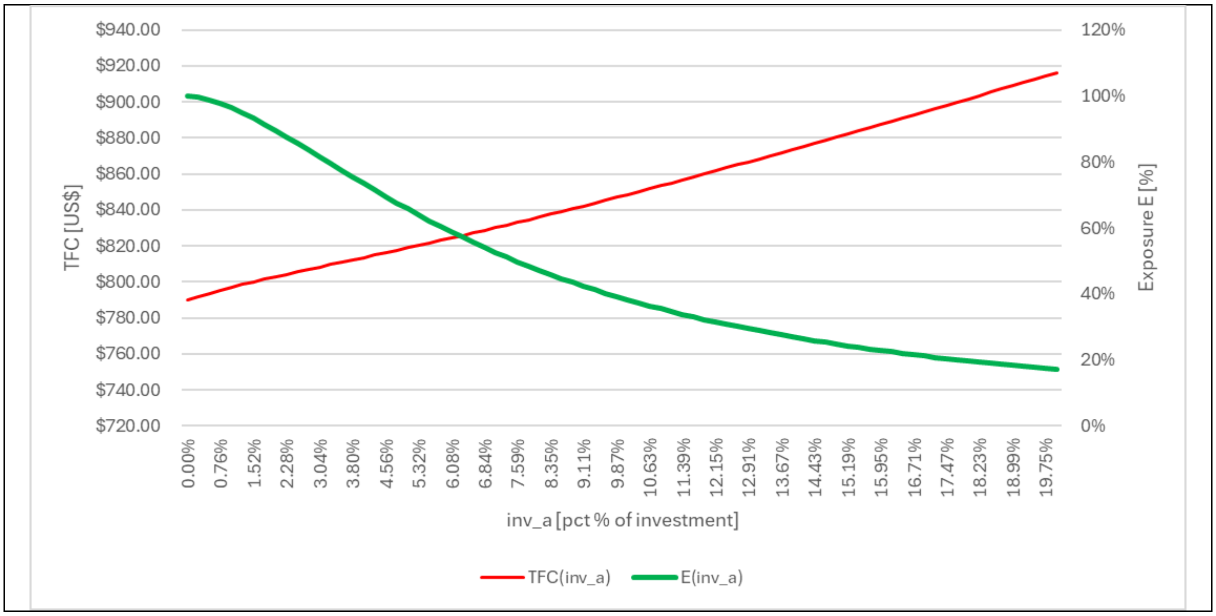

11.6.1.19 Project ID 235: Virginia Solar farm, 275MW, South Africa, private, 2024

Gross cost of debt (excl. climate):	4.57%
Cost of equity:	18.79%
Leverage:	77.02%
Gross investment (excl. adaptation):	$ 248.00
Loan tenure:	17
Wind β:	0.667%
Wind climate indicator, log(1+CI):	5.68
Scaling resilience investment as percentage of investment:	7.50%
Selected resilience strategy (name):	Wind breaks - structural
Effectiveness of resilience strategy:	49.50%
Level of protection of resilience strategy:	99.45%
Optimized level of investment in resilience strategy:	0.00%
Exposure factor:	100.00%
Resulting cost of debt:	8.53%
Resulting discount rate:	10.89%
Total funding cost:	$ 218.29
Exposure factor and total funding cost shown as a function of the investment in resilience measure:	

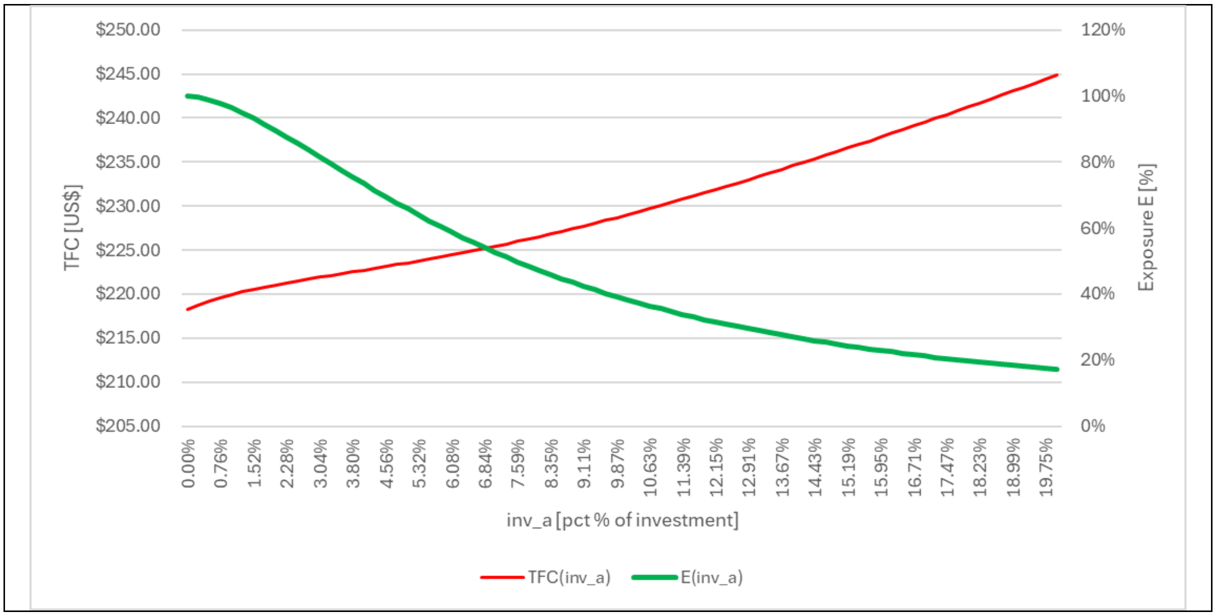

11.6.2 8.5.2 Sample 2: affected population climate indicator

11.6.2.1 Project ID 23: Thermal Power plant, Mozambique, concessional

Gross cost of debt (excl. climate):	5.17%
Cost of equity:	19.78%
Leverage:	57.00%
Gross investment (excl. adaptation):	$ 1,306.00
Loan tenure:	25
Wind β:	2.940%
Wind climate indicator, log(1+CI):	0.28
Scaling resilience investment as percentage of investment:	7.50%
Selected resilience strategy (name):	Wind breaks - structural
Effectiveness of resilience strategy:	49.50%
Level of protection of resilience strategy:	99.45%
Optimized level of investment in resilience strategy:	0.00%
Exposure factor:	100.00%
Resulting cost of debt:	6.00%
Resulting discount rate:	11.93%
Total funding cost:	$ 861.64
Exposure factor and total funding cost shown as a function of the investment in resilience measure:	

WORKING PAPER #6

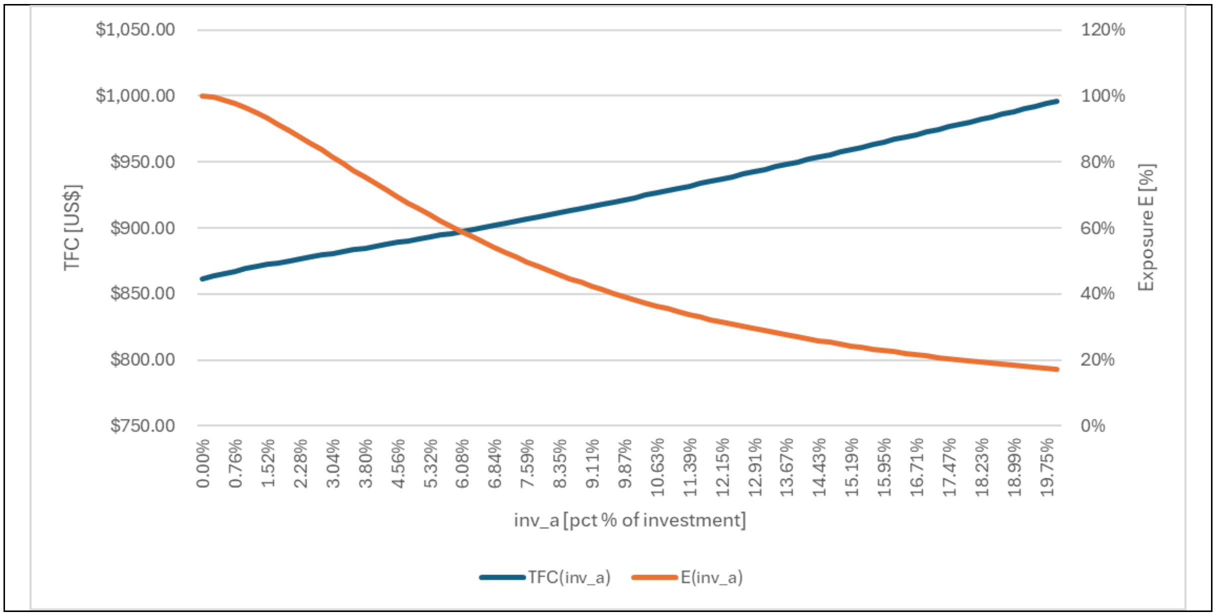

11.6.2.2 Project ID 174: Wind farm, South Africa, private

Gross cost of debt (excl. climate):	11.22%
Cost of equity:	10.42%
Leverage:	78.66%
Gross investment (excl. adaptation):	$ 253.00
Loan tenure:	19
Wind β:	2.940%
Wind climate indicator, log(1+CI):	0.04
Scaling resilience investment as percentage of investment:	5.00%
Selected resilience strategy (name):	Structural improvement
Effectiveness of resilience strategy:	79.50%
Level of protection of resilience strategy:	98.50%
Optimized level of investment in resilience strategy:	0.00%
Exposure factor:	100.00%
Resulting cost of debt:	11.35%
Resulting discount rate:	11.15%
Total funding cost:	$ 255.67
Exposure factor and total funding cost shown as a function of the investment in resilience measure:	

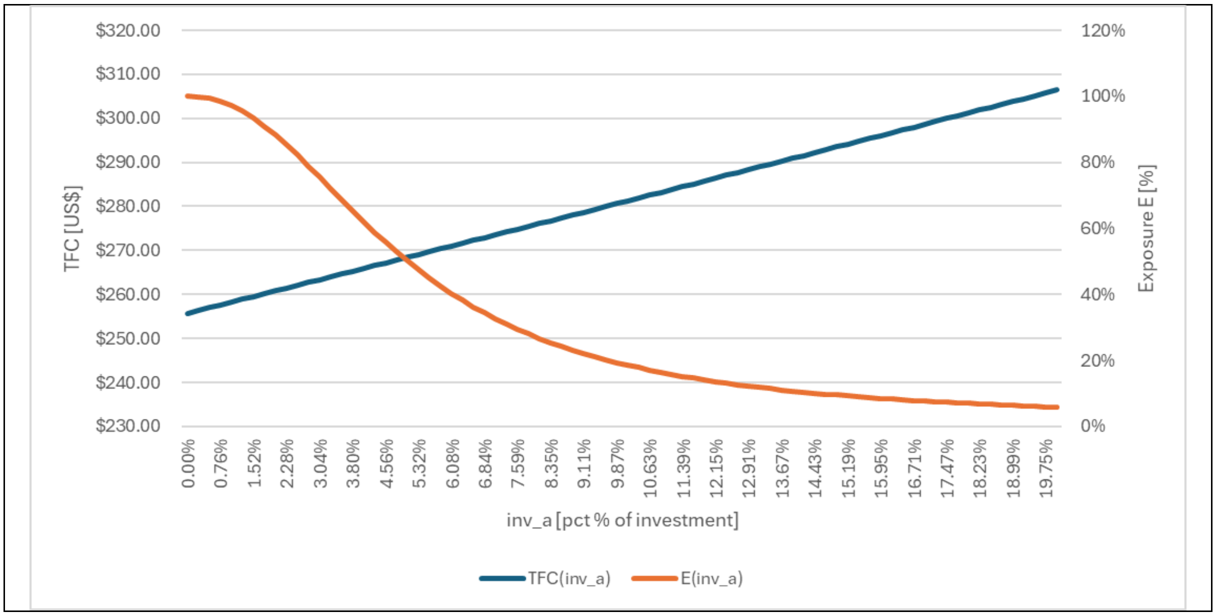

11.6.2.3 Project ID 175: Solar farm, South Africa, private

Gross cost of debt (excl. climate):	10.96%
Cost of equity:	10.42%
Leverage:	78.99%
Gross investment (excl. adaptation):	$ 119.00
Loan tenure:	17
Wind β:	2.940%
Wind climate indicator, log(1+CI):	0.04
Scaling resilience investment as percentage of investment:	7.50%
Selected resilience strategy (name):	Wind breaks - structural
Effectiveness of resilience strategy:	49.50%
Level of protection of resilience strategy:	99.45%
Optimized level of investment in resilience strategy:	0.00%
Exposure factor:	100.00%
Resulting cost of debt:	11.07%
Resulting discount rate:	10.94%
Total funding cost:	$ 119.83
Exposure factor and total funding cost shown as a function of the investment in resilience measure:	

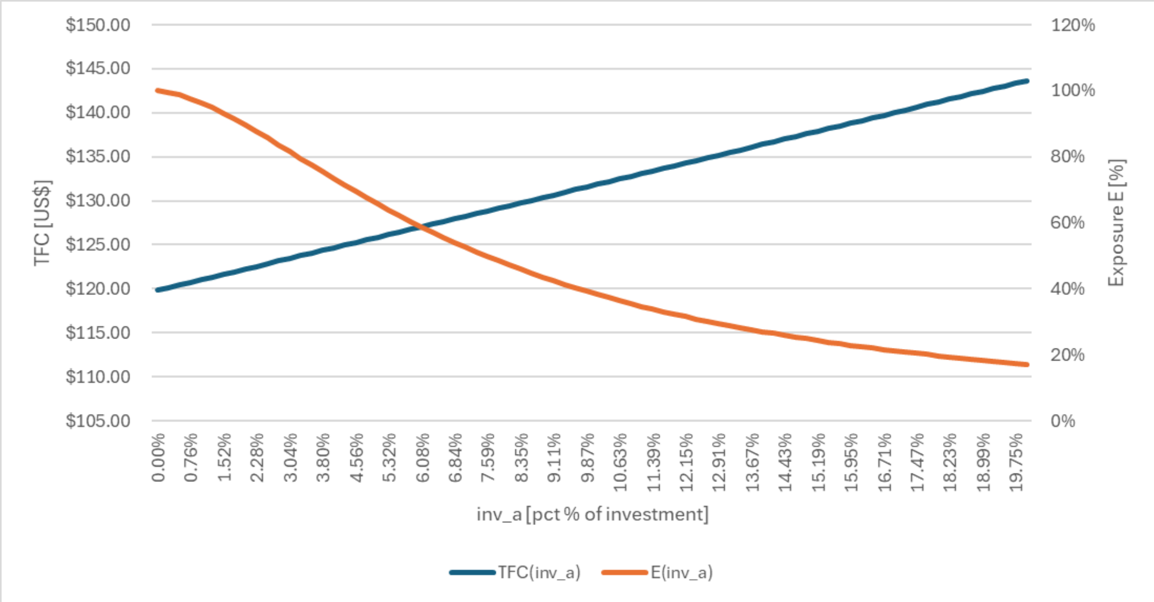

11.6.2.4 Project ID 176: Solar farm, South Africa, private

Gross cost of debt (excl. climate):	10.62%
Cost of equity:	10.42%
Leverage:	78.83%
Gross investment (excl. adaptation):	$ 137.00
Loan tenure:	16
Wind β:	2.940%
Wind climate indicator, log(1+CI):	0.03
Scaling resilience investment as percentage of investment:	7.50%
Selected resilience strategy (name):	Wind breaks - structural
Effectiveness of resilience strategy:	49.50%
Level of protection of resilience strategy:	99.45%
Optimized level of investment in resilience strategy:	0.00%
Exposure factor:	100.00%
Resulting cost of debt:	10.72%
Resulting discount rate:	10.65%
Total funding cost:	$ 137.43
Exposure factor and total funding cost shown as a function of the investment in resilience measure:	

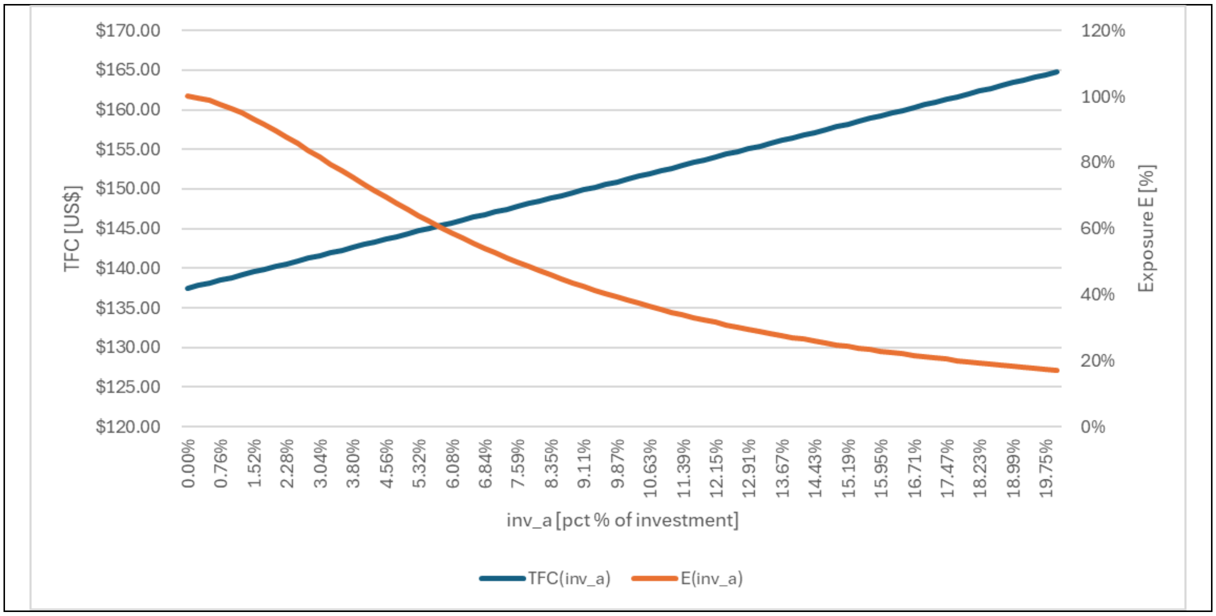

11.6.2.5 Project ID 177: Solar farm, South Africa, private

Gross cost of debt (excl. climate):	10.67%
Cost of equity:	10.42%
Leverage:	72.83%
Gross investment (excl. adaptation):	$ 92.00
Loan tenure:	16
Wind β:	2.940%
Wind climate indicator, log(1+CI):	0.04
Scaling resilience investment as percentage of investment:	7.50%
Selected resilience strategy (name):	Wind breaks - structural
Effectiveness of resilience strategy:	49.50%
Level of protection of resilience strategy:	99.45%
Optimized level of investment in resilience strategy:	0.00%
Exposure factor:	100.00%
Resulting cost of debt:	10.77%
Resulting discount rate:	10.68%
Total funding cost:	$ 92.44
Exposure factor and total funding cost shown as a function of the investment in resilience measure:	

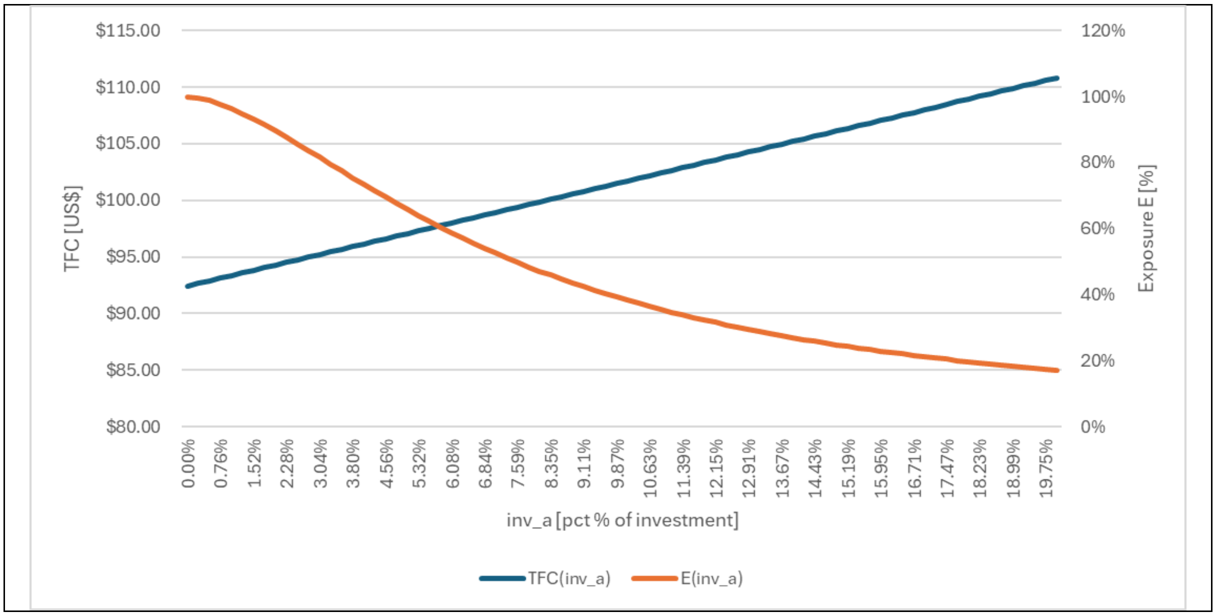

11.6.2.6 Project ID 178: Solar farm, South Africa, private

Gross cost of debt (excl. climate):	10.31%
Cost of equity:	10.42%
Leverage:	79.09%
Gross investment (excl. adaptation):	$ 110.00
Loan tenure:	18
Wind β:	2.940%
Wind climate indicator, log(1+CI):	0.04
Scaling resilience investment as percentage of investment:	7.50%
Selected resilience strategy (name):	Wind breaks - structural
Effectiveness of resilience strategy:	49.50%
Level of protection of resilience strategy:	99.45%
Optimized level of investment in resilience strategy:	0.00%
Exposure factor:	100.00%
Resulting cost of debt:	10.42%
Resulting discount rate:	10.42%
Total funding cost:	$ 110.01
Exposure factor and total funding cost shown as a function of the investment in resilience measure:	

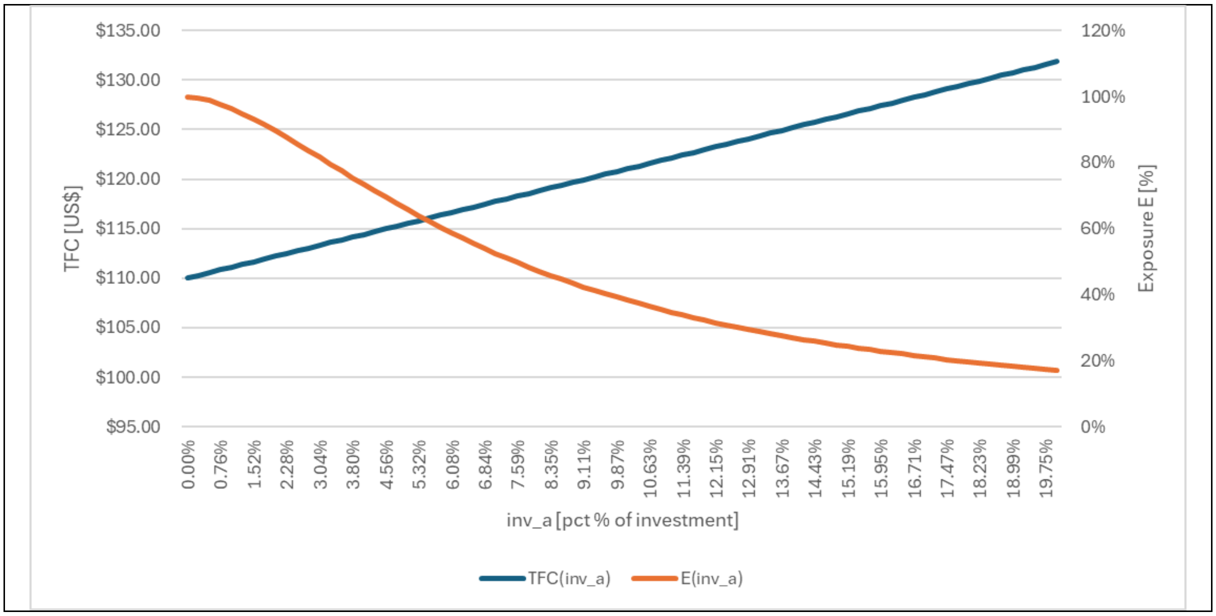

11.6.2.7 Project ID 179: Solar farm, South Africa, private

Gross cost of debt (excl. climate):	10.93%
Cost of equity:	10.42%
Leverage:	80.80%
Gross investment (excl. adaptation):	$ 125.00
Loan tenure:	17
Wind β:	2.940%
Wind climate indicator, log(1+CI):	0.04
Scaling resilience investment as percentage of investment:	7.50%
Selected resilience strategy (name):	Wind breaks - structural
Effectiveness of resilience strategy:	49.50%
Level of protection of resilience strategy:	99.45%
Optimized level of investment in resilience strategy:	0.00%
Exposure factor:	100.00%
Resulting cost of debt:	11.05%
Resulting discount rate:	10.93%
Total funding cost:	$ 125.77
Exposure factor and total funding cost shown as a function of the investment in resilience measure:	

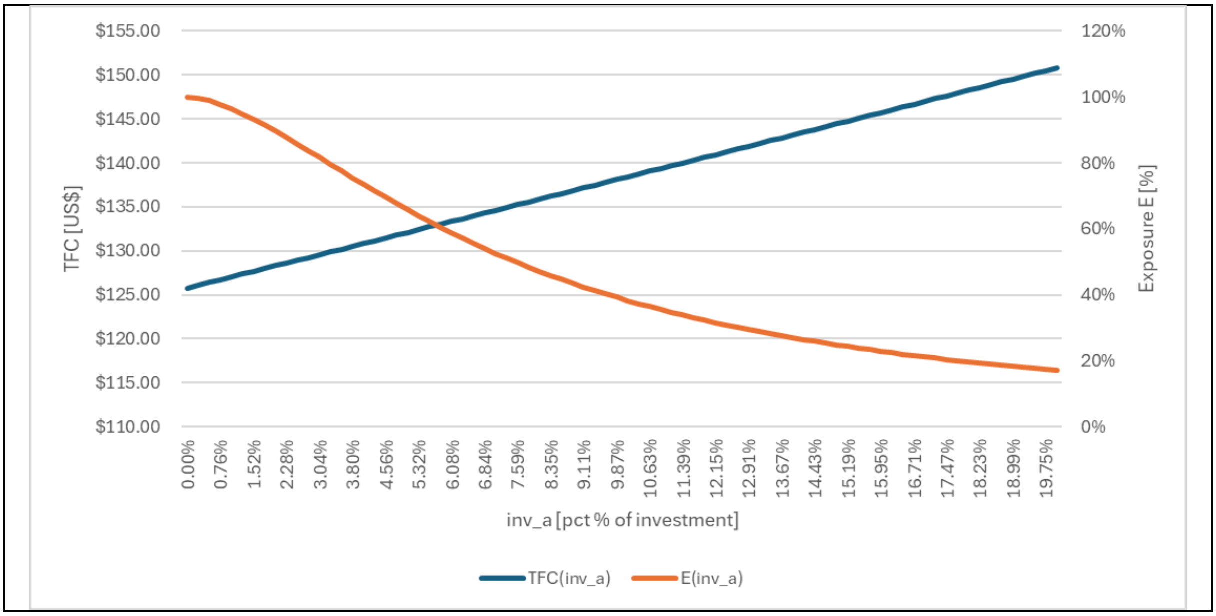

11.6.2.8 Project ID 180: Solar farm, South Africa, private

Gross cost of debt (excl. climate):	10.13%
Cost of equity:	10.42%
Leverage:	79.29%
Gross investment (excl. adaptation):	$ 140.00
Loan tenure:	17
Wind β:	2.940%
Wind climate indicator, log(1+CI):	0.04
Scaling resilience investment as percentage of investment:	7.50%
Selected resilience strategy (name):	Wind breaks - structural
Effectiveness of resilience strategy:	49.50%
Level of protection of resilience strategy:	99.45%
Optimized level of investment in resilience strategy:	0.00%
Exposure factor:	100.00%
Resulting cost of debt:	10.25%
Resulting discount rate:	10.28%
Total funding cost:	$ 139.74
Exposure factor and total funding cost shown as a function of the investment in resilience measure:	

WORKING PAPER #6

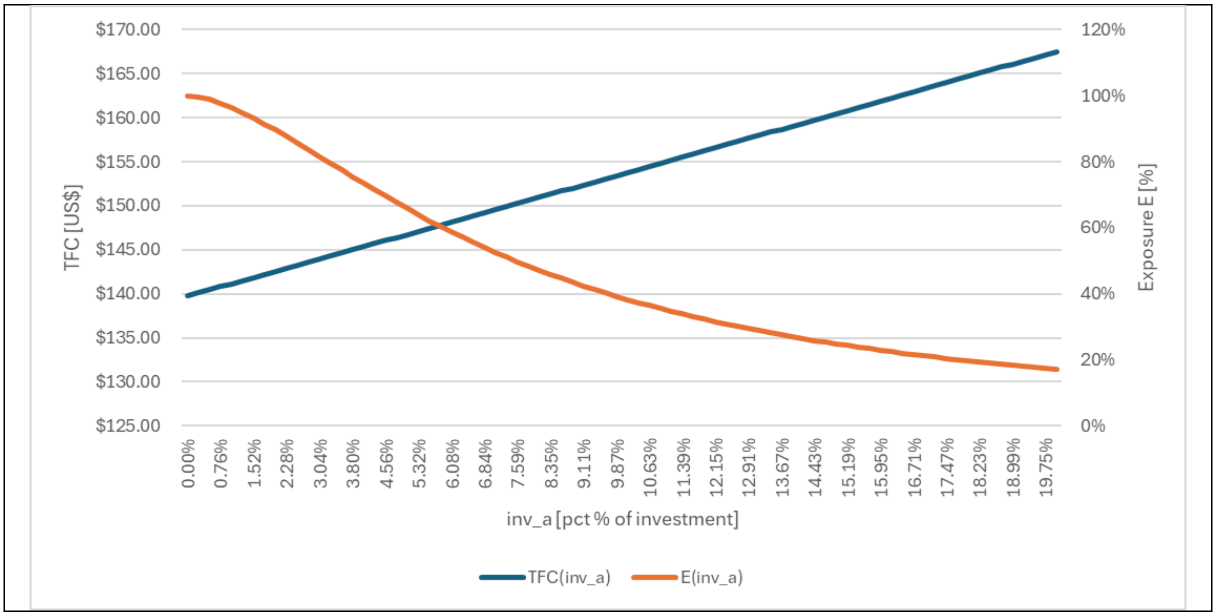

11.6.2.9 Project ID 181: Solar farm, South Africa, private

Gross cost of debt (excl. climate):	10.40%
Cost of equity:	10.42%
Leverage:	79.29%
Gross investment (excl. adaptation):	$ 140.00
Loan tenure:	18
Wind β:	2.940%
Wind climate indicator, log(1+CI):	0.04
Scaling resilience investment as percentage of investment:	7.50%
Selected resilience strategy (name):	Wind breaks - structural
Effectiveness of resilience strategy:	49.50%
Level of protection of resilience strategy:	99.45%
Optimized level of investment in resilience strategy:	0.00%
Exposure factor:	100.00%
Resulting cost of debt:	10.52%
Resulting discount rate:	10.50%
Total funding cost:	$ 140.16
Exposure factor and total funding cost shown as a function of the investment in resilience measure:	

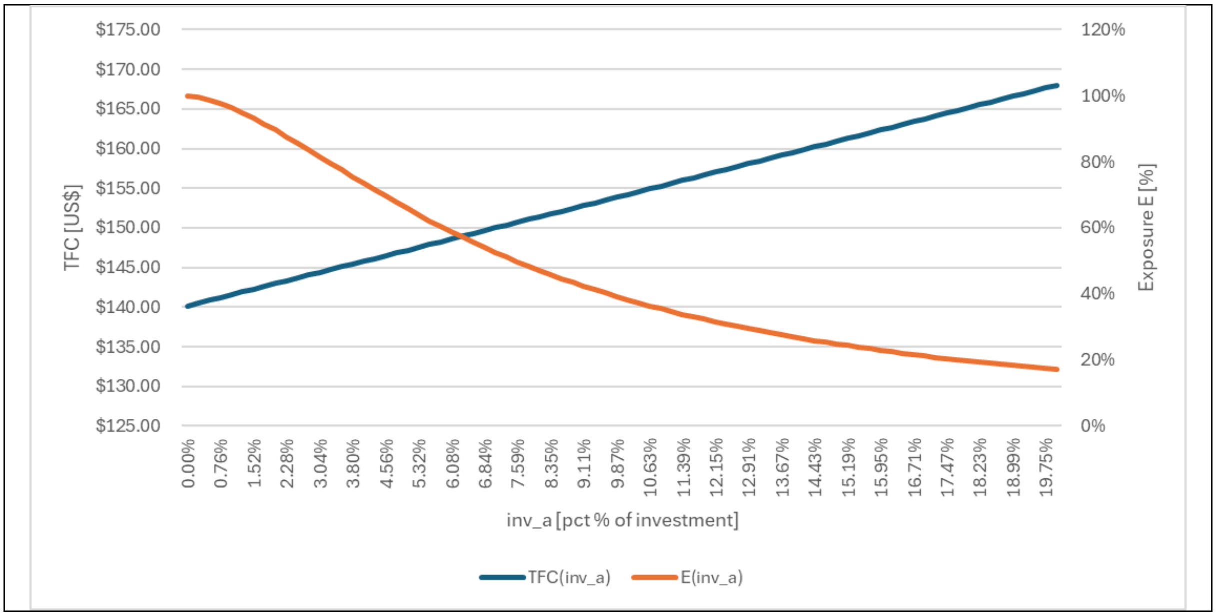

11.6.2.10 Project ID 182: Solar farm, South Africa, private

Gross cost of debt (excl. climate):	10.13%
Cost of equity:	10.42%
Leverage:	79.43%
Gross investment (excl. adaptation):	$ 141.00
Loan tenure:	18
Wind β:	2.940%
Wind climate indicator, log(1+CI):	0.04
Scaling resilience investment as percentage of investment:	7.50%
Selected resilience strategy (name):	Wind breaks - structural
Effectiveness of resilience strategy:	49.50%
Level of protection of resilience strategy:	99.45%
Optimized level of investment in resilience strategy:	0.00%
Exposure factor:	100.00%
Resulting cost of debt:	10.25%
Resulting discount rate:	10.28%
Total funding cost:	$ 140.73
Exposure factor and total funding cost shown as a function of the investment in resilience measure:	

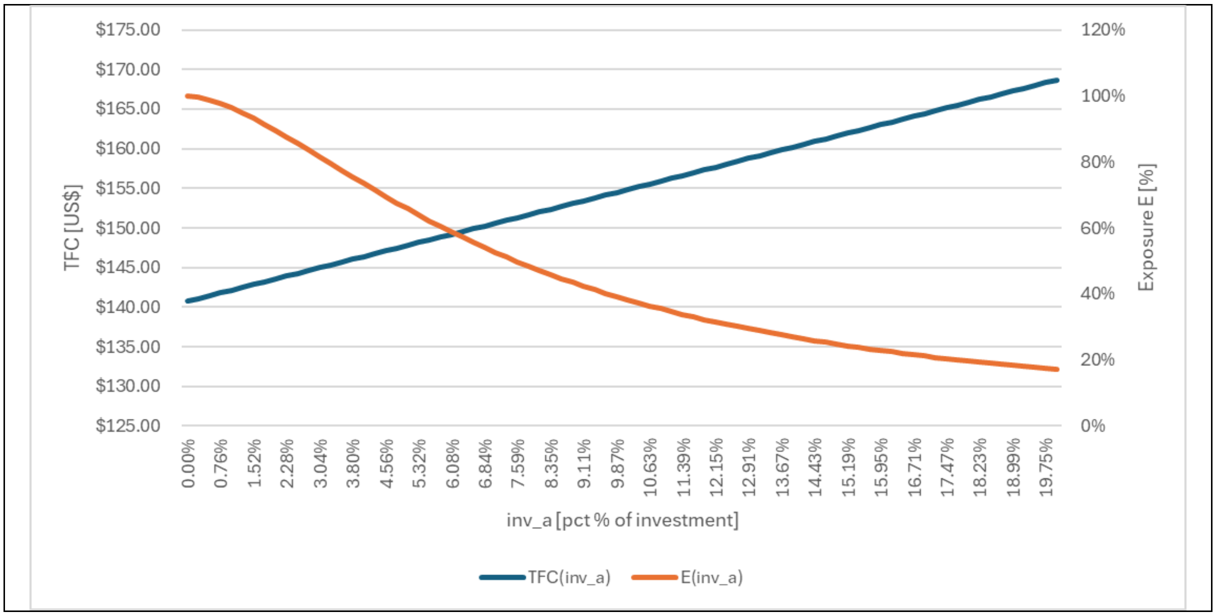

11.6.2.11 Project ID 204: Solar farm, South Africa, private

Gross cost of debt (excl. climate):	9.18%
Cost of equity:	8.33%
Leverage:	83.75%
Gross investment (excl. adaptation):	$ 800.00
Loan tenure:	17
Wind β:	2.940%
Wind climate indicator, log(1+CI):	0.04
Scaling resilience investment as percentage of investment:	7.50%
Selected resilience strategy (name):	Wind breaks - structural
Effectiveness of resilience strategy:	49.50%
Level of protection of resilience strategy:	99.45%
Optimized level of investment in resilience strategy:	0.00%
Exposure factor:	100.00%
Resulting cost of debt:	9.29%
Resulting discount rate:	9.13%
Total funding cost:	$ 806.88
Exposure factor and total funding cost shown as a function of the investment in resilience measure:	

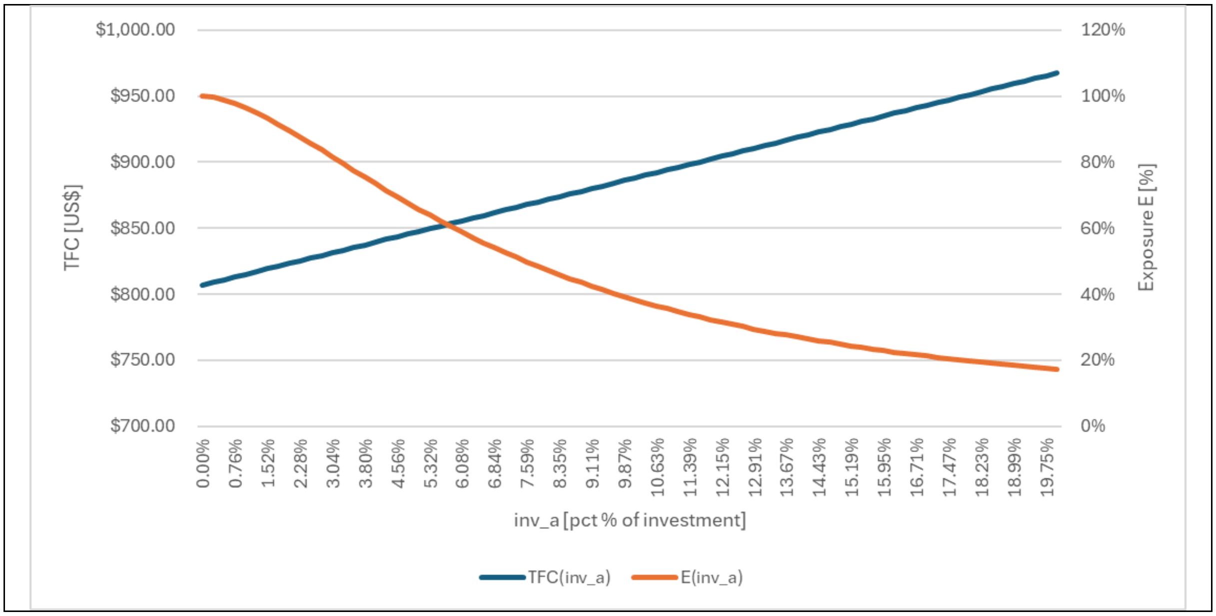

11.6.2.12 Project ID 223: Solar farm, South Africa, private

Gross cost of debt (excl. climate):	10.59%
Cost of equity:	10.42%
Leverage:	77.69%
Gross investment (excl. adaptation):	$ 121.00
Loan tenure:	17
Wind β:	2.940%
Wind climate indicator, log(1+CI):	0.04
Scaling resilience investment as percentage of investment:	7.50%
Selected resilience strategy (name):	Wind breaks - structural
Effectiveness of resilience strategy:	49.50%
Level of protection of resilience strategy:	99.45%
Optimized level of investment in resilience strategy:	0.00%
Exposure factor:	100.00%
Resulting cost of debt:	10.70%
Resulting discount rate:	10.64%
Total funding cost:	$ 121.40
Exposure factor and total funding cost shown as a function of the investment in resilience measure:	

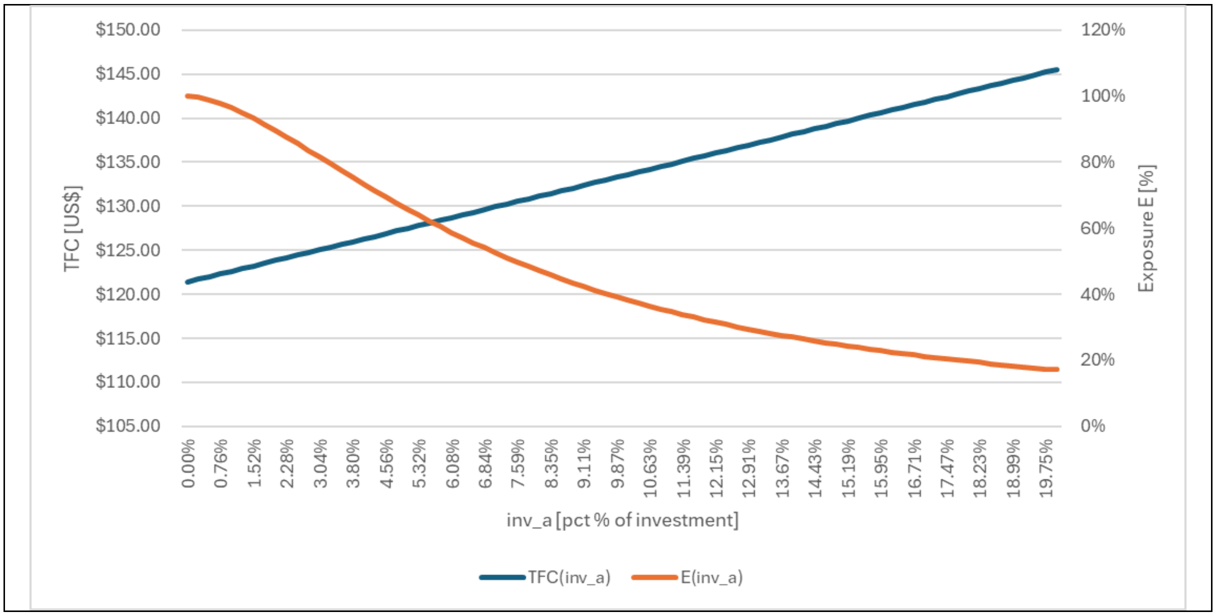

11.6.2.13 Project ID 226: Wind farm, South Africa, private

Gross cost of debt (excl. climate):	11.20%
Cost of equity:	10.42%
Leverage:	79.48%
Gross investment (excl. adaptation):	$ 268.00
Loan tenure:	19
Wind β:	2.940%
Wind climate indicator, log(1+CI):	0.04
Scaling resilience investment as percentage of investment:	5.00%
Selected resilience strategy (name):	Structural improvement
Effectiveness of resilience strategy:	79.50%
Level of protection of resilience strategy:	98.50%
Optimized level of investment in resilience strategy:	0.00%
Exposure factor:	100.00%
Resulting cost of debt:	11.32%
Resulting discount rate:	11.13%
Total funding cost:	$ 270.64
Exposure factor and total funding cost shown as a function of the investment in resilience measure:	

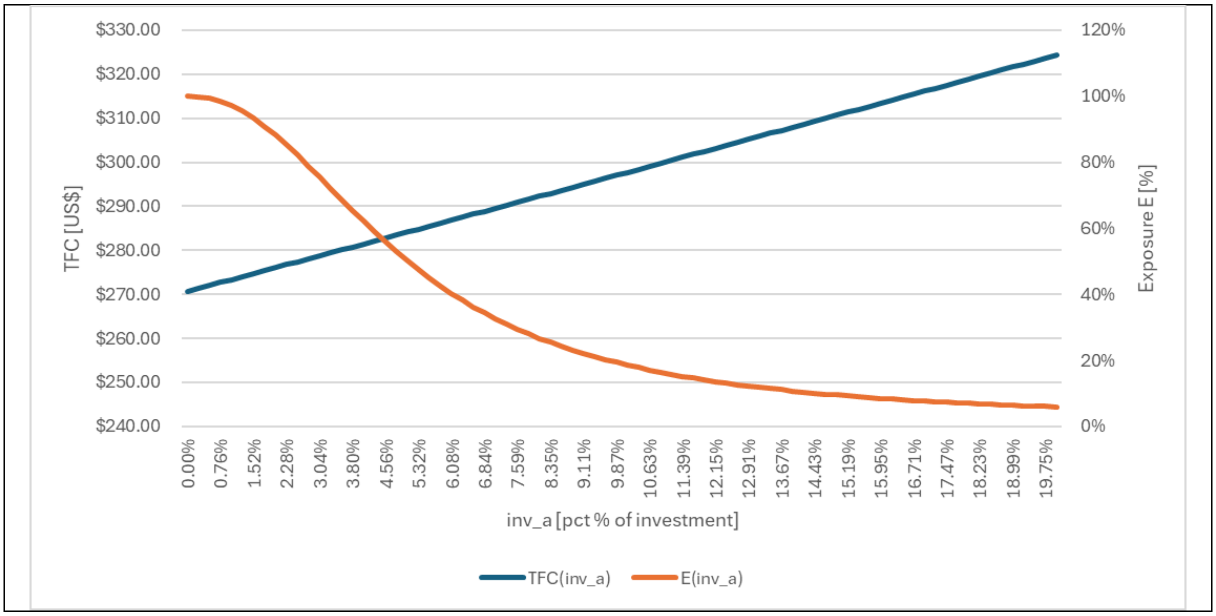

11.6.2.14 Project ID 227: Wind farm, South Africa, private

Gross cost of debt (excl. climate):	11.20%
Cost of equity:	10.42%
Leverage:	80.26%
Gross investment (excl. adaptation):	$ 304.00
Loan tenure:	18
Wind β:	2.940%
Wind climate indicator, log(1+CI):	0.04
Scaling resilience investment as percentage of investment:	5.00%
Selected resilience strategy (name):	Structural improvement
Effectiveness of resilience strategy:	79.50%
Level of protection of resilience strategy:	98.50%
Optimized level of investment in resilience strategy:	0.00%
Exposure factor:	100.00%
Resulting cost of debt:	11.32%
Resulting discount rate:	11.14%
Total funding cost:	$ 306.79
Exposure factor and total funding cost shown as a function of the investment in resilience measure:	

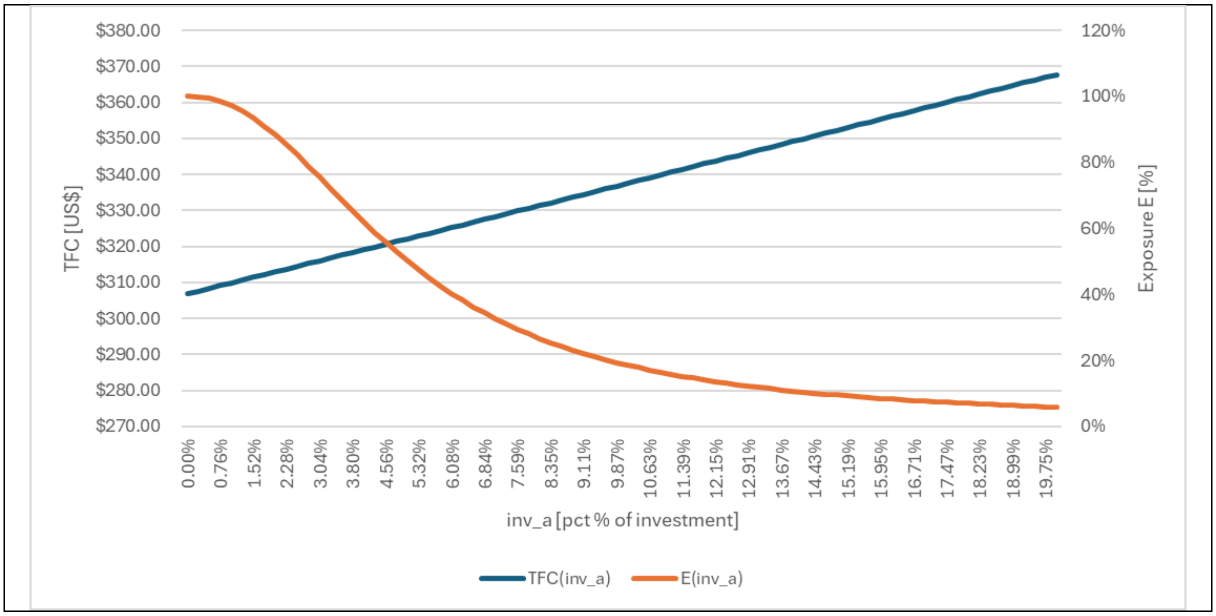

11.6.2.15 Project ID 228: Wind farm, South Africa, private

Gross cost of debt (excl. climate):	11.83%
Cost of equity:	10.42%
Leverage:	71.06%
Gross investment (excl. adaptation):	$ 387.00
Loan tenure:	19
Wind β:	2.940%
Wind climate indicator, log(1+CI):	0.04
Scaling resilience investment as percentage of investment:	5.00%
Selected resilience strategy (name):	Structural improvement
Effectiveness of resilience strategy:	79.50%
Level of protection of resilience strategy:	98.50%
Optimized level of investment in resilience strategy:	0.00%
Exposure factor:	100.00%
Resulting cost of debt:	11.95%
Resulting discount rate:	11.51%
Total funding cost:	$ 395.96
Exposure factor and total funding cost shown as a function of the investment in resilience measure:	

WORKING PAPER #6

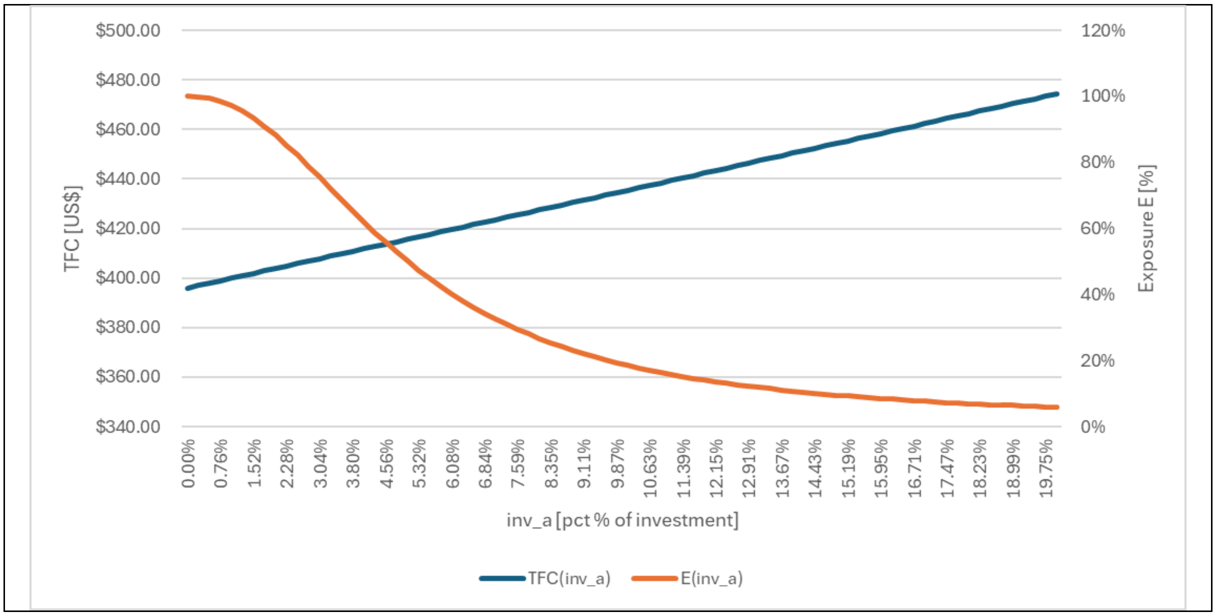

11.6.2.16 Project ID 229: Solar farm, South Africa, private

Gross cost of debt (excl. climate):	10.22%
Cost of equity:	8.96%
Leverage:	75.00%
Gross investment (excl. adaptation):	$ 4.00
Loan tenure:	17
Wind β:	2.940%
Wind climate indicator, log(1+CI):	0.04
Scaling resilience investment as percentage of investment:	7.50%
Selected resilience strategy (name):	Wind breaks - structural
Effectiveness of resilience strategy:	49.50%
Level of protection of resilience strategy:	99.45%
Optimized level of investment in resilience strategy:	0.00%
Exposure factor:	100.00%
Resulting cost of debt:	10.33%
Resulting discount rate:	9.99%
Total funding cost:	$ 4.07
Exposure factor and total funding cost shown as a function of the investment in resilience measure:	

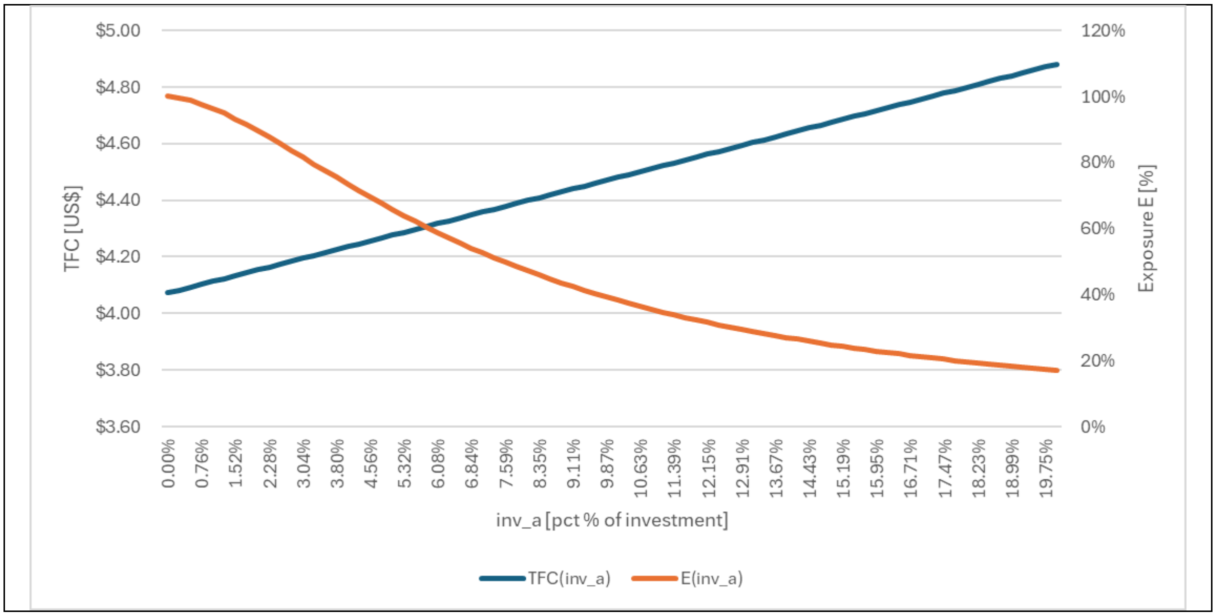

11.6.2.17 Project ID 232: Solar farm, South Africa, private

Gross cost of debt (excl. climate):	11.00%
Cost of equity:	18.79%
Leverage:	79.63%
Gross investment (excl. adaptation):	$ 594.00
Loan tenure:	16
Wind β:	2.940%
Wind climate indicator, log(1+CI):	0.03
Scaling resilience investment as percentage of investment:	5.00%
Selected resilience strategy (name):	Wind breaks - structural
Effectiveness of resilience strategy:	79.50%
Level of protection of resilience strategy:	98.50%
Optimized level of investment in resilience strategy:	0.00%
Exposure factor:	100.00%
Resulting cost of debt:	11.10%
Resulting discount rate:	12.66%
Total funding cost:	$ 551.37
Exposure factor and total funding cost shown as a function of the investment in resilience measure:	

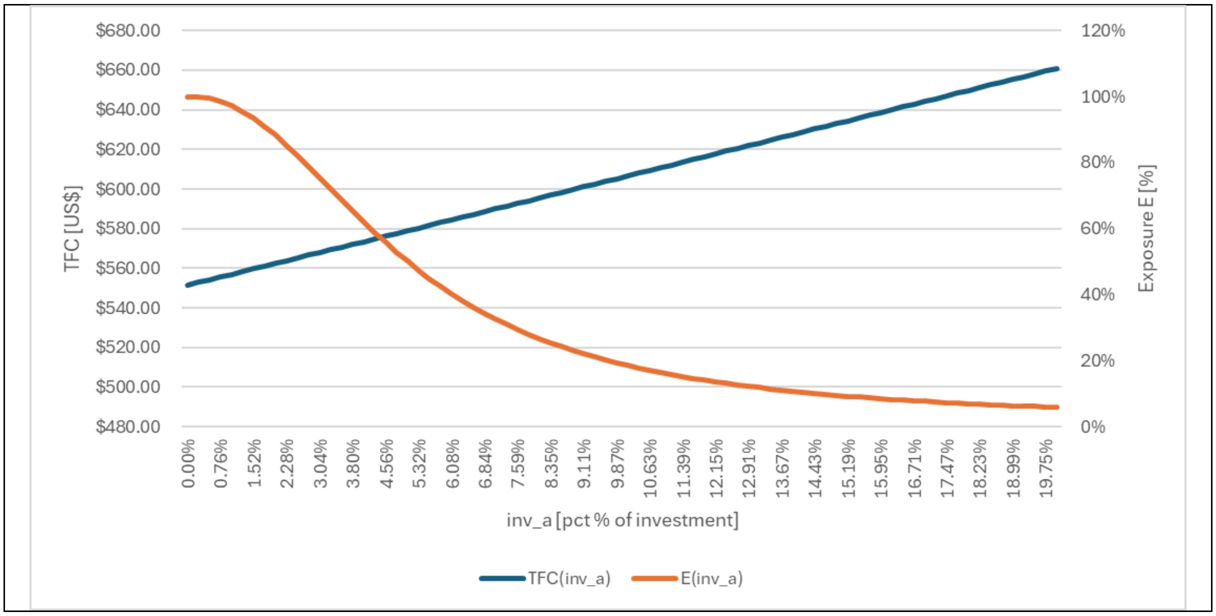

11.6.2.18 Project ID 234: Wind farm, South Africa, private

Gross cost of debt (excl. climate):	5.67%
Cost of equity:	10.25%
Leverage:	72.37%
Gross investment (excl. adaptation):	$ 854.00
Loan tenure:	17
Wind β:	2.940%
Wind climate indicator, log(1+CI):	0.04
Scaling resilience investment as percentage of investment:	7.50%
Selected resilience strategy (name):	Structural improvement
Effectiveness of resilience strategy:	49.50%
Level of protection of resilience strategy:	99.45%
Optimized level of investment in resilience strategy:	0.00%
Exposure factor:	100.00%
Resulting cost of debt:	5.80%
Resulting discount rate:	7.03%
Total funding cost:	$ 790.11
Exposure factor and total funding cost shown as a function of the investment in resilience measure:	

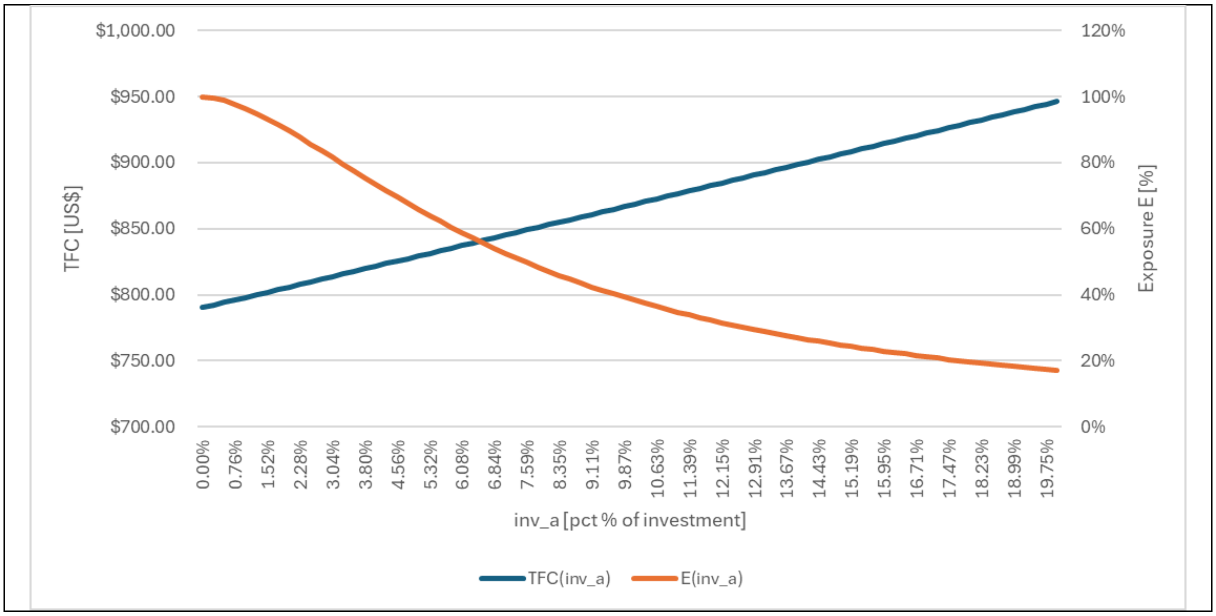

11.6.2.19 Project ID 235: Solar farm, South Africa, private

Gross cost of debt (excl. climate):	8.42%
Cost of equity:	18.79%
Leverage:	77.02%
Gross investment (excl. adaptation):	$ 248.00
Loan tenure:	17
Wind β:	2.940%
Wind climate indicator, log(1+CI):	0.04
Scaling resilience investment as percentage of investment:	7.50%
Selected resilience strategy (name):	Wind breaks - structural
Effectiveness of resilience strategy:	49.50%
Level of protection of resilience strategy:	99.45%
Optimized level of investment in resilience strategy:	0.00%
Exposure factor:	100.00%
Resulting cost of debt:	8.53%
Resulting discount rate:	10.89%
Total funding cost:	$ 218.29
Exposure factor and total funding cost shown as a function of the investment in resilience measure:	

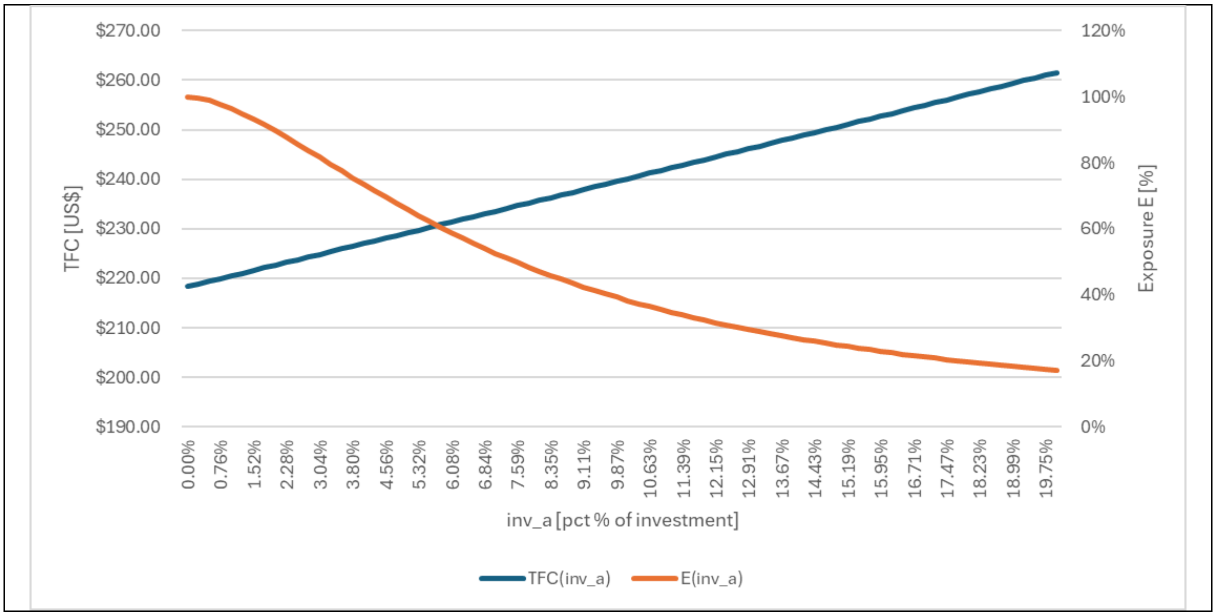

WORKING PAPER #6

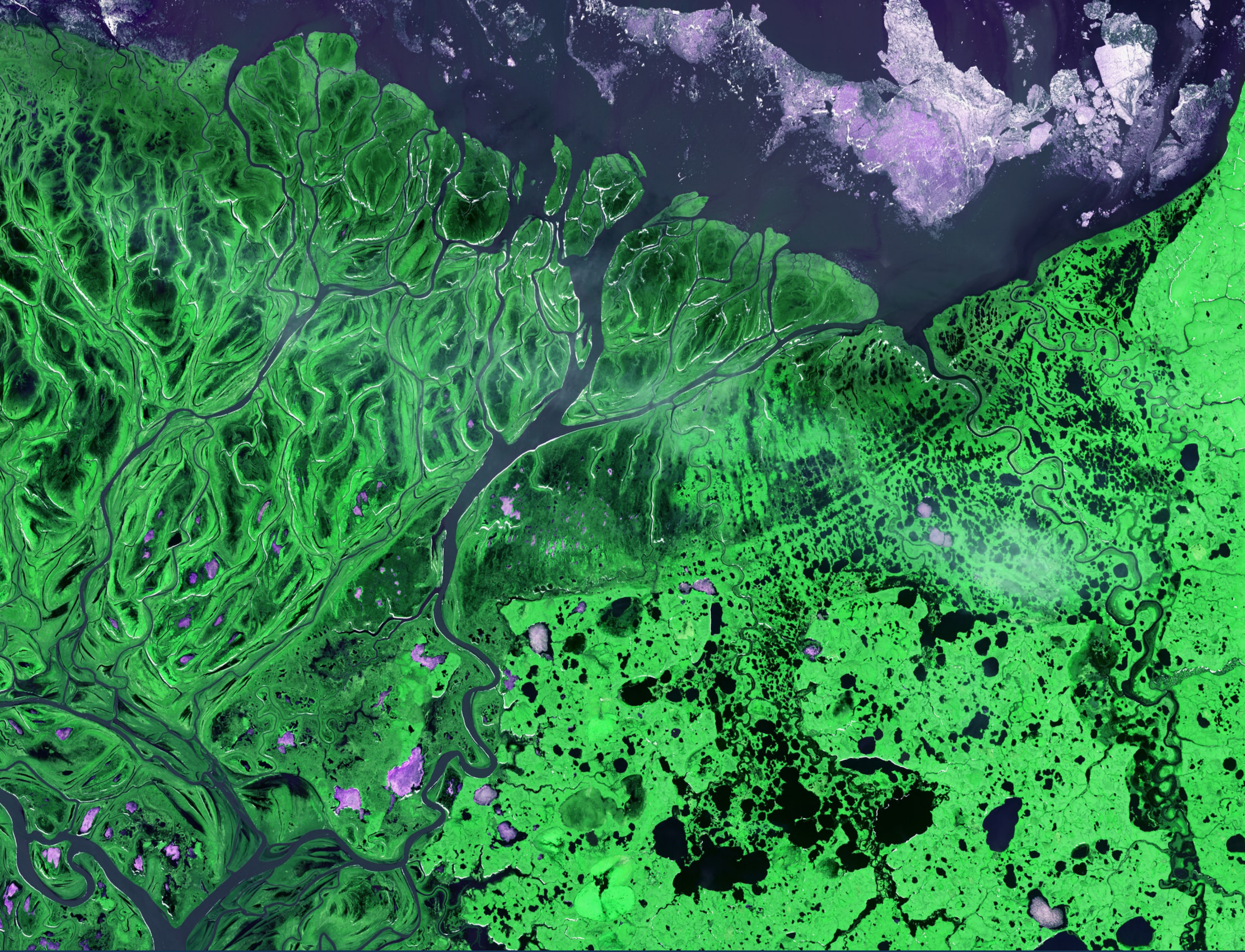

MINES PARIS | PSL | TTI.5° The Transition Institute

CONTACT

the-transition-institute.minesparis.psl.eu

tti.5@minesparis.psl.eu

WORKING PAPER #6